Inverse Problems for the Heat Equation Using Conjugate Gradient Methods

Kai Cao

Department of Applied Mathematics

The University of Leeds

Submitted in accordance with the requirements for the degree of

Doctor of Philosophy

September, 2018

Joint publications

At the time of publishing this thesis some of the work presented in it has already been published or has been accepted for publication, as follows:

- Some of the material of Chapters 2 and 4 is included in:
  Cao K. and Lesnic D. (2018). Determination of space-dependent coefficients from temperature measurements using the conjugate gradient method. *Numerical Methods for Partial Differential Equations*, 34 (4), 1370–1400.
- Some of the material of Chapter 3 is included in:
  Cao K., Lesnic D. and Colaco M.J. (2018). Determination of thermal conductivity of inhomogeneous orthotropic materials from temperature measurements. *Accepted by Inverse Problems in Science and Engineering*.
- Some of the material of Chapter 5 is included in:
  Cao K. and Lesnic D. (2018). Reconstruction of the space-dependent perfusion coefficient from final time or time-average temperature measurements. *Journal of Computational and Applied Mathematics*, 337, 150–165.
- Some of the material of Chapter 7 is included in:
  Cao K. and Lesnic D. (2018). Simultaneous reconstruction of the perfusion coefficient and initial temperature from time-average integral temperature measurements. *Accepted by Applied Mathematical Modelling*.

Acknowledgements

I would like to thank my supervisor Professor Daniel Lesnic for his great supervision, patience, continuous support and guidance throughout my PhD study. In fact, words cannot express my heartfelt gratitude, appreciation and thanks for all the support, guidance and time he had provided during my stay in Leeds.

I would like to give my thanks to all the staff at the School of Mathematics for their help with all the little things that keep everything running smoothly. I am thankful also to my postgraduate colleagues for their company and friendship during my time in Leeds.

My gratitude extends to Professor Jijun Liu for his valuable advice during his visit of the University of Leeds in April 2018.

My special thanks are due to my parents for their continuous love, tolerance and support.

Finally, many thanks go the China Scholarship Council (CSC) for financially supporting my postgraduate studies.

Kai Cao

Abstract

In many engineering systems, e.g., in heat exchanges, reflux condensers, combustion chambers, nuclear vessels, etc. concerned with high temperatures/pressures/loads and/or hostile environments, certain properties of the physical medium, geometry, boundary and initial conditions are not known and their direct measurement can be very inaccurate or even inaccessible. In such a situation, one can adopt an inverse approach and try to infer the unknowns from some extra accessible measurements of other quantities that may be available.

The purpose of this thesis is to determine the unknown space-dependent coefficients and/or initial temperature in inverse problems of heat transfer, especially to simultaneously reconstruct several unknown quantities. These inverse problems are investigated from additional pieces of information, such as internal temperature observations, final measured temperature and time-integral temperature measurement. The main difficulty involved in the solution of these inverse problems is that they are typically ill-posed. Thus, their solutions are unstable under small perturbations of the input data and classical numerical techniques fail to provide accurate and stable numerical results.

Throughout this thesis, the inverse problems are transformed into optimization problems, and their minimizers are shown to exist. A variational method is employed to obtain their Fréchet gradients with respect to the unknown quantities. Based on this gradient, the conjugate gradient method (CGM) is established together with the adjoint and sensitivity problems.

The stability of the numerical solution is investigated by introducing Gaussian random noise into the input measured data. Accurate and stable numerical solutions are obtained when using the CGM regularized by the discrepancy principle.

Nomenclature

$\mathcal{A}$	admissible set
C	heat capacity
$\mathcal{D}(\mathcal{T})$	domain of $\mathcal{T}$
d^n	direct of descent
E	accuracy error
e_1, e_2, Y, y	exact data
e_1^ϵ, e_2^ϵ, Y^ϵ, y^ϵ	perturbed data
F	space-dependent heat source component
f	heat source
g, h	space- and time-dependent heat source components
J	objective functional
J'	gradient of J
k	thermal conductivity
$\mathcal{L}$	parabolic operator
N	stopping iteration number
n	iteration number
$p\%$	percentage of noise
q	reaction coefficient
$\mathcal{R}(\mathcal{T})$	range of $\mathcal{T}$
T	final time
$\mathcal{T}$	operator
$\mathcal{T}^*$	adjoint operator
u	temperature
$\mathcal{U}$	bounded linear operator
x_0	a-priori information
$x^\dagger$	x_0-minimum-norm solution
$\mathcal{X}$, $\mathcal{Y}$	Hilbert spaces
$\mathcal{X}_D$	characteristic function of the domain D

Greek symbols

α	Robin coefficient
β	regularization parameter
β^n	search step size
γ^n, φ^n	conjugate coefficients
$\delta(\cdot)$	Dirac delta function
ϵ	noise level
λ	adjoint function
μ	heat flux
ν	outward unit normal
σ	standard deviation
ϕ	initial temperature
ω	weight function
Ω	bounded domain
$\partial\Omega$	boundary of Ω

Abbreviations

BEM	boundary element method
BHCP	backward heat conduction problem
CGM	conjugate gradient method
FDM	finite difference method
FEM	finite element method
FVM	finite volume method
HTC	heat transfer coefficient
IHTP	inverse heat transfer problem
MFS	method of fundamental solution
PDE	partial differential equation
RBF	radial basis function
SVD	singular value decomposition
TSVD	truncated singular value decomposition
TV	total variation

List of Figures

List of Tables

Contents

Chapter 1

Introduction

Inverse problems are considered as determining the cause of a desired or an observed effect, on the other hand, the direct problem is concerned with determining the effect when the cause is known. There is a natural distinction between the direct and the inverse problem if there is a real physical problem behind the mathematical model.

For instance, one shall call a problem direct when one wants to predict the future behaviour of a physical system if the present state and laws of the physical problem are known, whilst possible inverse problems are to identify the knowledge of the present state of the system from future observations or, the reconstruction of the physical parameters and/or coefficients from the measurements of the system.

Inverse heat transfer problems (IHTPs) are to determine the thermal parameters or coefficients, the temperature on an inaccessible part of the boundary and the initial temperature from over-specified temperature measurements, see e.g. Alifanov (1994); Özişik & Orlande (2000). Such inverse problems are encountered in almost every branch of science and engineering, and also found in aerospace, chemical and nuclear industry, etc. Thus, the interest has grown rapidly in the theory and application of IHTPs in recent years.

One example of an inverse problem is the following: It is difficult to directly measure the heat flux by applying conventional methods on the surface of a wall subjected to fire, in such case the inverse analysis in heat transfer can be employed to estimate the unknown heat flux from the transient temperature readings which are taken by temperature sensors at some specified locations beneath the heated surface.

Another practical application is about the aviation and rocket space technology using IHTPs. For instance, the surface temperature of the thermal shield is impossible to be measured directly by using temperature sensors, since the areodynamic heating of the

space vehicles is extremely high during the re-entry in the atmosphere. The surface temperature can be reconstructed by using inverse analysis from the measured temperature obtained by sensors placed beneath the hot shield surface. Finally, since the measurements of thermophysical properties based on classical methods to many materials can only be realized at lower temperatures and heating rates, such limitation can be avoided by estimating the thermophysical properties of the shield using the inverse analysis in heat transfer during operating conditions at high temperatures.

IHTPs are usually ill-posed, which is the main difficulty associated with the solution of such inverse problems, Alifanov (1994); Beck *et al.* (1985). As such, IHTPs are very sensitive to random errors inherent in the measured input data, which implies that special techniques are required to obtain stable solutions.

1.1 Direct problem

In mathematical physics, a direct problem is a problem of modelling some physical fields, processes, or phenomena, especially using partial differential equations (PDEs). The aim of solving a direct problem is to obtain the main dependent variable function that describes and governs naturally a physical field or process.

One example of a direct problem for a one-dimensional heat transfer process is given by

$$\begin{cases} \mathrm{C}(x)\frac{\partial u}{\partial t} = \frac{\partial}{\partial x}\left(k(x)\frac{\partial u}{\partial x}\right) + f(x,t), & (x,t) \in (0,1)\times(0,T), \\ -k(0)\frac{\partial u}{\partial x}(0,t) = \mu_1(t), \quad u(1,t) = \mu_2(t), & t \in (0,T), \\ u(x,0) = \phi(x), & x \in [0,1], \end{cases} \tag{1.1}$$

where $u(x,t)$ is the unknown temperature, $\mathrm{C}(x)$ is the heat capacity, $k(x)$ is the thermal conductivity, $f(x,t)$ is the source term, $\mu_1(t)$ is the heat flux at the left end point, $\mu_2(t)$ is the boundary temperature at the right end point, $\phi(x)$ is the initial temperature and T is the final time. The direct problem is to determine the temperature $u(x,t)$ satisfying the initial-boundary value problem (1.1) when the thermal coefficients $\mathrm{C}(x)$, $k(x)$, $f(x,t)$, the boundary data $\mu_1(t)$ and $\mu_2(t)$ and the initial temperature $\phi(x)$ are all specified.

We also present a two-dimensional heat transfer problem given by

$$\begin{cases} \mathrm{C}(x_1,x_2)\frac{\partial u}{\partial t} = \nabla\cdot(k(x_1,x_2)\nabla u) \\ \qquad\qquad -q(x_1,x_2,t)u + f(x_1,x_2,t), & (x_1,x_2,t) \in Q, \\ k(x_1,x_2)\frac{\partial u}{\partial \nu} + \alpha(x_1,x_2)u = \mu(x_1,x_2,t), & (x_1,x_2,t) \in S, \\ u(x_1,x_2,0) = \phi(x_1,x_2), & (x_1,x_2) \in \overline{\Omega}, \end{cases} \tag{1.2}$$

where $\Omega = (0,1)\times(0,1)$, $Q = \Omega\times(0,T)$, $S = \partial\Omega\times(0,T)$ and ν is the outward unit normal to the boundary $\partial\Omega$. The coefficients $\mathrm{C}(x_1,x_2)$, $k(x_1,x_2)$, $f(x_1,x_2,t)$, $\mu(x_1,x_2,t)$ and $\phi(x_1,x_2)$ have the same physical properties as those presented in (1.1), $q(x_1,x_2,t)$ is the reaction coefficient and $\alpha(x_1,x_2)$ is the Robin convective coefficient. Similarly, the direct problem is to identify the temperature $u(x_1,x_2,t)$ based on known coefficients, source, initial and boundary conditions in the problem (1.2).

Direct problems are in general well-posed by the concept of Hadamard (1923) if they satisfy:

(a) The solution to the problem exists;

(b) The solution is unique;

(c) The solution depends continuously on the input data.

The well-posedness of direct problems for parabolic PDEs has been extensively studied, see, e.g., Friedman (2008); Ladyzhenskaia *et al.* (1968). Besides analytical results, the methods to obtain numerical solutions play an important role in this thesis. There are various numerical discretisation methods to solve PDEs, for instance, the finite difference method (FDM), Smith (1985), the finite element method (FEM), Reddy (1993), the finite volume method (FVM), Versteeg & Malalasekera (2007), and the boundary element method (BEM), Banerjee & Butterfield (1981). Meshless spectral methods such as the method of fundamental solutions (MFS) or the radial basis functions (RBF) are also possible, but they are not discussed herein.

The FDM, which seems to be the easiest technique to numerically discretise a PDE, utilizes finite differences generated by the Taylor series expansion to approximate the partial derivatives involved in the PDE. The method becomes complicated when the FDM is employed to solve the PDE in irregular domains, and the convergence and stability analyses of FDM are quite difficult for nonliner PDEs.

The FEM uses variational methods to rewrite the original governing equation in a weak integral form. The large domain is subdivided into smaller, simpler parts that are called finite elements, then the solutions can be approximated using appropriate basis functions over each elements. The numerical solutions of the PDE over the entire domain is obtained by solving an assembled system of algebraic equations.

The FVM is based on integrating the PDE over a finite volume surrounding each node point. The volume integrals are converted to surface integrals by the divergence theorem. The FVM does not require a structured mesh, which is an advantage of FVM over FDM. In addition, the boundary conditions can be applied non-invasively in FVM.

The BEM can be applied to solve those PDEs with explicit fundamental solutions available. The PDEs then can be transformed into boundary integral equations by using the Green's formula, and the solutions can be computed using the given boundary conditions. One advantage is that only the boundary of the domain needs to be discretised in the BEM, which reduces the dimensionality of the problem by one.

1.2 Inverse heat transfer problems

In many engineering problems certain quantities of the direct problem (1.1) or (1.2) are not directly specified or measured, which leads to inverse problem formulations.

For instance, a similar problem to the initial-boundary value problem (1.1) is considered, but the thermal conductivity $k(x)$ is unknown, while all other physical quantities $\mathrm{C}(x)$, $f(x,t)$, $q(t)$, $\mu(t)$ and $\phi(x)$ are known. One inverse problem formulation is to determine the unknown thermal conductivity $k(x)$ from the temperature measurements

$$u(x,t) = Y(x,t), \quad (x,t) \in (0,1) \times (0,T). \tag{1.3}$$

Similarly, for the problem (1.2), one IHTP is to identify the unknown reaction coefficient $q(x_1, x_2, t)$ from the measured temperature in Q, when other thermal coefficients, initial and boundary conditions are known.

IHTPs can be classified based on the type of causal characteristics to be estimated, Özişik & Orlande (2000):

- unknown boundary conditions;
- unknown thermophysical properties;
- unknown initial temperature;
- unknown source term;
- unknown geometric characteristics.

The inverse boundary value problems of heat transfer are to determine the unknown boundary data on an inaccessible part of the boundary from over-prescribed boundary conditions provided on the remaining boundary part, when the thermal coefficients, the heat sources and the geometry of the domain are known. In the reference book by Alifanov (1994), analytical solutions and numerical methods for inverse boundary value problems are presented together with the stability analysis.

The thermophysical property identification problems in heat transfer are to determine the thermal coefficients in the governing heat equation characterising the material properties, such as the thermal conductivity $k(x_1, x_2)$, the heat capacity $\mathrm{C}(x_1, x_2)$ and the reaction coefficient $q(x_1, x_2, t)$ in (1.2). One example is that of the two-dimensional time- and space-dependent thermal conductivity $k(x_1, x_2, t)$ of a non-homogeneous medium reconstructed from the temperature measurements (1.3) using the conjugate gradient method (CGM), Huang & Chin (2000). Besides, the time- and space-dependent reaction coefficient $q(x, t)$ (or $q(x_1, x_2, t)$) was estimated from the measured temperature (1.3) using the CGM, Cao & Lesnic (2018a).

The IHTP to determine the initial temperature is usually called the backward heat conduction problem (BHCP). This inverse problem is to identify the unknown initial status from the temperature measurement at a latter time, when the thermal coefficients, source terms and boundary conditions are specified.

The inverse source problems are to identify the heat source, e.g., $f(x, t)$ in (1.1), or the heat source components, e.g., $f_1(x)$ in $f(x, t) = f_1(x)h(x, t)$, where $h(x, t)$ is a given function, when the thermal coefficients, initial and boundary conditions and geometry of domain are given. In Isakov (1990), the existence, uniqueness and stability of solutions to the inverse source problems of parabolic PDEs have been investigated from the final time or lateral boundary overdeterminations. The inverse source problems have also been reconstructed numerically, e.g., by using the CGM in Hào *et al.* (2017).

The inverse geometric problems are to determine the unknown location and shape of part of the boundary of the domain from the over specified boundary conditions on the known part of the boundary, when all the coefficients, heat source and initial temperature are specified. Such inverse geometric problems can be used to model defects such as obstacles, cavities, inclusions, flaws, faults, voids and cracks. Moreover, one typical medical application of the inverse geometric problem is the detection of anomalies such as tumours inside or on the skin of a body.

All the above categories of linear or nonlinear IHTPs are ill-posed, and the ill-posedness concept is introduced in the next section.

1.3 Ill-posed problems

For an inverse problem of mathematical physics, if one of the three conditions (a)–(c) of Section 1.1 fail to hold, then the problem is called ill-posed (in the sense of Hadamard). One main difficulty associated with IHTPs are that they are in general ill-posed, whereas the corresponding direct problem is well-posed.

A solution to an IHTP may exist, which can be established according to mathematical modelling and physical reasoning. The uniqueness of some IHTP can be proved under suitable sufficient conditions. The IHTP is not physical and cannot be computed if this problem does not satisfy the stability condition (c). In such case, the inverse problem becomes very sensitive to the noisy input data. Note that an unstable inverse problem may be rendered stable mathematically under suitably changing conditions (e.g., functional spaces), but such changes are not always possible for inverse problems in the realistic applications for which the input data is inevitably contaminated by random non-smooth noise.

In order to illustrate the ill-posedness of IHTP, we consider the one-dimensional heat equation with homogeneous Dirichlet boundary conditions given by

$$\begin{cases} \frac{\partial u}{\partial t} - \frac{\partial^2 u}{\partial x^2} = 0, & (x,t) \in (0,1) \times (0,1), \\ u(0,t) = u(1,t) = 0, & t \in (0,1). \end{cases} \tag{1.4}$$

The BHCP is to determine the initial temperature $u(x,0) = \phi(x)$ from the measured temperature at the final time $t = 1$,

$$u(x,1) = \phi_1(x), \quad x \in (0,1). \tag{1.5}$$

Taking $\phi_{1,n}(x) = \frac{\sin(n\pi x)}{n^2\pi^2}$, using the separation of variables to the problem (1.4) and (1.5), it is easy to see that

$$u_n(x,t) = \frac{1}{n^2\pi^2} e^{n^2\pi^2(1-t)} \sin(n\pi x), \quad n \in \mathbb{N}^*. \tag{1.6}$$

It is obvious that

$$\lim_{n\to\infty} \|\phi_{1,n}\|_{L_2(0,1)} = \lim_{n\to\infty} \frac{1}{\sqrt{2}n^2\pi^2} = 0,$$

and

$$\lim_{n\to\infty} \|u_n(\cdot,0)\|_{L_2(0,1)} = \lim_{n\to\infty} \frac{e^{n^2\pi^2}}{\sqrt{2}n^2\pi^2} = \infty.$$

Hence, when we consider $\phi_{1,n}$ as perturbation of $\phi_1 = 0$ with the L_2-error $\frac{1}{\sqrt{2}n^2\pi^2}$ decaying to 0 as $n \to \infty$, the corresponding error to the solution $u(\cdot,0)$ of the BHCP is amplified exponentially by $e^{n^2\pi^2}$, which implies that the initial temperature $u(x,0)$ to the BHCP is not continuously dependent on the final measured temperature $\phi_1(x)$.

Many IHTPs can be transformed into an operator equation:

$$\mathcal{T}x = y, \tag{1.7}$$

where $\mathcal{T} : \mathcal{D}(\mathcal{T}) \mapsto \mathcal{Y}$ is a linear or nonlinear operator with domain $\mathcal{D}(\mathcal{T}) \subset \mathcal{X}$, and $\mathcal{X}$, $\mathcal{Y}$ are infinite-dimensional Hilbert spaces. Then the solution of (1.7) exists when

$\mathcal{T} : \mathcal{D}(\mathcal{T}) \to \mathcal{R}(\mathcal{T})$ is surjective, i.e., when y belongs to the range $\mathcal{R}(\mathcal{T})$ of the operator $\mathcal{T}$. The solution is unique if and only if $\mathcal{T}$ is injective. In case $\mathcal{T} : \mathcal{D}(\mathcal{T}) \mapsto \mathcal{Y}$ is bijective, the stability is equivalent to the continuity of the inverse operator $\mathcal{T}^{-1} : \mathcal{R}(\mathcal{T}) \to \mathcal{D}(\mathcal{T})$. The equation (1.7) becomes an ill-posed problem if it violates one or more of the above conditions.

The operator equation (1.7) requires to determine $x \in \mathcal{D}(\mathcal{T})$ given the measured perturbed data $y^\epsilon \in \mathcal{Y}$ of the data $y \in \mathcal{R}(\mathcal{T})$, where $\epsilon \geq 0$ represents the noise level, satisfying

$$\|y - y^\epsilon\|_{\mathcal{Y}} \leq \epsilon. \tag{1.8}$$

For instance, in the IHTP (1.1) and (1.3), the nonlinear operator $\mathcal{T}$ maps the unknown thermal coefficient $k(x)$ onto the measured perturbed temperature Y^ϵ of Y in (1.3). Even if the inverse operator $\mathcal{T}^{-1} : \mathcal{R}(\mathcal{T}) \mapsto \mathcal{D}(\mathcal{T})$ exists, it is usually not continuous (e.g., in case $\mathcal{T}$ is compact[1], $\mathcal{T}^{-1}$ is unbounded) and therefore the problem becomes unstable. We can illustrate this easier in case of linear or nonlinear compact operators as follows.

For any compact linear operator $\mathcal{T}$ in the operator equation (1.7), the singular value decomposition (SVD) method is a widely used technique, e.g., Engl *et al.* (1996).

The non-zero eigenvalues of the selfadjoint operator $\mathcal{T}^*\mathcal{T}$ and $\mathcal{T}\mathcal{T}^*$, where $\mathcal{T}^*$ denotes the adjoint operator[2] of $\mathcal{T}$, are denoted by $\{\sigma_n^2\}_{n\in\mathbb{N}^*}$ with $\sigma_n > 0$, the $\{v_n\}_{n\in\mathbb{N}^*}$ are a corresponding complete orthonormal system of eigenvectors to $\mathcal{T}^*\mathcal{T}$, and $w_n = \mathcal{T}v_n/\|\mathcal{T}v_n\|$ are a complete orthonormal system of eigenvectors to $\mathcal{T}\mathcal{T}^*$. Then $(\sigma_n; v_n, w_n)$ is a singular system of the compact linear operator $\mathcal{T}$, and we have the following formulas:

$$\mathcal{T}x = \sum_{n=1}^{\infty} \sigma_n \langle x, v_n \rangle w_n, \quad x \in \mathcal{X}, \tag{1.9}$$

$$\mathcal{T}^* y = \sum_{n=1}^{\infty} \sigma_n \langle y, w_n \rangle v_n, \quad y \in \mathcal{Y}, \tag{1.10}$$

where (1.9) and (1.10) are the infinite-dimensional analogues of the SVD of a matrix, Golub & Van Loan (2012).

If $\dim \mathcal{R}(\mathcal{T}) < \infty$, $\mathcal{T}$ has only finitely many singular values, thus the infinite series (1.9) and (1.10) degenerate to finite sums, and the range $\mathcal{R}(\mathcal{T})$ is closed, which means

[1] Let $\mathcal{X}$ and $\mathcal{Y}$ be normed spaces and $\mathcal{T} : \mathcal{X} \to \mathcal{Y}$ be an operator, then $\mathcal{T}$ is a compact operator if for any bounded sequence $\{x^n\}$ in $\mathcal{X}$ the sequence $\{\mathcal{T}x^n\}$ contains a convergent subsequence in $\mathcal{Y}$.

[2] Given $\mathcal{T} : \mathcal{X} \mapsto \mathcal{Y}$ an operator, then its adjoint operator $\mathcal{T}^* : \mathcal{Y} \mapsto \mathcal{X}$ satisfies

$$\langle \mathcal{T}x, y \rangle = \langle x, \mathcal{T}^* y \rangle, \quad \forall x \in \mathcal{X}, y \in \mathcal{Y}.$$

that $\mathcal{T}$ is continuously invertible. However, if $\dim \mathcal{R}(\mathcal{T}) = \infty$, then $\lim_{n\to\infty} \sigma_n = 0$. Assuming further that $\mathcal{T} : \mathcal{D}(\mathcal{T}) \to \mathcal{R}(\mathcal{T})$ is invertible, on solving (1.7) we get that for $y \in \mathcal{R}(\mathcal{T})$

$$x = \mathcal{T}^{-1}y = \sum_{n=1}^{\infty} \frac{\langle y, w_n\rangle}{\sigma_n} v_n, \tag{1.11}$$

where $(\sigma_n; v_n, w_n)$ is a singular system of the compact linear operator $\mathcal{T}$.

Taking $y_n^\epsilon := y + \epsilon w_n$, then $\|y_n^\epsilon - y\|_{\mathcal{Y}} = \epsilon$ and using (1.11), we have

$$\mathcal{T}^{-1}y_n^\epsilon - \mathcal{T}^{-1}y = \sum_{i=1}^{\infty} \frac{\langle \epsilon w_n, w_i\rangle}{\sigma_i} v_i = \frac{\langle \epsilon w_n, w_n\rangle}{\sigma_n} v_n,$$

which implies that

$$\|\mathcal{T}^{-1}y - \mathcal{T}^{-1}y_n^\epsilon\|_{\mathcal{X}} = \frac{\epsilon}{\sigma_n} \to \infty, \quad \text{as } n \to \infty.$$

This result means that the above error can be amplified arbitrarily by the factors $\frac{1}{\sigma_n}$.

As for the nonlinear operator equation (1.7), we introduce the concept of the x_0-minimum-norm solution denoted by $x^\dagger$ of (1.7):

$$\mathcal{T}x^\dagger = y, \quad \|x^\dagger - x_0\|_{\mathcal{X}} = \min\{\|x - x_0\|_{\mathcal{X}} \mathcal{T}x = y\}, \tag{1.12}$$

where x_0 is some *a-priori* information on the solution of (1.7).

We close this subsection by highlighting a case when we can conclude that a nonlinear problem (1.7) is ill-posed. For a nonlinear, continuous and compact operator $\mathcal{T}$, suppose that $\mathcal{D}(\mathcal{T})$ is weakly closed[1]. We also assume that $\mathcal{T}x^\dagger = y$ and that there exists a $\rho > 0$ such that $\mathcal{T}x = \overline{y}$ has a unique solution for $\forall \overline{y} \in \mathcal{R}(\mathcal{T}) \cap \mathcal{B}_\rho(y)$, where $\mathcal{B}_\rho(y) := \{\overline{y} \in \mathcal{Y}; \|y - \overline{y}\|_{\mathcal{Y}} < \rho\}$ is the ball centred at y of radius ρ. If there exists a sequence $\{x^n\} \in \mathcal{D}(\mathcal{T})$ satisfying $x^n \rightharpoonup x^\dagger$ but $x^n \not\to x^\dagger$, then $\mathcal{T}^{-1}$ (defined on $\mathcal{R}(\mathcal{T}) \cap \mathcal{B}_\rho(y)$) is not continuous in y, see Proposition 10.1 of Engl *et al.* (1996). Note that if $\mathcal{D}(\mathcal{T})$ is compact and $\mathcal{T}^{-1}$ exists, then $\mathcal{T}^{-1}$ is continuous by the Arzela-Ascoli Theorem. This result implies that the nonlinear ill-posed problems can be regularized by simply restricting $\mathcal{D}(\mathcal{T})$ to a compact set, however, this usually does not yield qualitative stability estimates.

Regularization methods can be applied to overcome the difficulties arising from instability, as described in the next section.

[1]That is, for any $\{x^n\}$ in $\mathcal{D}(\mathcal{T})$, if $x^n \rightharpoonup x$ then $x \in \mathcal{D}(\mathcal{T})$.

1.4 Tikhonov's regularization

Some sort of regularization must be employed in order to retrieve the loss of stability for ill-posed problems. The Tikhonov regularization approach, see Phillips (1962); Tikhonov (1963a,b), is one of the most popular regularization procedure to deal with ill-posed inverse problems. In Engl *et al.* (1996), the Tikhonov regularization has been studied extensively for both the linear and nonlinear operator equation (1.7).

The quasi-solution to the ill-posed inverse problem (1.7) and (1.8) can be approximated by a minimizer of the Tikhonov functional given by:

$$J(x) = \|\mathcal{T}x - y^\epsilon\|_{\mathcal{Y}}^2 + \beta\|x\|_{\mathcal{X}}^2, \tag{1.13}$$

where β is a positive regularization parameter to be prescribed.

Convergence results for linear and nonlinear problems are presented in the following two sections, see further Engl *et al.* (1996).

1.4.1 Linear problems

If $\mathcal{T}$ is a linear operator, then there exists a unique minimizer x_β^ϵ of the Tikhonov functional (1.13) given by:

$$x_\beta^\epsilon = (\mathcal{T}^*\mathcal{T} + \beta\mathcal{I})^{-1}\mathcal{T}^* y^\epsilon, \tag{1.14}$$

where $\mathcal{I}$ is the identity operator. If the linear operator equation (1.7) is uniquely solvable and the regularization parameter $\beta := \beta(\epsilon)$ satisfies

$$\lim_{\epsilon\to 0}\beta(\epsilon) = 0, \quad \lim_{\epsilon\to 0}\frac{\epsilon^2}{\beta(\epsilon)} = 0, \tag{1.15}$$

then x_β^ϵ given by (1.14) tends to the solution $x = \mathcal{T}^{-1}y$ of (1.7), as $\epsilon \to 0$. It is also possible to derive convergence rates. For example, if we know a-priori that the solution x is in the range of the operator $(\mathcal{T}^*\mathcal{T})^\sigma$ for some $\sigma \in (0, 1]$ such that $x = (\mathcal{T}^*\mathcal{T})^\sigma v$ with $v \in \mathcal{X}$ and $\|v\|_{\mathcal{X}}$ sufficiently small, then choosing the regularization parameter $\beta \sim \epsilon^{2/(2\sigma+1)}$ we have the convergence rate, see Engl *et al.* (1996),

$$\|x_\beta^\epsilon - x\|_{\mathcal{X}} = O(\epsilon^{2\sigma/(2\sigma+1)}). \tag{1.16}$$

The condition that $x = (\mathcal{T}^*\mathcal{T})^\sigma v$ is called a source condition and $\mathcal{T}$ linear and compact operator can be rewritten in the form $x = \sum_{n=1}^\infty \sigma_n^{2\sigma}\langle v, v_n\rangle_{\mathcal{X}} v_n$. Equation (1.16) expresses that the convergence of x_β^ϵ to x can be arbitrary slow when σ is close to 0, and moreover it cannot be better than $O(\epsilon^{2/3})$ obtained when $\sigma = 1$.

For the linear problem, the truncated singular value decomposition (TSVD) of the linear compact operator $\mathcal{T}$, can be considered by replacing $\mathcal{T}$ with the finite-rank operator $\mathcal{T}_\beta$, given by

$$\mathcal{T}_\beta x := \sum_{n=1,\sigma_n^2\geq\beta}^{\infty} \sigma_n \langle x, v_n\rangle w_n,$$

where the positive constant β is a regularization/truncation parameter. Using (1.11) and assuming that $\mathcal{T}$ is invertible, we obtain the truncated regularized solution

$$\mathcal{T}_\beta^{-1} y = \sum_{n=1,\sigma_n^2\geq\beta}^{\infty} \frac{\langle y, w_n\rangle}{\sigma_n} v_n,$$

for exact data y and

$$x_\beta^\epsilon := \mathcal{T}_\beta^{-1} y^\epsilon = \sum_{n=1,\sigma_n^2\geq\beta}^{\infty} \frac{\langle y^\epsilon, w_n\rangle}{\sigma_n} v_n,$$

for noisy data y^ϵ. The choice of the threshold β can be based on the discrepancy principle, i.e., $\|\mathcal{T}x_\beta^\epsilon - y^\epsilon\|_{\mathcal{Y}} \leq \tau\epsilon$, $\tau \geq 1$, see Marin & Lesnic (2002).

1.4.2 Nonlinear problems

The quasi-solution to the nonlinear ill-posed inverse problem (1.7) and (1.8) can be approximated by a minimizer of the Tikhonov functional given by:

$$J(x) = \|\mathcal{T}x - y^\epsilon\|_{\mathcal{Y}}^2 + \beta\|x - x_0\|_{\mathcal{X}}^2. \tag{1.17}$$

A minimizer to the functional (1.17) is still denoted by x_β^ϵ. Let (1.15) hold. Then every sequence $\{x_{\beta^n}^{\epsilon^n}\}$, where $\epsilon^n \to 0$ as $n \to \infty$, $\beta^n := \beta(\epsilon^n)$ and $x_{\beta^n}^{\epsilon^n}$ is a solution of (1.17), has a convergent subsequence, and the limit of such subsequence is an x_0-minimum-norm solution of (1.7), see Engl *et al.* (1996). If in addition, the x_0-minimum-norm solution $x^\dagger$ is unique, then $\lim_{\epsilon\to 0} x_\beta^\epsilon = x^\dagger$.

Convergence rates can be established under stronger assumptions, as follows. Assume $\mathcal{D}(\mathcal{T}) \subset \mathcal{X}$ is convex and let $x^\dagger$ be an x_0-minimum-norm solution of (1.12). Then, if the following conditions hold:

(i) $\mathcal{T}$ is Fréchet differentiable[1];

[1]Let $\mathcal{V}$ and $\mathcal{W}$ be normed vector spaces, and $\mathcal{V}_1$ be an open subset of $\mathcal{V}$. An operator $\mathcal{T}$ is called Fréchet differentiable at point $x \in \mathcal{V}_1$, if there exists a bounded linear operator $\mathcal{U} : \mathcal{V} \mapsto \mathcal{W}$ such that

$$\lim_{\|h\|_{\mathcal{V}}\to 0} \frac{\|\mathcal{T}(x+h) - \mathcal{T}x - \mathcal{U}h\|_{\mathcal{W}}}{\|h\|_{\mathcal{V}}} = 0.$$

The operator $\mathcal{U}$ is called the Fréchet derivative of $\mathcal{T}$ at x.

(ii) there exist $M \geq 0$ such that

$$\|\mathcal{T}'(x^\dagger) - \mathcal{T}'(x)\|_{\mathcal{Y}} \leq M\|x^\dagger - x\|_{\mathcal{X}}, \quad \forall x \in \mathcal{D}(\mathcal{T}) \cap \mathcal{B}_\rho(x^\dagger) \text{ with } \rho \text{ sufficiently small;}$$

(iii) $x^\dagger$ satisfies the source condition

$$x^\dagger - x_0 = (\mathcal{T}'(x^\dagger)^*\mathcal{T}'(x^\dagger))^\sigma v$$

for some $\sigma \in [\frac{1}{2}, 1]$ and $v \in \mathcal{X}$ with $\|v\|_{\mathcal{X}} < 1/M$, then for the choice $\beta \sim \epsilon^{\frac{2}{2\sigma+1}}$, we have the convergence rate

$$\|x_\beta^\epsilon - x^\dagger\| = O(\epsilon^{\frac{2\sigma}{2\sigma+1}}). \tag{1.18}$$

1.5 Landweber's method

A regularized solution to the inverse problem (1.7) and (1.8) can also be obtained by using iterative regularization methods, e.g., the Landweber iteration method, see Engl *et al.* (1996); Hanke *et al.* (1995); Kaltenbacher *et al.* (2008); Landweber (1951). The Landweber method is given by

$$x^{n+1} = x^n + \mathcal{T}^*(y^\epsilon - \mathcal{T}x^n), \quad n = 0, 1, 2, \cdots, \tag{1.19}$$

where n denotes the number of iterations and x^0 is the initial guess.

Consider the linear operator equation (1.7) and suppose that $\|\mathcal{T}\| \leq 1$, otherwise we could introduce a relaxation parameter $0 < \gamma \leq \|\mathcal{T}\|^{-2}$, such that (1.19) becomes

$$x^{n+1} = x^n + \gamma\mathcal{T}^*(y^\epsilon - \mathcal{T}x^n), \quad n = 0, 1, 2, \cdots.$$

Thus, we can assume that $\|\mathcal{T}\| \leq 1$ and drop the parameter γ, without loss of generality.

For exact input data, i.e., $\epsilon = 0$, if $y \in \mathcal{D}(\mathcal{T}^{-1})$, then

$$\lim_{n\to\infty} x^n = \mathcal{T}^{-1}y, \tag{1.20}$$

otherwise if $y \notin \mathcal{D}(\mathcal{T}^{-1})$, then

$$\lim_{n\to\infty} \|x^n\|_{\mathcal{X}} = \infty.$$

For the noisy data y^ϵ satisfying (1.8), $x^n(\epsilon)$ obtained by (1.19) satisfies

$$\|x^n - x^n(\epsilon)\|_{\mathcal{X}} \leq \sqrt{n}\epsilon, \quad \forall n \in \mathbb{N}. \tag{1.21}$$

The behaviour of the Landweber iteration with y^ϵ can be seen by

$$\mathcal{T}^{-1}y - x^n(\epsilon) = \mathcal{T}^{-1}y - x^n + x^n - x^n(\epsilon),$$

which means that the error has two components, $\|\mathcal{T}^{-1}y - x^n\|_{\mathcal{X}}$ converging to zero from (1.20) and $\|x^n - x^n(\epsilon)\|_{\mathcal{X}}$ of the order at most $\sqrt{n}\epsilon$ from (1.21). Thus $x^n(\epsilon)$ converges to $\mathcal{T}^{-1}y$ for the first few iterations after which it diverges as $n \to \infty$, i.e., the Landweber method is semi-convergent, see Natterer (2001).

Thus, the proper stopping of the iterative algorithm plays an important regularizing role, and the Landweber method should be stopped before the iterates start to diverge. The iterative scheme can be regularized by the discrepancy principle, Morozov (1966), which terminates the Landweber method at the iteration threshold $n_* = n_*(\epsilon)$ for which

$$\|y^\epsilon - \mathcal{T}x^{n_*}\|_{\mathcal{Y}} \leq \tau\epsilon < \|y^\epsilon - \mathcal{T}x^{n_*-1}\|_{\mathcal{Y}}, \tag{1.22}$$

where $\tau \geq 1$ is a constant to be chosen. Under source conditions, convergence rates can be established, as described in Kaltenbacher *et al.* (2008).

1.6 Conjugate gradient method

The CGM was first introduced to solve finite dimensional systems of linear algebraic equations by Hestenes & Stiefel (1952), and then extended to continuous operator equations in infinite-dimensional Hilbert spaces by Patterson (1974).

We first consider the following system of linear algebraic equations

$$\mathbf{A}\mathbf{x} = \mathbf{y}, \tag{1.23}$$

for the vector $\mathbf{x} \in \mathbb{R}^{\mathrm{d}}$, where the vector $\mathbf{y} \in \mathbb{R}^{\mathrm{d}}$ is known and $\mathbf{A} \in \mathbb{R}^{\mathrm{d}\times\mathrm{d}}$ is a symmetric and positive definite matrix, i.e. $\mathbf{A}^{\mathrm{T}} = \mathbf{A}$ and $\mathbf{x}^{\mathrm{T}}\mathbf{A}\mathbf{x} > 0$ for all $\mathbf{x} \in \mathbb{R}^{\mathrm{d}} \setminus \{\mathbf{0}\}$.

The CGM for solving (1.23) is given by:

$$\begin{cases} \mathbf{d}^0 = \mathbf{r}^0 = \mathbf{y} - \mathbf{A}\mathbf{x}^0, & & \\ \mathbf{x}^{n+1} = \mathbf{x}^n + \beta^n\mathbf{d}^n, & \beta^n = \frac{|\mathbf{r}^n|^2}{(\mathbf{d}^n)^{\mathrm{T}}\mathbf{A}\mathbf{d}^n}, & n = 0, 1, 2, \cdots, \\ \mathbf{d}^n = \mathbf{r}^n + \gamma^n\mathbf{d}^{n-1}, & \mathbf{r}^n = \mathbf{r}^{n-1} - \beta^{n-1}\mathbf{A}\mathbf{d}^{n-1}, & n = 1, 2, \cdots, \\ \gamma^n = \frac{|\mathbf{r}^n|^2}{|\mathbf{r}^{n-1}|^2}, & & n = 1, 2, \cdots, \end{cases} \tag{1.24}$$

where n denotes the iteration number, $\mathbf{x}^0$ is the initial guess of the solution, $\mathbf{r}^n$ is the residual and the vectors $\mathbf{d}^n$ form a set of conjugate, or A-orthogonal, directions, i.e. $(\mathbf{d}^n)^{\mathrm{T}}\mathbf{A}\mathbf{d}^m = 0$ for all $m \neq n$. The convergence results and stability analysis of the method (1.24) are given in Hestenes & Stiefel (1952).

Note that the unique solution to the equation (1.23) is also the unique minimizer of the following quadratic function

$$f(\mathbf{x}) = \frac{1}{2}\mathbf{x}^{\mathrm{T}}\mathbf{A}\mathbf{x} - \mathbf{x}^{\mathrm{T}}\mathbf{y}, \quad \mathbf{x} \in \mathbb{R}^{\mathrm{d}}. \tag{1.25}$$

The first derivative of (1.25), $f'(\mathbf{x}) = \mathbf{A}\mathbf{x} - \mathbf{y}$, satisfies $f'(\mathbf{x}^n) = -\mathbf{r}^n$. Thus, the CGM given by (1.24) can be written as

$$\begin{cases} \mathbf{x}^{n+1} = \mathbf{x}^n + \beta^n \mathbf{d}^n, & n = 0, 1, 2, \cdots, \\ \mathbf{d}^0 = -f'(\mathbf{x}^0), & \\ \mathbf{d}^n = -f'(\mathbf{x}^n) + \gamma^n \mathbf{d}^{n-1}, & n = 1, 2, \cdots, \end{cases} \tag{1.26}$$

and β^n, γ^n can be computed using $f'(\mathbf{x}^n)$.

The CGM presented above can be naturally extended to the minimization of non-linear functions. For instance, it can be applied to the inverse operator problem (1.7) with the noisy data (1.8), whose solutions minimize the least-squares objective functional given by

$$J(x) = \frac{1}{2}\|\mathcal{T}x - y^\epsilon\|_y^2. \tag{1.27}$$

Using the algorithm (1.26), we can establish the CGM, which can be applied to reconstruct the minimizer of the optimization problem (1.27), given by:

$$\begin{cases} x^{n+1} = x^n + \beta^n d^n, & n = 0, 1, 2, \cdots, \\ d^0 = -s^0, & \\ d^n = -s^n + \gamma^n d^{n-1}, & n = 1, 2, \cdots, \end{cases} \tag{1.28}$$

where $s^n = J'^n = J'(x^n)$ is the Fréchet gradient of (1.27) at the point x^n. Note that the objective functional $J(x)$ given by (1.27) is Fréchet differentiable when the operator $\mathcal{T}$ is Fréchet differentiable, and its gradient is given by:

$$s^n = J'(x^n) = \mathcal{T}'(x^n)^*(\mathcal{T}(x^n) - y^\epsilon),$$

which means that the method (1.28) can be written as

$$\begin{cases} x^{n+1} = x^n + \beta^n d^n, & n = 0, 1, 2, \cdots, \\ d^0 = -s^0, \quad s^0 = \mathcal{T}'(x^0)^*(\mathcal{T}(x^0) - y^\epsilon), & \\ d^n = -s^n + \gamma^n d^{n-1}, \quad s^n = \mathcal{T}'(x^n)^*(\mathcal{T}(x^n) - y^\epsilon), & n = 1, 2, \cdots, \end{cases} \tag{1.29}$$

where x^0 is the initial guess, β^n is the search step size in passing from iteration n to iteration $n+1$, d^n is the direction of descent, γ^n is the conjugate coefficient, and $\mathcal{T}'(x^n)$ is the Fréchet gradient of $\mathcal{T}$ at the point x^n. Note that various choices of β^n and γ^n yield different iterative methods:

- Landweber iteration method, for $\beta^n = 1$ and $\gamma^n = 0$, see Section 1.5;
- Steepest descent method, for $\beta^n = \frac{\|d^n\|^2}{\|\mathcal{T}'(x^n)d^n\|^2}$ and $\gamma^n = 0$, Eicke *et al.* (1990); Kaltenbacher *et al.* (2008); Neubauer & Scherzer (1995);

- CGM, for $\beta^n \neq 0$, $\gamma^n \neq 0$ depending on n, $(x^i)_{i=\overline{0,n}}$ and y^ϵ.

In addition, there are many choices for the conjugate coefficient γ^n as shown in Table 1.1. Note that Powell (1977) introduced the so-called Powell-Beales version of the CGM with the search direction d^n given by

$$d^n = \begin{cases} -s^0, \\ -s^n + \gamma^n d^{n-1} + \psi^n d^p, \quad n = 1, 2, \cdots \end{cases} \tag{1.30}$$

where the superscript p in (1.30) denotes the iteration number where a restarting strategy is applied to the CGM, and γ^n and ψ^n are the conjugation coefficients given by

$$\gamma^n = \frac{\langle s^n, s^n - s^{n-1} \rangle}{\langle d^{n-1}, s^n - s^{n-1} \rangle}, \quad n = 1, 2, \cdots \tag{1.31}$$

$$\psi^n = \frac{\langle s^n, s^n - s^{n-1} \rangle}{\langle d^p, s^{p+1} - s^p \rangle}, \quad n = 1, 2, \cdots \tag{1.32}$$

According to Powell (1977), the application of the CGM with the conjugation coefficients given by (1.31) and (1.32) requires restarting when gradients s^n at successive iterations n tend to be non-orthogonal and when the search direction is not sufficiently downhill. The non-orthogonality of gradients at successive iterations is tested by

$$\left| \langle s^{n-1}, s^n \rangle \right| \geq 0.2 \|s^n\|^2, \tag{1.33}$$

and the non-sufficiently downhill search direction (i.e., the angle between the search direction and the negative gradient direction is too large) is identified if either of the following inequalities is satisfied

$$\langle d^n, s^n \rangle \leq -1.2 \|s^n\|^2, \tag{1.34}$$

or

$$\langle d^n, s^n \rangle \geq -0.8 \|s^n\|^2, \tag{1.35}$$

where the vales 0.2, -1.2 and -0.8 in (1.33)–(1.35) are empirical obtained by Powell (1977). Thus, d^n can be computed using the following algorithm, Colaço & Orlande (1999); Colaço *et al.* (2006); Powell (1977):

S1. Test the inequality (1.33), set $p = n - 1$ if it is true.

S2. Compute the conjugate gradient coefficient γ^n by (1.31).

S3. If $n = p + 1$ set the conjugate gradient coefficient $\psi^n = 0$, else compute the coefficient ψ^n with (1.32).

S4. Compute the search direction d^n by (1.30).

S5. If $n \neq p+1$ test the inequalities (1.34) and (1.35). If either one of them is satisfied set $p = n-1$ and $\psi^n = 0$. Then recompute the search direction d^n by (1.30).

$\gamma^n_{\mathrm{HS}} = \frac{\langle s^n, s^n - s^{n-1}\rangle}{\langle d^{n-1}, s^n - s^{n-1}\rangle}$	Hestenes & Stiefel (1952)
$\gamma^n_{\mathrm{FR}} = \frac{\|s^n\|^2}{\|s^{n-1}\|^2}$	Fletcher & Reeves (1964)
$\gamma^n_{\mathrm{PRP}} = \frac{\langle s^n, s^n - s^{n-1}\rangle}{\|s^{n-1}\|^2}$	Polak & Ribiere (1969)
$\gamma^n_{\mathrm{CD}} = -\frac{\|s^n\|^2}{\langle d^{n-1}, s^{n-1}\rangle}$	Fletcher (2013)
$\gamma^n_{\mathrm{LS}} = -\frac{\langle s^n, s^n - s^{n-1}\rangle}{\langle d^{n-1}, s^{n-1}\rangle}$	Liu & Storey (1991)
$\gamma^n_{\mathrm{DY}} = \frac{\|s^n\|^2}{\langle d^{n-1}, s^n - s^{n-1}\rangle}$	Dai & Yuan (1999)

Table 1.1: Several expressions for the conjugate coefficient γ^n.

The convergence and convergence rates of CGM (1.29) with the conjugate coefficient γ^n_{FR} given by Fletcher-Reeves formula in Table 1.1 for linear ill-posed inverse problems were investigated by Engl *et al.* (1996); Hanke (1995). For exact data, i.e. $\epsilon = 0$, x^n given by (1.29) converges to $\mathcal{T}^{-1}y$ of the linear problem (1.7) for all $y \in \mathcal{D}(\mathcal{T}^{-1}) = \mathcal{R}(\mathcal{T})$. For nosiy data y^ϵ, $\epsilon > 0$, the CGM is semi-convergent and should be stopped according to the discrepancy principle (1.22). Suppose that the linear ill-posed problem (1.7) and (1.8) is uniquely solvable and the CGM (1.29) is stopped according to the discrepancy principle (1.22) with $n_* = n_*(\epsilon)$. If $x - x^0 = (\mathcal{T}^*\mathcal{T})^\sigma v$, where $\sigma > 0$ and $\|v\|_{\mathcal{X}}$ is sufficiently small, see Engl *et al.* (1996), then

$$\|\mathcal{T}^{-1}y - x^{n_*}\|_{\mathcal{X}} = O(\epsilon^{\frac{2\sigma}{2\sigma+1}}), \quad \text{and } n_* = O(\epsilon^{-\frac{1}{2\sigma+1}}). \tag{1.36}$$

For nonlinear ill-posed problems a similar CGM (1.29) can be used to find the approximate solution, but convergence results are still open to be established, see Scherzer (1996).

1.6.1 Global convergence

Now, we consider the unconstrained minimization for a smooth function $J(\mathbf{x})$ of $\mathbf{x} \in \mathbb{R}^{\mathrm{d}}$, $\mathrm{d} \geq 1$, i.e., $\min_{\mathbf{x}\in\mathbb{R}^{\mathrm{d}}} J(\mathbf{x})$. For example, we can have $J(\mathbf{x})$ as a Tikhonov functional for the problem (1.23). CGMs are useful for minimizing $J(\mathbf{x})$, especially for large d, and are given by

$$\begin{cases} \mathbf{x}^{n+1} = \mathbf{x}^n + \beta^n \mathbf{d}^n, & n = 0, 1, 2, \cdots, \\ \mathbf{d}^0 = -J'^0, & \\ \mathbf{d}^n = -J'^n + \gamma^n \mathbf{d}^{n-1}, & n = 1, 2, \cdots, \end{cases} \tag{1.37}$$

where $J'^n = J'(\mathbf{x}^n)$ is the Fréchet gradient of $J(\mathbf{x})$ at the point $\mathbf{x}^n$. The global convergence of the CGM (1.37) is understood in the following sense:

$$\liminf_{n\to\infty} \|J'^n\| = 0. \tag{1.38}$$

Different choices of the conjugate coefficient γ^n, such as FR, PRP and HS formulae described in Table 1.1, yield different formulations of CGM. The non-negative step size β^n can be obtained by a line search for solving

$$\min_{\beta_c \geq 0} J(\mathbf{x}^n + \beta_c \mathbf{d}^n).$$

Some line search strategies for choosing suitable search step size β^n in the direction $\mathbf{d}^n$ satisfying the descent condition $\langle J'^n, \mathbf{d}^n \rangle < 0$, are as follows, see Schopfer (2016):

- Wolfe conditions: Let $0 < \sigma_1 < \sigma_2 < 1$ and choose β^n such that

$$\begin{cases} J(\mathbf{x}^{n+1}) - J(\mathbf{x}^n) \leq \sigma_1 \beta^n \langle J'^n, \mathbf{d}^n \rangle, \\ \langle J'^{n+1}, \mathbf{d}^n \rangle \geq \sigma_2 \langle J'^n, \mathbf{d}^n \rangle. \end{cases}$$

- Backtracking: Let $\sigma \in (0, 1)$ and $0 < \tau_1 < \tau_2 < 1$. If $\beta_c = 1$ satisfies

$$J(\mathbf{x}^n + \beta_c \mathbf{d}^n) - J(\mathbf{x}^n) \leq \sigma \langle J'^n, \mathbf{d}^n \rangle,$$

  then set $\beta^n = \beta_c$. Otherwise, choose a new $\beta_c \in [\tau_1 \beta_c, \tau_2 \beta_c]$ and repeat the test.

- Exact line search: Calculate β_c with $\langle J'(\mathbf{x}^n + \beta_c \mathbf{d}^n), \mathbf{d}^n \rangle = 0$ and set $\beta^n = \beta_c$.

The convergence analysis of the CGM requires a Lipschitz assumption given by: In some neighbourhood $\mathcal{A}$ of

$$\mathfrak{L} = \{\mathbf{x} \in \mathbb{R}^{\mathrm{d}} | J(\mathbf{x}) \leq J(\mathbf{x}^0)\},$$

the Fréchet gradient $J'(\mathbf{x})$ is Lipschitz continuous, i.e., there exists $L > 0$ such that

$$\|J'(\mathbf{x}_1) - J'(\mathbf{x}_2)\| \leq L \|\mathbf{x}_1 - \mathbf{x}_2\|, \quad \forall \mathbf{x}_1, \mathbf{x}_2 \in \mathcal{A}.$$

Consider the CGM (1.37) together with the direction $\mathbf{d}^n$ satisfying the descent condition and the search step size β^n satisfying the Wolfe conditions. Then, if the above Lipschitz condition holds, the CGM converges globally in the sense of (1.38), see Hager & Zhang (2006); Schopfer (2016).

1.6.2 Application of CGM to IHTPs

Throughout this thesis, the quasi-solutions to the IHTPs will be approximated by the minimizer of the least-squares objective functional, e.g., for the inverse problem (1.1) and (1.3) to reconstruct the unknown function, $k(x)$ is given by:

$$J(k) = \frac{1}{2}\|u(\cdot,\cdot;k) - Y\|^2_{L_2((0,1)\times(0,T))}.$$

Clearly, the Fréchet gradient $J'(k)$ is essential, and such gradient can be obtained from an auxiliary problem known as the adjoint problem. In fact, a variational method can be used to obtain the Fréchet gradient together with the adjoint problem. Many types of conjugate coefficient γ^n have been described in the above section, and the FR and PRP formulae are commonly utilized in the CGM for IHTPs. The search step size β^n can be determined by the Taylor series expansion and the sensitivity problem, which describes the perturbed temperature from the perturbation of the unknown quantity.

In summary, the CGM regularized by the discrepancy principle is based on the direct problem, the sensitivity problem, the adjoint problem, the Fréchet gradient, the iterative algorithm and the stopping criterion, Özişik & Orlande (2000). The procedure of the CGM for IHTP starts with an initial guess $n = 0$, e.g., k^0, for the unknown coefficient. Then the direct problem is solved with such initial guess in order to obtain the value of the objective functional. The adjoint problem and the Fréchet gradient are solved to determine the conjugate gradient coefficient γ^n and the search direction d^n. We then solve the sensitivity problem to compute the step size β^n, and update k^{n+1} by (1.37). Finally, the iteration is stopped when the discrepancy principle is satisfied.

The analysis of the global convergence of the CGM to IHTPs is interesting and novel. In such case, the conjugate gradient coefficient γ^n_{FR} given by FR formula is used in the iterative scheme and the exact line search method is applied to attain the step size β^n. Since the adjoint problem and the gradient can be expressed explicitly, the Lipschitz continuity of such gradient may be obtained from classical arguments described in Dai & Yuan (1996, 1999); Wolfe (1969); Zoutendijk (1970).

Finally, we present the general framework to reconstruct one or more unknown coefficients of the IHTPs by using the CGM, as follows:

1. Given the mathematical formulation of the direct heat transfer problem, define its weak solution, and present the well-posedness of the direct problem when all the coefficients and initial-boundary conditions are given;

2. State one or more unknown coefficients of the heat transfer problem, and give the temperature measurement, such as the interior measured temperature, the final temperature observation or the time-average temperature measurement. In addition, such information usually contains noise. Then, the inverse problem is to reconstruct the unknown coefficients from such measured temperature, and the problem is ill-posed;

3. Define a least-squares objective functional which is the gap between the computed and the measured temperatures. Here, the computed temperature is the weak solution to the heat transfer problem corresponding to the particular values of the unknown coefficients;

4. The solution of the inverse problem can be approximated by the minimizer of the objective functional, i.e. the inverse problem is transformed into an optimization problem. Then, based on the arguments of functional analysis, the existence of the minimizer to the optimization problem can be proved. Using the variational method, the Fréchet gradient of the objective functional and the adjoint problem can be obtained;

5. The CGM can be established using the gradient of the objective function, and the iteration process has been described above. Since the inverse problem is ill-posed, CGM regularized by the discrepancy principle can be used to obtain a stable numerical solution to the inverse problem;

6. Use the CGM to numerically reconstruct the minimizer of the objective functional, then such solution is also the numerical solution to the inverse problem. Thus, this method can be used to numerically estimate one or more coefficients from temperature measurements containing various level of noise.

1.7 Purpose and outline of the thesis

The identification of the unknown space-dependent thermal conductivity from various types of additional information was considered analytically by Cannon & DuChateau (1974); Cannon & Jones (1963); Cannon *et al.* (1963); Kohn & Vogelius (1984, 1985); Kravaris & Seinfeld (1986). The numerical estimation of the thermal conductivity was also investigated, when the unknown thermal conductivity is assumed to be a constant, Beck & Al-Araji (1974), space-dependent using CGM, Colaço *et al.* (2006); Huang &

Özişik (1990, 1991), time- and space-dependent, Huang & Chin (2000), and temperature-dependent, Colaço & Orlande (1999); Özişik & Orlande (2000); Tervola (1989).

The simultaneous reconstruction of the constant anisotropic thermal conductivity tensor was investigated by Harris *et al.* (2008); Sawaf & Özisik (1995); Thomas *et al.* (2010), but there is still no numerical estimation of the space-dependent thermal conductivity for an orthotropic material.

The identification of the reaction coefficient was investigated mainly theoretically, when is space-dependent, Gel'fand & Levitan (1951); Isakov (1991); Kamynin & Kostin (2010); Kozhanov (2004); Pierce (1979); Prilepko & Kostin (1993); Prilepko & Solovev (1987); Rundell (1987); Suzuki (1983), time-dependent, Cannon & Lin (1990); Cannon & Yin (1990); Cannon *et al.* (1992); Dehghan (2005); Trucu *et al.* (2008), time- and space-dependent, Deng *et al.* (2008, 2010), and temperature-dependent, Trucu *et al.* (2010a). Meanwhile, there were many works on the numerical reconstruction of the unknown reaction coefficient using FDM or FEM by Cao & Lesnic (2018a); Chen & Liu (2006); Trucu *et al.* (2008, 2010b, 2011), with regularization, but the CGM has not been applied yet for the estimation of the reaction coefficient from final or integral observation.

According to the above literature research, this thesis aims to fill in the gaps on the numerical solution for space-dependent thermal conductivity and reaction coefficient in one and two-dimensions using CGM, which model real phenomena such as heat conduction, melting or cooling process, blood perfusion, etc. Meanwhile, the simultaneous determination of the reaction coefficient and initial temperature will be numerically reconstructed using CGM from temperature observations. Finally, the reaction coefficient, initial temperature and some component of the source term shall also be recovered simultaneously by the CGM.

For all the IHTPs considered in this thesis, they are first transformed into optimization problems by the least-squares objective functional, then the quasi-solutions to IHTPs are approximated by the minimizers of these optimization problems. We prove the existence of the minimizer to each optimization problem using basic arguments of functional analysis. A variational method is utilized to obtain the Fréchet gradient of the objective functional, and the adjoint problem is also derived. Then we establish the CGM by the steps described in the previous section to reconstruct the unknown function(s). Several numerical examples for each IHTPs are calculated using the CGM and FDM, and stable and reasonably accurate solutions are also presented.

The reconstruction of the space-dependent thermal conductivity of an isotropic material from interior temperature observations is investigated in Chapter 2. The CGM is

established using the Fréchet gradient of the objective functional together with the adjoint and sensitivity problems. The Sobolev gradient is introduced in order to obtain smoother and more accurate numerical results. Three numerical examples for one- and two-dimensional inverse problems are presented and discussed.

In Chapter 3, the determination of the space-dependent thermal conductivity in a two-dimensional orthotropic material from the temperature observations is investigated using the similar approaches applied in Chapter 2. The numerical results obtained by the regular gradient and the Sobolev gradient are compared.

The simultaneous reconstruction of the space-dependent thermal conductivity and the reaction coefficient of an isotropic material is investigated in Chapter 4 from interior temperature observations. Three numerical examples are illustrated and discussed for one- and two-dimensional inverse problems.

The space-dependent reaction coefficient is identified from the final and/or integral observation in Chapter 5. Uniqueness of solution holds but continuous dependence on the input data is violated. This is the first time that the CGM is applied to solve the inverse problems under investigation. Three examples are investigated to verify the accuracy and stability of the numerical method.

In Chapter 6, the space-dependent reaction coefficient and the initial temperature are simultaneously identified from temperature observations at two distinct time instants. The numerical reconstruction process is based on the CGM regularized by the discrepancy principle. Accurate and stable numerical solutions are obtained for three examples.

The inverse problem investigated in Chapter 7 is to determine the same coefficients considered in Chapter 6 but from the integral temperature observations generated by two linearly independent time-dependent weight functions. The CGM is established similar to that of Chapter 6. The new part is the consideration of the global convergence of the CGM under the Lipschitz continuity property of the Fréchet gradient. In three numerical examples, the global convergence of CGM, and stable and accurate numerical solutions are presented.

In Chapter 8, the space-dependent reaction coefficient, initial temperature and one space-dependent component of the heat source are simultaneously reconstructed from the measured temperatures at three different time instants. Using the same methods of the previous chapters, the CGM can be established and used to obtain the numerical solutions of the three unknown quantities.

Finally, in Chapter 9, general conclusions and suggestions for possible future work are highlighted.

Chapter 2

Determination of the space-dependent thermal conductivity of an isotropic material

2.1 Introduction

The estimation of the thermal conductivity is very important in many heat transfer applications, see Alifanov & Tryanin (1985), e.g. in the cooling of continuously cast slabs and electronic chips, see Hibbins (1982); Orlande *et al.* (1997); Stewart *et al.* (1996).

The recent research about the space-dependent thermal conductivity identification has been reviewed in Section 1.7. Although the determination of the space-dependent thermal conductivity from temperature measurements has already been numerically attempted by Colaço *et al.* (2006); Huang & Özişik (1990, 1991) using the CGM, there is still need to be put on a firm mathematical solid basis, as described in this chapter. In particular, a variational framework is set up to rigorously establish the CGM. Moreover, the Sobolev gradient is utilized to improve the accuracy of the standard CGM.

The plan of the chapter is as follows. First, some preliminary notation is introduced in Section 2.2. In Section 2.3, the mathematical formulation of the IHTP that is investigated is given. Analysis is performed in Section 2.4 and the CGM is introduced in Section 2.5. Section 2.6 discusses the numerical schemes discretisation given by the Crank-Nicolson (C-N) scheme for one-dimensional problems and the alternating direction implicit (ADI) scheme for two-dimensional problems. Three numerical examples for one- and two-dimensional inverse problems are discussed, and stable and accurate numerical solutions are illustrated. Finally, conclusions are highlighted in Section 2.7.

2.2 Preliminaries and notations

In this section we give some notations on functional spaces from Isakov (2006); Ladyzhenskaia *et al.* (1968); Tröltzsch (2010). We denote by $\Omega \subset \mathbb{R}^{\mathrm{d}}$, $\mathrm{d} \geq 1$, a bounded domain with boundary $\partial\Omega$. The boundary $\partial\Omega$ is Lipschitz if it can be thought of as locally being the graph of a Lipschitz continuous function. We denote by $Q_T = \Omega \times (0,T)$ and $S_T = \partial\Omega \times (0,T)$ the lateral boundary of Q_T.

The space $L_p(\Omega)$, $p \in [1,\infty)$, consists of all p-integrable functions $u(x)$ over Ω, equipped with the norm

$$\|u\|_{L_p(\Omega)} = \left\{ \int_\Omega |u(x)|^p dx \right\}^{1/p}.$$

For $p = 2$, $L_2(\Omega)$ is a Hilbert space with the inner product defined by

$$\langle u, v \rangle_{L_2(\Omega)} = \int_\Omega u(x)v(x)dx, \quad \forall u, v \in L_2(\Omega).$$

The space $L_\infty(\Omega)$ comprises all essentially bounded functions $u(x)$ in Ω, endowed with the norm

$$\|u\|_{L_\infty(\Omega)} = \operatorname{ess\,sup}_{x\in\Omega} |u(x)| = \inf\{M \geq 0; |u(x)| \leq M, \text{a.e. } x \in \Omega\}.$$

The spaces $L_p(Q_T)$ and $L_\infty(Q_T)$ can be defined similarly.

The Sobolev space $H^m(\Omega)$, $m \in \mathbb{N}$, is defined by

$$H^m(\Omega) = \left\{ u \in L_2(\Omega) : D_x^j u \in L_2(\Omega) \text{ with } |j| \leq m \right\}$$

equipped with the norm

$$\|u\|_{H^m(\Omega)} = \left\{ \sum_{|j|\leq m} \|D_x^j u\|^2_{L_2(\Omega)} \right\}^{1/2},$$

where $j = (j_1, \ldots, j_d)$ is a multi-index, $j_i \geq 0$, $i = \overline{1,d}$, $|j| = \sum_{i=1}^d j_i$ and $D_x^j u = \frac{\partial^{|j|} u}{\partial x_1^{j_1} \cdots \partial x_d^{j_d}}$. For $m = 2$, with the inner product $\langle u, v \rangle_{H^1(\Omega)} = \int_\Omega (uv + \nabla u \cdot \nabla v) dx$, the space $H^1(\Omega)$ becomes a Hilbert space.

We denote by $H^{1,0}(Q_T)$ the normed space of all functions $u(x,t) \in L_2(Q_T)$ having first-order derivatives with respect to x in $L_2(Q_T)$ endowed with the norm

$$\|u\|_{H^{1,0}(Q_T)} = \left\{ \sum_{|j|\leq 1} \|D_x^j u\|^2_{L_2(Q_T)} \right\}^{1/2}.$$

The Sobolev space $H^{m,1}(Q_T)$ is defined as a Banach space of all functions u belonging to $L_2(Q_T)$ along with their space dependent partial derivatives up to the mth-order and the first-order time derivative. The norm in this space is defined by

$$\|u\|_{H^{m,1}(Q_T)} = \left\{ \sum_{|j|\leq m} \|D_x^j u\|^2_{L_2(Q_T)} + \left\| \frac{\partial u}{\partial t} \right\|^2_{L_2(Q_T)} \right\}^{1/2}.$$

The space $C([0,T]; L_2(\Omega))$ consists of all functions $u(x,t)$ that are square integrable with respect to $x \in \Omega$ for every $t \in [0,T]$, and continuous in t with respect to the norm of $L_2(\Omega)$, i.e.,

$$\lim_{\Delta t \to 0} \|u(\cdot, t+\Delta t) - u(\cdot, t)\|_{L_2(\Omega)} = 0.$$

The norm of such space is given by

$$\|u\|_{C([0,T];L_2(\Omega))} = \max_{t\in[0,T]} \|u(\cdot,t)\|_{L_2(\Omega)}.$$

We denote by $V_2^{1,0}(Q_T)$ the space $H^{1,0}(Q_T) \cap C([0,T]; L_2(\Omega))$, equipped with the norm

$$\|u\|_{V_2^{1,0}(Q_T)} = \max_{t\in[0,T]} \|u(\cdot,t)\|_{L_2(\Omega)} + \|\nabla u\|_{L_2(Q_T)}.$$

The space $C^m(\Omega)$ is the set of all continuous functions $u(x)$ in Ω having continuous derivatives up to order m in Ω, equipped with the norm

$$\|u\|_{C^m(\Omega)} = \sum_{|j|\leq m} \sup_{\Omega} |D_x^j u|.$$

The Hölder space $C^l(\Omega)$, $l \in (0,1)$ is the set of all continuous functions $u(x)$ in Ω which are Hölder continuous with exponent l, equipped with the norm

$$\|u\|_{C^l(\Omega)} = \sup_{\Omega} |u| + \sup_{x,x'\in\Omega} \frac{|u(x) - u(x')|}{|x-x'|^l}.$$

The Hölder space $C^{m+l}(\Omega)$ is the set of all continuous functions $u(x)$ in Ω satisfying $D_x^j u \in C^l(\Omega)$ for $|j| \leq m$, equipped with the norm

$$\|u\|_{C^{m+l}(\Omega)} = \sum_{|j|\leq m} \|D_x^j u\|_{C^l(\Omega)}.$$

The Hölder space $C^{l,l/2}(Q_T)$ is a Banach space of all functions $u(x,t)$ that are continuous on Q_T, which are Hölder continuous on x and t with exponents l and $l/2$, respectively. The norm on the space is defined by

$$\begin{aligned}\|u\|_{C^{l,l/2}(Q_T)} = &\sup_{Q_T} |u| + \sup_{(x,t),(x',t)\in Q_T} \frac{|u(x,t) - u(x',t)|}{|x-x'|^l} \\ &+ \sup_{(x,t),(x,t')\in Q_T} \frac{|u(x,t) - u(x,t')|}{|t-t'|^{l/2}}.\end{aligned}$$

We denote by $C^{m+l,(m+l)/2}(Q_T)$ the Banach space of functions $u(x,t)$ that are continuous in Q_T with $D_t^r D_x^j u \in C^{l,l/2}(Q_T)$ for $0 \leq 2r+|j| \leq m$, equipped with the norm

$$\|u\|_{C^{m+l,(m+l)/2}(Q_T)} = \sum_{2r+|j|\leq m} \|D_t^r D_x^j u\|_{C^{l,l/2}(Q_T)}.$$

2.3 Mathematical formulation

In this section, we consider the heat transfer problem in the bounded domain $\Omega \subset \mathbb{R}^{\mathrm{d}}$, $\mathrm{d} = 1,2,3$ for an isotropic material, from the initial time $t = 0$ to the given final time $t = T$, governed by the following mathematical model:

$$\begin{cases} \frac{\partial u}{\partial t} = \nabla \cdot (k(x)\nabla u) - q(x)u + f(x,t), & (x,t) \in Q_T, \\ k(x)\frac{\partial u}{\partial \nu} = \mu(x,t), \quad (x,t) \in S_T, \quad u(x,0) = \phi(x), & x \in \overline{\Omega}, \end{cases} \tag{2.1}$$

where $k(x) > 0$ is the thermal conductivity, $u(x,t)$ is the temperature, $q(x)$ is the reaction coefficient, $f(x,t)$ is the heat source, $\mu(x,t)$ is the heat flux, ν is the outward unit normal to the boundary $\partial\Omega$ and $\phi(x)$ is the initial temperature at $t = 0$. For simplicity, the heat capacity has been assumed constant and taken to be unity. Note that the Dirichlet, Robin or mixed boundary conditions can be prescribed instead of the Neumann boundary condition in (2.1).

The direct problem is concerned with the determination of the temperature field $u(x,t)$ in Q_T, when the thermal coefficients $k(x)$, $q(x)$, the heat source $f(x,t)$, the heat flux $\mu(x,t)$ and the initial temperature $\phi(x)$ are given. In such case, the problem (2.1) defines a well-posed process, i.e., the solution $u(x,t)$ to (2.1) is well-defined.

Definition 2.3.1. *A function $u(x,t) \in H^{1,0}(Q_T)$ is called as a weak solution to the initial-boundary value problem (2.1) if*

$$\begin{aligned} &\int_{Q_T} \left(-u\frac{\partial \eta}{\partial t} + k\nabla u \cdot \nabla \eta + qu\eta \right) dxdt \\ &= \int_{Q_T} f\eta dxdt + \int_{S_T} \mu\eta dsdt + \int_{\Omega} \phi\eta(\cdot,0)dx, \quad \forall \eta \in H^{1,1}(Q_T),\ \eta(\cdot,T) = 0. \end{aligned} \tag{2.2}$$

Note that we define the weak solution (2.2) in $H^{1,0}(Q_T)$ to the problem (2.1) rather than in $H^{1,1}(Q_T)$, since not only the result presented in Theorem 2.3.2 can be obtained, but also we shall carry out the mathematical analysis in $H^{1,0}(Q_T)$ in Section 2.4.

The existence and uniqueness of the weak solution $u \in H^{1,0}(Q_T)$ to the initial-boundary value problem (2.1) is presented in the following theorem (Tröltzsch (2010), p.373).

Theorem 2.3.2. *Let $\Omega \subset \mathbb{R}^{\mathrm{d}}$ be a bounded domain with a Lipschitz boundary $\partial\Omega$, and suppose that the functions $q \in L_\infty(\Omega)$, $f \in L_2(Q_T)$, $\mu \in L_2(S_T)$, $\phi \in L_2(\Omega)$ and $0 < k \in L_\infty(\Omega)$. Then the initial-boundary value problem (2.1) has a unique weak solution $u \in H^{1,0}(Q_T)$. Moreover, the solution satisfies the estimate*

$$\max_{t\in[0,T]} \|u(\cdot,t)\|_{L_2(\Omega)} + \|u\|_{H^{1,0}(Q_T)} \leq c\left(\|f\|_{L_2(Q_T)} + \|\mu\|_{L_2(S_T)} + \|\phi\|_{L_2(\Omega)}\right) \tag{2.3}$$

with a positive constant c which is independent of f, μ and ϕ.

The inverse problem, conversely, is concerned with the estimation of the unknown space-dependent thermal conductivity $k(x)$ using the measured temperature

$$u(x,t) = Y(x,t), \quad (x,t) \in Q_T, \tag{2.4}$$

where $Y(x,t)$ is given exact data. Note that at the steady-state, i.e. when all quantities in (2.1) and (2.4) are independent of time, the inverse problem was considered both analytically and numerically by Richter (1981a,b), respectively.

2.4 Analysis

Let $u(x,t;k)$ denote the solution of the initial-boundary value problem (2.1), that is, the temperature corresponding to conductivity function $k(x)$. The quasi-solution of the inverse problem (2.1) and (2.4) is obtained by minimizing the least-squares objective functional given by

$$J(k) = \frac{1}{2}\|u(k) - Y^\epsilon\|^2_{L_2(Q_T)}, \tag{2.5}$$

where we denote $u(k) = u(\cdot,\cdot;k)$, and $Y^\epsilon \in L_2(Q_T)$ represents the noisy measured temperature which satisfies

$$\|Y^\epsilon - Y\|_{L_2(Q_T)} \leq \epsilon, \tag{2.6}$$

and $\epsilon \geq 0$ represents the noise level, subject to $u \in H^{1,0}(Q_T)$ satisfying the (2.2), over the admissible set $\mathcal{A} = \{k \in L_\infty(\Omega) : 0 < \kappa_1 \leq k(x) \leq \kappa_2, \text{a.e. } x \in \Omega\}$, where κ_1 and κ_2 are given positive constants.

Penalizing (2.5) with a regularization parameter $\beta > 0$ we obtain the Tikhonov regularization, Engl *et al.* (1996),

$$J_1(k) = J(k) + \beta\|k - k^*\|^2_{L_2(\Omega)},$$

or the total variation (TV) regularization, Chen & Zou (1999),

$$J_2(k) = J(k) + \beta\int_\Omega |\nabla k| dx,$$

where k^* is an *a-priori* information on k.

Following the approach of Keung & Zou (1998) and using the variational principle in Zeidler (1995), the existence of a minimizer for the objective functional (2.5), over the the admissible set $\mathcal{A}$, can be established as follows.

Theorem 2.4.1. *A minimizer* $k^* = \arg\inf_{k\in\mathcal{A}} J(k)$ *exists.*

Proof. Since $\|u(x,t;k)\|_{L_2(Q_T)}$ is bounded by the *a-priori* estimate (2.3), it is obvious that $\min J(k)$ is finite over the admissible set $\mathcal{A}$ by the definition (2.5). Thus, there exists a minimizing sequence $\{k^n : n \in \mathbb{N}\} \subset \mathcal{A}$ such that

$$\lim_{n\to\infty} J(k^n) = \inf_{k\in\mathcal{A}} J(k).$$

The boundedness of $\{k^n\}$ in $L_\infty(\Omega)$ implies that there exists a subsequence, still denoted by $\{k^n\}$, and some $k^* \in L_\infty(\Omega)$ such that $\{k^n\}$ converges weakly[1] to k^*. Since the admissible set $\mathcal{A}$ is closed and convex, then $k^* \in \mathcal{A}$[2]. The *a-prior* estimate (2.3) implies that the sequence $\{u^n := u(x,t;k^n)\}$ is bounded in the space $H^{1,0}(Q_T)$. Thus a subsequence, still denoted by $\{u^n\}$, may be extracted, and some $u^* \in H^{1,0}(Q_T)$ such that $u^n \rightharpoonup u^*$ in $H^{1,0}(Q_T)$.

From the definition (2.2) of the weak solution in $H^{1,0}(Q_T)$ for the direct problem (2.1), for any $\eta \in H^{1,1}(Q_T)$ and $\eta(\cdot,T) = 0$, we have

$$\begin{aligned}&\int_{Q_T}\left(-u^n\frac{\partial\eta}{\partial t} + k^n\nabla u^n\cdot\nabla\eta + qu^n\eta\right)dxdt\\ &= \int_{Q_T} f\eta dxdt + \int_{S_T}\mu\eta dsdt + \int_\Omega \phi\eta(\cdot,0)dx.\end{aligned}$$

The weak convergence of u^n to u^* in $H^{1,0}(Q_T)$ and of k^n to k^* in $L_\infty(\Omega)$ imply that

$$\begin{aligned}&\lim_{n\to\infty}\int_{Q_T} -u^n\frac{\partial\eta}{\partial t}dxdt = \int_{Q_T} -u^*\frac{\partial\eta}{\partial t}dxdt, \quad \lim_{n\to\infty}\int_{Q_T} qu^n\eta dxdt = \int_{Q_T} qu^*\eta dxdt,\\ &\int_{Q_T} k^n\nabla u^n\cdot\nabla\eta dxdt = \int_{Q_T} k^*\nabla u^n\cdot\nabla\eta dxdt + \int_{Q_T}(k^n-k^*)\nabla u^n\cdot\nabla\eta dxdt,\\ &\lim_{n\to\infty}\int_{Q_T} k^*\nabla u^n\cdot\nabla\eta dxdt = \int_{Q_T} k^*\nabla u^*\cdot\nabla\eta dxdt.\end{aligned}$$

[1] A sequence $\{k^n\}$ is weakly convergent to k^* in $L_\infty(\Omega)$, i.e. $k^n \rightharpoonup k^*$ in $L_\infty(\Omega)$, if

$$\lim_{n\to\infty}\int_\Omega k^n v dx = \int_\Omega k^* v dx, \quad \forall v \in L_1(\Omega).$$

[2] **Theorem**. Let $\mathcal{A}$ be a closed, convex subset of a normed linear space $\mathcal{X}$, and $\{k^n\} \subset \mathcal{A}$ a sequence converging weakly to k^*. Then $k^* \in \mathcal{A}$, see Lax (2002).

Using (2.3) for u^n and the Lebesgue dominant convergence theorem[1] lead to

$$\int_{Q_T} (k^n - k^*)\nabla u^n \cdot \nabla \eta dxdt \to 0, \quad \text{as } n \to \infty.$$

Hence, we obtain

$$\int_{Q_T} k^n \nabla u^n \cdot \nabla \eta dxdt = \int_{Q_T} k^* \nabla u^* \cdot \nabla \eta dxdt,$$

and

$$\begin{aligned} &\int_{Q_T} \left(-u^* \frac{\partial \eta}{\partial t} + k^* \nabla u^* \cdot \nabla \eta + q u^* \eta \right) dxdt \\ =&\int_{Q_T} f\eta dxdt + \int_{S_T} \mu \eta ds dt + \int_{\Omega} \phi \eta(\cdot, 0) dx. \end{aligned}$$

Thus, $u^* = u(k^*)$, due to the uniqueness of a weak solution to the direct problem (2.1), and the lower semi-continuity of norms implies

$$\begin{aligned} J(k^*) =& \frac{1}{2} \|u^* - Y^\epsilon\|^2_{L_2(Q_T)} \leq \frac{1}{2} \lim_{n\to\infty} \|u^n - Y^\epsilon\|^2_{L_2(Q_T)} \\ \leq& \liminf_{n\to\infty} J(k^n) = \min_{k\in\mathcal{A}} J(k), \end{aligned}$$

which indicates that k^* is a minimizer of the objective functional $J(k)$ over $\mathcal{A}$. □

Lemma 2.4.2. *The mapping $k \mapsto u(k)$ is Lipschitz continuous from $\mathcal{A}$ to $H^{1,0}(Q_T)$, i.e.,*

$$\|u(k + \Delta k) - u(k)\|_{H^{1,0}(Q_T)} \leq c\|\Delta k\|_{L_\infty(\Omega)} \tag{2.7}$$

for any k, $k + \Delta k \in \mathcal{A}$ and the corresponding $u(k), u(k + \Delta k) \in H^{1,0}(Q_T)$.

Proof. Denote by $\Delta u = u(k + \Delta k) - u(k)$ the increment of the temperature u caused by the increment Δk of the coefficient k. Then, Δu and Δk satisfy the problem

$$\begin{cases} \frac{\partial(\Delta u)}{\partial t} = \nabla \cdot (k\nabla(\Delta u)) - q\Delta u + \nabla \cdot ((\Delta k)\nabla u(k + \Delta k)), & (x, t) \in Q_T, \\ k\frac{\partial(\Delta u)}{\partial \nu} + \Delta k \frac{\partial u(k+\Delta k)}{\partial \nu} = 0, \quad (x, t) \in S_T, \quad \Delta u(x, 0) = 0, \quad x \in \overline{\Omega}. \end{cases} \tag{2.8}$$

Multiplying (2.8) by Δu, and integrating it over Ω, we obtain

$$\begin{aligned} \frac{1}{2} \int_0^T \frac{d}{dt} \|\Delta u(\cdot, t)\|^2_{L_2(\Omega)} dt = &- \int_{Q_T} \left\{ k|\nabla(\Delta u)|^2 + q(\Delta u)^2 \right\} dxdt \\ &- \int_{Q_T} (\Delta k)\nabla u(k + \Delta k) \cdot \nabla(\Delta u) dxdt, \end{aligned} \tag{2.9}$$

[1] **Theorem** (Lebesgue's Dominated Convergence). Let $\{f_n(x)\}_{n=1}^\infty$ be a sequence of Lebesgue integrable functions that converges to a limit function $f(x)$ almost everywhere on a domain of definition I. Suppose that there exists a Lebesgue integrable function g such that $|f_n| \leq g$ almost everywhere on I and for all $n \in \mathbb{N}$. Then f is Lebesgue integrable on I and $\lim_{n\to\infty} \int_I f_n(x)dx = \int_I f(x)dx$.

and then $\frac{1}{2}\|\Delta u(\cdot,T)\|^2_{L_2(\Omega)} + c\|\Delta u\|^2_{H^{1,0}(Q_T)} \leq -\int_{Q_T}(\Delta k)\nabla u(k+\Delta k)\cdot\nabla(\Delta u)dxdt$, which implies that

$$\|\Delta u\|_{H^{1,0}(Q_T)} \leq c\|\Delta k\|_{L_\infty(\Omega)}\|u(k+\Delta k)\|_{H^{1,0}(Q_T)}.$$

Finally, by using (2.3), we can obtain that $\|\Delta u\|_{H^{1,0}(Q_T)} \leq c\|\Delta k\|_{L_\infty(\Omega)}$, which concludes the proof of the lemma. □

Note that the problem (2.8) represents the sensitivity problem subject to the thermal conductivity $k(x)$, which shall be utilized in the establishment of the CGM in Section 2.5 for the numerical estimation of the unknown thermal conductivity $k(x)$.

Lemma 2.4.3. *The mapping $k \mapsto u(k)$ is Fréchet differentiable with respect to k, i.e., for any $\Delta k \in L_\infty(\Omega)$ such that $k+\Delta k \in \mathcal{A}$ there exists a bounded linear operator $\mathcal{U}: \mathcal{A} \mapsto H^{1,0}(Q_T)$ such that*

$$\lim_{\|\Delta k\|_{L_\infty(\Omega)}\to 0} \frac{\|u(k+\Delta k)-u(k)-\mathcal{U}\Delta k\|_{H^{1,0}(Q_T)}}{\|\Delta k\|_{L_\infty(\Omega)}} = 0. \tag{2.10}$$

Proof. Consider the problem for the function $w \in H^{1,0}(Q_T)$ given by

$$\begin{cases} \frac{\partial w}{\partial t} = \nabla\cdot(k\nabla w) - qw + \nabla\cdot((\Delta k)\nabla u), & (x,t)\in Q_T, \\ k\frac{\partial w}{\partial \nu} + (\Delta k)\frac{\partial u}{\partial \nu} = 0, \quad (x,t)\in S_T, \quad w(x,0)=0, & x\in\overline{\Omega}. \end{cases} \tag{2.11}$$

Similarly as (2.9), we have

$$\frac{1}{2}\int_0^T \frac{d}{dt}\|w(t)\|^2_{L_2(\Omega)}dt = -\int_{Q_T}\left\{k(\nabla w)^2 + qw^2\right\}dxdt - \int_{Q_T}(\Delta k)\nabla u\cdot\nabla w dxdt.$$

Thus

$$\|w\|^2_{H^{1,0}(Q_T)} \leq c\|\Delta k\|_{L_\infty(\Omega)}\|u\|_{H^{1,0}(Q_T)}\|w\|_{H^{1,0}(Q_T)},$$

which implies that the mapping $\Delta k \mapsto w$ from $L_\infty(\Omega)$ to $H^{1,0}(Q_T)$ defines a bounded linear operator $\mathcal{U}$.

Denote $v = u(k+\Delta k) - u(k) - \mathcal{U}\Delta k = \Delta u - w$, where Δu satisfies the problem (2.8). Then, v satisfies the following problem:

$$\begin{cases} \frac{\partial v}{\partial t} = \nabla\cdot(k\nabla v) - qv + \nabla\cdot((\Delta k)\nabla(\Delta u)), & (x,t)\in Q_T, \\ k\frac{\partial v}{\partial \nu} + \Delta k\frac{\partial(\Delta u)}{\partial \nu} = 0, \quad (x,t)\in S_T, \quad v(x,0)=0, & x\in\overline{\Omega}, \end{cases}$$

and we have

$$\frac{1}{2}\int_0^T \frac{d}{dt}\|v(t)\|^2_{L_2(\Omega)}dt = -\int_{Q_T}\left\{k(\nabla v)^2 + qv^2\right\}dxdt - \int_{Q_T}(\Delta k)\nabla(\Delta u)\cdot\nabla v dxdt,$$

which implies $\|v\|^2_{H^{1,0}(Q_T)} \leq c\|\Delta k\|_{L_\infty(\Omega)}\|\Delta u\|_{H^{1,0}(Q_T)}\|v\|_{H^{1,0}(Q_T)}$. By (2.7), we obtain $\|v\|_{H^{1,0}(Q_T)} \leq c\|\Delta k\|^2_{L_\infty(\Omega)}$, therefore, the lemma is proved. □

In order to establish the CGM to obtain the minimizer of the objective functional $J(k)$, the adjoint problem is introduced and given by

$$\begin{cases} \frac{\partial \lambda}{\partial t} = -\nabla \cdot (k\nabla\lambda) + q\lambda - (u(x,t) - Y^\epsilon(x,t)), & (x,t) \in Q_T, \\ k\frac{\partial \lambda}{\partial \nu} = 0, \quad (x,t) \in S_T, \quad \lambda(x,T) = 0, & x \in \overline{\Omega}. \end{cases} \tag{2.12}$$

The weak solution $\lambda \in H^{1,0}(Q_T)$ of the adjoint problem (2.12) satisfies the variational equality

$$\int_{Q_T} \left(\lambda \frac{\partial \eta}{\partial t} + k\nabla\lambda \cdot \nabla\eta + q\lambda\eta \right) dxdt = \int_{Q_T} \lambda(u - Y^\epsilon) dxdt \tag{2.13}$$

for all $\eta \in H^{1,1}(Q_T)$ with $\eta(\cdot, 0) = 0$.

Lemma 2.4.4. *Under the assumptions of Theorem 2.3.2, there exists a constant $c > 0$, which does not depend on the given functions, such that*

$$\|\lambda\|_{H^{1,0}(Q_T)} \leq c\|u - Y^\epsilon\|_{L_2(Q_T)}. \tag{2.14}$$

Proof. Let $\tau \in [0, T]$ and $\tau := T - t$, then the functions $\overline{\lambda}$, $\overline{\eta}$, $\overline{u}$, and $\overline{Y}^\epsilon$ are given by $\overline{\lambda}(\tau) = \lambda(T - \tau)$, $\overline{\eta}(\tau) = \eta(T - \tau)$, $\overline{u}(\tau) = u(T - \tau)$ and $\overline{Y}^\epsilon(\tau) = Y^\epsilon(T - \tau)$. Then we have

$$\begin{cases} \frac{\partial \overline{\lambda}}{\partial \tau} = \nabla \cdot (k\nabla\overline{\lambda}) - q\overline{\lambda} + (\overline{u}(x,\tau) - \overline{Y}^\epsilon(x,\tau)), & (x,\tau) \in Q_T, \\ k\frac{\partial \overline{\lambda}}{\partial \nu} = 0, \quad (x,\tau) \in S_T, \quad \overline{\lambda}(x,0) = 0, & x \in \Omega. \end{cases} \tag{2.15}$$

By Theorem 2.3.2, there exists a unique weak solution $\overline{\lambda} \in H^{1,0}(Q_T)$, and the estimate (2.3) implies

$$\|\overline{\lambda}\|_{H^{1,0}(Q_T)} \leq c\|\overline{u} - \overline{Y}^\epsilon\|_{L_2(Q_T)}.$$

Since $\|\overline{\lambda}\|_{H^{1,0}(Q_T)} = \|\lambda\|_{H^{1,0}(Q_T)}$ and $\|\overline{u} - \overline{Y}^\epsilon\|_{L_2(Q_T)} = \|u - Y^\epsilon\|_{L_2(Q_T)}$, one can conclude that the estimate (2.14) holds. □

Theorem 2.4.5. *The objective functional (2.5) is Fréchet differentiable and its Fréchet derivative $J'(k)$ is given by*

$$J'(k) = -\int_0^T \nabla u \cdot \nabla\lambda dt, \tag{2.16}$$

where λ satisfies the adjoint problem (2.12).

Proof. Taking any $\Delta k \in L_\infty(\Omega)$ such that $k + \Delta k \in \mathcal{A}$, denoting by $\Delta J = J(k + \Delta k) - J(k)$ the increment of $J(k)$, and by equation (2.5), we obtain

$$\Delta J = \int_{Q_T} (u - Y^\epsilon)\Delta u dxdt + \frac{1}{2}\|\Delta u\|^2_{L_2(Q_T)}.$$

Using the adjoint problem (2.12), we have

$$\Delta J = \int_{Q_T} \left\{ -\frac{\partial \lambda}{\partial t} - \nabla \cdot (a \nabla \lambda) + q\lambda \right\} \Delta u dx dt + \frac{1}{2} \|\Delta u\|^2_{L_2(Q_T)},$$

and the sensitivity problem (2.8) implies that

$$\begin{aligned}
&\int_{Q_T} \left\{ -\frac{\partial \lambda}{\partial t} - \nabla \cdot (k \nabla \lambda) + q\lambda \right\} \Delta u dx dt \\
&= -\int_\Omega \Delta u \lambda|_0^T dx + \int_{S_T} k \left\{ \frac{\partial (\Delta u)}{\partial \nu} \lambda - \Delta u \frac{\partial \lambda}{\partial \nu} \right\} ds dt \\
&\quad + \int_{Q_T} \lambda \left\{ \frac{\partial (\Delta u)}{\partial t} - \nabla \cdot (k \nabla (\Delta u)) + q \Delta u \right\} dx dt \\
&= \int_{Q_T} \lambda \nabla \cdot ((\Delta k) \nabla u (k + \Delta k) dx dt + \int_{S_T} k \left\{ \frac{\partial (\Delta u)}{\partial \nu} \lambda - \Delta u \frac{\partial \lambda}{\partial \nu} \right\} ds dt.
\end{aligned}$$

Via integration by parts, we have

$$\begin{aligned}
&\int_{Q_T} \lambda \nabla \cdot ((\Delta k) \nabla u (k + \Delta k) dx dt \\
&= -\int_{Q_T} \Delta k \nabla u (k + \Delta k) \cdot \nabla \lambda dx dt + \int_{S_T} \lambda \Delta k \frac{\partial u (k + \Delta k)}{\partial \nu} ds dt \\
&= -\int_{Q_T} \Delta k \nabla u (k + \Delta k) \cdot \nabla \lambda dx dt - \int_{S_T} k \frac{\partial (\Delta u)}{\partial \nu} \lambda ds dt
\end{aligned}$$

which leads to

$$\int_{Q_T} \left\{ -\frac{\partial \lambda}{\partial t} - \nabla \cdot (k \nabla \lambda) + q\lambda \right\} \Delta u dx dt = -\int_{Q_T} \Delta k \nabla u (k + \Delta k) \cdot \nabla \lambda dx dt.$$

Thus, we obtain

$$\Delta J = -\int_{Q_T} \Delta k \nabla (u + \Delta u) \cdot \nabla \lambda dx dt + \frac{1}{2} \|\Delta u\|^2_{L_2(Q_T)}.$$

Using (2.7), we obtain that

$$\left| \int_{Q_T} \Delta k \nabla (\Delta u) \cdot \nabla \lambda dx dt \right| \leq \|\Delta k\|_{L_\infty(\Omega)} \|\Delta u\|_{H^{1,0}(Q_T)} \|\lambda\|_{H^{1,0}(Q_T)} \leq c \|\Delta k\|^2_{L_\infty(\Omega)},$$

which implies

$$\Delta J = -\int_{Q_T} \Delta k \nabla u \cdot \nabla \lambda dx dt + o(\|\Delta k\|_{L_\infty(\Omega)}),$$

which means the Fréchet derivative is given by (2.16). The theorem is proved. □

2.5 Conjugate gradient method

The following iterative process based on the CGM is applied for the numerical estimation of the unknown thermal conductivity $k(x)$ in (2.1) by minimizing the objective functional $J(k)$ given by (2.5):

$$k^{n+1}(x) = k^n(x) + \beta^n d^n, \quad n = 0, 1, 2, \cdots \tag{2.17}$$

with the search direction given by

$$d^n = \begin{cases} -J'^0, \\ -J'^n + \gamma^n d^{n-1}, \quad n = 1, 2, \cdots \end{cases} \tag{2.18}$$

where the subscripts n denotes the number of iteration, $J'^n = J'(k^n)$, k^0 is the initial guess of the thermal conductivity k, and β^n is search step size.

From the Fréchet gradient $J'(k)$ given by (2.16), the boundary condition in the adjoint problem (2.12) and the search direction (2.18), it is easy to see that $d^n|_{\partial\Omega} = 0$ for any $n \geq 0$. Thus, in the iterative process (2.17) the boundary values of the unknown thermal conductivity k will stay fixed and equal to those of the initial guess k^0.

Therefore, if the initial guess is not close to the exact solution on the boundary $\partial\Omega$, the numerical results will also be far from it. In order to deal with this difficulty, extra smoothness is imposed on the solution through the introduction of the Sobolev gradient, as described in the next section.

2.5.1 Sobolev gradient

We introduce the Sobolev gradient denoted by J'_H for the unknown thermal conductivity $k(x)$, which can be obtained via the inner product in $H^1(\Omega)$ rather than the gradient (2.16) which is generated in $L_2(\Omega)$. The Sobolev gradient J'_H is given by Alifanov (1994); Jin & Zou (2009); Neuberger (2009),

$$\Delta J = \langle J'_H, \Delta k \rangle_{H^1(\Omega)}, \tag{2.19}$$

where $\langle J'_H, \Delta k \rangle_{H^1(\Omega)}$ the weighted inner product in $H^1(\Omega)$ defined by

$$\langle J'_H, \Delta k \rangle_{H^1(\Omega)} = \int_\Omega \{\Delta k J'_H + \kappa \nabla J'_H \cdot \nabla(\Delta k)\}\, dx, \tag{2.20}$$

where κ is a positive constant representing the amount of regularization in the weighted inner product. Using Green's formula, equation (2.19) can be transformed into

$$\begin{aligned}\Delta J &= \int_\Omega \{\Delta k J'_H + \kappa \nabla J'_H \cdot \nabla(\Delta k)\}\, dx \\ &= \int_\Omega \Delta k \left(J'_H - \kappa \nabla^2 J'_H\right) dx + \int_{\partial\Omega} \kappa \Delta k \nabla J'_H ds \\ &= \langle \Delta k, J'_H - \kappa \nabla^2 J'_H \rangle_{L_2(\Omega)} + \int_{\partial\Omega} \kappa \Delta k \nabla J'_H ds.\end{aligned}$$

Setting $\nabla J'_H|_{\partial\Omega} = \mathbf{0}$, then we have

$$\Delta J = \langle \Delta k, J'_H - \kappa \nabla^2 J'_H \rangle_{L_2(\Omega)} = \langle \Delta k, J' \rangle_{L_2(\Omega)}.$$

Thus, the gradient J'_H can be calculated from the L_2-gradient J' (2.16) by solving the elliptic problem

$$\begin{cases} -\kappa \nabla^2 J'_H + J'_H = J', & x \in \Omega, \quad (2.21) \\ \dfrac{\partial J'_H}{\partial \nu} = 0, & x \in \partial\Omega. \quad (2.22) \end{cases}$$

Note that the Sobolev gradient J'_H obtained by solving the elliptic problem (2.21) and (2.22) is smoother than the conventional gradient J' (2.16). If the thermal conductivity k is known on the boundary $\partial\Omega$, the Neumann boundary condition (2.22) is replaced by the homogeneous Dirichlet boundary condition

$$J'_H = 0, \quad x \in \partial\Omega. \quad (2.23)$$

2.5.2 CGM

The search direction d^n given by (2.18) is defined by the gradient and the conjugate gradient coefficient γ^n. Several choices for the conjugate gradient coefficient γ^n have been given in Section 1.5. In this chapter and throughout the thesis, the Fletcher-Reeves formula is utilized for the conjugate gradient coefficient γ^n given by, see Fletcher & Reeves (1964),

$$\gamma^n = \frac{\|J'^n\|^2_{L_2(\Omega)}}{\|J'^{n-1}\|^2_{L_2(\Omega)}}, \quad n = 1, 2, \cdots. \quad (2.24)$$

The step size β^n can be found by minimizing

$$J(k^{n+1}) = \frac{1}{2} \int_{Q_T} (u(k^n + \beta^n d^n) - Y^\epsilon)^2 dx dt.$$

This expression implies that the step size β^n is implicit in the objective functional $J(k^{n+1})$. Such expression can be transformed into an explicit formula by applying the Taylor series expansion to approximate $u(k^n + \beta^n d^n)$. Thus, setting $\Delta k^n = d^n$, the function $u(k^n + \beta^n d^n)$ can be linearised by the Taylor series expansion in the form

$$u(k^n + \beta^n d^n) \approx u(k^n) + \beta^n d^n \frac{\partial u(k^n)}{\partial k^n} \approx u(k^n) + \beta^n \Delta u(k^n).$$

Denoting $u(x, t; k^n) = u^n$ and $\Delta u(x, t; k^n) = \Delta u^n$, we obtain

$$J(k^{n+1}) = \frac{1}{2} \int_{Q_T} (u^n + \beta^n \Delta u^n - Y^\epsilon)^2 dxdt.$$

The partial derivative of the objective functional $J(k^{n+1})$ with respect to β^n is given by

$$\frac{\partial J}{\partial \beta^n} = \int_{Q_T} (u^n + \beta^n \Delta u^n - Y^\epsilon) \Delta u^n dxdt.$$

We set $\frac{\partial J}{\partial \beta^n} = 0$, and obtain the step size β^n given by

$$\beta^n = -\frac{\langle u^n - Y^\epsilon, \Delta u^n \rangle_{L_2(Q_T)}}{\|\Delta u^n\|^2_{L_2(Q_T)}}. \tag{2.25}$$

The iteration process given by (2.17) and (2.18) does not provide the CGM with stabilization necessary for minimizing the objective functional (2.5) to be classified as well-posed because of the errors inherent in the temperature measurement (2.4). However, the method may become well-posed if the discrepancy principle, see Alifanov (1994); Engl *et al.* (1996); Hanke (1995); Jarny *et al.* (1991); Scherzer (1996), is applied to stop the iterative procedure. According to the discrepancy principle, the iterative procedure is stopped when the following criterion is satisfied:

$$J(k^n) \leq \bar{\epsilon}, \tag{2.26}$$

where $\bar{\epsilon}$ is a small positive value, e.g., $\bar{\epsilon} = 10^{-6}$, for exact temperature measurement, and

$$\bar{\epsilon} = \frac{1}{2} \|Y - Y^\epsilon\|^2_{L_2(Q_T)}, \tag{2.27}$$

when the temperature measurements contain noisy data. The exact temperature can be generated from the analytical solution, if available, or from solving the direct problem numerically (with care not to commit an inverse crime). In the absence of knowledge of any upper bound on the amount of noise in (2.27) popular heuristic error-free methods such as the generalized cross-validation, see Wahba (1990), or the L-curve method, see Hansen & OLeary (1993), may occasionally work well for a fixed noise level, but they cannot lead to convergence as the amount of noise tends to zero, see Engl *et al.* (1989).

The CGM established for reconstructing the unknown space-dependent thermal conductivity is presented as follows:

S1. Set $n = 0$ and choose an initial guess $k^0(x)$ for the unknown thermal conductivity $k(x)$.

S2. Solve the direct problem (2.1) numerically by applying the FDM scheme to compute the temperature $u(x, t; k^n)$ and the objective functional $J(k^n)$ given by (2.5).

S3. If the stopping criterion (2.26) is satisfied, then go to S7. Else go to S4.

S4. Solve the adjoint problem (2.12) to obtain the adjoint function $\lambda(x, t; k^n)$, and the gradient $J'(k^n)$ given by (2.16). Compute the conjugate gradient coefficient γ^n given by (2.24) and the search direction d^n given by (2.18).

S5. Solve the sensitivity problem (2.8) to numerically obtain the sensitivity function $\Delta u(x, t; k^n)$ by taking $\Delta k^n = d^n$, and compute the search step size β^n by (2.25).

S6. Update k^{n+1} by (2.17), set $n = n + 1$ and return to S2.

S7. End.

Note that the Sobolev gradient H^1-gradient $J'_H(k^n)$ can be applied in S4, and then the CGM with H^1-gradient can be established similarly.

2.6 Numerical results and discussions

In this section, the numerical methods for reconstructing the space-dependent thermal conductivity $k(x)$ are illustrated, and three numerical experiments based on the CGM established in the previous section are shown for one- and two-dimensional cases ($\mathrm{d} = 1, 2$). The Simpson's rule is utilized to deal with all the integrals within the CGM, e.g., the objective functional $J(k)$ in (2.5). The accuracy error, as a function of the iteration number n, for the thermal conductivity $k(x)$ is defined as

$$E(k^n) = \|k^n - k\|_{L_2(\Omega)}, \tag{2.28}$$

where k^n is the numerical solution obtained by the CGM at the iteration number n, and k is the analytical expression for the thermal conductivity, if available. The noisy temperature measurement Y^ϵ is numerically simulated by adding to the exact temperature Y an error term in the following form:

$$Y^\epsilon = Y + \sigma \times \mathrm{random}(1), \tag{2.29}$$

where $\sigma = \frac{p}{100} \times \max_{(x,t)\in\overline{Q}_T} |Y(x,t)|$ is the standard deviation, $\mathrm{random}(1)$ generates random values from a normal distribution with zero mean and unit standard deviation, and $p\%$ represents the percentage of noise.

In the following two sections, the FDM is applied to solve the PDEs of the CGM. The C-N and ADI methods are used for the one- and two-dimensional case $(\mathrm{d} = 1, 2)$, respectively.

2.6.1 The Crank-Nicolson scheme

The numerical scheme of the one-dimensional $(\mathrm{d} = 1)$ initial-boundary value problem (2.1) can be established using the C-N scheme, see e.g. Richtmyer & Morton (1967); Smith (1985), which is unconditionally stable and second-order accurate in space x and first-order accurate in time t. Set the domain $\Omega = (a_0, a_1)$, and $Q_T = (a_0, a_1) \times (0, T)$. For numerical discretization, a rectangular network is constructed by subdividing the domain Q_T into $I \times M$ subintervals of the step lengths Δx and Δt in space x and time t directions, where I, M are two positive integers. Taking $\Delta x = \frac{a_1-a_0}{I-1}$ and $\Delta t = \frac{T}{M-1}$, then

$$x_i = a_0 + (i-1)\Delta x, \quad i = \overline{1, I}, \quad t_m = (m-1)\Delta t, \quad m = \overline{1, M}.$$

The temperature $u(x,t)$ and the coefficients $k(x), q(x), f(x,t), \mu(x,t), \phi(x)$ at the node (i,m) are denoted by $u_i^m = u(x_i, t_m)$, $k_i = k(x_i)$, $q_i = q(x_i)$, $f_i^m = f(x_i, t_m)$, $\mu_i^m = \mu(x_i, t_m)$ and $\phi_i = \phi(x_i)$.

Denoting $k_{i\pm1/2} = \frac{1}{2}(k_i + k_{i\pm1})$, approximating

$$\begin{aligned}\nabla(k\nabla u)|_{i,m} = \frac{\partial}{\partial x}\left(k\frac{\partial u}{\partial x}\right)\Big|_{i,m} &\approx \frac{k_{i+1/2}\frac{u_{i+1}^m - u_i^m}{\Delta x} - k_{i-1/2}\frac{u_i^m - u_{i-1}^m}{\Delta x}}{\Delta x} \\ &= \frac{k_{i+1/2}}{(\Delta x)^2}u_{i+1}^m - \frac{k_{i+1/2}+k_{i-1/2}}{(\Delta x)^2}u_i^m + \frac{k_{i-1/2}}{(\Delta x)^2}u_{i-1}^m,\end{aligned}$$

and employing the C-N scheme, the heat transfer equation (2.1) can be discretised as

$$\begin{aligned}\frac{u_i^{m+1} - u_i^m}{\Delta t} = \frac{1}{2}\Bigg\{&\frac{k_{i+1/2}}{(\Delta x)^2}u_{i+1}^m - \frac{k_{i+1/2}+k_{i-1/2}}{(\Delta x)^2}u_i^m + \frac{k_{i-1/2}}{(\Delta x)^2}u_{i-1}^m - q_i u_i^m + f_i^m \\ &+ \frac{k_{i+1/2}}{(\Delta x)^2}u_{i+1}^{m+1} - \frac{k_{i+1/2}+k_{i-1/2}}{(\Delta x)^2}u_i^{m+1} + \frac{k_{i-1/2}}{(\Delta x)^2}u_{i-1}^{m+1} - q_i u_i^{m+1} + f_i^{m+1}\Bigg\}\end{aligned}$$

which implies that

$$\begin{aligned}&- A_{i-1/2}u_{i-1}^{m+1} + (2 + B_i)u_i^{m+1} - A_{i+1/2}u_{i+1}^{m+1} \\ =&A_{i-1/2}u_{i-1}^m + (2 - B_i)u_i^m + A_{i+1/2}u_{i+1}^m + \Delta t(f_i^m + f_i^{m+1}),\end{aligned} \tag{2.30}$$

where $A_i = k_i \frac{\Delta t}{(\Delta x)^2}$ and $B_i = q_i \Delta t + A_{i-1/2} + A_{i+1/2}$. The Neumann boundary condition in (2.1) can be approximated as

$$u_1^{m+1} = \frac{1}{3}\left(4u_2^{m+1} - u_3^{m+1} + 2\mu_1^{m+1}\frac{\Delta x}{k_1}\right), \tag{2.31}$$

$$u_I^{m+1} = \frac{1}{3}\left(4u_{I-1}^{m+1} - u_{I-2}^{m+1} + 2\mu_I^{m+1}\frac{\Delta x}{k_I}\right). \tag{2.32}$$

Thus, the difference equation (2.30) can be reformulated as a $(I-2)\times(I-2)$ system of linear equations of the form

$$\mathbf{A}\mathbf{u}^{m+1} = \mathbf{B}\mathbf{u}^m + \mathbf{F}^m, \quad m = \overline{1, M-1}, \tag{2.33}$$

where $\mathbf{u}^m = \left[u_2^m, \cdots, u_{I-1}^m\right]^{\mathrm{T}}$, and it is easy to see that $\mathbf{u}^1 = [\phi_2, \cdots, \phi_{I-1}]^{\mathrm{T}}$ is known by the given initial temperature $\phi(x)$ in (2.1), the $(I-2)\times(I-2)$ tridiagonal matrices $\mathbf{A}$ and $\mathbf{B}$ given by

$$\mathbf{A} = \begin{bmatrix} 2 + B_2 - \frac{4}{3}A_{\frac{3}{2}} & \frac{1}{3}A_{\frac{3}{2}} - A_{\frac{5}{2}} & 0 & \cdots\cdots\cdots\cdots \\ -A_{\frac{5}{2}} & 2 + B_3 & -A_{\frac{7}{2}} & \cdots\cdots\cdots\cdots \\ \cdots\cdots & \cdots\cdots & \cdots\cdots & \cdots\cdots\cdots\cdots \\ \cdots\cdots & -A_{I-\frac{5}{2}} & 2 + B_{I-2} & -A_{I-\frac{3}{2}} \\ \cdots\cdots & 0 & \frac{1}{3}A_{I-\frac{1}{2}} - A_{I-\frac{3}{2}} & 2 + B_{I-1} - \frac{4}{3}A_{I-\frac{1}{2}} \end{bmatrix},$$

$$\mathbf{B} = \begin{bmatrix} 2 - B_2 & A_{\frac{5}{2}} & 0 & \cdots & 0 & 0 & 0 \\ A_{\frac{5}{2}} & 2 - B_3 & A_{\frac{7}{2}} & \cdots & 0 & 0 & 0 \\ \vdots & \vdots & \vdots & \ddots & \vdots & \vdots & \vdots \\ 0 & 0 & 0 & \cdots & A_{I-\frac{5}{2}} & 2 - B_{I-2} & A_{I-\frac{3}{2}} \\ 0 & 0 & 0 & \cdots & 0 & A_{I-\frac{3}{2}} & 2 - B_{I-1} \end{bmatrix},$$

and

$$\mathbf{F}^m = \begin{bmatrix} \Delta t(f_2^m + f_2^{m+1}) + A_{\frac{3}{2}}u_1^m + \frac{2}{3}A_{\frac{3}{2}}\mu_1^{m+1}\frac{\Delta x}{k_1} \\ \Delta t(f_3^m + f_3^{m+1}) \\ \vdots \\ \Delta t(f_{I-2}^m + f_{I-2}^{m+1}) \\ \Delta t(f_{I-1}^m + f_{I-1}^{m+1}) + A_{I-\frac{1}{2}}u_I^m + \frac{2}{3}A_{I-\frac{1}{2}}\mu_I^{m+1}\frac{\Delta x}{k_I} \end{bmatrix}.$$

Note that for the direct problem (2.1) with the Dirichlet boundary condition given by $u(x,t) = \mu(x,t)$, $(x,t) \in S_T$, then such boundary condition can be approximated by

$$u_1^{m+1} = \mu_1^{m+1}, \quad u_I^{m+1} = \mu_I^{m+1}. \tag{2.34}$$

For the Robin convection type boundary condition given by $k(x)\frac{\partial u}{\partial \nu} + \alpha(x)u(x,t) = \mu(x,t)$, $(x,t) \in S_T$, where $\alpha(x)$ is a given Robin coefficient, the boundary condition can

be similarly approximated by

$$u_1^{m+1} = \frac{1}{3 + 2\Delta x \alpha_1 / k_1} \left(4u_2^{m+1} - u_3^{m+1} + 2\mu_1^{m+1} \frac{\Delta x}{k_1} \right), \tag{2.35}$$

$$u_I^{m+1} = \frac{1}{3 + 2\Delta x \alpha_I / k_I} \left(4u_{I-1}^{m+1} - u_{I-2}^{m+1} + 2\mu_I^{m+1} \frac{\Delta x}{k_I} \right). \tag{2.36}$$

Thus the C-N scheme for the initial-boundary value problem (2.1) with the Dirichlet or Robin boundary condition can be established by the above approach and (2.34) or (2.35), (2.36), respectively.

2.6.2 The alternating direction implicit (ADI) scheme

For the two dimensional case ($\mathrm{d} = 2$), setting the domain $\Omega = (a_0, a_1) \times (b_0, b_1)$ and $Q_T = (a_0, a_1) \times (b_0, b_1) \times (0, T)$, the parabolic equation (2.1) can be written as

$$\begin{aligned} \frac{\partial u}{\partial t} =& \frac{\partial}{\partial x_1} \left(k(x_1, x_2) \frac{\partial u}{\partial x_1} \right) + \frac{\partial}{\partial x_2} \left(k(x_1, x_2) \frac{\partial u}{\partial x_2} \right) \\ & - q(x_1, x_1) u(x_1, x_2, t) + f(x_1, x_2, t), \quad (x_1, x_2, t) \in Q_T. \end{aligned} \tag{2.37}$$

The ADI scheme, see Peaceman & Rachford (1955); Richtmyer & Morton (1967), is applied to compute the numerical solution for the two dimensional problem, which is unconditionally stable and second-order accurate in space (x_1, x_2) and first-order accurate time t.

For numerical discretization, a rectangular network is constructed by subdividing the domain Q_T into $I \times J \times M$ subintervals of the step lengths Δx_1, Δx_2 and Δt in space x_1, x_2 and time t directions, where I, J, M are positive integers.

Taking $\Delta x_1 = \frac{a_1 - a_0}{I-1}$, $\Delta x_2 = \frac{b_1 - b_0}{J-1}$ and $\Delta t = \frac{T}{M-1}$, then $(x_1)_i = a_0 + (i-1)\Delta x_1$, $i = \overline{1, I}$, $(x_2)_j = b_0 + (i-1)\Delta x_2$, $j = \overline{1, J}$, and $t_m = (m-1)\Delta t$, $m = \overline{1, M}$. The temperature $u(x_1, x_2, t)$, the thermal coefficients $k(x_1, x_2)$, $q(x_1, x_2)$, the heat source $f(x_1, x_2, t)$ and boundary and initial conditions $\mu(x_1, x_2, t)$, $\phi(x_1, x_2)$ at the node (i, j, m) are denoted by $u_{i,j}^m = u((x_1)_i, (x_2)_j, t_m)$, $k_{i,j} = k((x_1)_i, (x_2)_j)$, $q_{i,j} = q((x_1)_i, (x_2)_j)$, $f_{i,j}^m = f((x_1)_i, (x_2)_j, t_m)$, $\mu_{i,j}^m = \mu((x_1)_i, (x_2)_j, t_m)$, and $\phi_{i,j} = \phi((x_1)_i, (x_2)_j)$.

According to the ADI scheme, the equation (2.37) can be approximated by

$$\begin{aligned} \frac{u_{i,j}^{m+\frac{1}{2}} - u_{i,j}^m}{\frac{1}{2}\Delta t} =& \frac{k_{i+\frac{1}{2},j}}{(\Delta x_1)^2} u_{i+1,j}^{m+\frac{1}{2}} - \frac{k_{i+\frac{1}{2},j} + k_{i-\frac{1}{2},j}}{(\Delta x_1)^2} u_{i,j}^{m+\frac{1}{2}} + \frac{k_{i-\frac{1}{2},j}}{(\Delta x_1)^2} u_{i-1,j}^{m+\frac{1}{2}} \\ & + \frac{k_{i,j+\frac{1}{2}}}{(\Delta x_2)^2} u_{i,j+1}^m - \frac{k_{i,j+\frac{1}{2}} + k_{i,j-\frac{1}{2}}}{(\Delta x_2)^2} u_{i,j}^m + \frac{k_{i,j-\frac{1}{2}}}{(\Delta x_2)^2} u_{i,j-1}^m - q_{i,j} u_{i,j}^m + f_{i,j}^m, \end{aligned} \tag{2.38}$$

and

$$\frac{u_{i,j}^{m+1}-u_{i,j}^{m+\frac{1}{2}}}{\frac{1}{2}\Delta t}=\frac{k_{i+\frac{1}{2},j}}{(\Delta x_1)^2}u_{i+1,j}^{m+\frac{1}{2}}-\frac{k_{i+\frac{1}{2},j}+k_{i-\frac{1}{2},j}}{(\Delta x_1)^2}u_{i,j}^{m+\frac{1}{2}}+\frac{k_{i-\frac{1}{2},j}}{(\Delta x_1)^2}u_{i-1,j}^{m+\frac{1}{2}}$$
$$+\frac{k_{i,j+\frac{1}{2}}}{(\Delta x_2)^2}u_{i,j+1}^{m+1}-\frac{k_{i,j+\frac{1}{2}}+k_{i,j-\frac{1}{2}}}{(\Delta x_2)^2}u_{i,j}^{m+1}+\frac{k_{i,j-\frac{1}{2}}}{(\Delta x_2)^2}u_{i,j-1}^{m+1}-q_{i,j}u_{i,j}^{m+\frac{1}{2}}+f_{i,j}^{m+\frac{1}{2}}, \quad (2.39)$$

where $k_{i\pm\frac{1}{2},j}=\frac{1}{2}(k_{i,j}+k_{i\pm1,j})$ and $k_{i,j\pm\frac{1}{2}}=\frac{1}{2}(k_{i,j}+k_{i,j\pm1})$. Denoting

$$A_{i,j}=k_{i,j}\frac{\Delta t}{(\Delta x_1)^2}, \quad A1_{i,j}=2+A_{i-\frac{1}{2},j}+A_{i+\frac{1}{2},j},$$
$$A2_{i,j}=2-A_{i-\frac{1}{2},j}-A_{i+\frac{1}{2},j}-\Delta t q_{i,j}, \quad B_{i,j}=k_{i,j}\frac{\Delta t}{(\Delta x_2)^2},$$
$$B1_{i,j}=2+B_{i,j-\frac{1}{2}}+B_{i,j+\frac{1}{2}}, \quad B2_{i,j}=2-B_{i,j-\frac{1}{2}}-B_{i,j+\frac{1}{2}}-\Delta t q_{i,j},$$

the expressions (2.38) and (2.39) can be written as

$$-A_{i-\frac{1}{2},j}u_{i-1,j}^{m+\frac{1}{2}}+A1_{i,j}u_{i,j}^{m+\frac{1}{2}}-A_{i+\frac{1}{2},j}u_{i+1,j}^{m+\frac{1}{2}}$$
$$=B_{i,j-\frac{1}{2}}u_{i,j-1}^{m}+B2_{i,j}u_{i,j}^{m}+B_{i,j+\frac{1}{2}}u_{i,j+1}^{m}+\Delta t f_{i,j}^{m}, \quad (2.40)$$

and

$$-B_{i,j-\frac{1}{2}}u_{i,j-1}^{m+1}+B1_{i,j}u_{i,j}^{m+1}-B_{i,j+\frac{1}{2}}u_{i,j+1}^{m+1}$$
$$=A_{i-\frac{1}{2},j}u_{i-1,j}^{m+\frac{1}{2}}+A2_{i,j}u_{i,j}^{m+\frac{1}{2}}+A_{i+\frac{1}{2},j}u_{i+1,j}^{m+\frac{1}{2}}+\Delta t f_{i,j}^{m+\frac{1}{2}}. \quad (2.41)$$

The Neumann boundary condition of the problem (2.1) for the two-dimensional case can be approximated as

$$u_{1,j}^{m+1}=\frac{1}{3}\left(4u_{2,j}^{m+1}-u_{3,j}^{m+1}+2\mu_{1,j}^{m+1}\frac{\Delta x_1}{k_{1,j}}\right), \quad (2.42)$$
$$u_{I,j}^{m+1}=\frac{1}{3}\left(4u_{I-1,j}^{m+1}-u_{I-2,j}^{m+1}+2\mu_{I,j}^{m+1}\frac{\Delta x_1}{k_{I,j}}\right), \quad (2.43)$$
$$u_{i,1}^{m+1}=\frac{1}{3}\left(4u_{i,2}^{m+1}-u_{i,3}^{m+1}+2\mu_{i,1}^{m+1}\frac{\Delta x_2}{k_{i,1}}\right), \quad (2.44)$$
$$u_{i,J}^{m+1}=\frac{1}{3}\left(4u_{i,J-1}^{m+1}-u_{i,J-2}^{m+1}+2\mu_{i,J}^{m+1}\frac{\Delta x_2}{k_{i,J}}\right). \quad (2.45)$$

Thus, the difference equations (2.40) and (2.41) can be reformulated in the following forms:

$$\mathbf{A}_j\mathbf{u}_j^{m+\frac{1}{2}}=\mathbf{F}_j^m, \quad j=\overline{2,J-1}, \quad (2.46)$$
$$\mathbf{B}_i\mathbf{u}_i^{m+1}=\mathbf{F}_i^{m+\frac{1}{2}}, \quad i=\overline{2,I-1}, \quad (2.47)$$

for $m = \overline{1, M-1}$, where $\mathbf{u}_i^m = [u_{i,2}^m, \cdots, u_{i,J-1}^m]^{\mathrm{T}}$, $\mathbf{u}_j^m = [u_{2,j}^m, \cdots, u_{I-1,j}^m]^{\mathrm{T}}$,

$$\mathbf{A}_j = \begin{bmatrix} A1_{2,j} - \frac{4}{3}A_{\frac{3}{2},j} & \frac{1}{3}A_{\frac{3}{2},j} - A_{\frac{5}{2},j} & 0 & \cdots\cdots\cdots\cdots \\ -A_{\frac{5}{2},j} & A1_{3,j} & -A_{\frac{7}{2},j} & \cdots\cdots\cdots\cdots \\ \cdots\cdots & \cdots\cdots & \cdots\cdots & \cdots\cdots \\ \cdots\cdots\cdots\cdots & -A_{I-\frac{5}{2},j} & A1_{I-2,j} & -A_{I-\frac{3}{2},j} \\ \cdots\cdots\cdots\cdots & 0 & \frac{1}{3}A_{I-\frac{1}{2},j} - A_{I-\frac{3}{2},j} & A1_{I-1,j} - \frac{4}{3}A_{I-\frac{1}{2},j} \end{bmatrix},$$

$$\mathbf{F}_j^m = \begin{bmatrix} B_{2,j-\frac{1}{2}}u_{2,j-1}^m + B2_{2,j}u_{2,j}^m + B_{2,j+\frac{1}{2}}u_{2,j+1}^m + \frac{2}{3}A_{\frac{3}{2},j}\mu_{1,j}^{m+1}\frac{\Delta x_1}{k_{1,j}} + \Delta t f_{2,j}^m \\ B_{3,j-\frac{1}{2}}u_{3,j-1}^m + B2_{3,j}u_{3,j}^m + B_{3,j+\frac{1}{2}}u_{3,j+1}^m + \Delta t f_{3,j}^m \\ \vdots \\ B_{I-2,j-\frac{1}{2}}u_{I-2,j-1}^m + B2_{I-2,j}u_{I-2,j}^m + B_{I-2,j+\frac{1}{2}}u_{I-2,j+1}^m + \Delta t f_{I-2,j}^m \\ B_{I-1,j-\frac{1}{2}}u_{I-1,j-1}^m + B2_{I-1,j}u_{I-1,j}^m + B_{I-1,j+\frac{1}{2}}u_{I-1,j+1}^m + \Delta t f_{I-1,j}^m \\ +\frac{2}{3}A_{I-\frac{1}{2},j}\mu_{I,j}^{m+1}\frac{\Delta x_1}{k_{I,j}} \end{bmatrix},$$

and

$$\mathbf{B}_i = \begin{bmatrix} B1_{i,2} - \frac{4}{3}B_{i,\frac{3}{2}} & \frac{1}{3}B_{i,\frac{3}{2}} - B_{i,\frac{5}{2}} & 0 & \cdots\cdots\cdots\cdots \\ -B_{i,\frac{5}{2}} & B1_{i,3} & -B_{i,\frac{7}{2}} & \cdots\cdots\cdots\cdots \\ \cdots\cdots & \cdots\cdots & \cdots\cdots & \cdots\cdots \\ \cdots\cdots\cdots\cdots & -B_{i,J-\frac{5}{2}} & B1_{i,J-2} & -B_{i,J-\frac{3}{2}} \\ \cdots\cdots\cdots\cdots & 0 & \frac{1}{3}B_{i,J-\frac{1}{2}} - B_{i,J-\frac{3}{2}} & B1_{i,J-1} - \frac{4}{3}B_{i,J-\frac{1}{2}} \end{bmatrix},$$

$$\mathbf{F}_i^{m+\frac{1}{2}} = \begin{bmatrix} A_{i-\frac{1}{2},2}u_{i-1,2}^{m+\frac{1}{2}} + A2_{i,2}u_{i,2}^{m+\frac{1}{2}} + A_{i+\frac{1}{2},2}u_{i+1,2}^{m+\frac{1}{2}} + \Delta t f_{i,2}^{m+\frac{1}{2}} \\ +\frac{2}{3}B_{i,\frac{3}{2}}\mu_{i,1}^{m+1}\frac{\Delta x_2}{k_{i,1}} \\ A_{i-\frac{1}{2},3}u_{i-1,3}^{m+\frac{1}{2}} + A2_{i,3}u_{i,3}^{m+\frac{1}{2}} + A_{i+\frac{1}{2},3}u_{i+1,3}^{m+\frac{1}{2}} + \Delta t f_{i,3}^{m+\frac{1}{2}} \\ \vdots \\ A_{i-\frac{1}{2},J-2}u_{i-1,J-2}^{m+\frac{1}{2}} + A2_{i,J-2}u_{i,J-2}^{m+\frac{1}{2}} + A_{i+\frac{1}{2},J-2}u_{i+1,J-2}^{m+\frac{1}{2}} + \Delta t f_{i,J-2}^{m+\frac{1}{2}} \\ A_{i-\frac{1}{2},J-1}u_{i-1,J-1}^{m+\frac{1}{2}} + A2_{i,J-1}u_{i,J-1}^{m+\frac{1}{2}} + A_{i+\frac{1}{2},J-1}u_{i+1,J-1}^{m+\frac{1}{2}} + \Delta t f_{i,J-1}^{m+\frac{1}{2}} \\ +\frac{2}{3}B_{i,J-\frac{1}{2}}\mu_{i,J}^{m+1}\frac{\Delta x_2}{k_{i,J}} \end{bmatrix}.$$

Note that for the Dirichlet boundary condition $u(x_1, x_2, t) = \mu(x_1, x_2, t)$, $(x_1, x_2, t) \in S_T$, can be approximated as

$$u_{1,j}^m = \mu_{1,j}^m, \quad u_{I,j}^m = \mu_{I,j}^m, \quad u_{i,1}^m = \mu_{i,1}^m, \quad u_{i,J}^m = \mu_{i,J}^m. \tag{2.48}$$

Similarly, the Robin boundary condition $k(x_1, x_2)\frac{\partial u}{\partial \nu} + \alpha(x_1, x_2)u(x_1, x_2, t) = \mu(x_1, x_2, t)$,

$(x_1, x_2, t) \in S_T$, can be approximated by

$$u_{1,j}^{m+1} = \frac{1}{3 + 2\Delta x_1 \alpha_{1,j}/k_{1,j}} \left(4u_{2,j}^{m+1} - u_{3,j}^{m+1} + 2\mu_{1,j}^{m+1} \frac{\Delta x_1}{k_{1,j}} \right), \tag{2.49}$$

$$u_{I,j}^{m+1} = \frac{1}{3 + 2\Delta x_1 \alpha_{I,j}/k_{I,j}} \left(4u_{I-1,j}^{m+1} - u_{I-2,j}^{m+1} + 2\mu_{I,j}^{m+1} \frac{\Delta x_1}{k_{I,j}} \right), \tag{2.50}$$

$$u_{i,1}^{m+1} = \frac{1}{3 + 2\Delta x_2 \alpha_{i,1}/k_{i,1}} \left(4u_{i,2}^{m+1} - u_{i,3}^{m+1} + 2\mu_{i,1}^{m+1} \frac{\Delta x_2}{k_{i,1}} \right), \tag{2.51}$$

$$u_{i,J}^{m+1} = \frac{1}{3 + 2\Delta x_2 \alpha_{i,J}/k_{i,J}} \left(4u_{i,J-1}^{m+1} - u_{i,J-2}^{m+1} + 2\mu_{i,J}^{m+1} \frac{\Delta x_2}{k_{i,J}} \right). \tag{2.52}$$

Thus, the ADI for the problem (2.1) with with the Dirichlet or Robin boundary condition can be established by the above approach together with (2.48) or (2.49)–(2.52), respectively.

2.6.3 Example 1

In this section, the CGM proposed in Section 2.5 is used to reconstruct the unknown thermal conductivity $k(x)$ of the IHTP (2.1) and (2.4).

For the one-dimensional case $(\mathrm{d} = 1)$, we take $\Omega = (0, 1)$, the final time $T = 1$, the initial temperature $\phi \equiv 0$, and

$$\begin{aligned} f(x,t) &= (1 + x - xe^{-t})(\sin(\pi x) + (\pi + 1)x) \\ &\quad + \frac{1 - e^{-t}}{12}(\pi^2(1 + x)\sin(\pi x) - \pi\cos(\pi x) - \pi - 1), \\ q(x) &= 1 + x, \quad \mu(0,t) = -\frac{2\pi + 1}{12}(1 - e^{-t}), \quad \mu(1,t) = \frac{1}{6}(1 - e^{-t}), \\ Y(x,t) &= (1 - e^{-t})(\sin(\pi x) + (\pi + 1)x), \end{aligned} \tag{2.53}$$

and by the direct calculation for the parabolic problem (2.1), then the analytical solution of the inverse problem (2.1) and (2.4) is given by

$$k(x) = \frac{1 + x}{12}, \quad u(x,t) = (1 - e^{-t})(\sin(\pi x) + (\pi + 1)x). \tag{2.54}$$

Obviously, $u(x,t)$ in (2.54) coincides with $Y(x,t)$ in (2.53), however the latter one may contain noise as in (2.29) and solving the PDE in (2.1) as

$$\begin{aligned} \frac{\partial Y^\epsilon}{\partial t}(x,t) =& \nabla k(x) \cdot \nabla Y^\epsilon(x,t) + k(x)\nabla^2 Y^\epsilon(x,t) \\ & - q(x)Y^\epsilon(x,t) + f(x,t), \quad (x,t) \in Q_T \end{aligned}$$

constitutes an ill-posed problem of numerical differentiation.

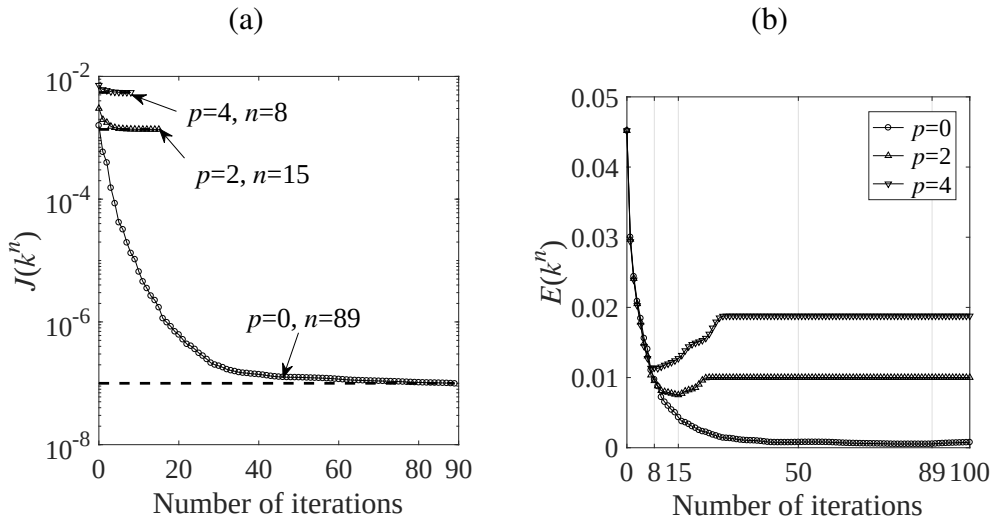

Figure 2.1: (a) The objective functional (2.5) and (b) the error $E(k^n)$ (2.28) with $p \in \{0, 2, 4\}$ noise and the initial guess k^0 (2.55) using the L_2-gradient J' (2.16), for Example 1.

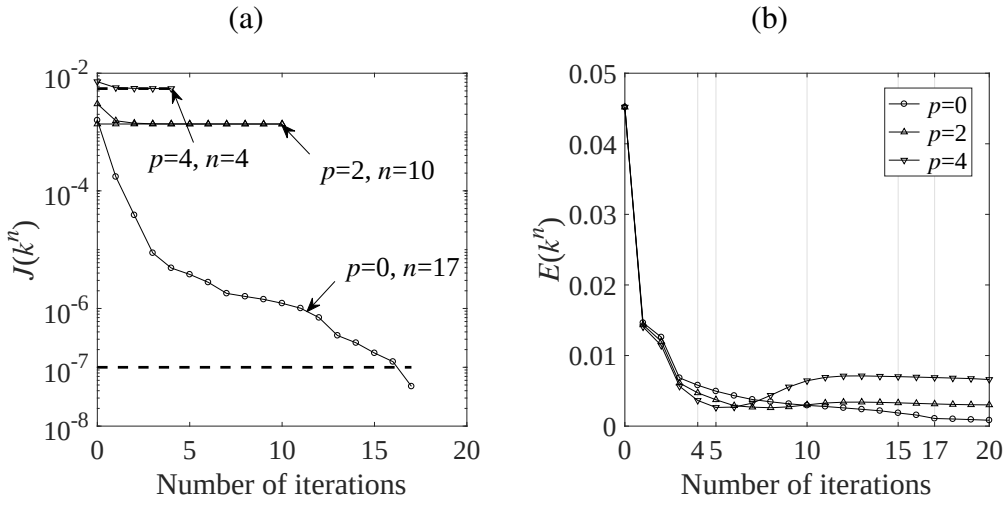

Figure 2.2: (a) The objective functional (2.5) and (b) the error $E(k^n)$ (2.28) with $p \in \{0, 2, 4\}$ noise and the initial guess k^0 (2.55) using the H^1-gradient J'_H (2.21) and (2.23), for Example 1.

The initial guess is taken as

$$k^0(x) = -\frac{1}{4}x^2 + \frac{1}{3}x + \frac{1}{12}, \tag{2.55}$$

which ensures that $k^0(x)$ coincides with the exact thermal conductivity (2.54) at the boundary points $x = 0$ and $x = 1$, and the quadratic initial guess (2.55) is also sufficiently far away from the linear exact function (2.54).

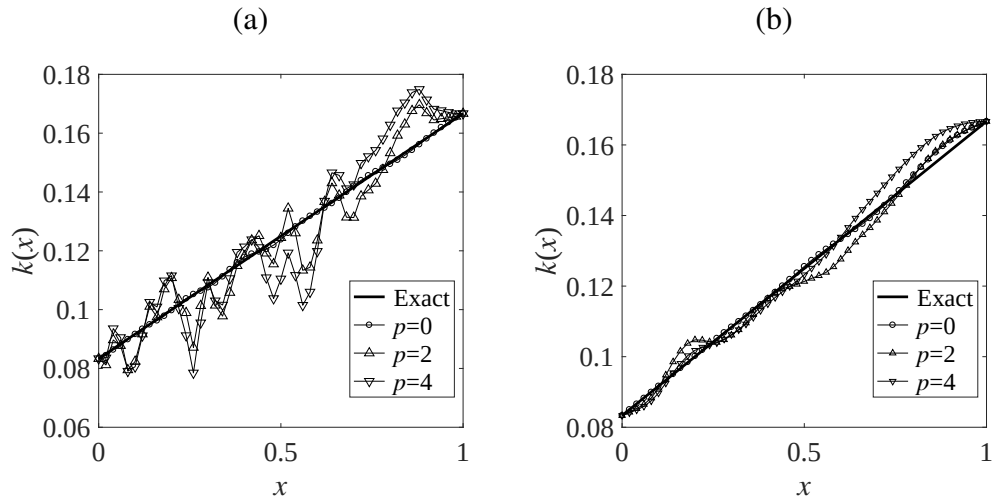

Figure 2.3: The numerical thermal conductivity $k(x)$ using (a) the L_2-gradient J' (2.16) and (b) the H^1-gradient J'_H (2.21), (2.23) with $p \in \{0, 2, 4\}$ noise and the initial guess k^0 (2.55), for Example 1.

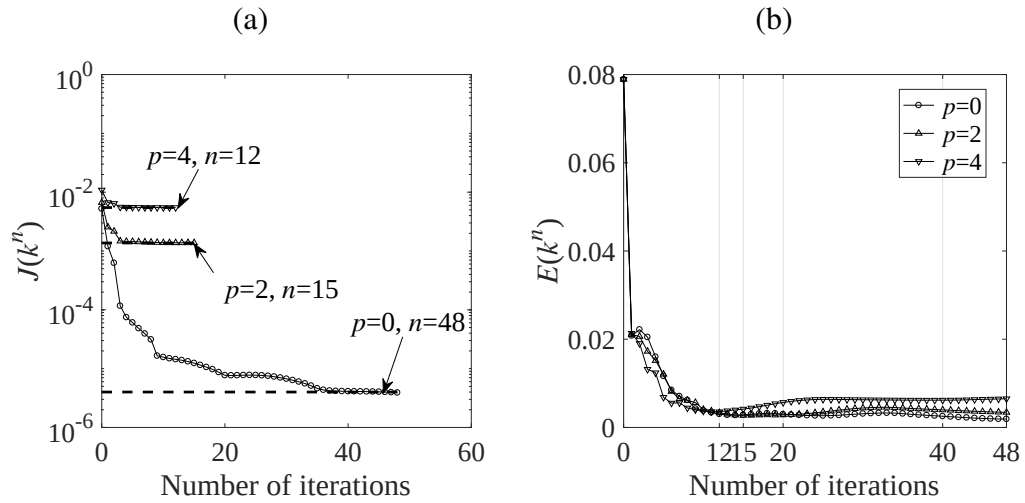

Figure 2.4: (a) The objective functional (2.5) and (b) the error $E(k^n)$ (2.28) with $p \in \{0, 2, 4\}$ noise and initial guess k^0 (2.56), using the H^1-gradient J'_H (2.21) and (2.22), for Example 1.

We consider this numerical example for estimating the unknown thermal conductivity $k(x)$ using the CGM, the C-N scheme of Section 2.6.1, and the L_2- and H^1-gradients. Figure 2.1(a) shows the monotonic decreasing convergence of the objective functional (2.5) that is minimized using the L_2-gradient J' (2.16), as a function of the number of iteration n, for various amounts of noise $p = 0$ (no noise) and $p \in \{2, 4\}$ noisy data generated by (2.29). For noisy data, the intersection of horizontal lines $y = \bar{\epsilon}$ with the

graphs of $J(k^n)$ yields that the stopping iteration numbers N_L for $p \in \{2, 4\}$, respectively, according to the discrepancy principle (2.26). These values are equal to the optimal ones obtained by plotting the error curves $E(k^n)$ (2.28) in Figure 2.1(b).

The numerical results using the L_2-gradient J' (2.16) are illustrated in Figure 2.3(a), and they are plotted at the stopping iteration numbers N_L in Table 2.1 for $p \in \{0, 2, 4\}$. From Figure 2.3(a) it can be seen that in the case of no noise $(p = 0)$, the retrieved solution is in very good agreement with the exact solution (2.54) (the curves are almost undistinguishable). However, in the case of noisy data, the retrieved numerical solution is less stable and accurate indicating the limitations of the CGM to deal with large amounts of noise, such as $p \in \{2, 4\}$, when inverting for the thermal conductivity coefficient.

				L_2-gradient (2.16)		H^1-gradient (2.21), (2.23)	
p	I	M	$\bar{\epsilon}$	N_L	$E(k^n)$	N_H	$E(k^n)$
0	51	51	1.0E-07	89	5.5E-04	17	1.1E-03
2	51	51	1.4E-03	15	7.5E-03	10	3.0E-03
4	51	51	5.5E-03	8	1.1E-02	4	3.6E-03

Table 2.1: The stopping iteration numbers N_L, N_H and the errors obtained by L_2- and H^1-gradient with $p \in \{0, 2, 4\}$ and the initial guess k^0 (2.55), for Example 1.

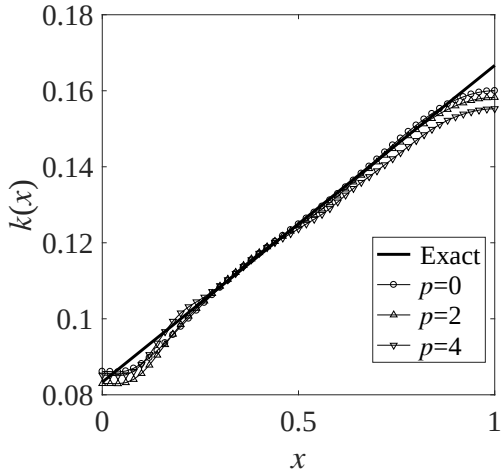

Figure 2.5: The numerical thermal conductivity $k(x)$ with $p \in \{0, 2, 4\}$ noise and initial guess k^0 (2.56), using the H^1-gradient J'_H (2.21) and (2.22), for Example 1.

In order to improve on the numerical results of Figure 2.3(a) for $p \in \{2, 4\}$ noise, the Sobolev gradient H^1-gradient (2.21) and the Dirichlet boundary condition (2.23) (instead of the conventional gradient L_2-gradient J' (2.16)) is employed, since the initial guess k^0

(2.55) provides the exact values of the thermal conductivity at the boundary values $x = 0$ and $x = 1$.

Figures 2.2(a) and 2.2(b) show the objective functional (2.5) and the error $E(k^n)$ (2.28) using the H^1-gradient (2.21) and (2.23), and by trial and error, $\kappa = 0.1$, with $p \in \{0, 2, 4\}$. Similar properties of the objective functional and errors as in Figures 2.1(a) and 2.1(b) are present, except for the different stopping iteration numbers. The numerical solutions in Figure 2.3(b) are stable and more accurate than those in Figure 2.3(a). The comparison of the stopping iteration numbers and errors are shown in Table 2.1, which indicates that the CGM with H^1-gradient (2.21) and (2.23) converges faster and obtain more accurate results than that using the L_2-gradient J' (2.16).

As there is a restriction on the initial guess k^0 (2.55) to ensure $k^0|_{\partial\Omega} = k|_{\partial\Omega}$ when using the L_2-gradient (2.16), in order to obtain a more robust method to reconstruct the unknown thermal conductivity, the H^1-gradient (2.21) and (2.22) is applied again for the arbitrary initial guess

$$k^0(x) = 0.2 \tag{2.56}$$

which does not satisfy that $k^0|_{\partial\Omega} = k|_{\partial\Omega}$.

Figures 2.4 and 2.5 illustrate the objective functional (2.5), the error $E(k^n)$ (2.28), and the numerical solutions of thermal conductivity $k(x)$ using the H^1-gradient J'_H (2.21), (2.22) and $\kappa = 0.1$, with $p \in \{0, 2, 4\}$ noise and initial guess k^0 (2.56). The stopping iteration numbers $n \in \{48, 15, 12\}$ in Figure 2.4(a) are obtained according to the discrepancy principle (2.26) with the values $\bar{\epsilon} \in \{4 \times 10^{-6}, 1.4 \times 10^{-3}, 5.5 \times 10^{-3}\}$, and the errors in Figure 2.4(b) at these iteration numbers are $\{1.9 \times 10^{-3}, 2.7 \times 10^{-3}, 3.5 \times 10^{-3}\}$ for $p \in \{0, 2, 4\}$.

The numerical results of the thermal conductivity in Figure 2.5 show that accurate and stable numerical results are achieved even for the initial guess (2.56). The numerical results in Figure 2.5 are almost as accurate as those in Figure 2.3(b), though the initial guess (2.56) is farther away from the exact solution (2.54) than the initial guess (2.55) which also satisfies $k^0|_{\partial\Omega} = k|_{\partial\Omega}$. The comparison of the numerical results in Figures 2.3(a), 2.3(b) and 2.5 confirms the conclusion that the CGM with the Sobolev gradient is a robust and stable method for retrieving the smooth space-dependent thermal conductivity.

2.6.4 Example 2

We now present a one-dimensional example where the input data for the temperature is numerically simulated by solving firstly the direct problem (2.1) using the C-N scheme

with $\mu(0,t) = -1$, $\mu(1,t) = 1$, $\phi \equiv 0$, $f \equiv 0$, $q \equiv 0$, and the discontinuous thermal conductivity

$$k(x) = \begin{cases} 2, & x \in \left(\frac{1}{5}, \frac{4}{5}\right), \\ 1, & \text{elsewhere.} \end{cases} \tag{2.57}$$

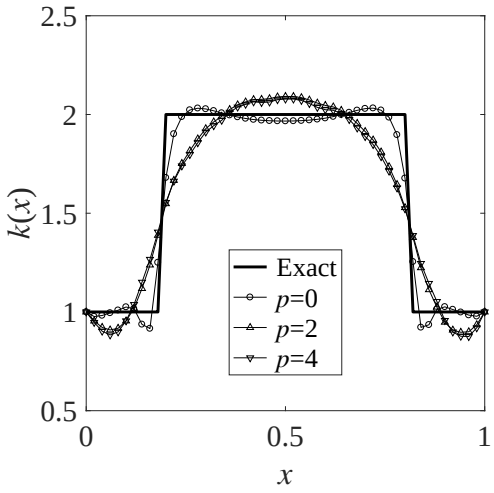

Figure 2.6: The numerical thermal conductivity $k(x)$ with $p \in \{0, 2, 4\}$ noise, for Example 2.

p	I	M	$\bar{\epsilon}$	N	$E(k^n)$
0	51	51	1.0E-07	18	0.0879
2	51	51	2.2E-05	11	0.1699
4	51	51	8.3E-05	5	0.1778

Table 2.2: The stopping iteration numbers N and the error with $p \in \{0, 2, 4\}$ noise in the estimation of $k(x)$, for Example 2.

We take the initial guess for the thermal conductivity $k(x)$ as

$$k^0(x) = 1. \tag{2.58}$$

The numerical solutions for the thermal conductivity $k(x)$ are presented in Figure 2.6 with $p \in \{0, 2, 4\}$ and the initial guess (2.58). The stopping iteration numbers and accuracy errors are shown in Table 2.2. From Figure 2.6 it is easy to see that the numerical results are stable and reasonably accurate bearing in mind the difficult discontinuous thermal conductivity (2.57) that had to be retrieved. There is also little difference between the numerical results obtained with $p = 2$ and $p = 4$ noise.

2.6.5 Example 3

For the two dimensional case $(\mathrm{d} = 2)$, we take $\Omega = (0,1) \times (0,1)$, the final time $T = 1$, the reaction coefficient $q \equiv 0$, the initial temperature $\phi \equiv 0$, and

$$\begin{aligned}
f(x_1,x_2,t) &= \left(e^{-t} + \frac{\pi^2}{6}(1+x_1+x_2)(1-e^{-t})\right)\sin(\pi x_1)\sin(\pi x_2) \\
&\quad + (\pi+1)e^{-t}(x_1+x_2) - \frac{1-e^{-t}}{12}(\pi\sin\pi(x_1+x_2) + 2\pi + 2), \\
\mu(0,x_2,t) &= -\frac{1+x_2}{12}(1-e^{-t})(\pi\sin\pi x_2 + \pi + 1), \\
\mu(1,x_2,t) &= \frac{2+x_2}{12}(1-e^{-t})(-\pi\sin\pi x_2 + \pi + 1), \\
\mu(x_1,0,t) &= -\frac{1+x_1}{12}(1-e^{-t})(\pi\sin\pi x_1 + \pi + 1), \\
\mu(x_1,1,t) &= \frac{2+x_1}{12}(1-e^{-t})(-\pi\sin\pi x_1 + \pi + 1),
\end{aligned}$$

and by the direct calculation for the problem (2.1), then the analytical solution of the inverse problem (2.1) and (2.4) is

$$\begin{aligned}
k(x_1,x_2) &= \frac{1+x_1+x_2}{12}, \\
u(x_1,x_2,t) &= (1-e^{-t})(\sin(\pi x_1)\sin(\pi x_2) + (\pi+1)(x_1+x_2)).
\end{aligned} \tag{2.59}$$

First, the initial guess is taken as

$$k^0(x_1,x_2) = \frac{1}{2}x_1x_2(1-x_1)(1-x_2) + \frac{1+x_1+x_2}{12} \tag{2.60}$$

so as to ensure that $k^0|_{\partial\Omega} = k|_{\partial\Omega}$. The numerical solutions are computed by using the ADI scheme in Section 2.6.2 with $I = J = 21$ and $M = 41$ to solve the two-dimensional parabolic differential equations. The standard L_2-gradient J' (2.16) and the Sobolev H^1-gradient J'_H (2.21), (2.23) shall be both applied in the CGM to obtain the numerical solution to the thermal conductivity $k(x_1,x_2)$ with the initial guess (2.60) and $p \in \{0,2,4\}$.

The stopping iteration numbers $N_L \in \{17,4,2\}$, $N_H \in \{3,2,2\}$ presented in Table 2.3 for L_2- and H^1-gradients, respectively, are generated by the discrepancy principle (2.26) with the values $\bar{\epsilon} \in \{1.6\times10^{-5}, 5.5\times10^{-3}, 2.1\times10^{-2}\}$ for $p \in \{0,2,4\}$. The comparison of the errors in Table 2.3 shows that the results obtained by H^1-gradient J'_H (2.21), (2.23) are more accurate. Meanwhile, by comparing the results in Figures 2.7 and 2.8, it can be seen that the use of the H^1-gradient J'_H improves significantly the smoothness and accuracy of the numerical solutions.

					L_2-gradient (2.16)		H^1-gradient (2.21), (2.23)	
p	I	J	M	$\bar{\epsilon}$	N_L	$E(k^n)$	N_H	$E(k^n)$
0	21	21	41	1.6E-05	17	3.8E-03	3	2.1E-03
2	21	21	41	5.5E-03	4	5.2E-03	2	2.9E-03
4	21	21	41	2.1E-02	2	6.5E-03	2	3.0E-03

Table 2.3: The stopping iteration numbers N_L, N_H and the errors obtained by L_2- and H^1-gradient with $p \in \{0, 2, 4\}$ and the initial guess (2.60) in the estimation of $k(x_1, x_2)$, for Example 3.

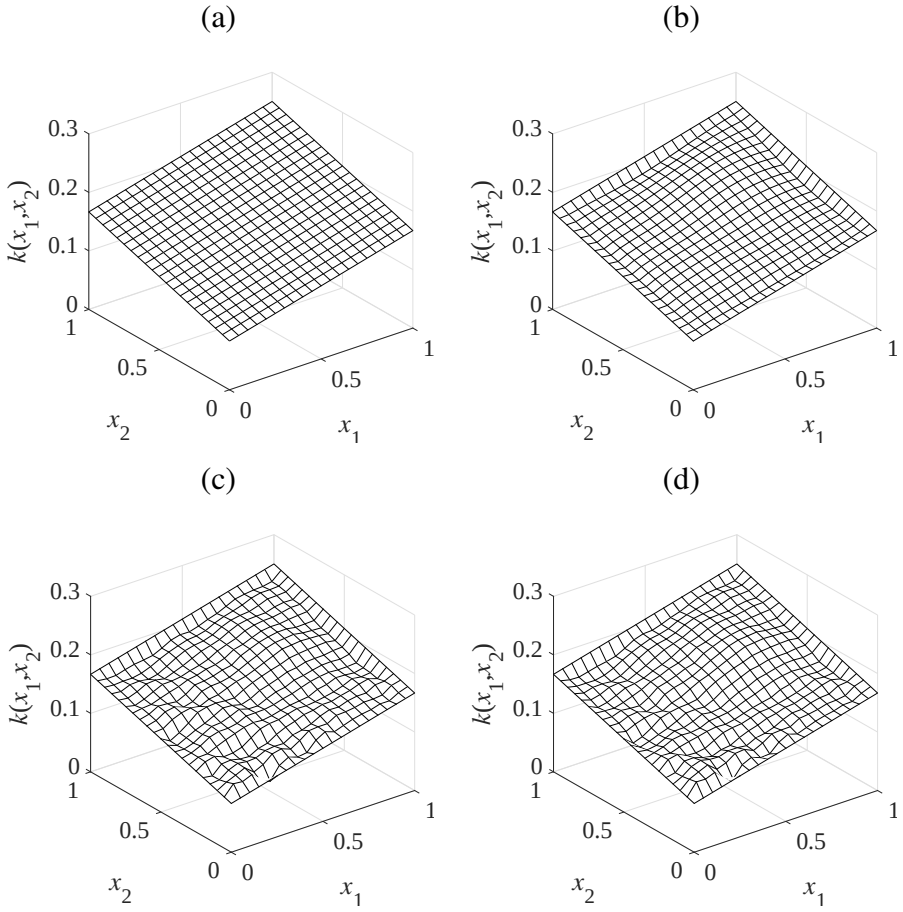

Figure 2.7: (a) The exact thermal conductivity $k(x_1, x_2)$ (2.59), and the estimated thermal conductivity $k(x_1, x_2)$ with (b) $p = 0$, (c) $p = 2$ and (d) $p = 4$ noise using the L_2-gradient J' (2.16) and the initial guess (2.60), for Example 3.

Like the discussions in Example 1, the initial guess is taken as

$$k^0(x_1, x_2) = \frac{1}{12}, \tag{2.61}$$

which is more arbitrary than the initial guess (2.60), and this initial guess is used to reconstruct the thermal conductivity $k(x_1, x_2)$ by the H^1-gradient (2.21) and (2.22).

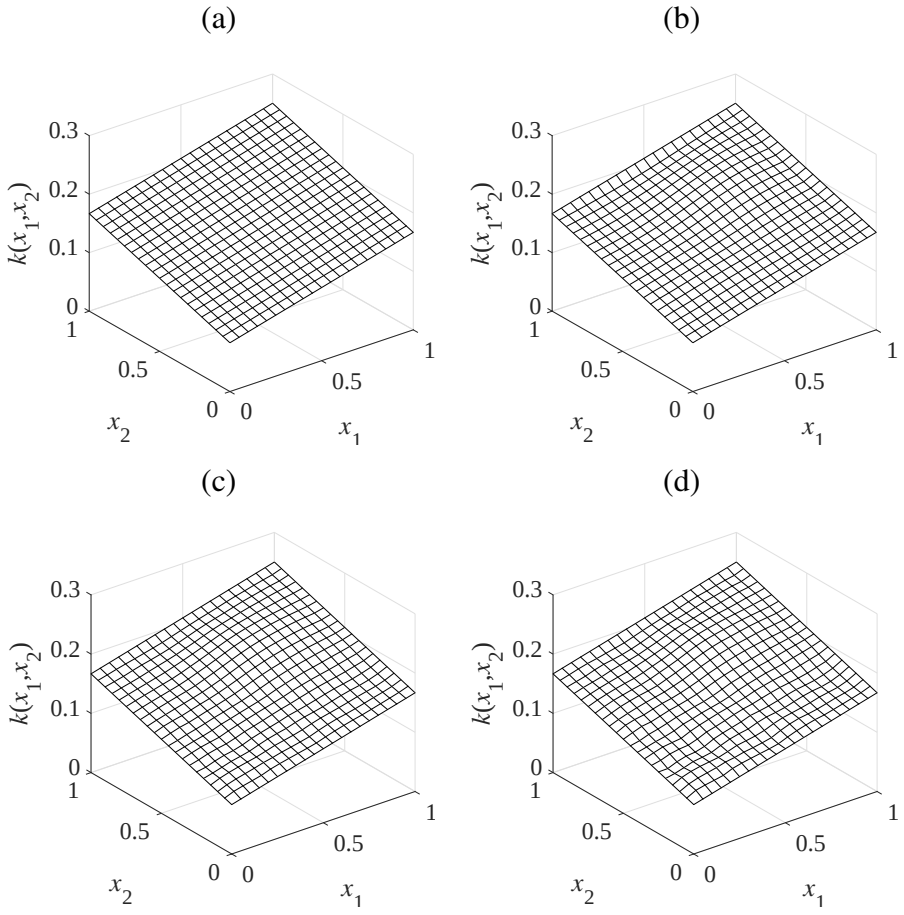

Figure 2.8: (a) The exact thermal conductivity $k(x_1, x_2)$ (2.59), and the estimated thermal conductivity $k(x_1, x_2)$ with (b) $p = 0$, (c) $p = 2$ and (d) $p = 4$ noise using the H^1-gradient J'_H (2.21), (2.23) and the initial guess (2.60), for Example 3.

					H^1-gradient (2.21),(2.22)	
p	I	J	M	$\bar{\epsilon}$	N_H	$E(k^n)$
0	21	21	41	1.3E-05	18	3.9E-03
2	21	21	41	5.5E-03	9	5.4E-03
4	21	21	41	2.1E-02	7	6.8E-03

Table 2.4: The stopping iteration numbers N_H and the error obtained by H^1-gradient (2.21) and (2.22) with $p \in \{0, 2, 4\}$ noise and the initial guess (2.61) in the estimation of $k(x_1, x_2)$, for Example 3.

The numerical solutions in Figure 2.9 for the thermal conductivity, and the stopping

iteration numbers N_H, errors in Table 2.4 are obtained by using the H^1-gradient (2.21) and $\kappa = 0.1$. The numerical results shown in Figure 2.9 confirm the stability of the obtained solutions as well as the robustness with respect to the initial guess of the iterative CGM with Sobolev gradient. It can also be remarked that the numerical results shown in Figure 2.8 are more accurate than those obtained in Figure 2.9, because the initial guess (2.60) is closer to the exact solution (2.59) than the initial guess (2.61), and especially because the initial guess (2.60) and the exact solution (2.59) share the same boundary values.

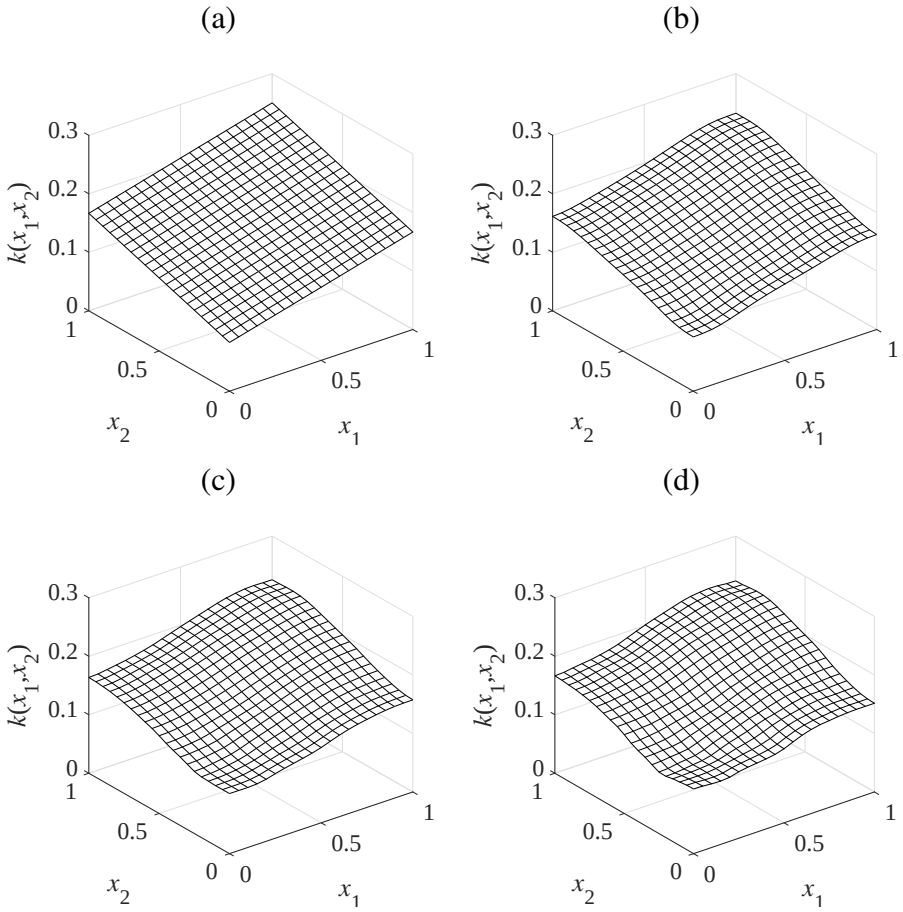

Figure 2.9: (a) The exact thermal conductivity $k(x_1, x_2)$ (2.59), and the estimated thermal conductivity $k(x_1, x_2)$ with (b) $p = 0$, (c) $p = 2$ and (d) $p = 4$ noise using the H^1-gradient J'_H (2.21), (2.22) and the initial guess (2.61), for Example 3.

2.7 Conclusions

The reconstruction of the space-dependent isotropic thermal conductivity in IHTP from interior temperature observations has been investigated using the CGM. The CGM is

based on the Fréchet gradient of the least-squares objective functional, minimizing the gap between the computed and the measured temperature. The use of the Sobolev gradient in the CGM yields smoother and more accurate numerical results. Regularization has been achieved by stopping the iterations at the level at which the objective functional becomes just below the noise threshold with which the data is contaminated. The numerical results show that CGM is an accurate, stable and robust regularization method for reconstructing the space-dependent thermal conductivity from interior temperature observations.

In the next chapter we extend the analysis for identifying a space-dependent orthotropic thermal conductivity from interior temperature observations.

Chapter 3

Determination of the space-dependent thermal conductivity of an orthotropic material

3.1 Introduction

Prior to this study, the identification of piecewise constant or linearly dependent functionally graded anisotropic materials was investigated in Harris *et al.* (2008); Lesnic *et al.* (2007) using the genetic algorithm for the resulting finite dimensional optimization problem. However, in many materials, e.g. thermally bonded nonwovens, Demirci *et al.* (2012), the principal directions are orthogonal and then the anisotropic structure is called orthotropic. Such simplified orthotropic structures have important characteristics and several inverse analyses have been undertaken, Mejias *et al.* (1999); Sawaf & Özisik (1995), for their estimation. Further, an experimental device for the simultaneous estimation of the constant thermal conductivity and the specific heat of orthotropic polymer composite materials was presented in Thomas *et al.* (2010). However, in all these studies the material properties were piecewise constant or linearly space-dependent and this restricts the generality of the materials that can be identified. In reality, many materials are highly heterogeneous and therefore simplified assumptions such as having uniform or linearly varying in space properties are not appropriate.

Therefore, in order to meet this generality manifested by inhomogeneous materials, the more general infinite dimensional problem is considered in which no prior information about the functional form of the space-dependent thermal conductivity is assumed. Furthermore, the CGM is developed for solving iteratively the resulting optimization problem and obtaining the numerical solution of the unknown thermal conductivity.

The mathematical formulation of the inverse problem to identify the unknown space-dependent orthotropic thermal conductivity is given in Section 3.2. Such inverse problem is analysed in Section 3.3, and the Fréchet gradient together with the adjoint problem are obtained. The gradient is then applied to establish the CGM in Section 3.4. Section 3.5 presents a numerical example illustrating that stable and accurate numerical results are obtained. Finally, conclusions are highlighted in Section 3.6.

3.2 Mathematical formulation

As a mathematical model, consider a two-dimensional, transient heat transfer problem in an orthotropic square plate $\Omega = (0,1)\times(0,1)$, over the time interval from the initial time $t = 0$ to a given final time $t = T > 0$. The governing equation is given by the following parabolic heat equation:

$$\begin{aligned}\frac{\partial u}{\partial t}(x_1,x_2,t) = \frac{\partial}{\partial x_1}\left(k_{11}(x_1,x_2)\frac{\partial u}{\partial x_1}(x_1,x_2,t)\right) + \frac{\partial}{\partial x_2}\left(k_{22}(x_1,x_2)\frac{\partial u}{\partial x_2}(x_1,x_2,t)\right)\\ - q(x_1,x_2)u(x_1,x_2,t) + f(x_1,x_2,t), \quad (x_1,x_2,t)\in Q_T = \Omega\times(0,T),\end{aligned} \tag{3.1}$$

where $u(x_1,x_2,t)$ is the temperature, $k_{11}(x_1,x_2)$ and $k_{22}(x_1,x_2)$ are the positive space-dependent components of the orthotropic thermal conductivity tensor $k = \begin{bmatrix} k_{11} & 0 \\ 0 & k_{22}\end{bmatrix}$, $q(x_1,x_2)$ is the reaction coefficient, $f(x_1,x_2,t)$ is the heat source term and, for simplicity, the heat capacity has been assumed constant and taken to be unity. For the boundary condition we assume that this is of Neumann type

$$\begin{cases} -k_{11}(0,x_2)\frac{\partial u}{\partial x_1}(0,x_2,t) = \mu_1(x_2,t), & (x_2,t)\in(0,1)\times(0,T),\\ k_{11}(1,x_2)\frac{\partial u}{\partial x_1}(1,x_2,t) = \mu_2(x_2,t), & (x_2,t)\in(0,1)\times(0,T),\\ -k_{22}(x_1,0)\frac{\partial u}{\partial x_2}(x_1,0,t) = \mu_3(x_1,t), & (x_1,t)\in(0,1)\times(0,T),\\ k_{22}(x_1,1)\frac{\partial u}{\partial x_2}(x_1,1,t) = \mu_4(x_1,t), & (x_1,t)\in(0,1)\times(0,T),\end{cases} \tag{3.2}$$

where $\mu_i|_{i=\overline{1,4}}$ are the given heat fluxes. Dirichlet, mixed or Robin boundary conditions can also be considered. The initial condition is

$$u(x_1,x_2,0) = \phi(x_1,x_2), \quad (x_1,x_2)\in\overline{\Omega}, \tag{3.3}$$

where $\phi(x_1,x_2)$ is the given initial temperature. The direct problem is concerned with the determination of the temperature $u(x_1,x_2,t)$ satisfying the initial-boundary value problem (3.1)–(3.3), when $q(x_1,x_2)$, $f(x_1,x_2,t)$ and the thermal conductivity components $k_{11}(x_1,x_2)$ and $k_{22}(x_1,x_2)$ are known.

Definition 3.2.1. *A function $u \in H^{1,0}(Q_T)$ is called as a weak solution to the initial-boundary value problem (3.1)–(3.3) if*

$$\begin{aligned}
&\int_{Q_T} \left(-u\frac{\partial \eta}{\partial t} + k_{11}\frac{\partial u}{\partial x_1}\frac{\partial \eta}{\partial x_1} + k_{22}\frac{\partial u}{\partial x_2}\frac{\partial \eta}{\partial x_2} + qu\eta \right) dx_1 dx_2 dt \\
&= \int_0^T \int_0^1 (\mu_1 + \mu_2)\eta dx_2 dt + \int_0^T \int_0^1 (\mu_3 + \mu_4)\eta dx_1 dt \\
&\quad + \int_{Q_T} f\eta dx_1 dx_2 dt + \int_\Omega \phi\eta(\cdot, 0) dx_1 dx_2, \quad \forall \eta \in H^{1,1}(Q_T),\ \eta(\cdot, T) = 0. \qquad (3.4)
\end{aligned}$$

The existence and uniqueness of the weak solution $u \in H^{1,0}(Q_T)$ to the initial-boundary value problem (3.1)–(3.3) is presented as follows (see Tröltzsch (2010), p.373):

Theorem 3.2.2. *Let $\Omega \subset \mathbb{R}^2$ be a bounded Lipschitz domain, and suppose that the functions $q \in L_\infty(\Omega)$, $f \in L_2(Q_T)$, $\mu_i \in L_2((0,1) \times (0,T))$, $i = \overline{1,4}$, $\phi \in L_2(\Omega)$, and $0 < \upsilon \leq k_{11}, k_{22} \in L_\infty(\Omega)$, where υ is a given positive constant. Then the initial-boundary value problem (3.1)–(3.3) has a unique weak solution $u \in H^{1,0}(Q_T)$. Moreover, the solution satisfies the estimate*

$$\begin{aligned}
&\max_{t\in[0,T]} \|u(\cdot, t)\|_{L_2(\Omega)} + \|u\|_{H^{1,0}(Q_T)} \\
&\leq c \left(\|f\|_{L_2(Q_T)} + \sum_{i=1}^{4} \|\mu_i\|_{L_2((0,1)\times(0,T))} + \|\phi\|_{L_2(\Omega)} \right) \qquad (3.5)
\end{aligned}$$

with a positive constant c which is independent of f, $\mu_i|_{i=\overline{1,4}}$, and ϕ.

The inverse problem, on the other hand, is to simultaneously determine the unknown thermal conductivity components $k_{11}(x_1, x_2)$ and $k_{22}(x_1, x_2)$ satisfying (3.1)–(3.3) and the additional interior temperature measurement

$$u(x_1, x_2, t) = Y(x_1, x_2, t), \quad (x_1, x_2, t) \in Q_T, \qquad (3.6)$$

where $Y(x_1, x_2, t)$ is the given exact data.

3.3 Analysis

Let $u(x_1, x_2, t; k_{11}, k_{22})$ denote the solution of the initial-boundary value problem (3.1)–(3.3), that is, the temperature corresponding to a particular value of the pair (k_{11}, k_{22}). The quasi-solution to the inverse problem (3.1)–(3.3), (3.6) is obtained by minimizing the following least-squares objective functional:

$$J(k_{11}, k_{22}) = \frac{1}{2} \|u(k_{11}, k_{22}) - Y^\epsilon\|^2_{L_2(Q_T)}, \qquad (3.7)$$

where $Y^\epsilon \in L_2(Q_T)$ is the noisy measured temperature satisfying

$$\|Y - Y^\epsilon\|_{L_2(Q_T)} \leq \epsilon,$$

and $\epsilon \geq 0$ represents the noise level, subject to $u \in H^{1,0}(Q_T)$ which is the weak solution to the initial-boundary value direct problem (3.1)–(3.3) satisfying (3.4), over the admissible set

$$\mathcal{A} = \{(k_{11}, k_{22}) \in L_\infty(\Omega) \times L_\infty(\Omega) : 0 < \kappa_1 \leq k_{11} \text{ and } k_{22} \leq \kappa_2\}, \tag{3.8}$$

where κ_1 and κ_2 are two given positive constants.

Theorem 3.3.1. *There exists at least one minimizer to the optimization problem* (3.7).

Theorem 3.3.1 can be proved using the methods in the proof of Theorem 2.4.1.

Lemma 3.3.2. *The mapping* $(k_{11}, k_{22}) \mapsto u(k_{11}, k_{22})$ *is Lipschitz continuous from* $\mathcal{A}$ *to* $H^{1,0}(Q_T)$*, i.e.,*

$$\|u(k_{11} + \Delta k_{11}, k_{22}) - u(k_{11}, k_{22})\|_{H^{1,0}(Q_T)} \leq c\|\Delta k_{11}\|_{L_\infty(\Omega)}, \tag{3.9}$$

$$\|u(k_{11}, k_{22} + \Delta k_{22}) - u(k_{11}, k_{22})\|_{H^{1,0}(Q_T)} \leq c\|\Delta k_{22}\|_{L_\infty(\Omega)}, \tag{3.10}$$

for any (k_{11}, k_{22}), $(k_{11} + \Delta k_{11}, k_{22} + \Delta k_{22}) \in \mathcal{A}$ *and the corresponding temperature* $u(k_{11}, k_{22}), u(k_{11} + \Delta k_{11}, k_{22}), u(k_{11}, k_{22} + \Delta k_{22}) \in H^{1,0}(Q_T)$.

Proof. Denote $\Delta u_{11} = u(k_{11}+\Delta k_{11}, k_{22}) - u(k_{11}, k_{22})$ and $\Delta u_{22} = u(k_{11}, k_{22}+\Delta k_{22}) - u(k_{11}, k_{22})$ be the increments of the temperature subject to increments in k_{11} and k_{22}, respectively. According to the initial-boundary value problem (3.1)–(3.3), Δu_{11} satisfies the following problem:

$$\begin{cases} \frac{\partial(\Delta u_{11})}{\partial t} = \frac{\partial}{\partial x_1}\left(k_{11}\frac{\partial(\Delta u_{11})}{\partial x_1}\right) + \frac{\partial}{\partial x_2}\left(k_{22}\frac{\partial(\Delta u_{11})}{\partial x_2}\right) \\ \qquad\qquad + \frac{\partial}{\partial x_1}\left(\Delta k_{11}\frac{\partial u}{\partial x_1}\right) - q\Delta u_{11}, & (x_1, x_2, t) \in Q_T, \\ -k_{11}\frac{\partial(\Delta u_{11})}{\partial x_1}\Big|_{x_1=0} = \Delta k_{11}\frac{\partial u}{\partial x_1}\Big|_{x_1=0}, & (x_2, t) \in (0,1)\times(0,T), \\ k_{11}\frac{\partial(\Delta u_{11})}{\partial x_1}\Big|_{x_1=1} = -\Delta k_{11}\frac{\partial u}{\partial x_1}\Big|_{x_1=1}, & (x_2, t) \in (0,1)\times(0,T), \\ -k_{22}\frac{\partial(\Delta u_{22})}{\partial x_2}\Big|_{x_2=0} = k_{22}\frac{\partial(\Delta u_{22})}{\partial x_2}\Big|_{x_2=1} = 0, & (x_1, t) \in (0,1)\times(0,T), \\ \Delta u_{11}(x_1, x_2, 0) = 0, & (x_1, x_2) \in \overline{\Omega}. \end{cases} \tag{3.11}$$

Multiplying Δu_{11} for (3.11), and integrating it over Q_T, then we get

$$\int_{Q_T} \frac{\partial}{\partial x_1}\left(k_{11}\frac{\partial(\Delta u_{11})}{\partial x_1}\right)\Delta u_{11}dx_1dx_2dt = \int_0^T\int_0^1 k_{11}\Delta u_{11}\frac{\partial(\Delta u_{11})}{\partial x_1}\Big|_{x_1=0}^1 dx_2dt - \int_{Q_T} k_{11}\left(\frac{\partial(\Delta u_{11})}{\partial x_1}\right)^2 dx_1dx_2dt,$$

$$\int_{Q_T} \frac{\partial}{\partial x_2}\left(k_{22}\frac{\partial(\Delta u_{11})}{\partial x_2}\right)\Delta u_{11}dx_1dx_2dt = \int_0^T\int_0^1 k_{22}\Delta u_{11}\left.\frac{\partial(\Delta u_{11})}{\partial x_2}\right|_{x_2=0}^1 dx_1dt - \int_{Q_T} k_{22}\left(\frac{\partial(\Delta u_{11})}{\partial x_2}\right)^2 dx_1dx_2dt,$$

and

$$\int_{Q_T} \frac{\partial}{\partial x_1}\left(\Delta k_{11}\frac{\partial u}{\partial x_1}\right)\Delta u_{11}dx_1dx_2dt = \int_0^T\int_0^1 \Delta k_{11}\Delta u_{11}\left.\frac{\partial u}{\partial x_1}\right|_{x=0}^1 dx_2dt - \int_{Q_T} \Delta k_{11}\frac{\partial u}{\partial x_1}\frac{\partial(\Delta u_{11})}{\partial x_1}dx_1dx_2dt.$$

Using the boundary conditions in (3.11), we obtain

$$\frac{1}{2}\int_0^T \frac{d}{dt}\|\Delta u_{11}(\cdot,t)\|^2_{L_2(\Omega)}dt = -\int_{Q_T}\Delta k_{11}\frac{\partial u}{\partial x_1}\frac{\partial(\Delta u_{11})}{\partial x_1}dx_1dx_2dt - \int_{Q_T}\left\{k_{11}\left(\frac{\partial(\Delta u_{11})}{\partial x_1}\right)^2 + k_{22}\left(\frac{\partial(\Delta u_{11})}{\partial x_2}\right)^2 + q(\Delta u_{11})^2\right\}dx_1dx_2dt \tag{3.12}$$

which implies that $\|\Delta u_{11}\|^2_{H^{1,0}(Q_T)} \le c\|\Delta k_{11}\|_{L_\infty(\Omega)}\left\|\frac{\partial u}{\partial x_1}\right\|_{L_2(Q_T)}\left\|\frac{\partial(\Delta u_{11})}{\partial x_1}\right\|_{L_2(Q_T)}$. Using the estimate (3.5) of Theorem 3.2.2, we obtain $\|\Delta u_{11}\|_{H^{1,0}(Q_T)} \le c\|\Delta k_{11}\|_{L_\infty(\Omega)}$.

Similarly, Δu_{22} satisfies the following problem:

$$\begin{cases} \frac{\partial(\Delta u_{22})}{\partial t} = \frac{\partial}{\partial x_1}\left(k_{11}\frac{\partial(\Delta u_{22})}{\partial x_1}\right) + \frac{\partial}{\partial x_2}\left(k_{22}\frac{\partial(\Delta u_{22})}{\partial x_2}\right) \\ \qquad\qquad + \frac{\partial}{\partial x_2}\left(\Delta k_{22}\frac{\partial u}{\partial x_2}\right) - q\Delta u_{22}, & (x_1,x_2,t)\in Q_T, \\ -k_{11}\left.\frac{\partial(\Delta u_{22})}{\partial x_1}\right|_{x_1=0} = k_{11}\left.\frac{\partial(\Delta u_{22})}{\partial x_1}\right|_{x_1=1} = 0, & (x_2,t)\in(0,1)\times(0,T), \\ -k_{22}\left.\frac{\partial(\Delta u_{22})}{\partial x_2}\right|_{x_2=0} = \Delta k_{22}\left.\frac{\partial u}{\partial x_2}\right|_{x_2=0}, & (x_1,t)\in(0,1)\times(0,T), \\ k_{22}\left.\frac{\partial(\Delta u_{22})}{\partial x_2}\right|_{x_2=1} = -\Delta k_{22}\left.\frac{\partial u}{\partial x_2}\right|_{x_2=1}, & (x_1,t)\in(0,1)\times(0,T), \\ \Delta u_{22}(x_1,x_2,0) = 0, & (x_1,x_2)\in\overline{\Omega}, \end{cases} \tag{3.13}$$

and we can obtain $\|\Delta u_{22}\|_{H^{1,0}(Q_T)} \le c\|\Delta k_{22}\|_{L_\infty(\Omega)}$. The lemma is proved. □

Note that the problems (3.11) and (3.13) are the sensitivity problems subject to the thermal conductivity components k_{11} and k_{22}, respectively, which shall be utilized in the establishment of the CGM later for the numerical reconstruction of the unknown thermal conductivity components k_{11} and k_{22}.

Lemma 3.3.3. *The mapping $(k_{11},k_{22}) \mapsto u(k_{11},k_{22})$ is Fréchet differentiable, i.e., for any $\Delta k_{11},\Delta k_{22}\in L_\infty(\Omega)$ such that $k_{11}+\Delta k_{11}, k_{22}+\Delta k_{22}\in\mathcal{A}$ there exist two bounded*

linear operators $\mathcal{U}_{11}, \mathcal{U}_{22} : \mathcal{A} \mapsto H^{1,0}(Q_T)$ *such that*

$$\lim_{\|\Delta k_{11}\|_{L_\infty(\Omega)}\to 0} \frac{\|u(k_{11}+\Delta k_{11}, k_{22}) - u(k_{11}, k_{22}) - \mathcal{U}_{11}\Delta k_{11}\|_{H^{1,0}(Q_T)}}{\|\Delta k_{11}\|_{L_\infty(\Omega)}} = 0, \tag{3.14}$$

$$\lim_{\|\Delta k_{22}\|_{L_\infty(\Omega)}\to 0} \frac{\|u(k_{11}, k_{22}+\Delta k_{22}) - u(k_{11}, k_{22}) - \mathcal{U}_{22}\Delta k_{22}\|_{H^{1,0}(Q_T)}}{\|\Delta k_{22}\|_{L_\infty(\Omega)}} = 0. \tag{3.15}$$

Proof. Consider the problem

$$\begin{cases} \frac{\partial w}{\partial t} = \frac{\partial}{\partial x_1}\left(k_{11}\frac{\partial w}{\partial x_1}\right) + \frac{\partial}{\partial x_2}\left(k_{22}\frac{\partial w}{\partial x_2}\right) - qw + \frac{\partial}{\partial x_1}\left(\Delta k_{11}\frac{\partial u}{\partial x_1}\right), & (x_1,x_2,t)\in Q_T,\\ -k_{11}\left.\frac{\partial w}{\partial x_1}\right|_{x_1=0} = \Delta k_{11}\left.\frac{\partial u}{\partial x_1}\right|_{x_1=0}, & (x_2,t)\in(0,1)\times(0,T),\\ k_{11}\left.\frac{\partial w}{\partial x_1}\right|_{x_1=1} = -\Delta k_{11}\left.\frac{\partial u}{\partial x_1}\right|_{x_1=1}, & (x_2,t)\in(0,1)\times(0,T),\\ -k_{22}\left.\frac{\partial w}{\partial x_2}\right|_{x_2=0} = k_{22}\left.\frac{\partial w}{\partial x_2}\right|_{x_2=1} = 0, & (x_1,t)\in(0,1)\times(0,T),\\ w(x_1,x_2,0) = 0, & (x_1,x_2)\in\overline{\Omega}. \end{cases} \tag{3.16}$$

where $\Delta k_{11} \in L_\infty(\Omega)$ is such that $k_{11} + \Delta k_{11} \in \mathcal{A}$. Similar as in (3.12), we have

$$\frac{1}{2}\int_0^T \frac{d}{dt}\|w(\cdot,t)\|^2_{L_2(\Omega)}dt = -\int_{Q_T}\left\{k_{11}\left(\frac{\partial w}{\partial x_1}\right)^2 + k_{22}\left(\frac{\partial w}{\partial x_2}\right)^2 + qw^2\right\}dx_1dx_2dt - \int_{Q_T}\Delta k_{11}\frac{\partial u}{\partial x_1}\frac{\partial w}{\partial x_1}dx_1dx_2dt,$$

which implies that $\|w\|^2_{H^{1,0}(Q_T)} \le c\|\Delta k_{11}\|_{L_\infty(\Omega)}\left\|\frac{\partial u}{\partial x_1}\right\|_{L_2(Q_T)}\left\|\frac{\partial w}{\partial x_1}\right\|_{L_2(Q_T)}$. Thus, the mapping $\Delta k_{11} \mapsto w$ from $L_\infty(\Omega)$ to $H^{1,0}(Q_T)$ defines a bounded linear operator $\mathcal{U}_{11}$.

Denote $v := u(k_{11}+\Delta k_{11}, k_{22}) - u(k_{11}, k_{22}) - \mathcal{U}_{11}\Delta k_{11} = \Delta u_{11} - \mathcal{U}_{11}\Delta k_{11}$, where Δu_{11} satisfies the problem (3.11). Thus, the function v satisfies the problem given by

$$\begin{cases} \frac{\partial v}{\partial t} = \frac{\partial}{\partial x_1}\left(k_{11}\frac{\partial v}{\partial x_1}\right) + \frac{\partial}{\partial x_2}\left(k_{22}\frac{\partial v}{\partial x_2}\right) - qv + \frac{\partial}{\partial x_1}\left(\Delta k_{11}\frac{\partial(\Delta u_{11})}{\partial x_1}\right), & (x_1,x_2,t)\in Q_T,\\ -k_{11}\left.\frac{\partial v}{\partial x_1}\right|_{x_1=0} = \Delta k_{11}\left.\frac{\partial(\Delta u_{11})}{\partial x_1}\right|_{x_1=0}, & (x_2,t)\in(0,1)\times(0,T),\\ k_{11}\left.\frac{\partial v}{\partial x_1}\right|_{x_1=1} = -\Delta k_{11}\left.\frac{\partial(\Delta u_{11})}{\partial x_1}\right|_{x_1=1}, & (x_2,t)\in(0,1)\times(0,T),\\ -k_{22}\left.\frac{\partial v}{\partial x_2}\right|_{x_2=0} = k_{22}\left.\frac{\partial v}{\partial x_2}\right|_{x_2=1} = 0, & (x_1,t)\in(0,1)\times(0,T),\\ v(x_1,x_2,0) = 0, & (x_1,x_2)\in\overline{\Omega}. \end{cases}$$

Then we have

$$\frac{1}{2}\int_0^T \frac{d}{dt}\|v(\cdot,t)\|^2_{L_2(\Omega)}dt = -\int_{Q_T}\left\{k_{11}\left(\frac{\partial v}{\partial x_1}\right)^2 + k_{22}\left(\frac{\partial v}{\partial x_2}\right)^2 + qv^2\right\}dx_1dx_2dt - \int_{Q_T}\Delta k_{11}\frac{\partial(\Delta u_{11})}{\partial x_1}\frac{\partial v}{\partial x_1}dx_1dx_2dt,$$

which implies that $\|v\|^2_{H^{1,0}(Q_T)} \leq c\|\Delta k_{11}\|_{L_\infty(\Omega)} \left\|\frac{\partial(\Delta u_{11})}{\partial x_1}\right\|_{L_2(Q_T)} \left\|\frac{\partial v}{\partial x_1}\right\|_{L_2(Q_T)}$. Using (3.9) of Lemma 3.3.2, we obtain $\|v\|_{H^{1,0}(Q_T)} \leq c\|\Delta k_{11}\|^2_{L_\infty(\Omega)}$, which means (3.14) holds, and (3.15) can be obtained by the same approach. The lemma is proved. □

To find the minimizer of the objective functional $J(k_{11}, k_{22})$ (3.7), the CGM, where the Fréchet gradient is required, shall be applied. Consequently, we introduce the adjoint problem given by:

$$\begin{cases} \frac{\partial \lambda}{\partial t} = -\frac{\partial}{\partial x_1}\left(k_{11}\frac{\partial \lambda}{\partial x_1}\right) - \frac{\partial}{\partial x_2}\left(k_{22}\frac{\partial \lambda}{\partial x_2}\right) + q\lambda - (u - Y^\epsilon), & (x_1, x_2, t) \in Q_T, \\ -k_{11}\left.\frac{\partial \lambda}{\partial x_1}\right|_{x_1=0} = k_{11}\left.\frac{\partial \lambda}{\partial x_1}\right|_{x_1=1} = 0, & (x_2, t) \in (0,1)\times(0,T), \\ -k_{22}\left.\frac{\partial \lambda}{\partial x_2}\right|_{x_2=0} = k_{22}\left.\frac{\partial \lambda}{\partial x_2}\right|_{x_2=1} = 0, & (x_1, t) \in (0,1)\times(0,T), \\ \lambda(x_1, x_2, T) = 0, & (x_1, x_2) \in \overline{\Omega}. \end{cases} \tag{3.17}$$

The weak solution $\lambda \in H^{1,0}(Q_T)$ of the adjoint problem (3.17) satisfies the variational equality

$$\int_{Q_T}\left(\lambda\frac{\partial \eta}{\partial t} + k_{11}\frac{\partial \lambda}{\partial x_1}\frac{\partial \eta}{\partial x_1} + k_{22}\frac{\partial \lambda}{\partial x_2}\frac{\partial \lambda}{\partial x_2} + q\lambda\eta\right)dx_1dx_2dt = \int_{Q_T}(u - Y^\epsilon)\eta dx_1dx_2dt,$$

for any $\eta \in H^{1,1}(Q_T)$ with $\eta(\cdot, 0) = 0$, and there exists a positive constant c, which does not depend on the given functions, such that

$$\|\lambda\|_{H^{1,0}(Q_T)} \leq c\|u - Y^\epsilon\|_{L_2(Q_T)}. \tag{3.18}$$

Theorem 3.3.4. *The objective functional $J(k_{11}, k_{22})$ given by (3.7) is Fréchet differentiable, and the gradients $J'_{11}(k_{11}, k_{22})$ and $J'_{22}(k_{11}, k_{22})$ with respect to k_{11} and k_{22} are given by*

$$J'_{11}(k_{11}, k_{22}) = -\int_0^T \frac{\partial u}{\partial x_1}\frac{\partial \lambda}{\partial x_1}dt, \tag{3.19}$$

$$J'_{22}(k_{11}, k_{22}) = -\int_0^T \frac{\partial u}{\partial x_2}\frac{\partial \lambda}{\partial x_2}dt. \tag{3.20}$$

Proof. Taking $\Delta k_{11} \in L_\infty(\Omega)$ such that $k_{11} + \Delta k_{11} \in \mathcal{A}$, denote $\Delta J_{11} = J(k_{11} + \Delta k_{11}, k_{22}) - J(k_{11}, k_{22})$, and by (3.7), we obtain

$$\Delta J_{11} = \int_{Q_T}(u - Y^\epsilon)\Delta u_{11}dx_1dx_2dt + \frac{1}{2}\|\Delta u_{11}\|^2_{L_2(Q_T)}.$$

Using the adjoint problem (3.17), we have

$$\Delta J_{11} = \int_{Q_T}\left\{-\frac{\partial \lambda}{\partial t} - \frac{\partial}{\partial x_1}\left(k_{11}\frac{\partial \lambda}{\partial x_1}\right) - \frac{\partial}{\partial x_2}\left(k_{22}\frac{\partial \lambda}{\partial x_2}\right) + q\lambda\right\}\Delta u_{11}dx_1dx_2dt + \frac{1}{2}\|\Delta u_{11}\|^2_{L_2(Q_T)},$$

and the sensitivity problem for Δu_{11} (3.11) implies

$$\begin{aligned}
&\int_{Q_T}\left\{-\frac{\partial\lambda}{\partial t}-\frac{\partial}{\partial x_1}\left(k_{11}\frac{\partial\lambda}{\partial x_1}\right)-\frac{\partial}{\partial x_2}\left(k_{22}\frac{\partial\lambda}{\partial x_2}\right)+q\lambda\right\}\Delta u_{11}dx_1dx_2dt\\
&=\int_{Q_T}\lambda\left\{\frac{\partial(\Delta u_{11})}{\partial t}-\frac{\partial}{\partial x_1}\left(k_{11}\frac{\partial(\Delta u_{11})}{\partial x_1}\right)-\frac{\partial}{\partial x_2}\left(k_{22}\frac{\partial(\Delta u_{11})}{\partial x_2}\right)\right\}dx_1dx_2dt\\
&\quad+\int_{Q_T}\lambda q\Delta u_{11}dx_1dx_2dt+\int_0^T\int_0^1\lambda k_{11}\left.\frac{\partial(\Delta u_{11})}{\partial x_1}\right|_{x_1=0}^{1}dx_2dt-\int_\Omega\Delta u_{11}\lambda|_{t=0}^{T}dx_1dx_2\\
&=\int_{Q_T}\lambda\frac{\partial}{\partial x_1}\left(\Delta k_{11}\frac{\partial u}{\partial x_1}\right)dx_1dx_2dt+\int_0^T\int_0^1\lambda k_{11}\left.\frac{\partial(\Delta u_{11})}{\partial x_1}\right|_{x_1=0}^{1}dx_2dt.
\end{aligned}$$

Via integration by parts, we get

$$\begin{aligned}
\int_{Q_T}\lambda\frac{\partial}{\partial x_1}\left(\Delta k_{11}\frac{\partial u}{\partial x_1}\right)dx_1dx_2dt=&\int_0^T\int_0^1\lambda\Delta k_{11}\left.\frac{\partial u}{\partial x_1}\right|_{x_1=0}^{1}dx_2dt\\
&-\int_{Q_T}\Delta k_{11}\frac{\partial u}{\partial x_1}\frac{\partial\lambda}{\partial x_1}dx_1dx_2dt,
\end{aligned}$$

and then

$$\begin{aligned}
&\int_{Q_T}\left\{-\frac{\partial\lambda}{\partial t}-\frac{\partial}{\partial x_1}\left(k_{11}\frac{\partial\lambda}{\partial x_1}\right)-\frac{\partial}{\partial x_2}\left(k_{22}\frac{\partial\lambda}{\partial x_2}\right)+q\lambda\right\}\Delta u_{11}dx_1dx_2dt\\
&=-\int_{Q_T}\Delta k_{11}\frac{\partial u}{\partial x_1}\frac{\partial\lambda}{\partial x_1}dx_1dx_2dt.
\end{aligned}$$

Thus, we obtain $\Delta J_{11}=-\int_{Q_T}\Delta k_{11}\frac{\partial u}{\partial x_1}\frac{\partial\lambda}{\partial x_1}dx_1dx_2dt+\frac{1}{2}\|\Delta u_{11}\|^2_{L_2(Q_T)}$, and (3.9) implies

$$\Delta J_{11}=-\int_{Q_T}\Delta k_{11}\frac{\partial u}{\partial x_1}\frac{\partial\lambda}{\partial x_1}dx_1dx_2dt+o(\|\Delta k_{11}\|_{L_\infty(\Omega)}).$$

By the same method, we have

$$\Delta J_{22}=-\int_{Q_T}\Delta k_{22}\frac{\partial u}{\partial x_2}\frac{\partial\lambda}{\partial x_2}dx_1dx_2dt+o(\|\Delta k_{22}\|_{L_\infty(\Omega)}).$$

Therefore, the Fréchet gradients J'_{11} and J'_{22} are given by (3.19) and (3.20), which concludes the theorem. □

3.4 Conjugate gradient method

The following iterative process based on the CGM is now applied for the simultaneous reconstruction of the two unknown space-dependent thermal conductivity components $k_{11}(x_1,x_2)$ and $k_{22}(x_1,x_2)$ by minimizing the objective functional $J(k_{11},k_{22})$ in (3.7):

$$k_{11}^{n+1}=k_{11}^n+\beta_{11}^nd_{11}^n,\quad k_{22}^{n+1}=k_{22}^n+\beta_{22}^nd_{22}^n,\quad n=0,1,2,\cdots \tag{3.21}$$

with the search directions d_{11}^n, d_{22}^n given by

$$d_{11}^n = \begin{cases} -J_{11}'^0, \\ -J_{11}'^n + \gamma_{11}^n d_{11}^{n-1}, \end{cases} \qquad d_{22}^n = \begin{cases} -J_{22}'^0, \\ -J_{22}'^n + \gamma_{22}^n d_{22}^{n-1}, \end{cases} \quad n = 1, 2, \cdots \tag{3.22}$$

where n is the subscript which indicates the number of iterations, $J_{11}'^n = J_{11}'(k_{11}^n, k_{22}^n)$, $J_{22}'^n = J_{22}'(k_{11}^n, k_{22}^n)$, k_{11}^0 and k_{22}^0 are the initial guesses for the two unknown coefficients in the inverse problem (3.1)–(3.6), β_{11}^n and β_{22}^n are the search step sizes in passing from iteration n to the next iteration $n+1$, and γ_{11}^n and γ_{22}^n are the conjugate gradient parameters, which are given by the Fletcher-Reeves formula, Fletcher & Reeves (1964),

$$\gamma_{11}^n = \frac{\|J_{11}'^n\|_{L_2(\Omega)}^2}{\|J_{11}'^{n-1}\|_{L_2(\Omega)}^2}, \quad \gamma_{22}^n = \frac{\|J_{22}'^n\|_{L_2(\Omega)}^2}{\|J_{22}'^{n-1}\|_{L_2(\Omega)}^2}, \quad n = 1, 2, \cdots \tag{3.23}$$

The search step sizes β_{11}^n and β_{22}^n are found by minimizing

$$J(k_{11}^{n+1}, k_{22}^{n+1}) = \frac{1}{2} \int_{Q_T} (u(k_{11}^n + \beta_{11}^n d_{11}^n, k_{22}^n + \beta_{22}^n d_{22}^n) - Y^\epsilon)^2 dx_1 dx_2 dt.$$

This formula shows that the step sizes β_{11}^n and β_{22}^n are implicit in the objective functional $J(k_{11}^{n+1}, k_{22}^{n+1})$. Such expression can be transformed into an explicit formula with step sizes β_{11}^n and β_{22}^n by applying the Taylor series expansion to approximate $u(k_{11}^n + \beta_{11}^n d_{11}^n, k_{22}^n + \beta_{22}^n d_{22}^n)$. Denoting $u(x_1, x_2, t; k_{11}^n, k_{22}^n) = u^n$, $\Delta u_{11}(x_1, x_2, t; k_{11}^n, k_{22}^n) = \Delta u_{11}^n$ and $\Delta u_{22}(x_1, x_2, t; k_{11}^n, k_{22}^n) = \Delta u_{22}^n$, and setting $\Delta k_{11}^n = d_{11}^n$ and $\Delta k_{22}^n = d_{22}^n$, the temperature $u(k_{11}^n + \beta_{11}^n d_{11}^n, k_{22}^n + \beta_{22}^n d_{22}^n)$ can be linearised by the Taylor series expansion in the form

$$\begin{aligned} u(k_{11}^n + \beta_{11}^n d_{11}^n, k_{22}^n + \beta_{22}^n d_{22}^n) &\approx u^n + \beta_{11}^n d_{11}^n \frac{\partial u^n}{\partial k_{11}^n} + \beta_{22}^n d_{22}^n \frac{\partial u^n}{\partial k_{22}^n} \\ &\approx u^n + \beta_{11}^n \Delta u_{11}^n + \beta_{22}^n \Delta u_{22}^n, \end{aligned}$$

where Δu_{11}^n and Δu_{22}^n are the solutions of the sensitivity problems (3.11) and (3.13). Then we obtain

$$J(k_{11}^{n+1}, k_{22}^{n+1}) = \frac{1}{2} \int_{Q_T} (u^n + \beta_{11}^n \Delta u_{11}^n + \beta_{22}^n \Delta u_{22}^n - Y^\epsilon)^2 dx_1 dx_2 dt.$$

The partial derivatives of the objective functional $J(k_{11}^{n+1}, k_{22}^{n+1})$ with respect to β_{11}^n and β_{22}^n are give by

$$\begin{aligned} \frac{\partial J}{\partial \beta_{11}^n} &= \int_{Q_T} (u^n + \beta_{11}^n \Delta u_{11}^n + \beta_{22}^n \Delta u_{22}^n - Y^\epsilon) \Delta u_{11}^n dx_1 dx_2 dt = C_1 + C_2 \beta_{11}^n + C_3 \beta_{22}^n, \\ \frac{\partial J}{\partial \beta_{22}^n} &= \int_{Q_T} (u^n + \beta_{11}^n \Delta u_{11}^n + \beta_{22}^n \Delta u_{22}^n - Y^\epsilon) \Delta u_{22}^n dx_1 dx_2 dt = C_4 + C_3 \beta_{11}^n + C_5 \beta_{22}^n, \end{aligned}$$

where

$$C_1 = \int_{Q_T} (u^n - Y^\epsilon)\Delta u_{11}^n dx_1 dx_2 dt, \quad C_2 = \|\Delta u_{11}^n\|^2_{L_2(Q_T)}, \quad C_5 = \|\Delta u_{22}^n\|^2_{L_2(Q_T)},$$
$$C_3 = \int_{Q_T} \Delta u_{11}^n \Delta u_{22}^n dx_1 dx_2 dt, \quad C_4 = \int_{Q_T} (u^n - Y^\epsilon)\Delta u_{22}^n dx_1 dx_2 dt.$$

Setting $\frac{\partial J}{\partial \beta_{11}^n} = \frac{\partial J}{\partial \beta_{22}^n} = 0$, the search step sizes β_{11}^n and β_{22}^n are given by

$$\beta_{11}^n = \frac{C_1 C_5 - C_3 C_4}{C_3^2 - C_2 C_5}, \quad \beta_{22}^n = \frac{C_2 C_4 - C_1 C_3}{C_3^2 - C_2 C_5}, \quad n = 0, 1, 2, \cdots . \tag{3.24}$$

The iteration process given by (3.21) and (3.22) does not provide the CGM with stabilization necessary for the minimizing of the objective functional $J(k_{11}, k_{22})$ in (3.7) to be classified as well-posed because of the errors inherently present in the measured temperature (3.6). However, the method may become well-posed if the discrepancy principle is applied to stop the iterative procedure. According to the discrepancy principle, the iterative procedure is stopped when the following criterion is satisfied

$$J(k_{11}^n, k_{22}^n) \leq \bar{\epsilon}, \tag{3.25}$$

where $\bar{\epsilon}$ is a small positive value, e.g., $\bar{\epsilon} = 10^{-5}$, for exact temperature measurement, or $\bar{\epsilon} = \frac{1}{2}\|Y^\epsilon - Y\|^2_{L_2(Q_T)}$, when the temperature measurements contain noisy data. The exact temperature data can be generated from the analytical solution, if available, or from solving the direct problem numerically (with care not to commit an inverse crime).

The CGM established for numerically reconstructing the unknown space-dependent thermal conductivity components $k_{11}(x_1, x_2)$ and $k_{22}(x_1, x_2)$ of an orthotropic material is presented as follows:

S1. Set $n = 0$ and choose initial guesses $k_{11}^0(x_1, x_2)$ and $k_{22}^0(x_1, x_2)$ for the unknown thermal conductivity components $k_{11}(x_1, x_2)$ and $k_{22}(x_1, x_2)$.

S2. Solve the direct problem (3.1)–(3.3) numerically by applying the ADI scheme introduced in Section 2.6.2 to compute the temperature $u(x_1, x_2, t; k_{11}^n, k_{22}^n)$, and the objective functional $J(k_{11}^n, k_{22}^n)$ (3.7).

S3. If the stopping criterion (3.25) is satisfied, then go to S7. Else go to S4.

S4. Solve the adjoint problem (3.17) to obtain $\lambda(x_1, x_2, t; k_{11}^n, k_{22}^n)$, and the gradients $J_{11}'^n$ (3.19) and $J_{22}'^n$ (3.20). Compute the conjugate gradient parameters γ_{11}^n and γ_{22}^n (3.23) and the search directions d_{11}^n and d_{22}^n (3.22).

S5. Solve the sensitivity problems (3.11) and (3.13) to gain the sensitivity functions $\Delta u_{11}(x_1, x_2, t; k_{11}^n, k_{22}^n)$ and $\Delta u_{22}(x_1, x_2, t; k_{11}^n, k_{22}^n)$ by taking $\Delta k_{11}^n = d_{11}^n$ and $\Delta k_{22}^n = d_{22}^n$, and compute the search step sizes β_{11}^n and β_{22}^n by (3.24).

S6. Update k_{11}^{n+1} and k_{22}^{n+1} by (3.21), set $n = n + 1$ and return to S2.

S7. End.

3.5 Numerical results and discussions

In this section, the numerical results for reconstructing the space-dependent thermal conductivity components $k_{11}(x_1, x_2)$ and $k_{22}(x_1, x_2)$ are illustrated. The accuracy errors for the thermal conductivity components $k_{11}(x_1, x_2)$ and $k_{22}(x_1, x_2)$ are defined as functions of the iteration number n, and are given by

$$E_1(k_{11}^n) = \|k_{11} - k_{11}^n\|_{L_2(\Omega)}, \tag{3.26}$$

$$E_2(k_{22}^n) = \|k_{22} - k_{22}^n\|_{L_2(\Omega)}, \tag{3.27}$$

where k_{11}^n and k_{22}^n are the numerical solutions at the iteration number n, and k_{11} and k_{22} are the analytical expressions for the thermal conductivity components, if available. The temperature measurement Y^ϵ containing random errors is generated by (2.29).

Example. The CGM is used to reconstruct simultaneously the unknown thermal conductivity components $k_{11}(x_1, x_2)$ and $k_{22}(x_1, x_2)$ of the two-dimensional inverse problem (3.1)–(3.3), (3.6) for an orthotropic material.

We take the final time $T = 1$, the coefficient $q \equiv 0$, and

$$\begin{aligned}
\phi(x_1, x_2) &= \sin(\pi x_1)\sin(\pi x_2) + (\pi + 1)(x_1 + x_2) + 1,\\
f(x_1, x_2, t) &= -e^{-t}(\sin(\pi x_1)\sin(\pi x_2) + (\pi + 1)(x_1 + x_2) + 1)\\
&\quad - \frac{e^{-t}}{12}(\pi \sin\pi(x_1 + x_2) + 2\pi + 2) + \frac{\pi^2 e^{-t}}{12}(2 + 1.5x_1 + 2x_2)\sin(\pi x_1)\sin(\pi x_2),\\
\mu_1(x_2, t) &= -\frac{1 + x_2}{12}(\pi \sin(\pi x_2) + \pi + 1)e^{-t},\\
\mu_2(x_2, t) &= \frac{2 + x_2}{12}(-\pi \sin(\pi x_2) + \pi + 1)e^{-t},\\
\mu_3(x_1, t) &= -\frac{1 + 0.5x_1}{12}(\pi \sin(\pi x_1) + \pi + 1)e^{-t},\\
\mu_3(x_1, t) &= \frac{2 + 0.5x_1}{12}(-\pi \sin(\pi x_1) + \pi + 1)e^{-t}.
\end{aligned}$$

By direct calculation, the analytical solution of the inverse problem (3.1)–(3.3), (3.6) is

$$k_{11}(x_1, x_2) = \frac{1 + x_1 + x_2}{12}, \tag{3.28}$$

$$k_{22}(x_1, x_2) = \frac{1 + 0.5x_1 + x_2}{12}, \tag{3.29}$$

$$u(x_1, x_2, t) = e^{-t}\left(\sin(\pi x_1)\sin(\pi x_2) + (\pi + 1)(x_1 + x_2) + 1\right). \tag{3.30}$$

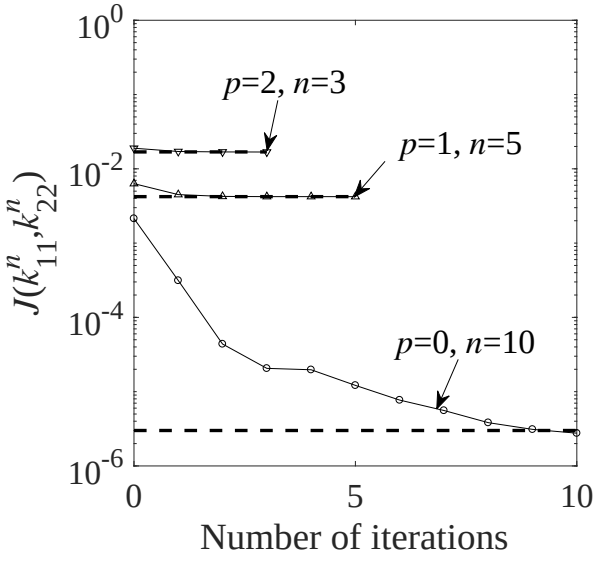

Figure 3.1: The objective functional $J(k_{11}, k_{22})$ in (3.7) with $p \in \{0, 1, 2\}$ noise using the L_2-gradients J'_{11} in (3.19) and J'_{22} in (3.20).

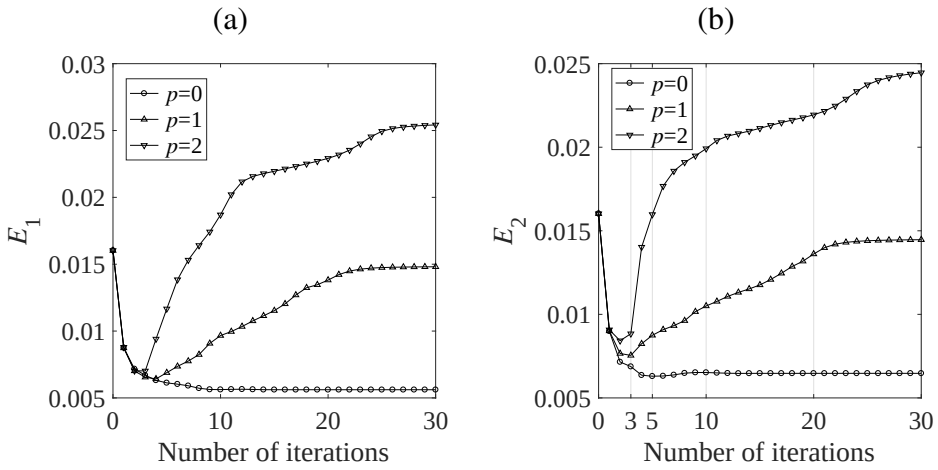

Figure 3.2: The errors (a) $E_1(k_{11}^n)$ (3.26) and (b) $E_2(k_{22}^n)$ (3.27) for k_{11} and k_{22} with $p \in \{0, 1, 2\}$ noise, using the L_2-gradients J'_{11} (3.19) and J'_{22} (3.20).

We take the initial guesses for $k_{11}(x_1, x_2)$ and $k_{22}(x_1, x_2)$ as

$$k_{11}^0(x_1, x_2) = \frac{1}{2}x_1x_2(1-x_1)(1-x_2) + \frac{1+x_1+x_2}{12}, \tag{3.31}$$

$$k_{22}^0(x_1, x_2) = \frac{1}{2}x_1x_2(1-x_1)(1-x_2) + \frac{1+0.5x_1+x_2}{12}, \tag{3.32}$$

which ensure that the boundary values of the initial approximations are equal to the exact ones (3.28) and (3.29).

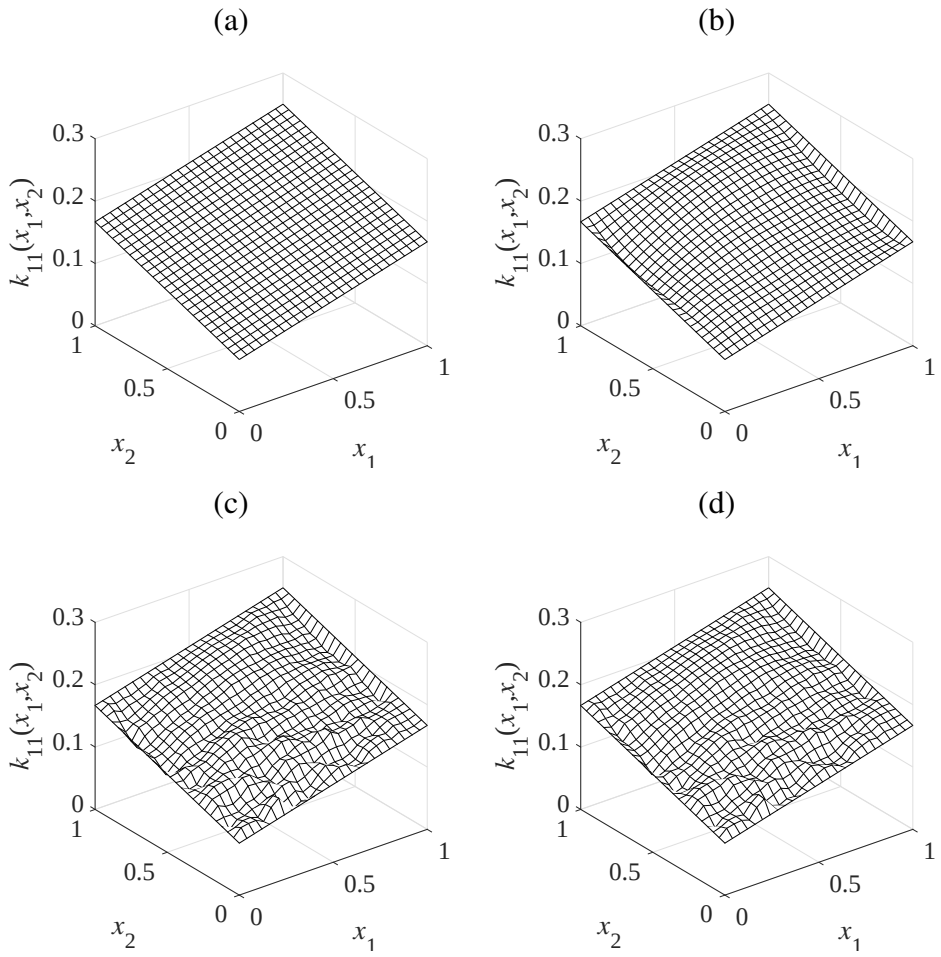

Figure 3.3: (a) The exact thermal conductivity component $k_{11}(x_1, x_2)$ (3.28), and the estimated solutions with (b) $p = 0$, (c) $p = 1$ and (d) $p = 2$ noise using the L_2-gradients J'_{11} (3.19) and J'_{22} (3.20) and the initial guesses (3.31) and (3.32).

All the numerical results are obtained by using the ADI scheme with $I = J = M = 26$. The standard L_2-gradients J'_{11} in (3.19) and J'_{22} in (3.20) and the Sobolev H^1-gradient (2.21) with the homogeneous Dirichlet boundary condition (2.23) and $\kappa = 0.1$ are applied to obtain the numerical solutions.

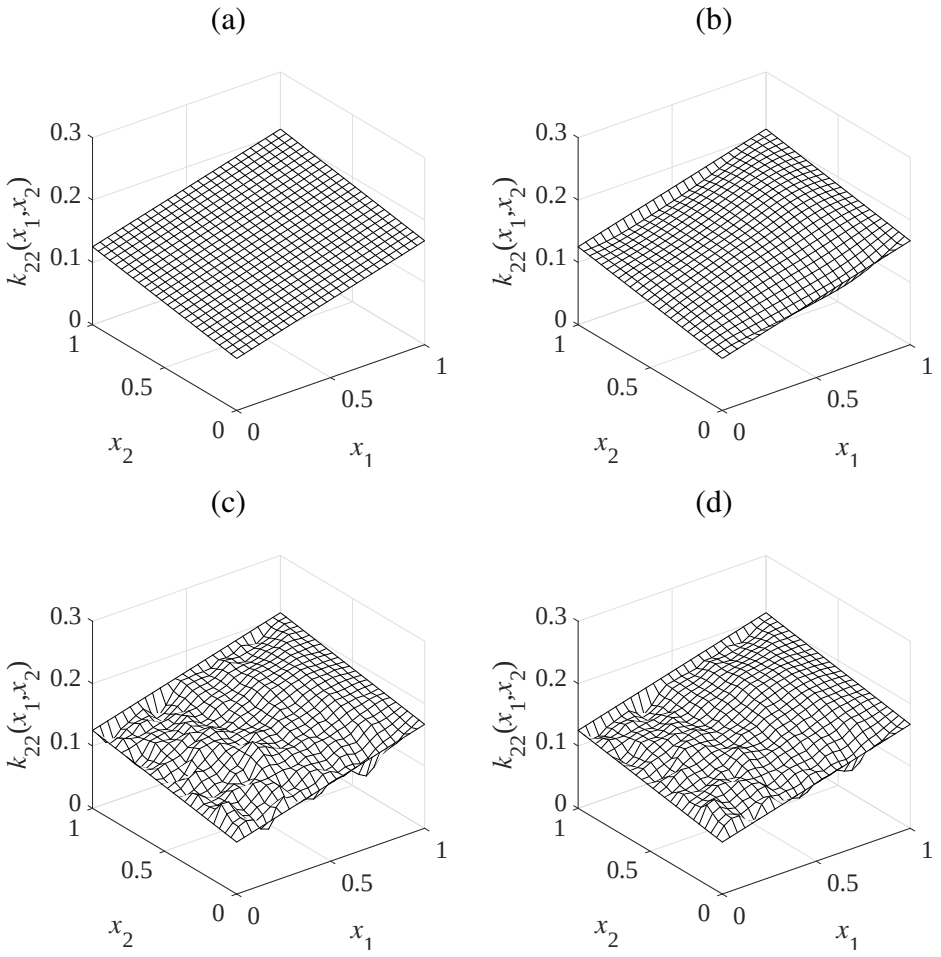

Figure 3.4: (a) The exact thermal conductivity component $k_{22}(x_1, x_2)$ (3.29), and the estimated solutions with (b) $p = 0$, (c) $p = 1$ and (d) $p = 2$ noise using the L_2-gradients J'_{11} (3.19) and J'_{22} (3.20) and the initial guesses (3.31) and (3.32).

p	I	J	M	$\bar{\epsilon}$	N	E_1	E_2
0	26	26	26	3.0E-06	10	5.6E-03	6.5E-03
1	26	26	26	4.2E-03	5	6.9E-03	8.7E-03
2	26	26	26	1.7E-02	3	7.0E-03	8.8E-03

Table 3.1: The stopping iteration numbers N and the errors obtained by L_2-gradients J'_{11} (3.19) and J'_{22} (3.20), with $p \in \{0, 1, 2\}$ noise and the initial guesses (3.31) and (3.32).

Figure 3.1 shows the monotonic decrease of the objective functional $J(k_{11}, k_{22})$ (3.7) as a function of the number of iteration n, and the stopping iterations numbers for $p \in \{0, 1, 2\}$ are obtained by the discrepancy principle (3.25) with the parameter ϵ presented in Table 3.1. The errors E_1 (3.26) and E_2 (3.27) for k_{11} and k_{22} are plotted in Figure 3.2,

and it is obvious that the errors at the stopping iteration numbers are quite close to the optimal ones.

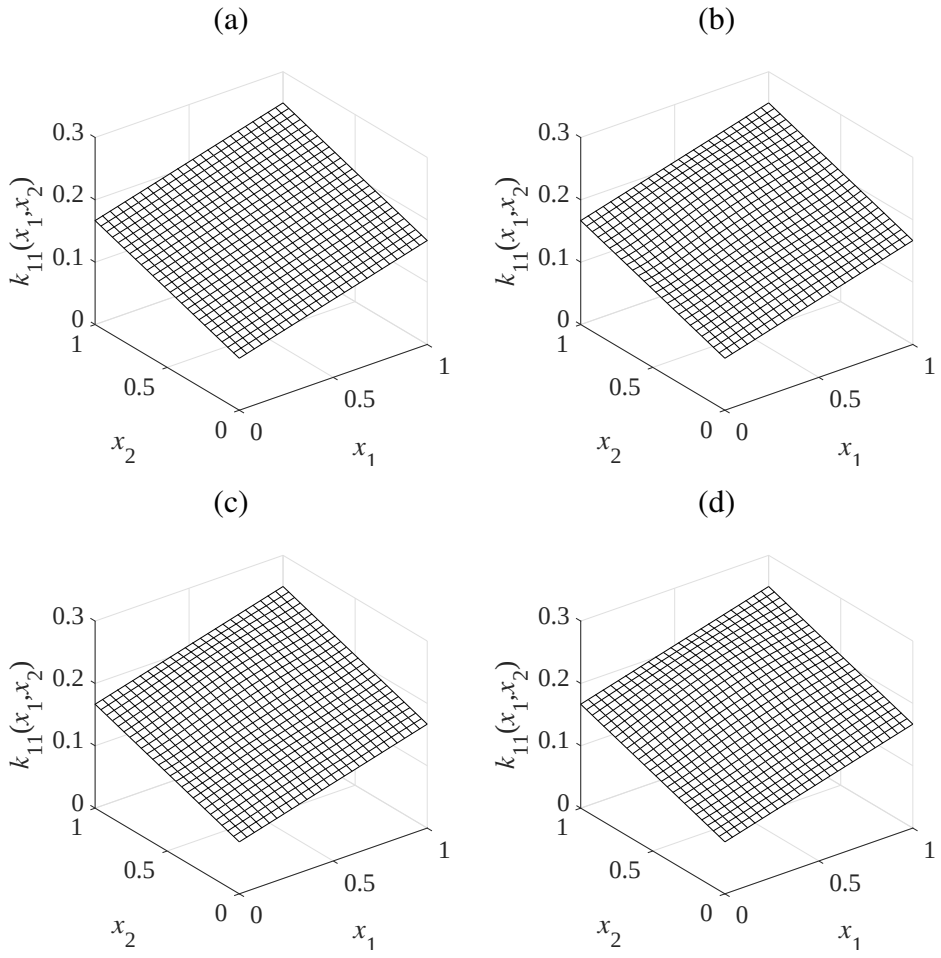

Figure 3.5: (a) The exact thermal conductivity component $k_{11}(x_1, x_2)$ (3.28), and the estimated solutions with (b) $p = 0$, (c) $p = 1$ and (d) $p = 2$ noise using the H^1-gradients and the initial guesses (3.31) and (3.32).

The numerical solutions for the thermal conductivity components $k_{11}(x_1, x_2)$ and $k_{22}(x_1, x_2)$ with the L_2-gradients are shown in Figures 3.3 and 3.4, whilst the numerical results with the H^1-gradients at the iteration numbers in Table 3.2 are presents in Figures 3.5 and 3.6.

By comparing the results in Figures 3.3 and 3.4 with Figures 3.5 and 3.6, it is easy to see that the numerical solutions obtained with the standard L_2-gradient are not so smooth, but the employment of the Sobolev H^1-gradient alleviates this problem and the improvement obtained is quite significant. Furthermore, the results obtained with the Sobolev H^1-gradient are more accurate than the ones obtained using the L_2-gradient

according to the errors shown in Tables 3.1 and 3.2. Thus, the numerical results are significantly smoother, more accurate and stable when using the Sobolev H^1-gradient than when using the L_2-gradient.

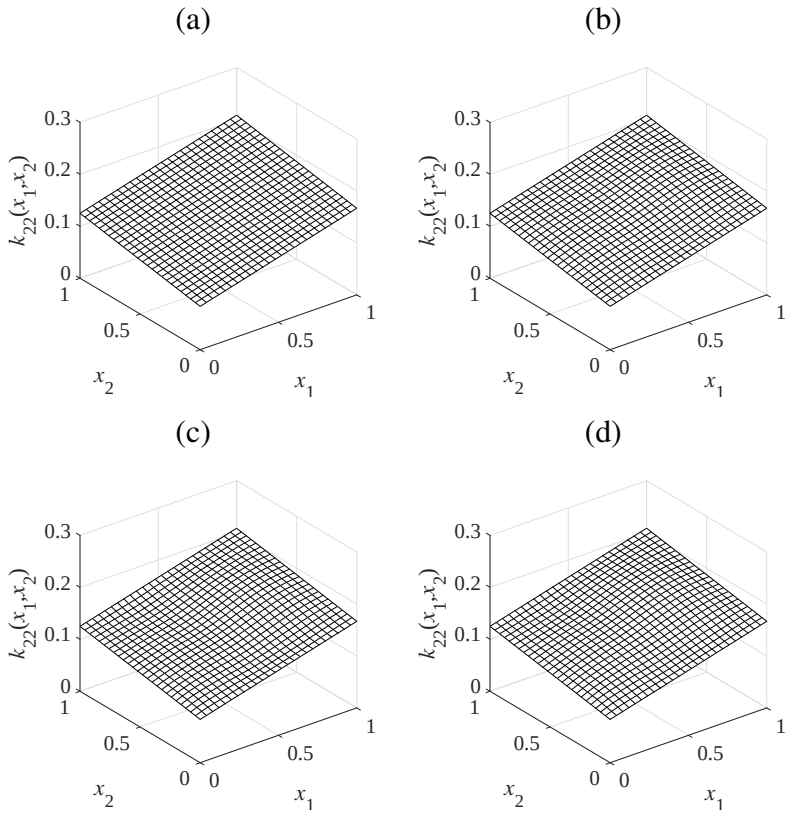

Figure 3.6: (a) The exact thermal conductivity component $k_{22}(x_1, x_2)$ (3.29), and the estimated solutions with (b) $p = 0$, (c) $p = 1$ and (d) $p = 2$ noise using the H^1-gradients and the initial guesses (3.31) and (3.32).

Next, for an arbitrary initial guesses for the thermal conductivity components k_{11} and k_{22}, say

$$k_{11}^0 = k_{22}^0 = \frac{1}{4}, \tag{3.33}$$

we apply the Sobolev H^1-gradient (2.21).

With the initial guesses (3.33), the stopping criterion (3.25) yields the stopping iteration numbers presented in Table 3.3. Figures 3.7 and 3.8 show that the numerical solutions for the thermal conductivity components k_{11} and k_{22} are smooth, stable and they become more accurate as the amount of noise p decreases. Remark also that the standard L_2-gradient produced very inaccurate results for the initial guess (3.33) due to the incompatibility between (3.33) and (3.28), (3.29) on the boundary.

p	I	J	M	$\bar{\epsilon}$	N	E_1	E_2
0	26	26	26	5.0E-06	5	2.0E-03	2.3E-03
1	26	26	26	4.2E-03	3	2.1E-03	2.5E-03
2	26	26	26	1.7E-02	2	4.0E-03	4.6E-03

Table 3.2: The stopping iteration numbers N and the errors obtained by H^1-gradients, with $p \in \{0, 1, 2\}$ noise and the initial guesses (3.31) and (3.32).

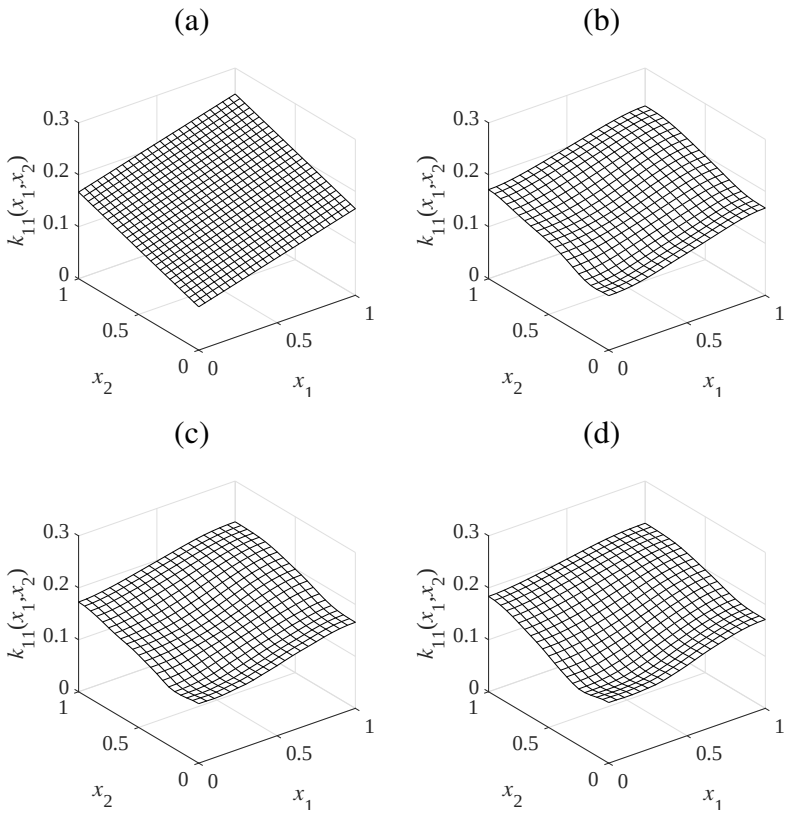

Figure 3.7: (a) The exact thermal conductivity component $k_{11}(x_1, x_2)$ (3.28), and the estimated solutions with (b) $p = 0$, (c) $p = 1$ and (d) $p = 2$ noise using the H^1-gradients and the initial guesses (3.33).

p	I	J	M	$\bar{\epsilon}$	N	E_1	E_2
0	26	26	26	3.0E-05	18	5.8E-03	4.7E-03
1	26	26	26	4.2E-03	17	7.2E-03	5.6E-03
2	26	26	26	1.7E-02	7	9.0E-03	7.5E-03

Table 3.3: The stopping iteration numbers N and the errors obtained by H^1-gradients, with $p \in \{0, 1, 2\}$ noise and the initial guesses (3.33).

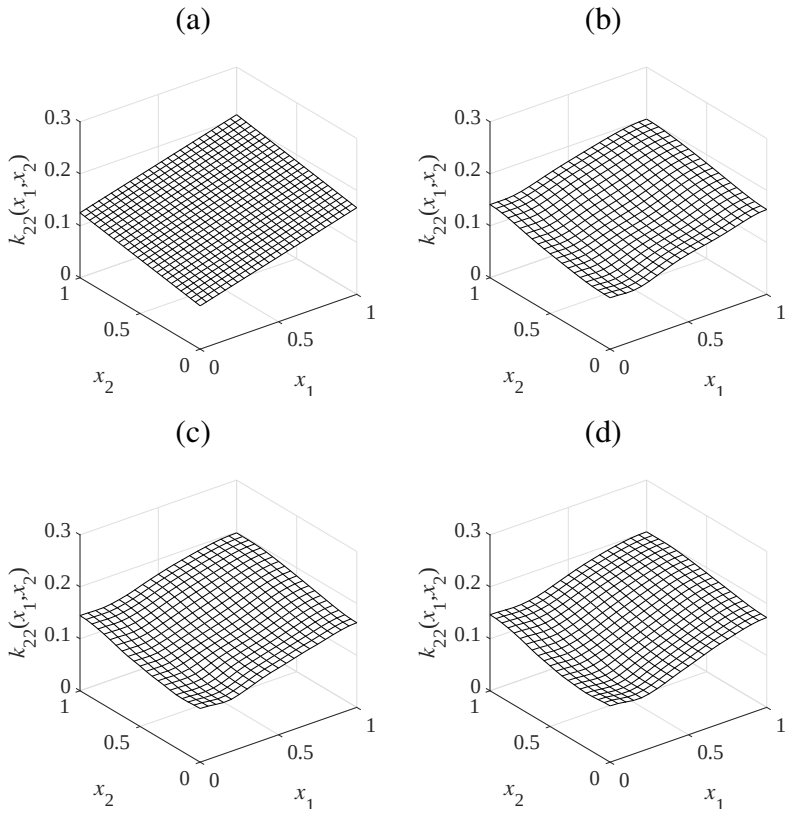

Figure 3.8: (a) The exact thermal conductivity component $k_{22}(x_1, x_2)$ (3.29), and the estimated solutions with (b) $p = 0$, (c) $p = 1$ and (d) $p = 2$ noise using the H^1-gradients and the initial guesses (3.33).

3.6 Conclusions

The determination of two-dimensional space-dependent orthotropic thermal conductivity from internal temperature measurement has been accomplished using the CGM together with the discrepancy principle. The Sobolev gradient has been utilized in the CGM to reconstruct smoother and significantly more accurate and stable numerical solutions. Regularization has been achieved by stopping the iterations at the level at which the least-squares objective functional, minimizing the gap between the computed and the measured temperature, becomes just below the noise threshold with which the data is contaminated. The numerical results illustrate that the CGM regularized by the discrepancy principle is an efficient and stable method. Furthermore, its robustness with respect to the independence on the initial guess has been further enhanced by using the Sobolev gradient.

Chapter 4

Simultaneous determination of the space-dependent thermal conductivity and reaction coefficient

4.1 Introduction

This chapter extends the inverse analysis of Chapter 2 from one coefficient, $k(x)$, to two coefficients, $k(x)$ and $q(x)$. This problem was previously investigated by Colaço *et al.* (2006) in the one-dimensional case.

In this chapter, the mathematical analysis of the inverse problem shall be carried out by some basic arguments of functional analysis and a variational method. The existence of the minimizer to the optimization problem, and the Fréchet gradient are derived. The CGM regularized by the discrepancy principle shall be established to simultaneously estimate both two unknown coefficients, for one- and two-dimensional inverse problems.

The plan of the chapter is as follows. In Section 4.2, the mathematical formulation is given and analysis is performed in Section 4.3. The CGM based on the Fréchet gradient and the adjoint problem is introduced in Section 4.4. Three numerical examples for one- and two-dimensional inverse problems are discussed, and stable and accurate numerical solutions are illustrated in Section 4.5. Finally, conclusions are highlighted in Section 4.6.

4.2 Mathematical formulation

We consider the same heat transfer mathematical model (2.1) in an isotropic material as in Chapter 2. Obviously, the direct problem is to determine the temperature $u(x,t)$

from the specified thermal coefficients, heat source and initial and boundary conditions. In the inverse problem, the space-dependent thermal conductivity $k(x)$ and the reaction coefficient $q(x)$ are unknown, and have to be determined from (2.1) and the temperature measurement (2.4).

4.3 Analysis

Let $u(x,t;k,q)$ denote the solution of the initial-boundary value direct problem (2.1), that is, the temperature corresponding to a particular pair $(k(x),q(x))$. The quasi-solution to the inverse problem (2.1), (2.4) is obtained by minimizing the least-squares objective functional given by

$$J(k,q)=\frac{1}{2}\left\|u(\cdot,\cdot;k,q)-Y^{\epsilon}(\cdot,\cdot)\right\|^2_{L_2(Q_T)}, \tag{4.1}$$

where Y^{ϵ} is the measured temperature satisfying $\|Y-Y^{\epsilon}\|_{L_2(\Omega)}\leq\epsilon$, and $\epsilon\geq 0$ represents noise level, where $u\in H^{1,0}(Q_T)$ is the weak solution satisfying (2.2), over the admissible set $\mathcal{A}_1\times\mathcal{A}_2$, where

$$\mathcal{A}_1=\{k\in L_\infty(\Omega):0<\kappa_1\leq k(x)\leq\kappa_2,\text{a.e. } x\in\Omega\},$$
$$\mathcal{A}_2=\{q\in L_\infty(\Omega):0\leq q(x)\leq\kappa_3,\text{a.e. } x\in\Omega\},$$

and κ_1, κ_2 and κ_3 are three known positive constants.

Based on the approaches in Keung & Zou (1998); Yamamoto & Zou (2001), the existence of a minimizer to the objective functional (4.1) over the the admissible set $\mathcal{A}_1\times\mathcal{A}_2$ is established as follows.

Theorem 4.3.1. *There exists at least one minimizer to the optimization problem* (4.1).

Proof. Since $\|u(x,t;k,q)\|_{L_2(Q_T)}$ is bounded by (2.3), it is obvious that $\min J(k,q)$ is finite over the admissible set $\mathcal{A}_1\times\mathcal{A}_2$ by the definition (4.1). Thus there exists a minimizing sequence $\{k^n,q^n\}$ from $\mathcal{A}_1\times\mathcal{A}_2$ such that

$$\lim_{n\to\infty}J(k^n,q^n)=\inf_{k\in\mathcal{A}_1,q\in\mathcal{A}_2}J(k,q).$$

By the boundedness of $\{k^n,q^n\}$ in $L_\infty(\Omega)\times L_\infty(\Omega)$, there exists a subsequence, still denoted by $\{k^n,q^n\}$, and some $k^*\in L_\infty(\Omega)$, $q^*\in L_\infty(\Omega)$ such that both k^n, q^n converge weakly to k^* and q^* respectively in $L_\infty(\Omega)$, and $k^*\in\mathcal{A}_1$, $q^*\in\mathcal{A}_2$. The estimate (2.3) implies that the sequence $\{u^n:=u(x,t;k^n,q^n)\}$ is bounded in the space $H^{1,0}(Q_T)$. Thus a subsequence, still denoted by $\{u^n\}$, may be extracted, and some $u^*\in H^{1,0}(Q_T)$ such that $u^n\to u^*$ weakly in $H^{1,0}(Q_T)$.

From the definition (2.2) of the weak solution in $H^{1,0}(Q_T)$ for the direct problem (2.1), for any $\eta \in H^{1,1}(Q_T)$ and $\eta(\cdot, T) = 0$, we have

$$\begin{aligned}\int_{Q_T} \left(-u^n \frac{\partial \eta}{\partial t} + k^n \nabla u^n \cdot \nabla \eta + q^n u^n \eta \right) dxdt \\ = \int_{Q_T} f\eta dxdt + \int_{S_T} \mu \eta ds dt + \int_{\Omega} \phi \eta(\cdot, 0) dx.\end{aligned}$$

The weak convergence of u^n to u^* implies that

$$\lim_{n\to\infty} \int_{Q_T} -u^n \frac{\partial \eta}{\partial t} dxdt = \int_{Q_T} -u^* \frac{\partial \eta}{\partial t} dxdt,$$

Since u^n weakly converges to u^* in $H^{1,0}(Q_T)$ and k^n, q^n both weakly converge to k^*, q^* in $L_\infty(\Omega)$, respectively, we have

$$\begin{aligned}\int_{Q_T} k^n \nabla u^n \cdot \nabla \eta dxdt = \int_{Q_T} k^* \nabla u^n \cdot \nabla \eta dxdt + \int_{Q_T} (k^n - k^*) \nabla u^n \cdot \nabla \eta dxdt, \\ \lim_{n\to\infty} \int_{Q_T} k^* \nabla u^n \cdot \nabla \eta dxdt = \int_{Q_T} k^* \nabla u^* \cdot \nabla \eta dxdt,\end{aligned}$$

and

$$\begin{aligned}\int_{Q_T} q^n u^n \eta dxdt = \int_{Q_T} q^* u^n \eta dxdt + \int_{Q_T} (q^n - q^*) u^n \eta dxdt, \\ \lim_{n\to\infty} \int_{Q_T} q^* u^n \eta dxdt = \int_{Q_T} q^* u^* \eta dxdt,\end{aligned}$$

using the estimate (2.3) for u^n and the Lebesgue dominant convergence theorem leads to the terms $\int_{Q_T} (k^n - k^*) \nabla u^n \cdot \nabla \eta dxdt$ and $\int_{Q_T} (q^n - q^*) u^n \eta dxdt$ converge to zero, hence we obtain

$$\begin{aligned}\lim_{n\to\infty} \int_{Q_T} k^n \nabla u^n \cdot \nabla \eta dxdt = \int_{Q_T} k^* \nabla u^* \cdot \nabla \eta dxdt, \\ \lim_{n\to\infty} \int_{Q_T} q^n u^n \eta dxdt = \int_{Q_T} q^* u^* \eta dxdt,\end{aligned}$$

and

$$\begin{aligned}\int_{Q_T} \left(-u^* \frac{\partial \eta}{\partial t} + k^* \nabla u^* \cdot \nabla \eta + q^* u^* \eta \right) dxdt \\ = \int_{Q_T} f\eta dxdt + \int_{S_T} \mu \eta ds dt + \int_{\Omega} \phi \eta(\cdot, 0) dx.\end{aligned}$$

Thus $u^* = u(k^*, q^*)$ by the definition 2.3.1 and $k = k^*$, $q = q^*$ in the direct problem (2.1), and the lower semi-continuity of norms implies that

$$\begin{aligned}J(k^*, q^*) =& \frac{1}{2} \|u^* - Y^\epsilon\|^2_{L_2(Q_T)} \leq \frac{1}{2} \lim_{n\to\infty} \|u^n - Y^\epsilon\|^2_{L_2(Q_T)} \\ \leq& \liminf_{n\to\infty} J(k^n, q^n) = \min_{k\in\mathcal{A}_1, q\in\mathcal{A}_2} J(k, q),\end{aligned}$$

which indicates that (k^*, q^*) is a minimizer of the objective functional $J(k, q)$ (4.1) over the admissible set $\mathcal{A}_1 \times \mathcal{A}_2$. □

Lemma 4.3.2. *The mapping $(k, q) \mapsto u(k, q)$ is Lipschitz continuous from $\mathcal{A}_1$ to $H^{1,0}(Q_T)$ with respect to k, and from $\mathcal{A}_2$ to $H^{1,0}(Q_T)$ with respect to q, i.e.,*

$$\|u(k + \Delta k, q) - u(k, q)\|_{H^{1,0}(Q_T)} \leq c\|\Delta k\|_{L_\infty(\Omega)}, \tag{4.2}$$

$$\|u(k, q + \Delta q) - u(k, q)\|_{H^{1,0}(Q_T)} \leq c\|\Delta q\|_{L_\infty(\Omega)}, \tag{4.3}$$

for any $k, k+\Delta k \in \mathcal{A}_1$, $q, q+\Delta q \in \mathcal{A}_2$ and the corresponding $u(k, q), u(k+\Delta k, q), u(k, q+\Delta q) \in H^{1,0}(Q_T)$.

Proof. The inequality (4.2) can be obtained according to Lemma 2.4.2. Thus, our work is to prove (4.3). Denoted by $\Delta u_q = u(k, q+\Delta q) - u(k, q)$ the increment of the temperature with respect to q, then Δu_q satisfies the following parabolic problem generated based on the direct problem (2.1)

$$\begin{cases} \frac{\partial(\Delta u_q)}{\partial t} = \nabla \cdot (k\nabla(\Delta u_q)) - q\Delta u_q - \Delta q u(k, q + \Delta q), & (x, t) \in Q_T, \\ k\frac{\partial(\Delta u_q)}{\partial \nu} = 0, \quad (x, t) \in S_T, \quad \Delta u_q(x, 0) = 0, & x \in \overline{\Omega}. \end{cases} \tag{4.4}$$

Using the estimate (2.3) to the parabolic problem (4.4), we obtain

$$\begin{aligned} \|\Delta u_q\|_{H^{1,0}(Q_T)} \leq & c\|\Delta q u(k, q + \Delta q)\|_{L_2(Q_T)} \\ \leq & c\|\Delta q\|_{L_\infty(\Omega)}\|u(k, q + \Delta q)\|_{L_2(Q_T)} \leq c\|\Delta q\|_{L_\infty(\Omega)}. \end{aligned}$$

This concludes the proof of the lemma. □

Lemma 4.3.3. *The mapping $(k, q) \mapsto u(k, q)$ is Fréchet differentiable with respect to k and q, i.e., for any $\Delta k, \Delta q \in L_\infty(\Omega)$ such that $k + \Delta k \in \mathcal{A}_1$ and $q + \Delta q \in \mathcal{A}_2$ there exist two bounded linear operators $\mathcal{U}_k : \mathcal{A}_1 \mapsto H^{1,0}(Q_T)$ and $\mathcal{U}_q : \mathcal{A}_2 \mapsto H^{1,0}(Q_T)$ such that*

$$\lim_{\|\Delta k\|_{L_\infty(\Omega)} \to 0} \frac{\|u(k + \Delta k, q) - u(k, q) - \mathcal{U}_k \Delta k\|_{H^{1,0}(Q_T)}}{\|\Delta k\|_{L_\infty(\Omega)}} = 0, \tag{4.5}$$

$$\lim_{\|\Delta q\|_{L_\infty(\Omega)} \to 0} \frac{\|u(k, q + \Delta q) - u(k, q) - \mathcal{U}_q \Delta q\|_{H^{1,0}(Q_T)}}{\|\Delta q\|_{L_\infty(\Omega)}} = 0. \tag{4.6}$$

Proof. The main work is to obtain (4.6), since (4.5) has been proved in Lemma 2.4.3. Consider the problem

$$\begin{cases} \frac{\partial w}{\partial t} = \nabla \cdot (k\nabla w) - qw - \Delta q u(k, q), & (x, t) \in Q_T, \\ k\frac{\partial w}{\partial \nu} = 0, \quad (x, t) \in S_T, \quad w(x, 0) = 0, & x \in \overline{\Omega}, \end{cases} \tag{4.7}$$

where $\Delta q \in L_\infty(\Omega)$ such that $q + \Delta q \in \mathcal{A}_2$. Then, there exists a unique solution $w \in H^{1,0}(Q_T)$ for the initial-boundary value problem (4.7) by Theorem 2.3.2, and by (2.3) the mapping $\Delta q \mapsto w$ from $L_\infty(\Omega)$ to $H^{1,0}(Q_T)$ defines a bounded linear operator $\mathcal{U}_q$.

Denote $v = u(k, q + \Delta q) - u(k, q) - \mathcal{U}_q \Delta q = \Delta u_q - w$, where Δu_q satisfies the problem (4.4), then v satisfies the problem

$$\begin{cases} \frac{\partial v}{\partial t} = \nabla \cdot (k \nabla v) - qv - \Delta q \Delta u_q, & (x,t) \in Q_T, \\ k \frac{\partial v}{\partial \nu} = 0, \quad (x,t) \in S_T, \quad v(x,0) = 0, & x \in \overline{\Omega}. \end{cases}$$

Using (2.3), we obtain $\|v\|_{H^{1,0}(Q_T)} \leq c\|\Delta q \Delta u_q\|_{L_2(\Omega)} \leq c\|\Delta q\|_{L_\infty(\Omega)}\|\Delta u_q\|_{L_2(\Omega)}$, and via (4.3) of Lemma 4.3.2, we obtain that

$$\|u(k, q + \Delta q) - u(k, q) - \mathcal{U}_q \Delta q\|_{H^{1,0}(Q_T)} = \|v\|_{H^{1,0}(Q_T)} \leq c\|\Delta q\|^2_{L_\infty(\Omega)},$$

thus, the lemma is proved. □

Theorem 4.3.4. *The objective functional $J(k, q)$ defined in (4.1) is Fréchet differentiable and its Fréchet derivatives $J'_k(k, q)$ and $J'_q(k, q)$ are given by*

$$J'_k(k, q) = -\int_0^T \nabla u \cdot \nabla \lambda dt, \quad x \in \Omega, \tag{4.8}$$

$$J'_q(k, q) = -\int_0^T u\lambda dt, \quad x \in \Omega. \tag{4.9}$$

Proof. The gradient $J'_k(k, q)$ in (4.8) is obtained in Theorem 2.4.5, then our work is to obtain the gradient $J'_q(k, q)$ in (4.9). Taking any $\Delta q \in L_\infty(\Omega)$ such that $q + \Delta q \in \mathcal{A}_2$, denote $\Delta J_q = J(k, q + \Delta q) - J(k, q)$, and by (4.1), we obtain

$$\Delta J_q = \int_{Q_T} (u - Y^\epsilon) \Delta u_q dx dt + \frac{1}{2}\|\Delta u_q\|^2_{L_2(Q_T)}.$$

Using the adjoint problem (2.12), then we have

$$\Delta J_q = \int_{Q_T} \left\{ -\frac{\partial \lambda}{\partial t} - \nabla \cdot (k \nabla \lambda) + q\lambda \right\} \Delta u_q dx dt + \frac{1}{2}\|\Delta u_q\|^2_{L_2(Q_T)},$$

and the sensitivity problem (4.4) implies that

$$\begin{aligned} &\int_{Q_T} \left\{ -\frac{\partial \lambda}{\partial t} - \nabla \cdot (k \nabla \lambda) + q\lambda \right\} \Delta u_q dx dt \\ =& -\int_\Omega \Delta u_q \lambda|_0^T dx + \int_{S_T} k \left\{ \frac{\partial (\Delta u_q)}{\partial \nu} \lambda - \Delta u_q \frac{\partial \lambda}{\partial \nu} \right\} ds dt \\ &+ \int_{Q_T} \lambda \left\{ \frac{\partial (\Delta u_q)}{\partial t} - \nabla \cdot (k \nabla (\Delta u_q)) + q \Delta u_q \right\} dx dt \\ =& -\int_{Q_T} \Delta q u(k, q + \Delta q) \lambda dx dt = -\int_{Q_T} \Delta q \Delta u_q \lambda dx dt - \int_{Q_T} \Delta q u \lambda dx dt. \end{aligned}$$

Since Δu_q is the solution to the problem (4.4), in virtue of Lemma 4.3.2, we have $\|\Delta u_q\|^2_{L_2(Q_T)} \leq c\|\Delta q\|^2_{L_\infty(\Omega)}$, and

$$\left|\int_{Q_T} \Delta q \Delta u_q \lambda dx dt\right| \leq \|\Delta q\|_{L_\infty(\Omega)} \|\Delta u_q\|_{L_2(Q_T)} \|\lambda\|_{L_2(Q_T)} \leq c\|\Delta q\|^2_{L_\infty(\Omega)} \|\lambda\|_{L_2(Q_T)}.$$

Thus,

$$\Delta J_q = -\int_{Q_T} \Delta q u \lambda dx dt + o(\|\Delta q\|_{L_\infty(\Omega)}),$$

which means that the Fréchet derivative $J'_q(k,q)$ is given by (4.9). The theorem is proved. □

4.4 Conjugate gradient method

The following iterative process based on the CGM is applied for the numerical estimation of the unknown thermal conductivity $k(x)$ and reaction coefficient $q(x)$ by minimizing the objective functional $J(k,q)$ in (4.1):

$$k^{n+1}(x) = k^n(x) + \beta^n_k d^n_k, \quad q^{n+1}(x) = q^n(x) + \beta^n_q d^n_q, \quad n = 0, 1, 2, \cdots \tag{4.10}$$

with the search direction given by

$$d^n_k = \begin{cases} -J'^0_k, \\ -J'^n_k + \gamma^n_k d^{n-1}_k, \end{cases} \qquad d^n_q = \begin{cases} -J'^0_q, \\ -J'^n_q + \gamma^n_q d^{n-1}_q, \end{cases} \quad n = 1, 2, \cdots \tag{4.11}$$

where the subscripts n denotes the number of iteration, $J'^n_k = J'_k(k^n, q^n)$, $J'^n_q = J'_q(k^n, q^n)$, k^0, q^0 are the initial guesses of the thermal conductivity $k(x)$ and reaction coefficient $q(x)$, β^n_k, β^n_q are search step sizes for k and q, respectively, in passing from iteration n to iteration $n+1$. γ^n_k and γ^n_q are the conjugate gradient parameters, which are given by the Fletcher-Reeves formula, Fletcher & Reeves (1964),

$$\gamma^n_k = \frac{\|J'^n_k\|^2_{L_2(\Omega)}}{\|J'^{n-1}_k\|^2_{L_2(\Omega)}}, \quad \gamma^n_q = \frac{\|J'^n_q\|^2_{L_2(\Omega)}}{\|J'^{n-1}_q\|^2_{L_2(\Omega)}}, \quad n = 1, 2, \cdots \tag{4.12}$$

The search step sizes β^n_k and β^n_q are found by minimizing

$$J(k^{n+1}, q^{n+1}) = \frac{1}{2}\int_{Q_T} (u(k^n + \beta^n_k d^n_k, q^n + \beta^n_q d^n_q) - Y^\epsilon)^2 dx dt.$$

Denoting $u(x,t;k^n,q^n) = u^n$, $\Delta u_k(x,t;k^n,q^n) = \Delta u^n_k$ and $\Delta u_q(x,t;k^n,q^n) = \Delta u^n_q$, and setting $\Delta k^n = d^n_k$ and $\Delta q^n = d^n_q$, the temperature $u(k^n + \beta^n_k d^n_k, q^n + \beta^n_q d^n_q)$ can be linearised by the Taylor series expansion in the form

$$u(k^n + \beta^n_k d^n_k, q^n + \beta^n_q d^n_q) \approx u^n + \beta^n_k d^n_k \frac{\partial u^n}{\partial k^n} + \beta^n_q d^n_q \frac{\partial u^n}{\partial q^n} \approx u^n + \beta^n_k \Delta u^n_k + \beta^n_q \Delta u^n_q,$$

where Δu_k^n and Δu_q^n are the solutions of the sensitivity problems (2.8) and (4.4). Then we obtain

$$J(k^{n+1}, q^{n+1}) = \frac{1}{2}\int_{Q_T} (u^n + \beta_k^n \Delta u_k^n + \beta_q^n \Delta u_q^n - Y^\epsilon)^2 dxdt.$$

The partial derivatives of the objective functional $J(k^{n+1}, q^{n+1})$ with respect to β_k^n and β_q^n are give by

$$\frac{\partial J}{\partial \beta_k^n} = \int_{Q_T} (u^n + \beta_k^n \Delta u_k^n + \beta_q^n \Delta u_q^n - Y^\epsilon)\Delta u_k^n dxdt = C_1 + C_2\beta_k^n + C_3\beta_q^n,$$
$$\frac{\partial J}{\partial \beta_q^n} = \int_{Q_T} (u^n + \beta_k^n \Delta u_k^n + \beta_q^n \Delta u_q^n - Y^\epsilon)\Delta u_q^n dxdt = C_4 + C_3\beta_k^n + C_5\beta_k^n,$$

where

$$C_1 = \int_{Q_T} (u^n - Y^\epsilon)\Delta u_k^n dxdt, \quad C_2 = \|\Delta u_k^n\|^2_{L_2(Q_T)},$$
$$C_3 = \int_{Q_T} \Delta u_k^n \Delta u_q^n dxdt, \quad C_4 = \int_{Q_T} (u^n - Y^\epsilon)\Delta u_q^n dxdt, \quad C_5 = \left\|\Delta u_q^n\right\|^2_{L_2(Q_T)}.$$

Setting $\frac{\partial J}{\partial \beta_k^n} = \frac{\partial J}{\partial \beta_q^n} = 0$, the search step sizes β_k^n and β_q^n are given by

$$\beta_k^n = \frac{C_1C_5 - C_3C_4}{C_3^2 - C_2C_5}, \quad \beta_q^n = \frac{C_2C_4 - C_1C_3}{C_3^2 - C_2C_5}, \quad n = 0, 1, \cdots. \tag{4.13}$$

To summarise, the CGM established for numerically reconstructing the unknown space-dependent thermal conductivity $k(x)$ and reaction coefficient $q(x)$ is presented as follows:

S1. Set $n = 0$ and choose initial guesses $k^0(x)$ and $q^0(x)$ for the unknown thermal conductivity $k(x)$ and reaction coefficient $q(x)$.

S2. Solve the direct problem (2.1) to compute the temperature $u(x, t; k^n, q^n)$ numerically by applying the FDM scheme introduced in Subsections 2.6.1 and 2.6.2, and the objective functional $J(k^n, q^n)$ in (4.1).

S3. If the stopping criterion

$$J(k^n, q^n) \leq \bar{\epsilon}, \tag{4.14}$$

is satisfied, where $\bar{\epsilon}$ is a small positive value defined below equation (2.26), then go to S7. Else go to S4.

S4. Solve the adjoint problem (2.12) to obtain the adjoint function $\lambda(x_1, x_2, t; k^n, q^n)$, and the gradients $J_k'^n$ (4.8) and $J_q'^n$ (4.9). Compute the conjugate gradient parameters γ_k^n and γ_q^n (4.12) and the search directions d_k^n and d_q^n (4.11).

S5. Solve the sensitivity problems (2.8) and (4.4) to obtain the sensitivity functions $\Delta u_k(x,t;k^n,q^n)$ and $\Delta u_q(x,t;k^n,q^n)$ by taking $\Delta k^n = d_k^n$ and $\Delta q^n = d_q^n$, and compute the search step sizes β_k^n and β_q^n by (4.13).

S6. Update k^{n+1} and q^{n+1} by (4.10), set $n = n+1$ and return to S2.

S7. End.

4.5 Numerical results and discussions

In this section, the numerical method for reconstructing the space-dependent thermal conductivity $k(x)$ and reaction coefficient $q(x)$ simultaneously is illustrated, and three numerical experiments based on the CGM are shown for one and two dimensional cases $(\mathrm{d} = 1, 2)$. The accuracy errors for $k(x)$ and $q(x)$ are defined as functions of the iteration number n, as given by

$$E_k(n) = \|k - k^n\|_{L_2(\Omega)}, \tag{4.15}$$

$$E_q(n) = \|q - q^n\|_{L_2(\Omega)}, \tag{4.16}$$

where k^n and q^n are the numerical solutions for thermal conductivity and reaction coefficient at iteration number n, respectively. The temperature measurements Y^ϵ containing random errors are generated by (2.29).

4.5.1 Example 1

In this section, the CGM is used to reconstruct the unknown thermal conductivity $k(x)$ and reaction coefficient $q(x)$ of the IHTP (2.1) and (2.4), simultaneously. For the one dimensional case $(\mathrm{d} = 1)$, we take $\Omega = (0,1)$, the final time $T = 1$, the initial temperature $\phi \equiv 0$, and

$$\begin{aligned} f(x,t) &= (1 + x - xe^{-t})(\sin(\pi x) + (\pi+1)x) \\ &\quad + \frac{1-e^{-t}}{12}(\pi^2(1+x)\sin(\pi x) - \pi\cos(\pi x) - \pi - 1), \\ \mu(0,t) &= -\frac{2\pi+1}{12}(1-e^{-t}), \quad \mu(1,t) = \frac{1}{6}(1-e^{-t}). \end{aligned}$$

Then the analytical solution of the inverse problem (2.1), (2.4) is

$$k(x) = \frac{1+x}{12}, \tag{4.17}$$

$$q(x) = 1 + x, \quad u(x,t) = (1-e^{-t})(\sin(\pi x) + (\pi+1)x). \tag{4.18}$$

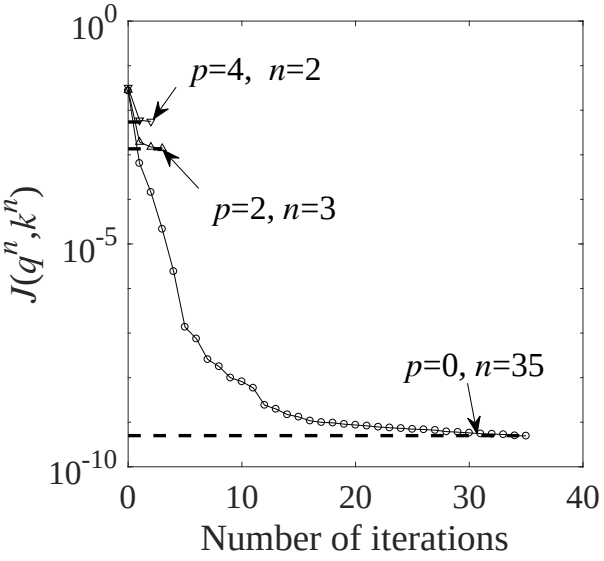

Figure 4.1: The objective functional $J(k,q)$ in (4.1) for $p \in \{0,2,4\}$ noise, for Example 1.

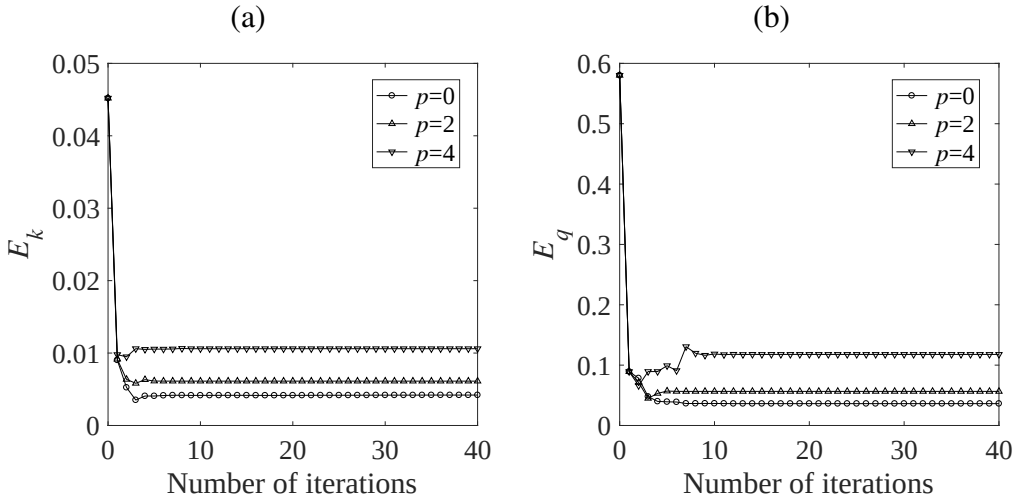

Figure 4.2: The errors (a) $E_k(n)$ (4.15) and (b) $E_q(n)$ (4.16) for the thermal conductivity k and reaction coefficient q with $p \in \{0,2,4\}$ noise, for Example 1.

We take the initial guesses for the thermal conductivity $k(x)$ and reaction coefficient $q(x)$ as

$$k^0(x) = -\frac{1}{4}x^2 + \frac{1}{3}x + \frac{1}{12}, \tag{4.19}$$

$$q^0(x) = 1, \tag{4.20}$$

which ensure that the boundary value of the initial approximation k^0 is equal to the exact one (4.17). All the numerical results illustrated in the figures of Example 1 are obtained

by using the C-N scheme 2.6.1 with $I = M = 51$, $p \in \{0, 2, 4\}$ noise and the initial guesses (4.19) and (4.20).

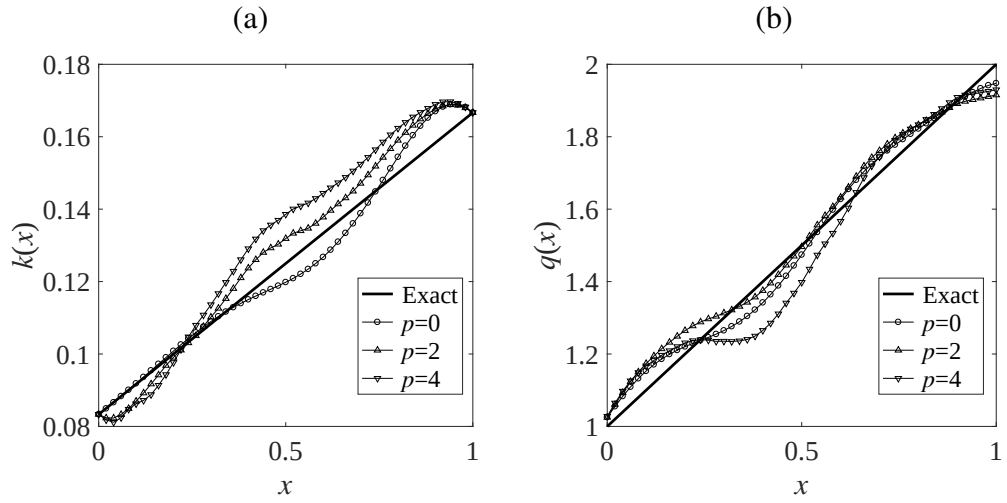

Figure 4.3: (a) The numerical thermal conductivity $k(x)$ and (b) reaction coefficient $q(x)$ with $p \in \{0, 2, 4\}$ noise, for Example 1.

Figure 4.1 shows the monotonic decrease of the objective functional $J(k, q)$ in (4.1), as a function of the number of iterations n, and the stopping iteration numbers for $p \in \{0, 2, 4\}$ are obtained by the discrepancy principle (4.14) with the value of $\bar{\epsilon}$ presented in Table 4.1. The errors $E_k(n)$ (4.15) and $E_q(n)$ (4.16) for k and q are plotted in Figure 4.2. The numerical solutions for the thermal conductivity $k(x)$ and reaction coefficient $q(x)$ are shown in Figure 4.3, and they are plotted at the stopping iteration numbers N in Table 4.1 for $p \in \{0, 2, 4\}$. From Figure 4.3 it can be seen that the retrieved numerical solutions are stable and accurate.

p	I	M	$\bar{\epsilon}$	N	E_k	E_q
0	51	51	5.0E-10	35	4.2E-03	3.6E-02
2	51	51	1.4E-03	3	5.8E-03	4.5E-02
4	51	51	5.4E-03	2	9.5E-03	6.6E-02

Table 4.1: The stopping iteration numbers N and the errors E_k and E_q for $p \in \{0, 2, 4\}$ noise in the simultaneous estimation of $k(x)$ and $q(x)$, for Example 1.

4.5.2 Example 2

We now present a one-dimensional example where the input data for the temperature is numerically simulated by solving firstly the direct problem (2.1) using the C-N scheme

in Subsection 2.6.1 with

$$\mu(0,t) = -2, \quad \mu(1,t) = 2, \quad \phi \equiv 0, \quad f \equiv 0, \tag{4.21}$$

the discontinuous thermal conductivity and reaction coefficient

$$k(x) = \begin{cases} 2, & x \in \left(\frac{1}{4}, \frac{3}{4}\right), \\ 1, & \text{elsewhere.} \end{cases} \tag{4.22}$$

$$q(x) = 2 + \cos(\pi x). \tag{4.23}$$

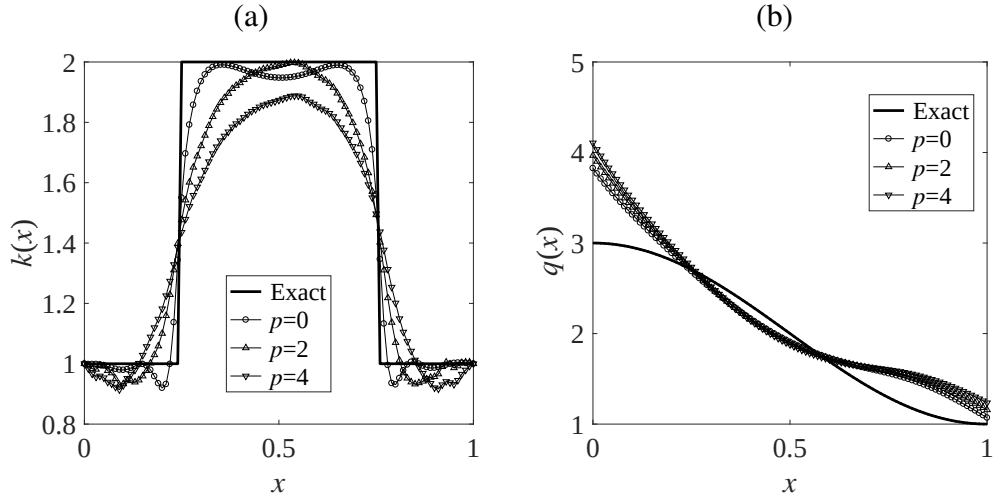

Figure 4.4: (a) The numerical thermal conductivity $k(x)$ and (b) reaction coefficient $q(x)$ for $p \in \{0, 2, 4\}$ noise, for Example 2.

p	I	M	$\bar{\epsilon}$	N	E_k	E_q
0	101	101	1.0E-06	19	0.1027	0.2603
2	101	101	1.3E-04	7	0.1680	0.3065
4	101	101	5.3E-04	4	0.2207	0.3532

Table 4.2: The stopping iteration numbers N and the errors E_k and E_q for $p \in \{0, 2, 4\}$ noise and the initial guesses (4.24) and (4.25) in the simultaneous estimation of $k(x)$ and $q(x)$, for Example 2.

We take the initial guesses for the thermal conductivity $k(x)$ and reaction coefficient $q(x)$ as

$$k^0(x) = 1, \tag{4.24}$$

$$q^0(x) = 2. \tag{4.25}$$

The numerical solutions for the thermal conductivity $k(x)$ and reaction coefficient $q(x)$ are presented in Figure 4.4 with $p \in \{0, 2, 4\}$ and the initial guesses (4.24) and (4.25). The stopping iteration numbers are shown in Table 4.2, which are obtained by the stopping criterion (4.14) with the quantity $\bar{\epsilon}$. From Figure 4.4 it is easy to see that the numerical results are stable and reasonably accurate bearing in mind the difficult discontinuous thermal conductivity (4.22) that had to be retrieved.

4.5.3 Example 3

For the two-dimensional case $(\mathrm{d} = 2)$, we take $\Omega = (0, 1) \times (0, 1)$, the final time $T = 1$, the initial temperature $\phi \equiv 0$, and the source term

$$
\begin{aligned}
f(x_1, x_2, t) &= 2\pi^2(1 + \sin(\pi x_1)\sin(\pi x_2))\sin(\pi x_1)\sin(\pi x_2)(1 - e^{-t}) \\
&+ (\sin(\pi x_1)\sin(\pi x_2) + (\pi + 1)(x_1 + x_2))((1 + x_1^2 + x_2^2)(1 - e^{-t}) + e^{-t}) \\
&- \pi(1 - e^{-t})(\pi\cos^2(\pi x_1)\sin^2(\pi x_2) + \pi\sin^2(\pi x_1)\cos^2(\pi x_2) + (\pi + 1)\sin(x_1 + x_2)).
\end{aligned}
$$

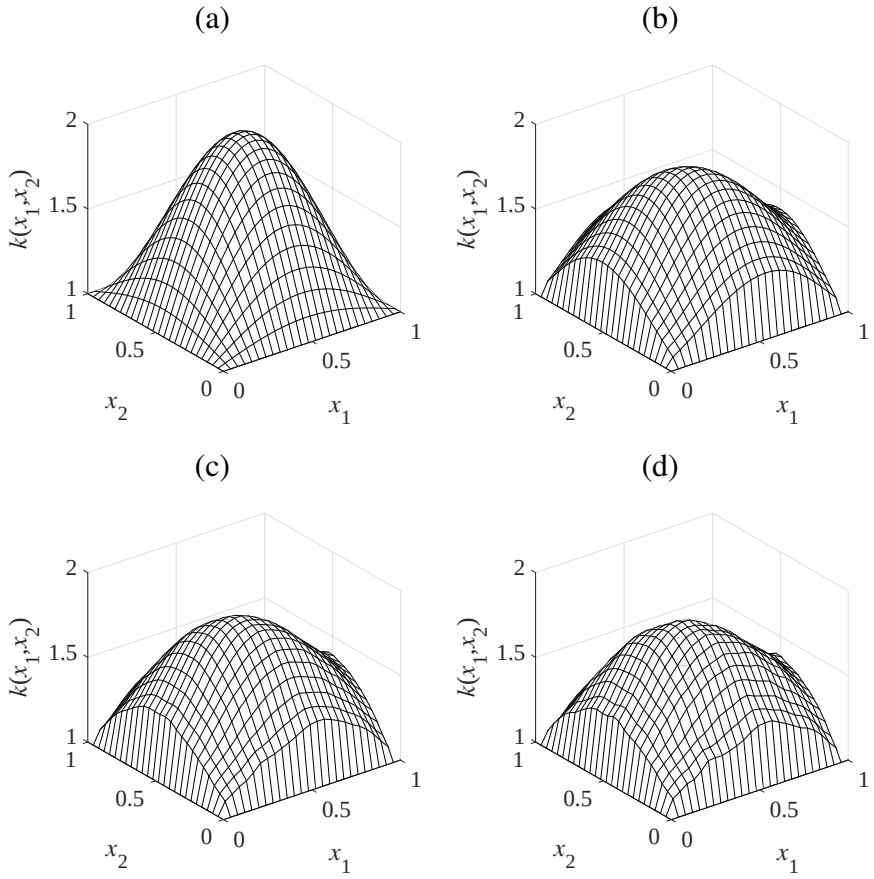

Figure 4.5: (a) The exact thermal conductivity $k(x_1, x_2)$, and the estimated solutions for (b) $p = 0$, (c) $p = 2$ and (d) $p = 4$ noise, for Example 3.

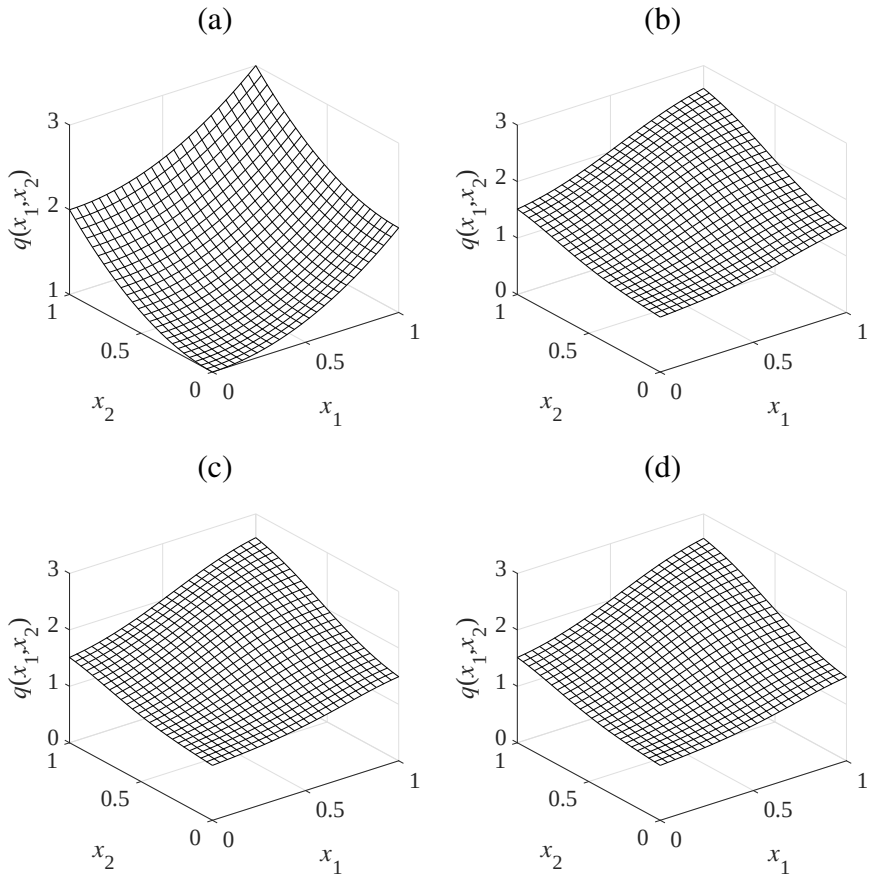

Figure 4.6: (a) The exact reaction coefficient $q(x_1, x_2)$, and the estimated solutions for (b) $p = 0$, (c) $p = 2$ and (d) $p = 4$ noise, for Example 3.

With the boundary conditions

$$\mu(0, x_2, t) = -(1 - e^{-t})(\pi \sin(\pi x_2) + \pi + 1),$$
$$\mu(1, x_2, t) = (1 - e^{-t})(-\pi \sin(\pi x_2) + \pi + 1),$$
$$\mu(x_1, 0, t) = -(1 - e^{-t})(\pi \sin(\pi x_1) + \pi + 1),$$
$$\mu(x_1, 1, t) = (1 - e^{-t})(-\pi \sin(\pi x_1) + \pi + 1),$$

the analytical solution of the inverse problem (2.1), (2.4) is given by

$$k(x_1, x_2) = 1 + \sin(\pi x_1) \sin(\pi x_2), \quad q(x_1, x_2) = 1 + x_1^2 + x_2^2, \tag{4.26}$$
$$u(x_1, x_2, t) = (1 - e^{-t}) \left(\sin(\pi x_1) \sin(\pi x_2) + (\pi + 1)(x_1 + x_2)\right). \tag{4.27}$$

The initial guesses for the simultaneous reconstruction of the thermal conductivity $k(x_1, x_2)$ and reaction coefficient $q(x_1, x_2)$ are taken as

$$k^0(x_1, x_2) = 1, \tag{4.28}$$
$$q^0(x_1, x_2) = 1. \tag{4.29}$$

The numerical solutions are computed by using the ADI scheme in Subsection 2.6.2 with $I = J = 21$ and $M = 26$ to solve the two-dimensional parabolic differential equations with the initial guesses (4.28) and (4.29) and the level of noise $p \in \{0, 2, 4\}$ in the following figures.

Figures 4.5 and 4.6 show the retrieved solutions of the space-dependent thermal conductivity $k(x_1, x_2)$ and reaction coefficient $q(x_1, x_2)$ at the stopping iteration numbers in Table 4.3 generated by the discrepancy principle (4.14), with $p \in \{0, 2, 4\}$ noise and the initial guesses (4.28) and (4.29). From these figures it can be seen that the numerical solutions are reasonably stable and they become more accurate as the amount of noise p decreases.

p	I	J	M	$\bar{\epsilon}$	N	E_k	E_q
0	21	21	26	3.0E-04	49	0.1316	0.1583
2	21	21	26	5.2E-03	39	0.1324	0.1606
4	21	21	26	2.0E-02	28	0.1355	0.1627

Table 4.3: The stopping iteration numbers N and the errors E_k and E_q for $p \in \{0, 2, 4\}$ noise and the initial guesses (4.28) and (4.29) in the simultaneous estimation of $k(x_1, x_2)$ and $q(x_1, x_2)$, for Example 3.

4.6 Conclusions

In this chapter, the determination of the space-dependent thermal conductivity and reaction coefficient from the temperature measurements has been investigated using the CGM. The quasi-solution for the inverse problem is obtained by minimizing the least-squares objective functional, and the existence of a minimizer is proved. The variational method is utilized to obtain the Fréchet gradient which is used in the CGM. Regularization has been achieved by stopping the iterations according to the discrepancy principle at the level at which the least-squares objective functional, minimizing the gap between the computed and the measured temperature, becomes just below the noise threshold with which the data is contaminated. The numerical results show that CGM is an accurate and stable regularization method for reconstructing spatially-varying coefficients.

In the next chapter, we give a different inverse formulation to the task of recovering the reaction coefficient $q(x)$ from measurement of the temperature at the final time or from a time-average temperature measurement.

Chapter 5

Determination of the space-dependent reaction coefficient from final or time-average data

5.1 Introduction

In this chapter, the space-dependent reaction coefficient is sought to be retrieved from the final or time-average temperature measurements. The reaction coefficient can also be considered as the blood perfusion coefficient in biomedical applications, Pennes (1948). Blood perfusion is defined as the blood volume flow exchange per volume of tissue, which refers to the local, multidirectional blood flow through the capillaries and intracellular space of living tissue, and its measurements can determine the success or failure of skin grafts and any related healing, Robinson *et al.* (1998).

Prior to this study, several parameter estimation least-squares techniques were utilized for the determination of blood perfusion using non-invasive measurements from minimally surface probe, Robinson *et al.* (1998); Scott *et al.* (1997, 1998); Yue *et al.* (2008).

The uniqueness of the space-dependent reaction coefficient in Hölder spaces for the heat equation with homogeneous Neumann boundary condition, initial and final data was established in Rundell (1987). In Isakov (1991), the uniqueness in the same Hölder space of functions with the same data, but with zero initial condition and non-homogeneous Dirichlet boundary condition was proved. In Prilepko & Solovev (1987), existence and uniqueness for the space-dependent reaction coefficient in Hölder spaces were established for the heat equation with non-homogeneous initial and Dirichlet boundary conditions and two distinct types of over-determination: the final temperature data and the

temperature at a fixed point in the interior of the relevant space region for all values of time.

In Kamynin & Kostin (2010); Kozhanov (2004), the existence and uniqueness of the space-dependent reaction coefficient in Sobolev spaces for the heat equation with non-homogeneous Dirichlet boundary condition and time-average temperature measurement were established. Finally, the uniqueness of the space-dependent reaction coefficient in Sobolev spaces from homogeneous initial and boundary conditions with inhomogeneous source and final or time-average temperature data was established in Prilepko & Kostin (1993).

In Yang *et al.* (2008), the space-dependent reaction coefficient was determined in the one-dimensional heat equation with homogeneous Neumann boundary condition, and initial and final observations, as in the inverse problem formulated and theoretically investigated in Rundell (1987). The unknown coefficient was reconstructed by minimizing the first-order nonlinear Tikhonov regularization functional. Numerical results were obtained using the FDM and an elliptic bilateral variational inequality. In Deng *et al.* (2009), the same inverse problem as in Yang *et al.* (2008) was discussed from discrete final temperature observations. On the basis of an interpolation technique, a new way was found to reconstruct the coefficient by minimizing the same Tikhonov regularization functional. In Chen & Liu (2006), the space-dependent reaction coefficient was determined in the heat equation with homogeneous Dirichlet boundary condition and final temperature measurement. A different weighted objective gradient functional was minimized to identify the coefficient. The coefficient was obtained numerically by applying the Armijo algorithm combined with the FEM. Finally, in Trucu *et al.* (2010b), the space-dependent reaction coefficient was determined in the one-dimensional heat equation with non-homogeneous Dirichlet boundary condition and heat flux or time-average temperature measurement. The first-order Tikhonov regularization functional was minimized using the NAG routine E04FCF together with the FDM to obtain the numerical solution for the unknown coefficient.

In this chapter, the determination of the space-dependent reaction coefficient from final time or time-average temperature measurements in the inverse parabolic with initial and boundary conditions is obtained by minimizing the nonlinear least-squares objective functional. The Fréchet gradient of the objective functional is obtained using a variational method. In order to obtain a stable numerical solution, the CGM regularized by the discrepancy principle, Alifanov (1994); Özişik & Orlande (2000), is developed apparently for the first time for the inverse problems under investigation. Three examples are presented, and the numerical results obtained using the CGM and the FDM show that

the CGM algorithm regularized by the discrepancy principle is efficient and stable for identifying the space-dependent reaction coefficient.

The mathematical formulations of the coefficient identification problems under investigation are presented in Section 5.2. This inverse problem is analysed in Section 5.3, and the Fréchet gradient together with the adjoint problem is obtained. The numerical CGM algorithm based on the sensitivity and adjoint problems is presented in Section 5.4. Numerical results are presented and discussed in Section Section 5.5. Finally, Section 5.6 highlights the conclusions of the work.

5.2 Mathematical formulation

The most common heat transfer model in tissue is obtained by balancing the accumulation of energy with the diffusion, heat transfer due to the blood flow through the capillary network and heat generation due to cell metabolism, to result in the well-known Pennes' bio-heat equation, Pennes (1948). As such, we consider the heat transfer problem in a bounded domain $\Omega \subset \mathbb{R}^{\mathrm{d}}$ with sufficient smooth boundary $\partial\Omega$, over the time interval $t \in (0, T)$, given by

$$\begin{cases} \frac{\partial u}{\partial t}(x,t) = \nabla \cdot (k(x)\nabla u(x,t)) - q(x)u(x,t) + f(x,t), & (x,t) \in Q_T, \\ u(x,t) = \mu(x,t), \quad (x,t) \in S_T, \quad u(x,0) = \phi(x), & x \in \overline{\Omega}. \end{cases} \tag{5.1}$$

The operator

$$\mathcal{L} := \frac{\partial}{\partial t} - \nabla \cdot (k\nabla) + q\mathcal{I}, \tag{5.2}$$

where $\mathcal{I}$ is the identity, is assumed to be uniformly parabolic, i.e.,

$$\upsilon_1 |\xi|^2 \leq \sum_{i,j=1}^{\mathrm{d}} k_{ij}(x)\xi_i\xi_j \leq \upsilon_2 |\xi|^2, \quad \text{a.e. } x \in \Omega, \ \forall \xi \in \mathbb{R}^{\mathrm{d}}, \tag{5.3}$$

for two given positive constants υ_1 and υ_2, and usually $k_{ij} = k_{ji}$.

In the above, Ω represents the tissue with $\mathrm{d} = 1, 2, 3$ usually, $k = (k_{ij}(x))_{i,j=\overline{1,\mathrm{d}}}$ denotes the thermal conductivity of the tissue satisfying (5.3) which states and the physical property that the thermal conductivity tensor is symmetric and positive definite, and leads to the operator $\mathcal{L}$ (5.2) being uniformly parabolic. The perfusion coefficient $q(x)$ in the bio-heat equation is the product between the heat capacity of the blood C_b and the blood perfusion rate ω_b. The arterial blood temperature has been assumed to be uniform and taken, for simplicity, equal to zero, and $f(x,t)$ is the given metabolic heat source. Neumann heat flux or Robin convective boundary conditions can also be considered instead of the Dirichlet boundary condition in (5.1).

5. DETERMINATION OF THE SPACE-DEPENDENT REACTION COEFFICIENT FROM FINAL OR TIME-AVERAGE DATA

Since the coefficient $q(x)$ in (5.1) is unknown we need additional information, and in this chapter we supply either the final temperature at $t = T$, namely,

$$e_1(x) = u(x, T), \quad x \in \Omega, \tag{5.4}$$

or the time-average temperature measurement

$$e_2(x) = \int_0^T \omega(t) u(x, t) dt, \quad x \in \Omega, \tag{5.5}$$

where $\omega(t) \in L_2(0, T)$ is some given weight function, and $e_1(x)$ and $e_2(x)$ are given data which may be subjected to noise due to measurement errors. Compatibility conditions between (5.1), (5.4) and (5.5) require that

$$e_1(x) = \mu(x, T), \quad x \in \partial\Omega, \tag{5.6}$$

and

$$e_2(x) = \int_0^T \omega(t) \mu(x, t) dt, \quad x \in \partial\Omega, \tag{5.7}$$

respectively.

There are two inverse problems, namely, (5.1), (5.4) and (5.1), (5.5) termed IP1 and IP2, respectively, which may be formulated for the determination of the space-dependent reaction coefficient $q(x) \geq 0$ together with the temperature $u(x, t)$. These two inverse problems possess in common the fundamental property that both the input data, $e_1(x)$ or $e_2(x)$, and output data, $q(x)$, are space-dependent. A different inverse Cauchy-type problem in which, instead of (5.4) or (5.5), we have a time-dependent boundary measurement of the heat flux,

$$k(x) \frac{\partial u}{\partial \nu}(x, t) = \tilde{\mu}(x, t), \quad (x, t) \in S_T, \tag{5.8}$$

is not investigated herein, but we mention Tadi *et al.* (2002); Trucu *et al.* (2008).

The existence and uniqueness of the classical solution in Hölder spaces of the IP1 was established in Prilepko & Solovev (1987). For the IP2, existence of a generalized solution was established in Kozhanov (2004) and Kamynin & Kostin (2010), whilst Prilepko & Kostin (1993) established uniqueness of generalized solutions in Sobolev spaces for both IP1 and IP2.

First, we state the existence and uniqueness of the solution for the direct problem (5.1) when all the coefficients and boundary and initial conditions are known functions (see Ladyzhenskaia *et al.* (1968), p.341).

Theorem 5.2.1. *Suppose that $k \in C^1(\Omega)$ satisfies (5.3), $q \in L_\infty(\Omega)$, $f \in L_2(Q_T)$, $\phi \in H^1(\Omega)$ and $\mu \in H^{3/2,3/4}(S_T)$. Then the direct problem (5.1) satisfying the compatibility condition of zero order $\phi|_{\partial\Omega} = \mu|_{t=0}$ has a unique solution $u \in H^{2,1}(Q_T)$ which satisfies the estimate*

$$\|u\|_{H^{2,1}(Q_T)} \leq c(\|f\|_{L_2(Q_T)} + \|\phi\|_{H^1(\Omega)} + \|\mu\|_{H^{3/2,3/4}(S_T)}), \tag{5.9}$$

where c is a positive constant.

Next, we state the uniqueness results for the inverse problems IP1 and IP2.

Theorem 5.2.2 (Prilepko & Kostin (1993))**.** *Let Ω be a bounded simply connected domain in $\mathbb{R}^{\mathrm{d}}$, $\mathrm{d} \geq 1$ with boundary $\partial\Omega \in C^2$. Suppose that $\phi = \mu \equiv 0$, $0 \leq f \in L_2(Q_T)$, $0 \leq f_t \in L_2(Q_T)$, $0 \leq \omega \in L_2(0,T)$. Then:*

(i) if $e_1 > 0$ in Ω (or $e_2 > 0$ in Ω) the solution of the IP1 (or IP2) is unique in the class of functions $u \in H^{2,1}(Q_T)$ and $0 \leq q \in L_\infty(\Omega)$;

(ii) the same uniqueness result holds if $f(\cdot,T) \not\equiv 0$ for IP1, or $\int_0^T \omega(t) f(\cdot,t)dt \not\equiv 0$ for IP2.

5.3 Analysis

Let $u(x,t;q)$ denote the solution of the direct problem, that is, the temperature corresponding to a particular value of the unknown function $q(x)$. The quasi-solution of the IP1 or IP2 is obtained such that the following least-squares objective functionals are minimized:

$$J_1(q) = \frac{1}{2}\|u(\cdot,T;q) - e_1^\epsilon(\cdot)\|^2_{L_2(\Omega)}, \tag{5.10}$$

or

$$J_2(q) = \frac{1}{2}\left\|\int_0^T \omega(t)u(\cdot,t;q)dt - e_2^\epsilon(\cdot)\right\|^2_{L_2(\Omega)}, \tag{5.11}$$

where e_1^ϵ or e_2^ϵ is the noisy temperature measurement satisfying

$$\|e_1 - e_1^\epsilon\|_{L_2(\Omega)} \leq \epsilon,$$
$$\|e_2 - e_2^\epsilon\|_{L_2(\Omega)} \leq \epsilon,$$

and ϵ is the level of noise, subject to $u \in H^{2,1}(Q_T)$ satisfying the direct problem (5.1), over the admissible set $\mathcal{A} = \{q \in L_\infty(\Omega) : q(x) \geq 0, \text{a.e. } x \in \Omega\}$.

The following result states the existence of the minimizer to the optimization problem (5.10) or (5.11), which can be proved according to the approach of Theorem 4.3.1.

Theorem 5.3.1. *There exists at least one minimizer to the optimization problem* (5.10) *or* (5.11).

Lemma 5.3.2. *The mapping $q \mapsto u(q)$ is Lipschitz continuous from $\mathcal{A}$ to $H^{2,1}(Q_T)$, i.e., for any $q, q+\Delta q \in \mathcal{A}$ and the corresponding $u(q), u(q+\Delta q) \in H^{2,1}(Q_T)$, there holds*

$$\|u(q+\Delta q) - u(q)\|_{H^{2,1}(Q_T)} \leq c\|\Delta q\|_{L_\infty(\Omega)}. \tag{5.12}$$

Proof. Denote $\Delta u = u(q+\Delta q) - u(q)$ which is the increment of the temperature u subject to q, then Δu satisfies the problem

$$\begin{cases} \frac{\partial(\Delta u)}{\partial t} = \nabla\cdot(k\nabla(\Delta u)) - q\Delta u - \Delta q u(q+\Delta q), & (x,t)\in Q_T, \\ \Delta u(x,t) = 0, \quad (x,t)\in S_T, \quad \Delta u(x,0) = 0, & x\in\overline{\Omega}. \end{cases} \tag{5.13}$$

Using the estimate (5.9) in Theorem 5.2.1 to the problem (5.13), we obtain

$$\|\Delta u\|_{H^{2,1}(Q_T)} \leq c\|\Delta q u\|_{L_2(Q_T)} \leq c\|\Delta q\|_{L_\infty(\Omega)}\|u\|_{L_2(Q_T)}.$$

Since $\|u\|_{L_2(Q_T)}$ is bounded by (5.9), this concludes the proof of the lemma. □

Lemma 5.3.3. *The mapping $q \mapsto u(q)$ from $\mathcal{A}$ to $H^{2,1}(Q_T)$ is Fréchet differentiable in the sense that for any $\Delta q \in L_\infty(\Omega)$ such that $q+\Delta q \in \mathcal{A}$ there exists a bounded linear operator $\mathfrak{U} : L_\infty(\Omega) \mapsto H^{2,1}(Q_T)$ such that*

$$\lim_{\|\Delta q\|_{L_\infty(\Omega)}\to 0} \frac{\|u(q+\Delta q) - u(q) - \mathfrak{U}\Delta q\|_{H^{2,1}(Q_T)}}{\|\Delta q\|_{L_\infty(\Omega)}} = 0. \tag{5.14}$$

Proof. Consider the problem

$$\begin{cases} \frac{\partial w}{\partial t} = \nabla\cdot(k\nabla w) - qw - \Delta q u(q), & (x,t)\in Q_T, \\ w(x,t) = 0, \quad (x,t)\in S_T, \quad w(x,0) = 0, & x\in\overline{\Omega}, \end{cases} \tag{5.15}$$

where $\Delta q \in L_\infty(\Omega)$ such that $q+\Delta q \in \mathcal{A}$. Theorem 5.2.1 shows that there exists a unique solution $w(x,t) \in H^{2,1}(Q_T)$ of (5.15), and the map $\Delta q \mapsto w$ from $L_\infty(\Omega)$ to $H^{2,1}(Q_T)$ defines a bounded linear operator $\mathfrak{U}$ by the estimate (5.9).

Denote $v = u(q+\Delta q) - u(q) - \mathfrak{U}\Delta q = \Delta u - w$, where Δu satisfies the problem (5.13), thus the function v satisfies the problem

$$\begin{cases} \frac{\partial v}{\partial t} = \nabla\cdot(k\nabla v) - qv - \Delta q\Delta u, & (x,t)\in Q_T, \\ v(x,t) = 0, \quad (x,t)\in S_T, \quad v(x,0) = 0, & x\in\overline{\Omega}. \end{cases} \tag{5.16}$$

Utilizing the estimate (5.9), we obtain

$$\|v\|_{H^{2,1}(Q_T)} \leq c\|\Delta q\Delta u\|_{L_2(Q_T)} \leq c\|\Delta q\|_{L_\infty(\Omega)}\|\Delta u\|_{L_2(Q_T)}, \tag{5.17}$$

and (5.12) implies that $\|v\|_{H^{2,1}(Q_T)} \leq c\|\Delta q\|^2_{L_\infty(\Omega)}$. The lemma is proved. □

Theorem 5.3.4. *The functional $J_1(q)$ in (5.10) is Fréchet differentiable and its gradient is*

$$J_1'(q) = -\int_0^T u(x,t)\lambda_1(x,t)dt, \tag{5.18}$$

where $\lambda_1(x,t)$ satisfies the following adjoint problem:

$$\begin{cases} \frac{\partial \lambda_1}{\partial t} = -\nabla\cdot(k\nabla\lambda_1) + q\lambda_1 - 2(u(x,T;q) - e_1^\epsilon(x))\delta(t-T), & (x,t)\in Q_T, \\ \lambda_1(x,t) = 0, \quad (x,t)\in S_T, \quad \lambda_1(x,T) = 0, & x\in\overline{\Omega}, \end{cases} \tag{5.19}$$

and δ is the Dirac delta function.

Proof. Taking any $\Delta q \in L_\infty(\Omega)$ such that $q+\Delta q \in \mathcal{A}$, and $\Delta J_1(q) = J_1(q+\Delta q) - J_1(q)$, we have

$$\begin{aligned} \Delta J_1(q) =& \frac{1}{2}\int_\Omega (u(x,T;q+\Delta q) - e_1^\epsilon(x))^2 dx - \frac{1}{2}\int_\Omega (u(x,T;q) - e_1^\epsilon(x))^2 dx \\ =& \int_\Omega \Delta u(x,T)(u(x,T;q) - e_1^\epsilon(x))dx + \frac{1}{2}\|\Delta u(\cdot,T)\|^2_{L_2(\Omega)}. \end{aligned}$$

Now we introduce a function $\lambda_1(x,t)$, being the solution to the final-boundary value problem (5.19). Using the problem (5.13) and integration by parts, we have

$$\begin{aligned} &\int_\Omega \Delta u(x,T)(u(x,T;q) - e_1^\epsilon(x))dx \\ =& \int_{Q_T} 2\Delta u(x,t)(u(x,T;q) - e_1^\epsilon(x))\delta(t-T)dxdt \\ =& \int_{Q_T} \Delta u\left(-\frac{\partial\lambda_1}{\partial t} - \nabla\cdot(k\nabla\lambda_1) + q\lambda_1\right)dxdt \\ =& \int_{Q_T} \lambda_1\left(\frac{\partial(\Delta u)}{\partial t} - \nabla\cdot(k\nabla(\Delta u)) + q\Delta u\right)dxdt - \int_\Omega \Delta u\lambda_1|_0^T dx \\ &+ \int_{S_T} k\left(\lambda_1\frac{\partial(\Delta u)}{\partial\nu} - \Delta u\frac{\partial\lambda_1}{\partial\nu}\right)dsdt = -\int_{Q_T}\Delta q u(q+\Delta q)\lambda_1 dxdt. \end{aligned}$$

Hence

$$\begin{aligned} \Delta J_1(q) =& -\int_{Q_T}\Delta q u(q+\Delta q)\lambda_1 dxdt + \frac{1}{2}\|\Delta u(\cdot,T)\|^2_{L_2(\Omega)} \\ =& -\int_{Q_T}\Delta q\Delta u\lambda_1 dxdt - \int_{Q_T}\Delta q u\lambda_1 dxdt + \frac{1}{2}\|\Delta u(\cdot,T)\|^2_{L_2(\Omega)}. \end{aligned}$$

Since Δu is the solution of the parabolic problem (5.13), in virtue of Lemma 5.3.2, we have $\|\Delta u(\cdot,T)\|^2_{L_2(\Omega)} \le c\|\Delta q\|^2_{L_\infty(\Omega)}$, and

$$\left|\int_{Q_T}\Delta q\Delta u\lambda_1 dxdt\right| \le \|\Delta q\|_{L_\infty(\Omega)}\|\Delta u\|_{L_2(Q_T)}\|\lambda_1\|_{L_2(Q_T)} \le c\|\Delta q\|^2_{L_\infty(\Omega)}\|\lambda_1\|_{L_2(Q_T)},$$

thus $\Delta J_1(q) = -\int_{Q_T}\Delta q u\lambda_1 dxdt + o(\|\Delta q\|_{L_\infty(\Omega)})$, which means the functional $J_1(q)$ is Fréchet differentiable, and its gradient is given by (5.18). The theorem is proved. □

Similarly, we can obtain the following result by applying the approach in the proof of Theorem 5.3.4 for the objective functional $J_2(q)$ in (5.11):

Theorem 5.3.5. *The functional $J_2(q)$ in (5.11) is Fréchet differentiable and its gradient is*

$$J_2'(q) = -\int_0^T u(x,t)\lambda_2(x,t)dt, \tag{5.20}$$

where $\lambda_2(x,t)$ satisfies the following adjoint problem:

$$\begin{cases} \frac{\partial \lambda_2}{\partial t} = -\nabla\cdot(k\nabla\lambda_2) + q\lambda_2 \\ \qquad -\omega(t)\left(\int_0^T \omega(\tau)u(x,\tau;q)d\tau - e_2^\epsilon(x)\right), \quad (x,t)\in Q_T, \\ \lambda_2(x,t) = 0, \quad (x,t)\in S_T, \quad \lambda_2(x,T) = 0, \qquad x\in\overline{\Omega}. \end{cases} \tag{5.21}$$

5.4 Conjugate gradient method

The following iterative process based on the CGM is used for the numerical estimation of the reaction coefficient $q(x)$ in (5.1) by minimizing the objective functional $J(q)$, where J stands for J_1 or J_2:

$$q^{n+1}(x) = q^n(x) + \beta^n d^n, \quad n = 0,1,2,\cdots \tag{5.22}$$

with the search direction given by

$$d^n = \begin{cases} -J'^0, \\ -J'^n + \gamma^n d^{n-1}, \quad n = 1,2,\cdots, \end{cases} \tag{5.23}$$

where the subscripts n denotes the number of iteration, $J'^n = J'(q^n)$, $q^0(x)$ is the initial guess for $q(x)$, β^n is search step size in passing from iteration n to iteration $n+1$. The conjugate gradient parameter γ^n is given by the Fletcher-Reeves formula, Fletcher & Reeves (1964),

$$\gamma^n = \frac{\|J'^n\|^2_{L_2(\Omega)}}{\|J'^{n-1}\|^2_{L_2(\Omega)}}, \quad n = 1,2,\cdots \tag{5.24}$$

For the problem IP1, the search step size β^n is found by minimizing

$$J_1(q^{n+1}) = \frac{1}{2}\int_\Omega (u(x,T;q^n+\beta^n d^n) - e_1^\epsilon(x))^2 dx. \tag{5.25}$$

Setting $\Delta q^n = d^n$, the estimated temperature $u(x,T;q^n+\beta^n d^n)$ is linearized by a Taylor series expression in the form

$$u(x,T;q^n+\beta^n d^n) \approx u(x,T;q^n) + \beta^n d^n \frac{\partial u(x,T;q^n)}{\partial q^n} \approx u(x,T;q^n) + \beta^n \Delta u(x,T;q^n)$$

and $\Delta u(x,T;q^n)$ is the solution of the sensitivity problem (5.13) when $t=T$. Then, we have

$$J_1(q^{n+1}) = \frac{1}{2}\int_\Omega (u(x,T;q^n) + \beta^n \Delta u(x,T;q^n) - e_1^\epsilon(x))^2 dx.$$

The partial derivative of the objective functional $J_1(q^{n+1})$ with respect to β^n is give by

$$\frac{\partial J_1(q^{n+1})}{\partial \beta^n} = \int_\Omega \Delta u(x,T;q^n)(u(x,T;q^n) + \beta^n \Delta u(x,T;q^n) - e_1^\epsilon(x))dx.$$

Setting $\frac{\partial J_1(q^{n+1})}{\partial \beta^n} = 0$, the search step size β^n is given by

$$\beta^n = \frac{\int_\Omega (u(x,T;q^n) - e_1^\epsilon(x))\Delta u(x,T;q^n)dx}{\|\Delta u(\cdot,T;q^n)\|^2_{L_2(\Omega)}}. \tag{5.26}$$

We also can obtain β^n for the inverse problem IP2 via a similar method. We have

$$\begin{aligned} J_2(q^{n+1}) =& \frac{1}{2}\int_\Omega \left[\int_0^T \omega(t)u(x,t;q^n+\beta^n d^n)dt - e_2^\epsilon(x)\right]^2 dx \\ =& \frac{1}{2}\int_\Omega \left[\int_0^T \omega(t)u(x,t;q^n)dt + \beta^n \int_0^T \omega(t)\Delta u dt - e_2^\epsilon(x)\right]^2 dx. \end{aligned}$$

Then the derivative of $J_2(q^{n+1})$ with respect to β^n is

$$\frac{\partial J_2}{\partial \beta^n} = \int_\Omega \left[\int_0^T \omega(t)u dt + \beta^n \int_0^T \omega(t)\Delta u dt - e_2^\epsilon\right]\left(\int_0^T \omega(t)\Delta u dt\right) dx.$$

Again we set $\frac{\partial J_2}{\partial \beta^n} = 0$, and obtain

$$\beta^n = -\frac{\int_\Omega \left(\int_0^T \omega(t)u dt - e_2^\epsilon\right)\left(\int_0^T \omega(t)\Delta u dt\right) dx}{\|\omega \Delta u\|^2_{L_2(Q_T)}}. \tag{5.27}$$

According to the discussion in Section 2.5, the CGM regularized by the discrepancy principle, for the numerical reconstruction of the reaction coefficient $q(x)$ for the inverse problem IP1 or IP2, may become well-posed. Hence, the iterative procedure is stopped when the following criterion is satisfied:

$$J(q^n) \le \bar{\epsilon}, \tag{5.28}$$

where $\bar{\epsilon}$ is a small positive value, e.g., $\bar{\epsilon} = 10^{-5}$, for exact measured data, or

$$\bar{\epsilon} = \frac{1}{2}\|e - e^\epsilon\|^2_{L_2(\Omega)}, \tag{5.29}$$

when the temperature measurement contains noisy data, e denote the final temperature measurement e_1 for the inverse problem IP1, or the time-average temperature measurement e_2 for the inverse problem IP2.

The steps of the CGM algorithm for the estimation of the reaction coefficient $q(x)$ for the inverse problem IP1 (and similarly for the inverse problem IP2) are shown as follows:

S1. Set $n = 0$ and choose an initial guess q^0 for the unknown reaction coefficient $q(x)$.

S2. Solve the direct problem (5.1) numerically by applying the FDM scheme to compute the temperature $u(x, t; q^n)$, and the objective functional $J_1(q^n)$ (5.10).

S3. If the stopping criterion (5.28) is satisfied, then go to S7. Else go to S4.

S4. Solve the adjoint problem (5.19) to compute the adjoint function $\lambda_1(x, t; q^n)$, and the gradient $J_1'(q^n)$ from (5.18). Compute the conjugate coefficient γ^n (5.24), and the search direction d^n in (5.23).

S5. Solve the sensitivity problem (5.13) to compute $\Delta u(x, t; q^n)$ by taking $\Delta q^n = d^n$, and compute the search step size β^n (5.26).

S6. Update q^{n+1} by (5.22). In case $q^{n+1}(x)$ takes negative values replace it utilizing $\max\{0, q^{n+1}(x)\}$ in order to enforce the physical constraint that the reaction coefficient cannot be negative. Set $n = n + 1$ and return to S2.

S7. End.

5.5 Numerical results and discussions

In this section, the space-dependent reaction coefficient $q(x)$ is numerically reconstructed by the CGM proposed in Section 5.4. We use the FDM, based on the C-N method to one dimension $\mathrm{d} = 1$, or the ADI method to two dimension $\mathrm{d} = 2$, to solve the direct, sensitivity and adjoint problems. We define the accuracy error at the iteration number n for the reaction coefficient $q(x)$ as

$$E(q^n) = \|q^n - q\|_{L_2(\Omega)}. \tag{5.30}$$

The final temperature e_1^ϵ for the inverse problem IP1 containing random errors are simulated by adding to the exact data an error term generated from a normal distribution by MATLAB in the form:

$$e_1^\epsilon = e_1 + \sigma_1 \times \mathrm{random}(1), \tag{5.31}$$

where $\sigma_1 = \frac{p}{100} \times \max_{x \in \overline{\Omega}} |e_1(x)|$ is the standard deviation and $p\%$ represents the percentage of noise. Similarly, the time-average temperature measurements e_2^ϵ for the inverse problem IP2 containing random errors are simulated as

$$e_2^\epsilon = e_2 + \sigma_2 \times \mathrm{random}(1), \tag{5.32}$$

where $\sigma_2 = \frac{p}{100} \times \max_{x \in \overline{\Omega}} |e_2(x)|$.

5.5.1 Example 1

In this example, we take $\Omega = (0,1)$, $T = 1$, $\omega(t) = 1$ and

$$k \equiv 1, \quad f \equiv 0, \quad \mu(0,t) = \mu(1,t) = 20e^{-t}, \quad \phi(x) = (x - x^2)^2 + 20, \tag{5.33}$$

$$e_1(x) = e^{-1}((x - x^2)^2 + 20), \quad \text{for IP1}, \tag{5.34}$$

$$e_2(x) = (1 - e^{-1})((x - x^2)^2 + 20), \quad \text{for IP2}, \tag{5.35}$$

we obtain the analytical solution, Trucu *et al.* (2010b),

$$u(x,t) = e^{-x}((x - x^2)^2 + 20), \quad q(x) = \frac{x^4 - 2x^3 + 13x^2 - 12x + 22}{(x - x^2)^2 + 20}. \tag{5.36}$$

We take the initial guess as $q^0(x) = 1.1$ such that on the boundary $\partial\Omega = \{0,1\}$, the initial guess is equal to the exact solution for the reaction coefficient $q(x)$ in (5.36), with the mesh size $\Delta x = \Delta t = 0.01$ applied in the FDM for solving the direct, sensitivity and adjoint problems involved.

Figures 5.1 and 5.3 show the monotonic decreasing convergence of the objective functional $J_1(q^n)$ given by (5.10) and $J_2(q^n)$ given by (5.11) that are minimized for the inverse problems IP1 and IP2, respectively, as functions of the number of iterations n, for various amounts of noise $p \in \{0,1,2\}$. For noisy data $p \in \{1,2\}$, the stopping iteration numbers $\{1,1\}$ are generated according to the discrepancy principle (5.28). It is clear that the stopping iteration numbers are quite close to the optimal ones in Figures 5.2(a) and 5.4(a) which present the error curve (5.30).

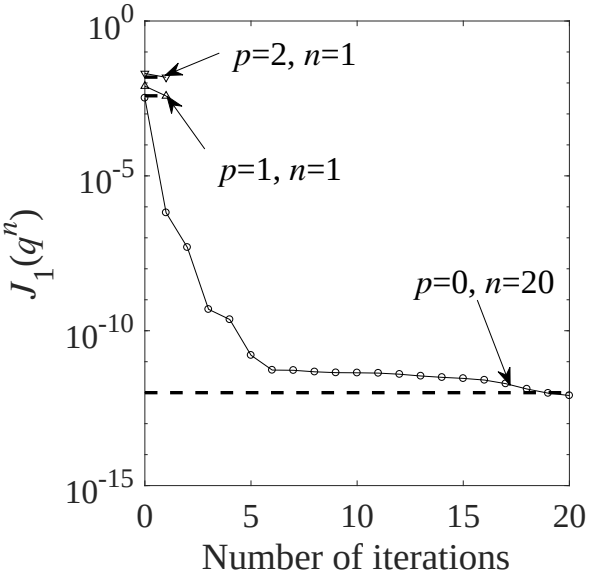

Figure 5.1: The objective functional $J_1(q^n)$ (5.10) with $p \in \{0,1,2\}$ noise, for the IP1 of Example 1.

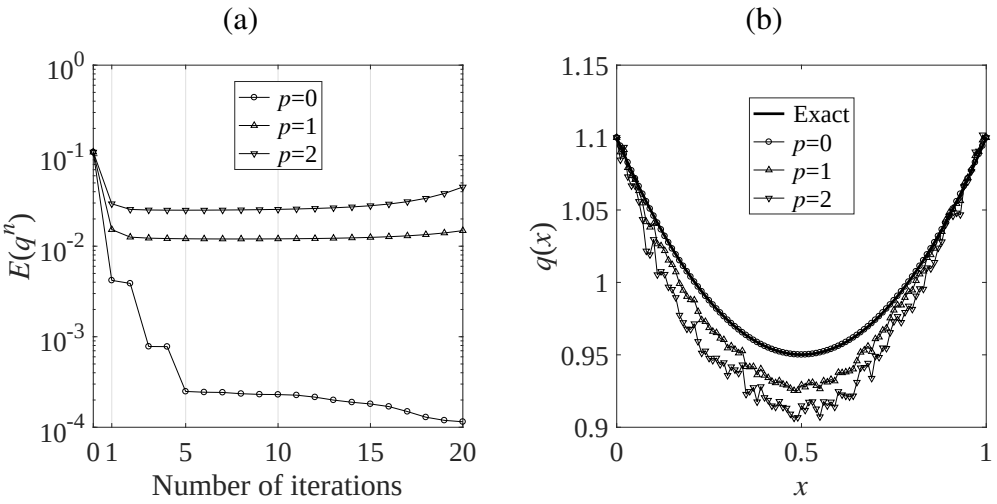

Figure 5.2: (a) The error $E(q^n)$ (5.30) and (b) the exact and numerical coefficient $q(x)$ with $p \in \{0, 1, 2\}$ noise, for the IP1 of Example 1.

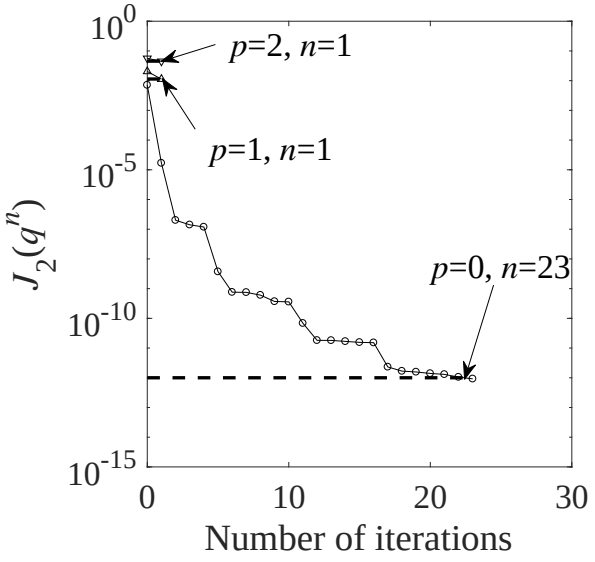

Figure 5.3: The objective functional $J_2(q^n)$ (5.11) with $p \in \{0, 1, 2\}$ noise, for the IP2 of Example 1.

The numerical solutions for IP1 and IP2 are presented in Figures 5.2(b) and 5.4(b), respectively. In the case of no noise, the results are plotted after 24 iterations, whilst for noisy data the results are plotted after 1 iterations. First, it can be seen that in the case of no noise, the retrieved solutions for both IP1 and IP2 are in very good agreement with the exact solution (5.36). Second, in the case of noisy data, the retrieved solutions are stable and they become more accurate as the amount of noise p decreases. The errors for IP1

and IP2 for various amounts of noise $p \in \{0, 1, 2\}$ are shown in Table 5.1, and it can be seen that the numerical results for IP2 are more accurate than the numerical results for IP1.

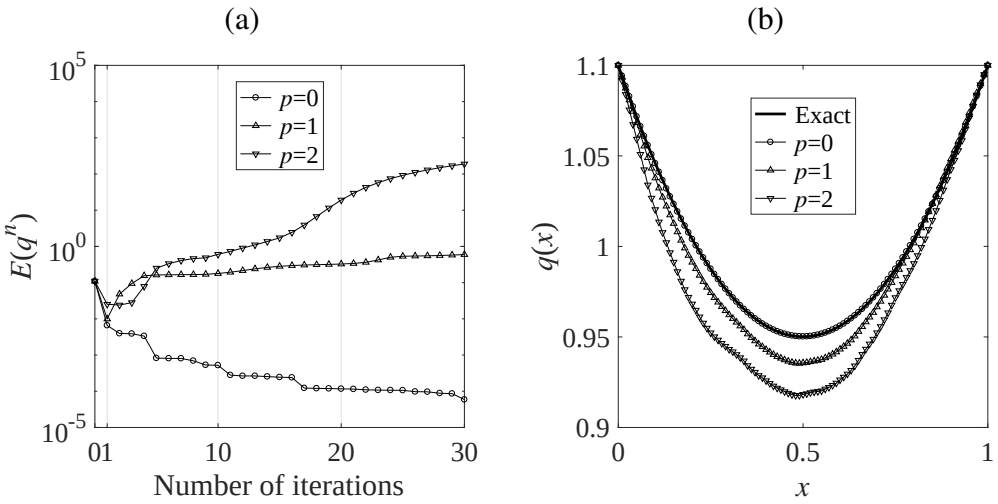

Figure 5.4: (a) The error $E(q^n)$ (5.30) and (b) the exact and numerical coefficient $q(x)$ with $p \in \{0, 1, 2\}$ noise, for the IP2 of Example 1.

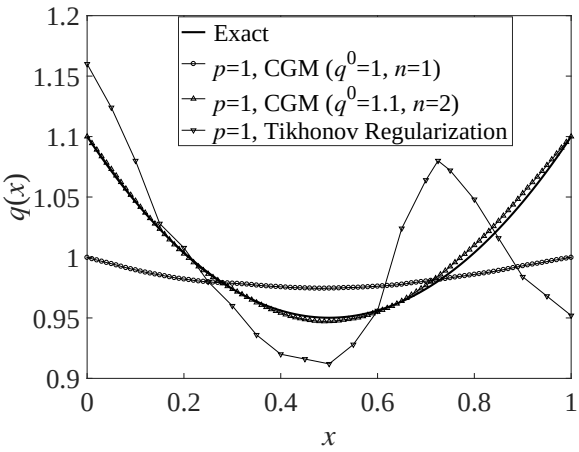

Figure 5.5: The exact solution (5.36), the numerical results of Trucu *et al.* (2010b) (with regularization parameter 0.8 and initial guess $q^0 = 1$), and of the CGM with initial guesses $q^0 = 1$ and $q^0 = 1.1$ for $p\% = 1\%$ noise, for the IP2 of Example 1.

Comparison with other method. For Example 1, a comparison for the IP2 can be made with the previous numerical results of Trucu *et al.* (2010b) obtained by minimizing the first-order Tikhonov regularization functional using the NAG routine E04FCF. In order to keep the numerical simulations as similar as possible the time-average temperature

Inverse problem			IP1			IP2		
p	I	M	$\bar{\epsilon}$	N	E	$\bar{\epsilon}$	N	E
0	101	101	1.0E-12	20	1.0E-04	1.0E-12	23	5.9E-05
1	101	101	3.8E-03	1	1.5E-02	1.1E-02	1	9.9E-03
2	101	101	1.5E-02	1	2.9E-02	4.5E-02	1	2.4E-02

Table 5.1: The stopping iteration numbers N and the errors E with $p \in \{0, 1, 2\}$ noise, for IP1 and IP2 of Example 1.

measurement (5.35) is perturbed by the multiplicative noise

$$e_2^\epsilon = e_2 \left(1 + \frac{p}{100} \times \eta\right), \tag{5.37}$$

where η are random variables generated from a uniform distribution in $[-1, 1]$, as in Trucu *et al.* (2010b), rather than the additive noise (5.32). In Trucu *et al.* (2010b), the initial guess $q^0(x) = 1$, but in our CGM, because of (5.18) and (5.19), as the value of $q^n(x)$ remains to $q^0(x)$ on $x \in \partial\Omega$, throughout iteration, we take the initial guess as $q^0(x) = 1.1$.

For $p\% = 1\%$ noise in (5.37), Figure 5.5 illustrates the comparison between the analytical solution (5.36), the Tikhonov's regularization numerical results of Trucu *et al.* (2010b) and those obtained by our CGM with the initial guesses $q^0(x) = 1$ (and stopped after $n = 1$ iteration according to (5.28)) and $q^0(x) = 1.1$ (and stopped after $n = 2$ iteration according to (5.28)). From this figure it can be seen that for $p\% = 1\%$ noise in the data (5.37), both the Tikhonov's regularization of Trucu *et al.* (2010b) and our CGM under-perform in achieving good agreement with the exact solution (5.36) when the initial guess is $q^0 = 1$. The CGM over-regularizes the numerical solution when stopped only after $n = 1$ iteration, according to the discrepancy principle (5.28), whilst the Tikhonov's method of Trucu *et al.* (2010b), with the regularization parameter 0.8, under-regularizes the numerical solution, which manifests some unstable oscillations. However, when the initial guess is $q^0 = 1.1$, which ensures that $q^0(x) = q(x)$ for $x \in \Omega$ our CGM is very accurate in comparison with the exact solution (5.36). Unfortunately, we do not have available the numerical results of Trucu *et al.* (2010b) for the initial guess $q^0 = 1.1$ to compare with. Finally, on comparing Figures 5.4 and 5.5 for $p\% = 1\%$ noise and initial guess $q^0 = 1.1$, it can be remarked that the CGM inversion of the data (5.35) perturbed by the multiplicative noise (5.37) is more accurate than when the data is perturbed by the additive noise (5.32).

5.5.2 Example 2

In this example, we take $\Omega = (0,1)$, $T = 1$, $\omega(t) = 1$,

$$k \equiv 1, \quad \phi \equiv 0, \quad \mu \equiv 0, \tag{5.38}$$

$$f(x,t) = 2t + x(1-x) + \begin{cases} tx(1-x)(2-x), & x \in [0, 0.3], \\ tx(1-x)(1-x+4x^2), & x \in (0.3, 0.7), \\ 3tx(1-x), & x \in [0.7, 1], \end{cases} \tag{5.39}$$

$$e_1(x) = x(1-x), \quad x \in (0,1), \quad \text{for IP1}, \tag{5.40}$$

$$e_2(x) = \frac{1}{2}x(1-x), \quad x \in (0,1), \quad \text{for IP2}. \tag{5.41}$$

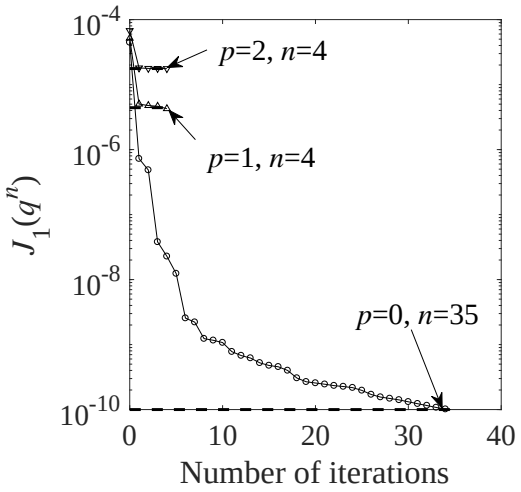

Figure 5.6: The objective functional $J_1(q^n)$ (5.10) with $p \in \{0, 1, 2\}$ noise, for the IP1 of Example 2.

One can observe that the conditions of Theorem 5.2.2 are satisfied and hence the solutions of the IP1 and IP2 are unique. In fact it can be verified by direct substitution that the analytical solution is given by

$$q(x) = \begin{cases} 2-x, & x \in [0, 0.3], \\ 1-x+4x^2, & x \in (0.3, 0.7), \\ 3, & x \in [0.7, 1], \end{cases} \qquad u(x,t) = tx(1-x). \tag{5.42}$$

The initial guess is chosen as $q^0(x) = 2+x$ which is a linear function passing through the end points $q(0) = 2$ and $q(1) = 3$. Figures 5.6 and 5.8 show the monotonic decreasing convergence of the objective functional $J_1(q^n)$ given by (5.10) and $J_2(q^n)$ given by (5.11) that are minimized for IP1 and IP2, respectively. For exact data, i.e., $p = 0$ numerical results are plotted after 35 and 38 iterations for IP1 and IP2, while for noisy data $p \in \{1, 2\}$, the stopping iteration numbers generated by the discrepancy principle (5.28) are

$\{4, 4\}$ and $\{4, 5\}$ for IP1 and IP2, respectively. The error curves (5.30) are shown in Figures 5.7(a) and 5.9(a), and the numerical solutions are presented in Figures 5.7(b) and 5.9(b). It is obvious that the numerical results deviate from the exact solution (5.42) near the discontinuity points $x = 0.3$ and $x = 0.7$. The errors for IP1 and IP2 are shown in Table 5.2 with $p \in \{0, 1, 2\}$ noise and it can be seen that the errors are quite close to each other for both IP1 and IP2.

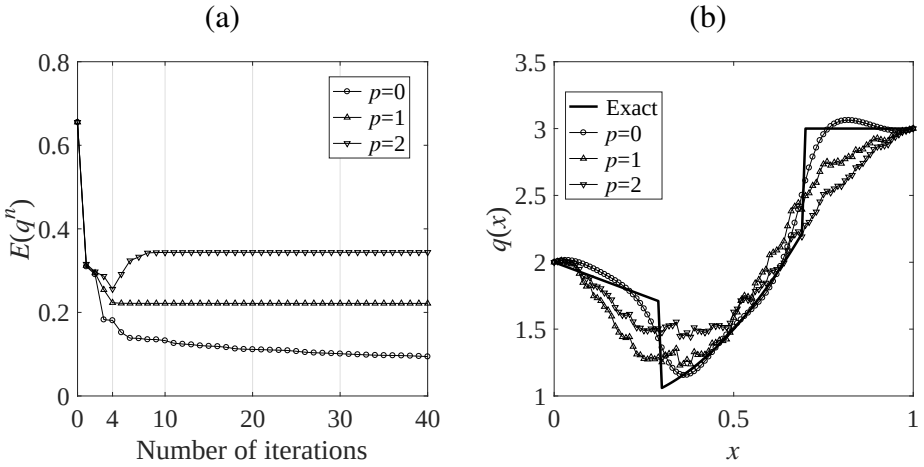

Figure 5.7: (a) The error $E(q^n)$ (5.30) and (b) the exact and numerical coefficient $q(x)$ with $p \in \{0, 1, 2\}$ noise, for the IP1 of Example 2.

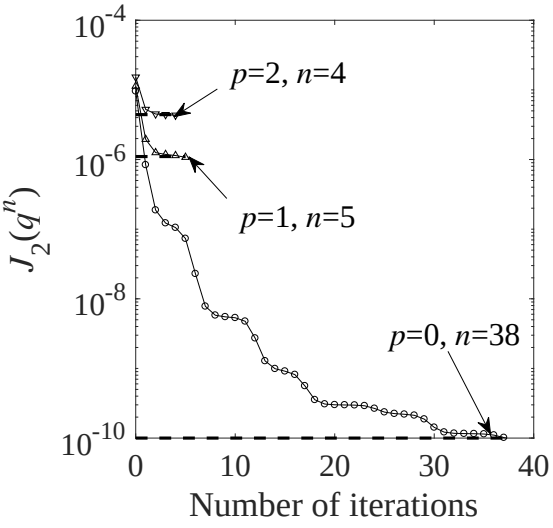

Figure 5.8: The objective functional $J_2(q^n)$ (5.11) with $p \in \{0, 1, 2\}$ noise, for the IP2 of Example 2.

Inverse problem			IP1			IP2		
p	I	M	$\bar{\epsilon}$	N	E	$\bar{\epsilon}$	N	E
0	101	101	1.0E-10	35	0.0972	1.0E-10	38	0.1184
1	101	101	4.4E-06	4	0.2233	1.1E-06	5	0.2188
2	101	101	1.8E-05	4	0.2558	4.4E-06	4	0.2504

Table 5.2: The stopping iteration numbers N and the errors E with $p \in \{0, 1, 2\}$ noise, for IP1 and IP2 of Example 2.

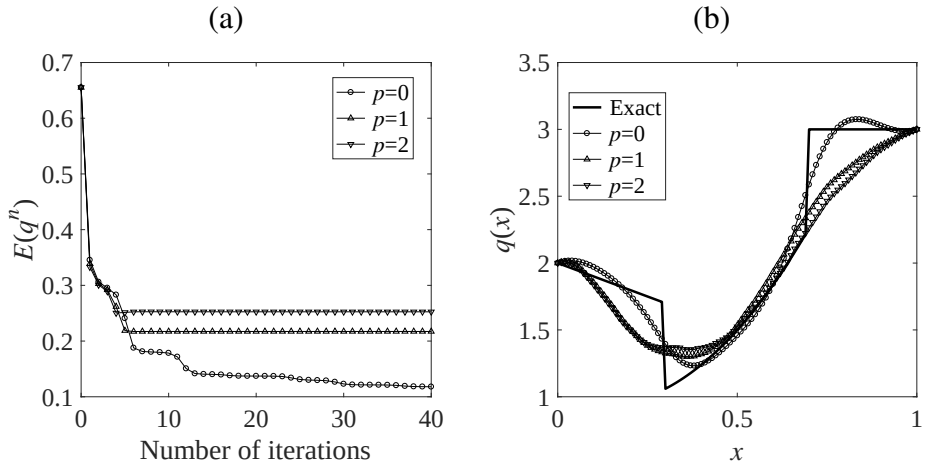

Figure 5.9: (a) The error $E(q^n)$ (5.30) and (b) the exact and numerical coefficient $q(x)$ with $p \in \{0, 1, 2\}$ noise, for the IP2 of Example 2.

5.5.3 Example 3

We consider now a two-dimensional ($\mathrm{d} = 2$) example in the domain $\Omega = (0, 1) \times (0, 1)$, $T = 1$, and

$$\begin{aligned} \omega(t) =& 1, \quad k = \mathbf{I}_2, \quad \mu \equiv 0, \quad \phi \equiv 0, \\ f(x_1, x_2, t) =& (1 + t(1 + x_1^2 + x_2^2))x_1x_2(1 - x_1)(1 - x_2) \\ &+ t(x_1(1 - x_1) + x_2(1 - x_2)), \\ e_1(x_1, x_2) =& x_1x_2(1 - x_1)(1 - x_2), \quad \text{for IP1}, \qquad (5.43) \\ e_2(x_1, x_2) =& \frac{1}{2}x_1x_2(1 - x_1)(1 - x_2), \quad \text{for IP2}. \qquad (5.44) \end{aligned}$$

One can observe that the conditions of Theorem 5.2.2 are satisfied and hence the solutions of the IP1 and IP2 are unique. In fact, it can be verified by direct substitution that the analytical solution is given by

$$q(x_1, x_2) = 1 + x_1^2 + x_2^2, \quad u(x_1, x_2, t) = tx_1x_2(1 - x_1)(1 - x_2). \qquad (5.45)$$

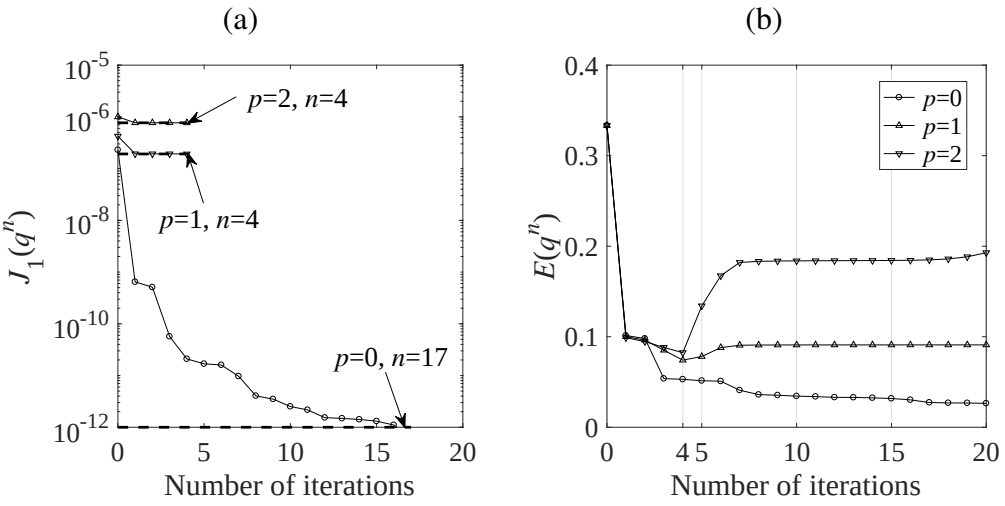

Figure 5.10: (a) The objective functional $J_1(q^n)$ (5.10) and (b) the error $E(q^n)$ (5.30) with $p \in \{0, 1, 2\}$ noise, for the IP1 of Example 3.

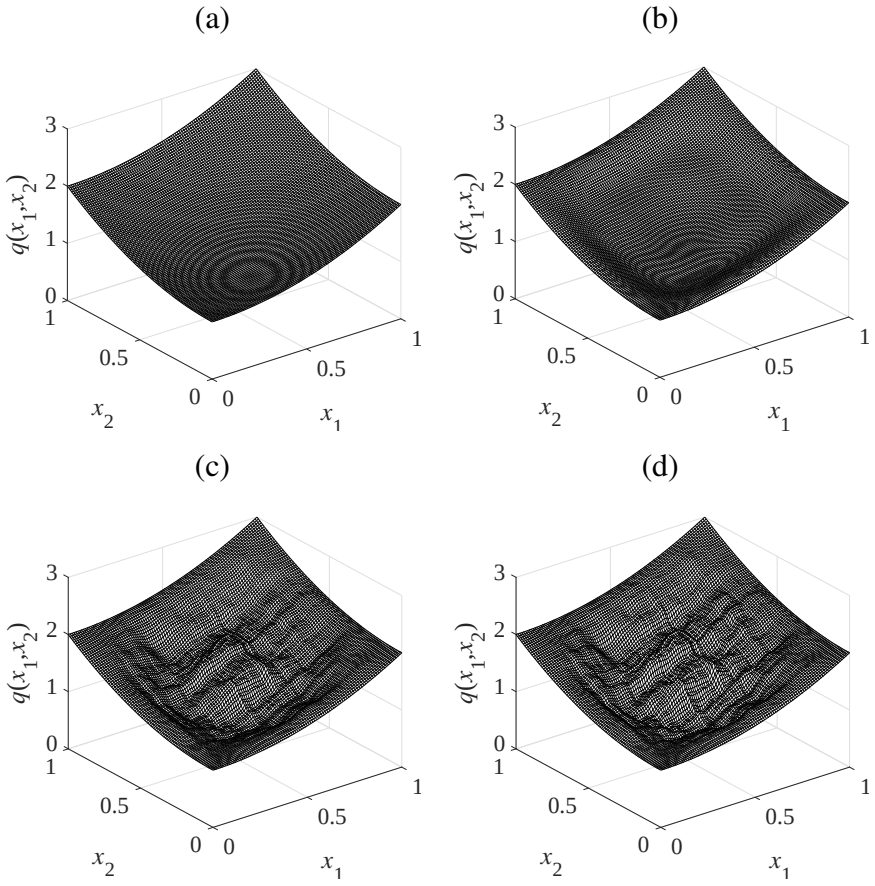

Figure 5.11: (a) The exact and numerical reaction coefficient $q(x_1, x_2)$ for (b) $p = 0$, (c) $p = 1$ and (d) $p = 1$ noise, for the IP1 of Example 3.

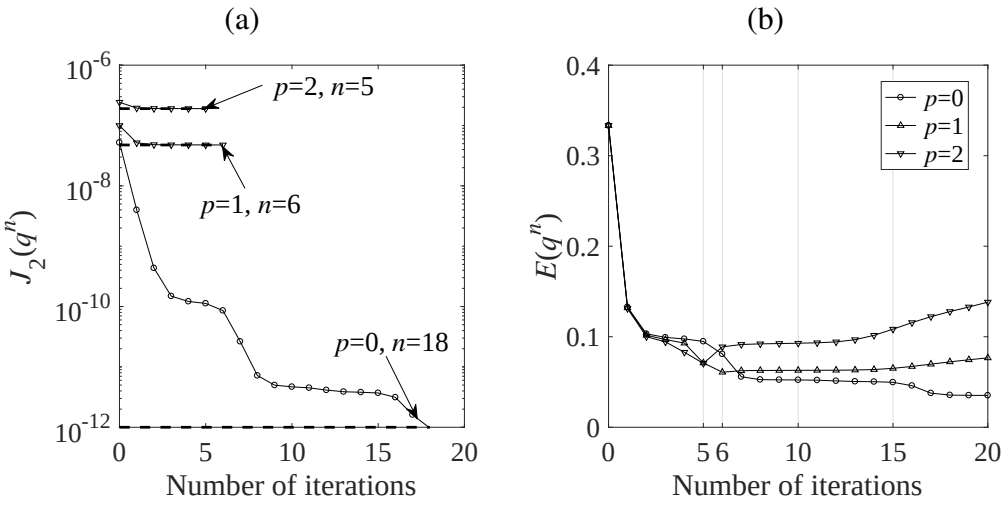

Figure 5.12: (a) The objective functional $J_2(q^n)$ (5.11) and (b) the error $E(q^n)$ (5.30) with $p \in \{0, 1, 2\}$ noise, for the IP2 of Example 3.

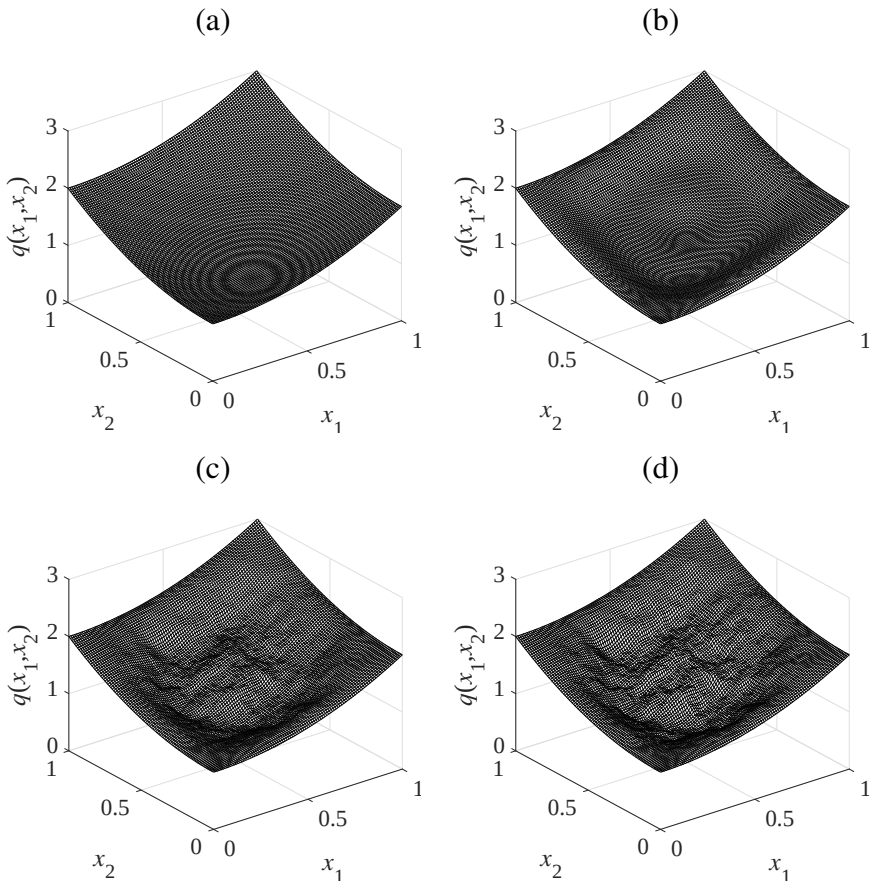

Figure 5.13: (a) The exact and numerical reaction coefficient $q(x_1, x_2)$ for (b) $p = 0$, (c) $p = 1$ and (d) $p = 1$ noise, for the IP2 of Example 3.

We take $I = J = M = 101$ and the initial guess

$$q^0(x_1, x_2) = 1 + x_1^2 + x_2^2 + 10x_1x_2(1 - x_1)(1 - x_2)$$

which ensures that $q^0 = q$ on the boundary $\partial\Omega$. Numerical results and errors presented in Figures 5.10–5.13 and Table 5.3 reveal the same conclusions as those drawn for Examples 1 and 2.

Inverse problem				IP1			IP2		
p	I	J	M	$\bar{\epsilon}$	N	E	$\bar{\epsilon}$	N	E
0	101	101	101	1.0E-12	17	0.0273	1.0E-12	18	0.0355
1	101	101	101	1.9E-07	4	0.0741	4.8E-08	6	0.0608
2	101	101	101	7.7E-07	4	0.0824	1.9E-07	5	0.0706

Table 5.3: The stopping iteration numbers N and the errors E with $p \in \{0, 1, 2\}$ noise, for IP1 and IP2 of Example 3.

5.6 Conclusions

The numerical CGM analysis developed and verified in this study overcomes the state of the art limits in reconstructing accurately and stably the space-dependent reaction coefficient from noisy final temperature or time-average temperature measurements. The Fréchet gradient together with the adjoint problems is obtained using the variational method. Regularization has been achieved by stopping the iterations at the level at which the least-squares objective functional, minimizing the gap between the computed and the measured data, becomes just below the noise threshold with which the data is contaminated. We have tested three examples for both inverse problems, and found that the numerical solutions are stable and become more accurate as the amount of noise decreases. From Example 2, we also understand that the error becomes larger when the exact reaction coefficient is discontinuous but still stable and reasonable. The numerical results show that the CGM is an efficient and stable iterative algorithm for reconstructing the reaction coefficient from minimal data which makes the solution of the inverse problems unique. We have also found out that the numerical solution for the IP2 based on the time-average temperature data (5.5), which is also more practically realistic, is slightly more accurate than the numerical solution for the IP1 based on the final instant temperature measurement (5.4).

In the next chapter, we extend the inverse analysis to the case when the initial temperature $\phi(x)$ is also unknown in addition to the reaction/perfusion coefficient $q(x)$.

Chapter 6

Simultaneous reconstruction of the space-dependent reaction coefficient and initial temperature

6.1 Introduction

Managing and controlling the complex process of heat transfer involves solving a wide-range of inverse problems concerned with the identification of physical properties and heat transfer coefficients, internal sources, boundary and/or initial conditions, Kurpisz & Nowak (1995). In particular, the efficient and safe performance of heat transfer apparatus and equipment requires knowledge of the heat transfer coefficients (HTCs). Therefore, an important but difficult problem of reconstructing the reaction coefficient, which are assumed to be spacewise dependent, from temperature measurements at interior points inside the heat conductor at prescribed times is proposed. Moreover, in certain applications, e.g., steel melting, data assimilation or deblurring, the initial status of the diffusion process cannot be prescribed directly, but instead the temperature at a later time is available. This BHCP is also well-known to be severely ill-posed, Miranker (1961).

When the initial temperature is known, the identification of the space-dependent reaction coefficient from final temperature measurements has been investigated theoretically and numerically, see Chapter 5. On the other hand, when the initial temperature is unknown, this BHCP is well-known to be severely ill-posed, but conditions under which it can become stable are well-known, Cannon & Douglas (1967); Miranker (1961). Moreover, there were many numerical techniques to reconstruct the unknown initial temperature, including the iterative CGM algorithm, Alifanov (1994); Özişik & Orlande (2000), the BEM, Han *et al.* (1995), the elliptic approximation together with the BEM, Lesnic

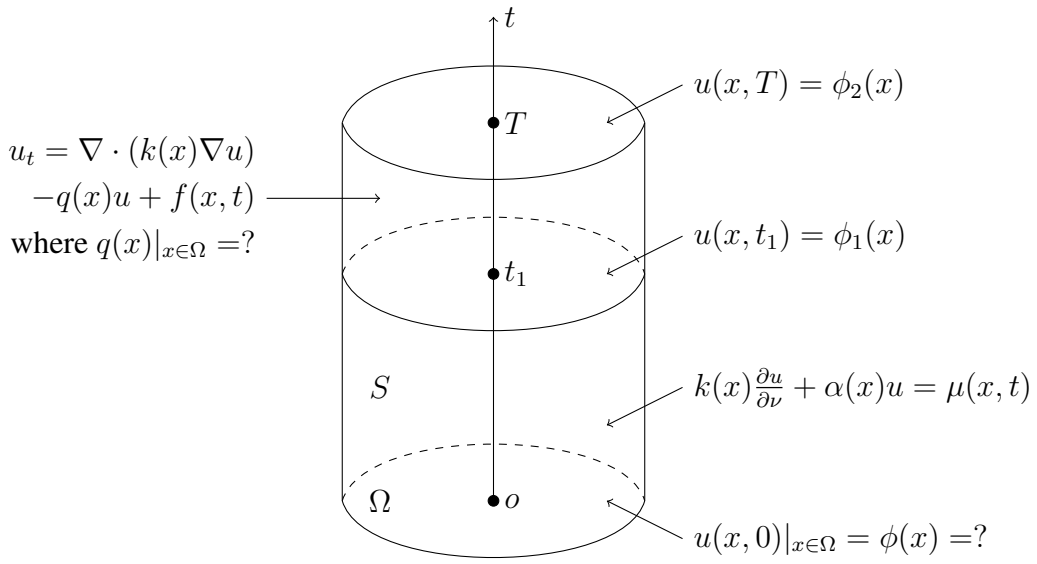

Figure 6.1: Schematic of the inverse problem under investigation.

et al. (1998), the Tikhonov regularization approach, Muniz *et al.* (1999), the Fourier regularization method, Fu *et al.* (2007), and the non-local boundary value problem method, Hào *et al.* (2009). It is also worth noting, Colton (1979), for the solution of the BHCP for the heat equation with heterogeneous thermal conductivity and the more recent investigation, Tuan *et al.* (2017), of the BHCP for the nonlinear heat equation.

Prior to this study, the space-dependent reaction coefficient and the initial temperature were simultaneously reconstructed in Yamamoto & Zou (2001) from temperature measurements at a fixed time and in a subregion of the space-time domain. The stability of the inverse problem and the existence of a minimizer to the Tikhonov's first-order regularization functional were proved. The multi-grid gradient method was used to obtain the numerical solution of the nonlinear finite element minimization problem. In a subsequent paper, Choulli & Yamamoto (2008), the previous reaction coefficient and the initial temperature were determined simultaneously with the Robin coefficient, which appears in a convection Robin boundary condition, from final time measurements only, provided that the reaction coefficient is *a-priori* known on a sub-domain of the heat conductor. The uniqueness and stability for this inverse problem were obtained.

In this chapter, the space-dependent reaction coefficient and initial temperature are determined from temperature observations at the final time T and at a instant of time t_1, where $t_1 \in (0,T)$. This is a completely new inverse problem, sketched in Figure 6.1, which has never been investigated before. The reaction coefficient is proved to be unique from the contraction mapping principle for the problem during the time-layer

$[t_1, T]$, and finally the initial temperature is obtained uniquely from the energy estimate for the BHCP during the time-layer $[0, t_1]$, Cao *et al.* (2018). Next, the simultaneous and numerical reconstruction of the reaction coefficient and initial temperature is carried out by minimizing the least-squares objective functional. The Fréchet gradient components with respect to the two unknowns are obtained together with the adjoint problem. Since the inverse problem is nonlinear and unstable, the CGM is regularized by the discrepancy principle, Alifanov (1994); Özişik & Orlande (2000), to obtain a stable and accurate numerical solution.

The mathematical formulation of the multi-component inverse problem under investigation is presented in section 6.2 together with the uniqueness result for the inverse problem. The variational formulation and the iterative CGM are presented in Sections 6.3 and 6.4. Numerical results are presented and discussed in Section 6.5 and finally, Section 6.6 highlights the conclusions.

6.2 Mathematical formulation

In the bounded domain $\Omega \subset \mathbb{R}^{\mathrm{d}}$ with boundary $\partial\Omega \in C^{2+l}$[1], consider the transient heat transfer process given by the following mathematical model:

$$\begin{cases} \frac{\partial u}{\partial t}(x,t) = \nabla \cdot (k(x)\nabla u(x,t)) - q(x)u(x,t) + f(x,t), & (x,t) \in Q_T, \\ k(x)\frac{\partial u}{\partial \nu} + \alpha(x)u(x,t) = \mu(x,t), \quad (x,t) \in S_T, \quad u(x,0) = \phi(x), & x \in \overline{\Omega}, \end{cases} \tag{6.1}$$

where $k(x) = (k_{ij}(x))_{i,j=\overline{1,\mathrm{d}}}$ is the thermal conductivity, $q(x)$ is the reaction coefficient, $\alpha(x)$ represents the Robin coefficient, and $f(x,t)$, $\mu(x,t)$ and $\phi(x)$ represent an internal source, heat flux and initial temperature, respectively. The convective boundary condition in (6.1) involving the Robin coefficient, $\alpha(x)$ on $x \in \partial\Omega$, is the most important boundary condition for quenching process simulation, Trombe *et al.* (2003).

For known system functions $(k(x), q(x), \alpha(x))$, if we consider (f, μ, ϕ) as the inputs for the heat conduction process, then (6.1) defines a well-posed process, namely, the temperature solution $u(x,t)$ to (6.1) is well-defined. However, in some engineering situations, the system parameters as well as some inputs may be unknown. To be precise, we assume that the thermal conductivity $k(x)$ and the Robin coefficient $\alpha(x)$ are known, but $q(x)$ and $\phi(x)$ are unknown. We are interested in the determination of

[1] That is, each point of $\partial\Omega$ has a neighbourhood in which $\partial\Omega$ is the graph of a function $x_{\mathrm{d}} = f(x_1, \ldots, x_{\mathrm{d}-1})$ of class C^{2+l} consisting of functions which themselves and all derivatives up to the second-order are Hölder continuous with exponent $l \in (0,1)$.

$(q(x), \phi(x), u(x,t))$ satisfying (6.1) and the extra temperature measurements at some internal time $t_1 \in (0,T)$ and the final time $t = T$, i.e., we are given

$$u(x,t_1) = \phi_1(x), \quad u(x,T) = \phi_2(x), \quad x \in \overline{\Omega}. \tag{6.2}$$

A sketch of the inverse problem under investigation is presented in Figure 6.1.

Remark 6.2.1. *A weighted time-average temperature observation*

$$\phi_2(x) = \int_{t_1}^{T} \omega(t) u(x,t) dt$$

for $x \in \overline{\Omega}$, with $\omega > 0$ a given weight function, may be specified in place of the second condition $u(x,T) = \phi_2(x)$ for $x \in \overline{\Omega}$, in (6.2), see Prilepko & Kostin (1993) and Chapter 5. Note that the input data (6.2) and the output components $q(x)$ and $\phi(x)$ of the inverse problem are both spatially distributed for $x \in \Omega$ and therefore, the rule of thumb of trace functionals in prescribing the extra data with respect to the unknowns is followed, Cannon et al. (1990). In case the destructive temperature measurements (6.2) are not permitted or available, non-destructive boundary temperature (or heat flux) measurements can be used instead, but this resulting non-characteristic, nonlinear and ill-posed inverse problem is deferred to a future work .

In practical cases, measurements unavoidably contain some noise. Therefore, from the numerical implementations point of view, we are in fact seeking the solution only approximately from the noisy data $(\phi_1^\epsilon, \phi_2^\epsilon)$ of (ϕ_1, ϕ_2) satisfying

$$\|\phi_1^\epsilon - \phi_1\|_{L_2(\Omega)} \le \epsilon, \quad \|\phi_2^\epsilon - \phi_2\|_{L_2(\Omega)} \le \epsilon, \tag{6.3}$$

where $\epsilon \ge 0$ represents the noise level.

In summary, our inverse problem is to identify the reaction coefficient $q(x)$, the initial status $\phi(x)$, and the temperature $u(x,t)$ throughout Q_T, from (6.1), and (6.2) or the noisy data $(\phi_1^\epsilon, \phi_2^\epsilon)$ satisfying (6.3). To analyse the above inverse problem, we need the following well-posedness result for the direct problem (6.1) (see Ladyzhenskaia *et al.* (1968), p.320).

Lemma 6.2.2. *Suppose $k_{ij} = k_{ji} \in C^{1+l}(\Omega)$, $i,j = \overline{1,\mathrm{d}}$, satisfying (5.3), $q \in C^l(\Omega)$ and $\alpha \in C^{1+l}(\partial\Omega)$. Then, for given $f \in C^{l,l/2}(Q_T)$, $\phi \in C^{2+l}(\Omega)$, $\mu \in C^{1+l,(1+l)/2}(S_T)$ satisfying the compatibility condition*

$$k(x)\frac{\partial \phi}{\partial \nu}(x) + \alpha(x)\phi(x) = \mu(x,0), \quad x \in \partial\Omega,$$

the direct problem (6.1) has a unique solution $u \in C^{2+l,1+l/2}(Q_T)$ satisfying the estimate

$$\|u\|_{C^{2+l,1+l/2}(Q_T)} \le c\left(\|f\|_{C^{l,l/2}(Q_T)} + \|\phi\|_{C^{2+l}(\Omega)} + \|\mu\|_{C^{1+l,(1+l)/2}(S_T)}\right). \tag{6.4}$$

Notice, the inverse problem (6.1) and (6.2) is nonlinear for unknown pair (q, ϕ). We state below the uniqueness for this inverse problem. Define $\mathcal{Q} := \{q(x) : q \in C^l(\Omega), 0 < q^- \leq q(x) \leq q^+\}$, $\Phi := \{\phi(x) : 0 < \phi_0 \leq \phi \in C^{2+l}(\Omega)\}$ where $q^\pm$ and ϕ_0 are given positive constants.

Theorem 6.2.3 (Cao *et al.* (2018)). *For known $0 < k_0 \leq k \in C^{1+l}(\Omega)$, $0 \leq \alpha \in C^{1+l}(\partial\Omega)$, $0 < f_0 \leq f \in C^{l,l/2}(Q)$ and $0 \leq \mu \in C^{1+l,(1+l)/2}(S)$, the solution to the inverse problem (6.1) and (6.2) is unique in $\mathcal{Q} \times \Phi$.*

6.3 Analysis

The unique reconstruction of $q(x)$ and $\phi(x)$ for $x \in \Omega$, together with the temperature $u(x,t)$ for $(x,t) \in Q_T$, from specified temperatures (6.2) at two instants t_1 and T is implemented by the following two steps:

- S1: Recover the solution $(q(x), u(x,t))$ satisfying the inverse problem

$$\begin{cases} \frac{\partial u}{\partial t}(x,t) = \nabla \cdot (k(x)\nabla u(x,t)) - q(x)u(x,t) + f(x,t), & (x,t) \in \Omega \times (t_1, T), \\ k(x)\frac{\partial u}{\partial \nu} + \alpha(x)u(x,t) = \mu(x,t), & (x,t) \in \partial\Omega \times [t_1, T], \\ u(x,t_1) = \phi_1(x), \quad u(x,T) = \phi_2(x), & x \in \overline{\Omega}; \end{cases}$$

- S2: With $q(x)$ in Ω already determined in S1, recover the solution $(\phi(x), T(x,t))$ of the BHCP given by

$$\begin{cases} \frac{\partial u}{\partial t}(x,t) = \nabla \cdot (k(x)\nabla u(x,t)) - q(x)u(x,t) + f(x,t), & (x,t) \in \Omega \times (0, t_1), \\ k(x)\frac{\partial u}{\partial \nu} + \alpha(x)u(x,t) = \mu(x,t), \ (x,t) \in \partial\Omega \times [0, t_1], \ u(x,t_1) = \phi_1(x), \ x \in \overline{\Omega}. \end{cases}$$

Although the above reconstruction process, which recovers three unknowns step by step, is clear for the formal uniqueness, the numerical implementation is not so easy, since the reconstruction error in one step will contaminate the recovery in the next step. Step S1 is the challenging since the inverse problem is both nonlinear and ill-posed, whilst Step S2 considers a linear BHCP which has been investigated in many studies but which is still challenging due to its severe ill-posedness and heterogeneity of the material.

In the following, we reconstruct $q(x)$ and $\phi(x)$ simultaneously using the noisy data $(\phi_1^\epsilon(x), \phi_2^\epsilon(x))$. To deal with these noisy situations, we reformulate the inverse problem as its optimization version. Let $u(x,t;q,\phi)$ be the solution of the direct problem (6.1). Introduce the admissible sets

$$\mathcal{A}_1 = \{q \in L_\infty(\Omega) : 0 < q^- \leq q(x) \leq q^+, \text{ a.e. } x \in \Omega\},$$
$$\mathcal{A}_2 = \{\phi \in L_2(\Omega) : 0 \leq \phi(x) \leq F_0, \text{ a.e. } x \in \Omega\}.$$

The quasi-solution of the inverse problem is obtained by minimizing the least-squares objective functional $J(q,\phi) : \mathcal{A}_1 \times \mathcal{A}_2 \to \mathbb{R}_+$ defined by

$$J(q,\phi) = \frac{1}{2}\left(\|u(\cdot,t_1;q,\phi) - \phi_1^\epsilon(\cdot)\|^2_{L_2(\Omega)} + \|u(\cdot,T;q,\phi) - \phi_2^\epsilon(\cdot)\|^2_{L_2(\Omega)}\right), \tag{6.5}$$

where $u(x,t;q,\phi) \in H^{1,0}(Q_T)$ is the weak solution to (6.1) satisfying the variational form

$$\begin{aligned}&\int_{Q_T}\left(-u\frac{\partial\eta}{\partial t} + (k\nabla u)\cdot\nabla\eta + qu\eta\right)dxdt + \int_{S_T}\alpha u\eta dsdt\\ &= \int_{Q_T} f\eta dxdt + \int_{S_T}\mu\eta dsdt + \int_\Omega \phi\eta(x,0)dx, \quad \forall\eta \in H^{1,1}(Q_T),\ \eta(\cdot,T) = 0.\end{aligned} \tag{6.6}$$

The existence and uniqueness of $u(q,\phi) \in H^{1,0}(Q_T)$ satisfying (6.6) for the direct problem (6.1) can be found in Tröltzsch (2010). Moreover,

$$\|u\|_{H^{1,0}(Q_T)} + \max_{t\in[0,T]}\|u(\cdot,t)\|_{L_2(\Omega)} \le c\left(\|f\|_{L_2(Q_T)} + \|\mu\|_{L_2(S_T)} + \|\phi\|_{L_2(\Omega)}\right) \tag{6.7}$$

for some constant $c > 0$ independent of f, μ and ϕ.

Inspired by the approaches in Hào *et al.* (2013); Keung & Zou (1998); Yamamoto & Zou (2001), the existence of a minimizer for the objective functional (6.5) over the admissible set $\mathcal{A}_1 \times \mathcal{A}_2$ is established as follows.

Theorem 6.3.1. *There exists at least one minimizer to the optimization problem* (6.5) *and* (6.6).

Proof. Since $\inf_{\mathcal{A}_1\times\mathcal{A}_2} J(q,\phi) =: J_0 \ge 0$, there exists a minimizing sequence

$$\{(q^n,\phi^n) : n \in \mathbb{N}\} \subset \mathcal{A}_1 \times \mathcal{A}_2$$

such that

$$\lim_{n\to\infty} J(q^n,\phi^n) = J_0.$$

Since $\{(q^n,\phi^n) : n \in \mathbb{N}\}$ is uniformly bounded in $L_\infty(\Omega)\times L_2(\Omega)$ and thus there exists a subsequence, still denoted by $\{q^n,\phi^n\}$, such that $(q^n,\phi^n) \rightharpoonup (q^*,\phi^*)$ in $L_\infty(\Omega)\times L_2(\Omega)$ with $(q^*,\phi^*) \in \mathcal{A}_1\times\mathcal{A}_2$. The *a-priori* estimate (6.7) implies that the sequence $\{u^n := u(q^n,\phi^n) : n \in \mathbb{N}\}$ is uniformly bounded in $H^{1,0}(Q_T)$, noticing that the constant c depends only on q^+. Thus we may extract a subsequence, still denoted by $\{u^n : n \in \mathbb{N}\}$ such that $u^n \rightharpoonup u^* \in H^{1,0}(Q_T)$ in $H^{1,0}(Q_T)$.

From the definition (6.6) of the weak solution, for any $\eta \in H^{1,1}(Q_T)$, $\eta(\cdot,T) = 0$, we have

$$\begin{aligned}&\int_{Q_T}\left(-u^n\frac{\partial\eta}{\partial t} + (k\nabla u^n)\cdot\nabla\eta + q^n u^n\eta\right)dxdt + \int_{S_T}\alpha u^n\eta dsdt\\ &= \int_{Q_T} f\eta dxdt + \int_{S_T}\mu\eta dsdt + \int_\Omega \phi^n\eta(x,0)dx.\end{aligned} \tag{6.8}$$

The third term in the left-hand side of (6.8) can be rewritten as

$$\int_{Q_T} q^n u^n \eta dxdt = \int_{Q_T} q^* u^n \eta dxdt + \int_{Q_T} (q^n - q^*) u^n \eta dxdt.$$

Since $q^n \rightharpoonup q^*$ in $L_\infty(\Omega)$, using the estimate (6.6) for u^n and the Lebesgue dominant convergence theorem giving $\int_{Q_T}(q^n - q)u^n \eta dxdt \to 0$, finally (6.8) leads to

$$\begin{aligned}
&\int_{Q_T} \left(-u^* \frac{\partial \eta}{\partial t} + (k\nabla u^*) \cdot \nabla \eta + q^* u^* \eta \right) dxdt + \int_{S_T} \alpha u^* \eta ds dt \\
&= \int_{Q_T} f\eta dxdt + \int_{S_T} \mu \eta ds dt + \int_\Omega \phi^* \eta(x,0) dx,
\end{aligned}$$

by $u^n \rightharpoonup u^*$ in $H^{1,0}(Q_T)$, $H^{1,0}(Q_T) \hookrightarrow L_2(Q_T)$ compactly and $u^n|_{S_T} \rightharpoonup u^*|_{S_T}$ in $L_2(S_T)$.

Thus we have $u^* = u(q^*, \phi^*)$ due to the uniqueness of weak solution to direct problem (6.1). Now the lower semi-continuity of norms implies

$$\begin{aligned}
J(q^*, \phi^*) &= \frac{1}{2}\left(\|u^*(\cdot, t_1) - \phi_1^\epsilon(\cdot)\|^2_{L_2(\Omega)} + \|u^*(\cdot, T) - \phi_2^\epsilon(\cdot)\|^2_{L_2(\Omega)} \right) \\
&\le \frac{1}{2} \lim_{n\to\infty} \left(\|u^n(\cdot, t_1) - \phi_1^\epsilon(\cdot)\|^2_{L_2(\Omega)} + \|u^n(\cdot, T) - \phi_2^\epsilon(\cdot)\|^2_{L_2(\Omega)} \right) \\
&\le \liminf_{n\to\infty} J(q^n, \phi^n) = \inf_{\mathcal{A}_1 \times \mathcal{A}_2} J(q, \phi),
\end{aligned}$$

i.e., $\{q^*, \phi^*\}$ is a minimizer of the optimization problem over $\mathcal{A}_1 \times \mathcal{A}_2$. The proof is complete. □

To find the minimizer, we will apply CGM where the gradient of $J(q, \phi)$ is required, which is ensured by the following lemma.

Lemma 6.3.2. *The mapping $(q, \phi) \mapsto u(q, \phi)$ is Lipschitz continuous from $\mathcal{A}_1$ to $H^{1,0}(Q_T)$ with respect to q, and from $\mathcal{A}_2$ to $H^{1,0}(Q_T)$ with respect to ϕ, i.e.,*

$$\|u(q + \Delta q, \phi) - u(q, \phi)\|_{H^{1,0}(Q_T)} \le c\|\Delta q\|_{L_\infty(\Omega)}, \tag{6.9}$$

$$\|u(q, \phi + \Delta\phi) - u(q, \phi)\|_{H^{1,0}(Q_T)} \le c\|\Delta\phi\|_{L_2(\Omega)} \tag{6.10}$$

for any $q, q+\Delta q \in \mathcal{A}_1$, $\phi, \phi+\Delta\phi \in \mathcal{A}_2$ and the corresponding $u(q, \phi), u(q+\Delta q, \phi), u(q, \phi+\Delta\phi) \in H^{1,0}(Q_T)$.

Proof. The proof is just a straightforward application of (6.7) to the initial-boundary value problems for $\Delta u_q := u(q + \Delta q, \phi) - u(q, \phi)$ and $\Delta u_\phi := u(q, \phi + \Delta\phi) - u(q, \phi)$. We omit the details. □

Based on the above lemma, now we can prove the differentiability of $u(q, \phi)$.

Lemma 6.3.3. *The mapping $(q,\phi) \mapsto u(q,\phi)$ is Fréchet differentiable with respect to q and ϕ, i.e., there exist two bounded linear operators $\mathcal{U}_q : \mathcal{A}_1 \mapsto H^{1,0}(Q_T)$ and $\mathcal{U}_\phi : \mathcal{A}_2 \mapsto H^{1,0}(Q_T)$ such that*

$$\lim_{\|\Delta q\|_{L_\infty(\Omega)}\to 0} \frac{\|u(q+\Delta q,\phi)-u(q,\phi)-\mathcal{U}_q\Delta q\|_{H^{1,0}(Q_t)}}{\|\Delta q\|_{L_\infty(\Omega)}} = 0, \tag{6.11}$$

$$\lim_{\|\Delta \phi\|_{L_2(\Omega)}\to 0} \frac{\|u(q,\phi+\Delta \phi)-u(q,\phi)-\mathcal{U}_\phi\Delta \phi\|_{H^{1,0}(Q_T)}}{\|\Delta \phi\|_{L_2(\Omega)}} = 0. \tag{6.12}$$

Proof. For given $q \in \mathcal{A}_1$, consider the problem

$$\begin{cases} \frac{\partial w}{\partial t} = \nabla\cdot(k\nabla w) - qw - \Delta q u(q,\phi), & (x,t)\in Q_T, \\ k(x)\frac{\partial w}{\partial \nu} + \alpha(x)w = 0, \quad (x,t)\in S_T, \quad w(x,0)=0, & x\in\overline{\Omega}, \end{cases} \tag{6.13}$$

for $\Delta q \in L_\infty(\Omega)$ such that $q+\Delta q \in \mathcal{A}_1$, where $u(q,\phi)$ is the solution to direct problem (6.1). Then there exists a unique solution $w(x,t) \in H^{1,0}(Q_T)$ for (6.13) depending on Δq linearly, and by (6.7), the mapping $\Delta q \mapsto w$ is from $L_\infty(\Omega)$ to $H^{1,0}(Q_T)$, which is defined as $\mathcal{U}_q$.

Define $v := u(q+\Delta q,\phi) - u(q,\phi) - \mathcal{U}_q\Delta q = \Delta u_q - w$. Then, it is easy to verify that Δu_q satisfies the parabolic problem

$$\begin{cases} \frac{\partial(\Delta u_q)}{\partial t} = \nabla\cdot(k\nabla(\Delta u_q)) - q\Delta u_q - \Delta q(\Delta u_q + u(q,\phi)), & (x,t)\in Q_T, \\ k(x)\frac{\partial(\Delta u_q)}{\partial \nu} + \alpha(x)\Delta u_q = 0, \quad (x,t)\in S_T, \quad \Delta u_q(x,0)=0, & x\in\overline{\Omega}. \end{cases} \tag{6.14}$$

Using (6.13), then v satisfies

$$\begin{cases} \frac{\partial v}{\partial t} = \nabla\cdot(k\nabla v) - qv - \Delta q\Delta u_q, & (x,t)\in Q_T, \\ k(x)\frac{\partial v}{\partial \nu} + \alpha(x)v = 0, \quad (x,t)\in S_T, \quad v(x,0)=0, & x\in\overline{\Omega}. \end{cases}$$

Applying (6.7) to this problem, we obtain

$$\|v\|_{H^{1,0}(Q_T)} \le c\|\Delta q\Delta u_q\|_{L_2(Q_T)} \le c\|\Delta q\|_{L_\infty(\Omega)}\|\Delta u_q\|_{H^{1,0}(Q_T)},$$

Using (6.9) in Lemma 6.3.2, the above estimate leads to

$$\|u(q+\Delta q,\phi)-u(q,\phi)-\mathcal{U}_q\Delta q\|_{H^{1,0}(Q_T)} = \|v\|_{H^{1,0}(Q_T)} \le c\|\Delta q\|^2_{L_\infty(\Omega)}.$$

So we have proven (6.11).

Similarly, the function $\Delta u_\phi = u(q,\phi+\Delta\phi) - u(q,\phi)$ satisfies the problem

$$\begin{cases} \frac{\partial \Delta u_\phi}{\partial t} = \nabla\cdot(k\nabla(\Delta u_\phi)) - q\Delta u_\phi, & (x,t)\in Q_T, \\ k(x)\frac{\partial(\Delta u_\phi)}{\partial \nu} + \alpha(x)\Delta u_\phi = 0, \quad (x,t)\in S_T, \quad \Delta u_\phi(x,0)=\Delta\phi(x), & x\in\overline{\Omega}, \end{cases} \tag{6.15}$$

which defines a linear operator $\mathcal{U}_\phi$ on $\Delta\phi$. Then, the relation (6.12) can be proven analogously. The proof is complete. □

Theorem 6.3.4. *The objective functional $J(q,\phi)$ is Fréchet differentiable and its Fréchet derivatives $J'_q(q,\phi)$ and $J'_\phi(q,\phi)$ are given by*

$$J'_q(q,\phi) = -\int_0^T u(x,t)\lambda(x,t)dt, \quad x \in \Omega, \tag{6.16}$$

$$J'_\phi(q,\phi) = \lambda(x,0), \quad x \in \Omega, \tag{6.17}$$

where λ satisfies the following adjoint problem:

$$\begin{cases} \frac{\partial \lambda}{\partial t} = -\nabla\cdot(k\nabla\lambda) + q\lambda - (u(x,t_1;q,\phi) - \phi_1^\epsilon)\delta(t-t_1) \\ \qquad -2(u(x,T;q,\phi) - \phi_2^\epsilon)\delta(t-T), & (x,t) \in Q_T, \\ k(x)\frac{\partial \lambda}{\partial \nu} + \alpha(x)\lambda = 0, \quad (x,t) \in S_T, \quad \lambda(x,T) = 0, & x \in \overline{\Omega}, \end{cases} \tag{6.18}$$

where $\delta(\cdot)$ denotes the Dirac delta function.

Proof. Taking any $\Delta q \in L_\infty(\Omega)$ such that $q + \Delta q \in \mathcal{A}_1$, we have

$$\begin{aligned} &J(q+\Delta q,\phi) - J(q,\phi) \\ =&\frac{1}{2}\|\Delta u_q(\cdot,t_1)\|^2_{L_2(\Omega)} + \int_{Q_T} \Delta u_q(x,t)\left[u(x,t_1;q,\phi) - \phi_1^\epsilon(x)\right]\delta(t-t_1)dxdt \\ &+ \frac{1}{2}\|\Delta u_q(\cdot,T)\|^2_{L_2(\Omega)} + 2\int_{Q_T} \Delta u_q(x,t)\left[u(x,T;q,\phi) - \phi_2^\epsilon(x)\right]\delta(t-T)dxdt. \end{aligned}$$

Let λ be the weak solution of the problem (6.18). Integrating by parts in the above identity, we have

$$\begin{aligned} J(q+\Delta q,\phi) - J(q,\phi) = &\int_{Q_T} \Delta u_q \left\{-\frac{\partial \lambda}{\partial t} - \nabla\cdot(k\nabla\lambda) + q\lambda\right\} dxdt \\ &+ \frac{1}{2}\|\Delta u_q(\cdot,t_1)\|^2_{L_2(\Omega)} + \frac{1}{2}\|\Delta u_q(\cdot,T)\|^2_{L_2(\Omega)}, \end{aligned}$$

and

$$\begin{aligned} &\int_{Q_T} \Delta u_q \left\{-\frac{\partial \lambda}{\partial t} - \nabla\cdot(k\nabla\lambda) + q\lambda\right\} dxdt \\ =&\int_{Q_T} \lambda\left\{\frac{\partial(\Delta u_q)}{\partial t} - \nabla\cdot(k\nabla(\Delta u_q)) + q\Delta u_q\right\} dxdt - \int_\Omega \Delta u_q\lambda|_0^T dx \\ &+ \int_{S_T}\left(k\frac{\partial(\Delta u_q)}{\partial \nu}\lambda - k\frac{\partial \lambda}{\partial \nu}\Delta u_q\right) dsdt = -\int_{Q_T} \Delta q u(q+\Delta q,\phi)\lambda dxdt. \end{aligned}$$

Using the decomposition on the first term of the right-hand side

$$-\int_{Q_T} \Delta q u(q+\Delta q,\phi)\lambda dxdt = -\int_{Q_T} \Delta q \Delta u_q \lambda dxdt - \int_{Q_T} \Delta q u \lambda dxdt$$

and noticing Δu_q the problem (6.14) with zero boundary and initial conditions and by (6.7), we have $\max\left\{\|\Delta u_q(\cdot,t_1)\|^2_{L_2(\Omega)}, \|\Delta u_q(\cdot,T)\|^2_{L_2(\Omega)}\right\} \leq c\|u\|^2_{L_2(Q_T)}\|\Delta q\|^2_{L_\infty(\Omega)}$, from Lemma 6.3.2 and

$$\left|\int_{Q_T} \Delta q \Delta u_q \lambda dx dt\right| \leq \|\Delta q\|_{L_\infty(\Omega)}\|\Delta u_q\|_{L_2(Q_T)}\|\lambda\|_{L_2(Q_T)} \leq c\|\Delta q\|^2_{L_\infty(\Omega)}.$$

Thus, $J(q+\Delta q,\phi) - J(q,\phi) = -\int_{Q_T} \Delta q u \lambda dx dt + o(\|\Delta q\|_{L_\infty(\Omega)})$, which means that the Fréchet derivative $J'_q(q,\phi)$ is given by (6.16). Using a similar approach, we obtain $J(q,\phi+\Delta\phi) - J(q,\phi) = \int_\Omega \Delta\phi\lambda(x,0)dx + o(\|\Delta\phi\|_{L_2(\Omega)})$, thus the Fréchet derivative $J'_\phi(q,\phi)$ is given by (6.17). The proof is complete. □

6.4 Conjugate gradient method

The following iterative process based on the CGM is now used for the estimation of $q(x)$ and $\phi(x)$ by minimizing the objective functional $J(q,\phi)$:

$$q^{n+1}(x) = q^n(x) + \beta^n_q d^n_q, \quad \phi^{n+1}(x) = \phi^n(x) + \beta^n_\phi d^n_\phi, \quad n = 0,1,2,\cdots, \tag{6.19}$$

where n denotes the number of iterations, $q^0(x)$ and $\phi^0(x)$ are the initial guesses for $q(x)$ and $\phi(x)$, β^n_q and β^n_ϕ are the step search sizes for $q(x)$ and $\phi(x)$ in passing from iteration n to iteration $n+1$, and d^n_q and d^n_ϕ are the directions of descent given by

$$d^n_q = \begin{cases} -J'^0_q, \\ -J'^n_q + \gamma^n_q d^{n-1}_q, \end{cases} \qquad d^n_\phi = \begin{cases} -J'^0_\phi, \\ -J'^n_\phi + \gamma^n_\phi d^{n-1}_\phi, \end{cases} \quad n = 1,2,\cdots \tag{6.20}$$

The Fletcher–Reeves type conjugate gradient coefficients γ^n_q and γ^n_ϕ are given by

$$\gamma^n_q = \frac{\|J'^n_q\|^2_{L_2(\Omega)}}{\|J'^{n-1}_q\|^2_{L_2(\Omega)}}, \quad \gamma^n_\phi = \frac{\|J'^n_\phi\|^2_{L_2(\Omega)}}{\|J'^{n-1}_\phi\|^2_{L_2(\Omega)}}, \quad n = 1,2,\cdots \tag{6.21}$$

The search step sizes β^n_q and β^n_ϕ are found by minimizing

$$\begin{aligned} J(q^{n+1},\phi^{n+1}) =& \frac{1}{2}\int_\Omega [u(x,t_1;q^n+\beta^n_q d^n_q, \phi^n+\beta^n_\phi d^n_\phi) - \phi^\epsilon_1(x)]^2 dx \\ &+ \frac{1}{2}\int_\Omega [u(x,T;q^n+\beta^n_q d^n_q, \phi^n+\beta^n_\phi d^n_\phi) - \phi^\epsilon_2(x)]^2 dx. \end{aligned}$$

Setting $\Delta q^n = P^n_q$ and $\Delta\phi^n = P^n_\phi$, the temperature $u(x,t_1;q^n+\beta^n_q d^n_q, \phi^n+\beta^n_\phi d^n_\phi)$ and $u(x,T;q^n+\beta^n_q d^n_q, \phi^n+\beta^n_\phi d^n_\phi)$ are linearised by a Taylor series expansion in the form

$$\begin{aligned} &u(x,t';q^n+\beta^n_q d^n_q, \phi^n+\beta^n_\phi d^n_\phi) \\ \approx& u(x,t';q^n,\phi^n) + \beta^n_q \Delta u_q(x,t';q^n,\phi^n) + \beta^n_\phi \Delta u_\phi(x,t';q^n,\phi^n) \end{aligned}$$

where t' represents t_1 and T, respectively. Then, denoting

$$\begin{aligned}
&u_1^n = u(x, t_1; q^n, \phi^n), \quad u_2^n = u(x, T; q^n, \phi^n),\\
&\Delta u_{q,1}^n = \Delta u_q(x, t_1; q^n, \phi^n), \quad \Delta u_{q,2}^n = \Delta u_q(x, T; q^n, \phi^n),\\
&\Delta u_{\phi,1}^n = \Delta u_\phi(x, t_1; q^n, \phi^n), \quad \Delta u_{\phi,2}^n = \Delta u_\phi(x, T; q^n, \phi^n),
\end{aligned}$$

we have

$$\begin{aligned}
J(q^{n+1}, \phi^{n+1}) =& \frac{1}{2}\int_\Omega [u_1^n + \beta_q^n \Delta u_{q,1}^n + \beta_\phi^n \Delta u_{\phi,1}^n - \phi_1^\epsilon(x)]^2 dx\\
&+ \frac{1}{2}\int_\Omega [u_2^n + \beta_q^n \Delta u_{q,2}^n + \beta_\phi^n \Delta u_{\phi,2}^n - \phi_2^\epsilon(x)]^2 dx.
\end{aligned}$$

We calculate the partial derivatives with respect to β_q^n and β_ϕ^n to obtain

$$\frac{\partial J}{\partial \beta_q^n} = C_1\beta_q^n + C_2\beta_\phi^n + C_3, \quad \frac{\partial J}{\partial \beta_\phi^n} = C_2\beta_q^n + C_4\beta_\phi^n + C_5,$$

where

$$\begin{aligned}
&C_1 = \int_\Omega \left[(\Delta u_{q,1}^n)^2 + (\Delta u_{q,2}^n)^2\right] dx, \quad C_2 = \int_\Omega \left(\Delta u_{q,1}^n \Delta u_{\phi,1}^n + \Delta u_{q,2}^n \Delta u_{\phi,2}^n\right) dx,\\
&C_3 = \int_\Omega \left[(u_1^n - \phi_1^\epsilon)\Delta u_{q,1}^n + (u_2^n - \phi_2^\epsilon)\Delta u_{q,2}^n\right] dx, \quad C_4 = \int_\Omega \left[(\Delta u_{\phi,1}^n)^2 + (\Delta u_{\phi,2}^n)^2\right] dx,\\
&C_5 = \int_\Omega \left[(u_1^n - \phi_1^\epsilon)\Delta u_{\phi,1}^n + (u_2^n - \phi_2^\epsilon)\Delta u_{\phi,2}^n\right] dx.
\end{aligned}$$

Next, we set $\frac{\partial J}{\partial \beta_q^n} = \frac{\partial J}{\partial \beta_\phi^n} = 0$, and obtain the search step sizes β_q^n and β_ϕ^n as follows:

$$\beta_q^n = \frac{C_2C_5 - C_3C_4}{C_2^2 - C_1C_4}, \quad \beta_\phi^n = \frac{C_2C_3 - C_1C_5}{C_2^2 - C_1C_4}, \quad n = 0, 1, \cdots. \tag{6.22}$$

The unregularized iterative procedure given by (6.19) does not provide the CGM with the stabilization necessary for the minimization of the function (6.5) to be classified as well-posed because of the errors inherent in the measurements (6.2). However, the CGM algorithm may become well-posed if the discrepancy principle is used to stop the iterative procedure when the following criterion is satisfied:

$$J(q^n, \phi^n) \le \bar{\epsilon} \tag{6.23}$$

where $\bar{\epsilon}$ is some small positive value, e.g., $\bar{\epsilon} = 10^{-5}$, for the exact temperature measurements, and

$$\bar{\epsilon} = \frac{1}{2}\left(\|\phi_1 - \phi_1^\epsilon\|_{L_2(\Omega)}^2 + \|\phi_2 - \phi_2^\epsilon\|_{L_2(\Omega)}^2\right),$$

when the measured temperatures contain noise.

To summarise, the steps of the CGM for reconstructing the unknown space-dependent coefficients $q(x)$ and $\phi(x)$ numerically, are as follows:

S1. Set $n = 0$ and choose initial guesses $q^0(x)$ and $\phi^0(x)$ for the unknown $q(x)$ and $\phi(x)$, respectively.

S2. Solve the direct problem (6.1) (using e.g., FDM) to compute $u(x,t;q^n,\phi^n)$ and $J(q^n,\phi^n)$.

S3. If the stopping condition (6.23) is satisfied, then go to S7. Else go to S4.

S4. Solve the adjoint problem (6.18) to compute the function $\lambda(x,t;q^n,\phi^n)$, and the gradients $J'_q(q^n,\phi^n)$ in (6.16) and $J'_\phi(q^n,\phi^n)$ in (6.17). Compute the conjugate coefficients γ_q^n and γ_ϕ^n in (6.21), and the directions of descent d_q^n and d_ϕ^n in (6.20).

S5. Solve the sensitivity problems (6.14) and (6.15) to compute $\Delta u_q(x,t;q^n,\phi^n)$ and $\Delta u_\phi(x,t;q^n,\phi^n)$ by taking $\Delta q^n(x) = d_q^n(x)$ and $\Delta\phi^n(x) = d_\phi^n(x)$, and compute the search step sizes β_q^n and β_ϕ^n in (6.22).

S6. Compute q^{n+1} and ϕ^{n+1} by (6.19). In case q^{n+1} takes negative values replace it by $\max\{0, q^{n+1}\}$ in order to enforce the physical constraint that the coefficient $q(x)$ cannot be negative. Set $n = n+1$ and return to S2.

S7. End.

Remark 6.4.1. *At this stage it is worth mentioning that another possible approach, motivated by Johansson & Lesnic (2008), was also developed based on decoupling the simultaneously identification into first obtaining the reaction coefficient $q(x)$ using the CGM in Chapter 5 by solving the inverse coefficient problem in the region $\Omega\times(t_1,T)$, after which the initial temperature $\phi(x)$ is obtained using an elliptic approximation method, Lesnic et al. (1998), for solving the BHCP in the region $\Omega\times(0,t_1)$. However, due to the uncontrollable noise present or accumulated in $q(x)$, $\phi_1(x)$ and $\partial_t u(x,t_1)$, which are needed as input in this latter method, the numerically obtained results were rather inconsistent and therefore they are not presented.*

6.5 Numerical results and discussions

In this section we show the numerical results for the initial temperature $\phi(x)$ and the reaction coefficient $q(x)$ reconstructed simultaneously by the nonlinear CGM, as described in Section 6.4. The FDM based on the C-N scheme in one dimension $\mathrm{d}=1$, or the ADI scheme in two dimension $\mathrm{d}=2$, is employed to solve the direct, sensitivity and adjoint

problems. Note that the source term in (6.18) contains the Dirac delta function which is approximated by

$$\delta_a(t-\bar{t}) \approx \frac{1}{a\sqrt{\pi}} e^{-(t-\bar{t})^2/a^2},$$

where $\bar{t}$ denotes t_1 and T, and a is a small positive constant taken as $a = 10^{-3}$. The Simpson's rule is used to approximate all the integrals involved. We define the errors at the iteration number n for $q(x)$ and $\phi(x)$ as

$$E_1(q^n) = \|q - q^n\|_{L_2(\Omega)}, \tag{6.24}$$

$$E_2(\phi^n) = \|\phi - \phi^n\|_{L_2(\Omega)}. \tag{6.25}$$

The temperature measurement ϕ_1^ϵ at time t_1 and the final temperature measurement ϕ_2^ϵ at T containing random noise are simulated by adding to the exact data ϕ_1 and ϕ_2 error terms generated from a normal distribution in the following forms:

$$\phi_1^\epsilon = \phi_1 + \sigma \times \text{random}(1), \quad \phi_2^\epsilon = \phi_2 + \sigma \times \text{random}(1), \tag{6.26}$$

where $\sigma = \frac{p}{100} \times \max_{x\in\bar{\Omega}}\{|\phi_1(x)|, |\phi_2(x)|\}$ is the standard deviation, $p\%$ represents the percentage of noise, and the term $\text{random}(1)$ generates random values from the normal distribution with zero mean and standard deviation equal to unity using MATLAB.

6.5.1 Example 1

In the one-dimensional case we take $\Omega = (0, 1)$. We also take $t_1 = 0.5$, $T = 1$ and

$$k \equiv 1, \quad f(x,t) = x(1+2x+x^2)e^{-t}, \quad \alpha(x) = 1, \quad \mu(0,t) = e^{-t},$$
$$\mu(1,t) = 4e^{-t}, \quad \phi_1(x) = e^{-0.5}(1+x^2), \quad \phi_2(x) = e^{-1}(1+x^2).$$

Then the analytical solution of the inverse problem is

$$q(x) = 3 + x, \quad \phi(x) = 1 + x^2, \quad x \in \Omega,$$
$$u(x,t) = e^{-t}(1+x^2), \quad (x,t) \in Q_T. \tag{6.27}$$

For obtaining the components $q(x)$, $\phi(x)$ and $u(x,t)$ of the solution we use the FDM Crank-Nicolson scheme with $I = 101$ and $M = 21$ to solve the PDEs involved in the CGM. In this example, the initial guesses q^0 and ϕ^0 for $q(x)$ and $\phi(x)$ are chosen as $q^0(x) = 2$ and $\phi^0(x) = x + 2$.

In Figures 6.2, 6.3(a) and 6.3(b), the objective functional $J(q^n, \phi^n)$ given by (6.5), and the errors $E_1(q^n)$ given by (6.24) and $E_2(\phi^n)$ given by (6.25) are illustrated for the

simultaneous numerical reconstruction of the initial temperature $\phi(x)$ and the reaction coefficient $q(x)$ using the CGM algorithm of Section 6.4. Figure 6.2 shows the monotonic decreasing convergence of the objective functional (6.5), as a function of the number of iterations n, for $p \in \{0, 1\}$ noise. The stopping number for the iterations is 9 for no noise $p = 0$, and 2 iterations according to the discrepancy principle (6.23) for $p = 1$ noise. These values are in good agreement with the optimal values of the iteration numbers, which can be inferred from Figures 6.3(a) and 6.3(b) included herein only for illustrative purposes.

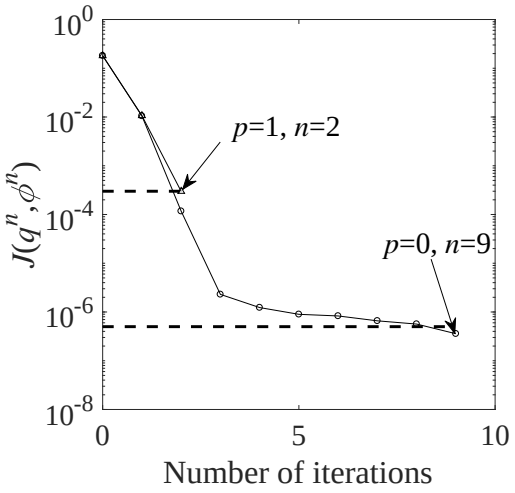

Figure 6.2: The objective functional $J(q^n, \phi^n)$ (6.5) with $p \in \{0, 1, 2\}$ noise, for Example 1.

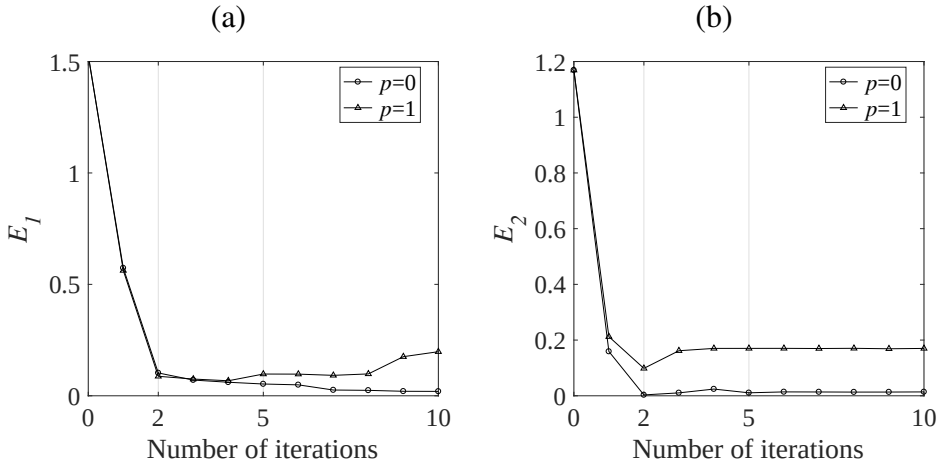

Figure 6.3: The errors (a) (6.24) and (b) (6.25) with $p \in \{0, 1\}$ noise, for Example 1.

The corresponding numerical solutions for $q(x)$ and $\phi(x)$ are shown in Figures 6.4(a)

and 6.4(b), respectively. First, it can be seen that in the case of no noise, the retrieved solutions for both reaction coefficient $q(x)$ and initial temperature $\phi(x)$ are in very good agreement (see Table 6.1) with the exact solutions (6.27). Second, in the case of noisy data $p = 1$, the retrieved solutions are stable and also in reasonable agreement (see Table 6.1) with the exact solutions (6.27) for both functions.

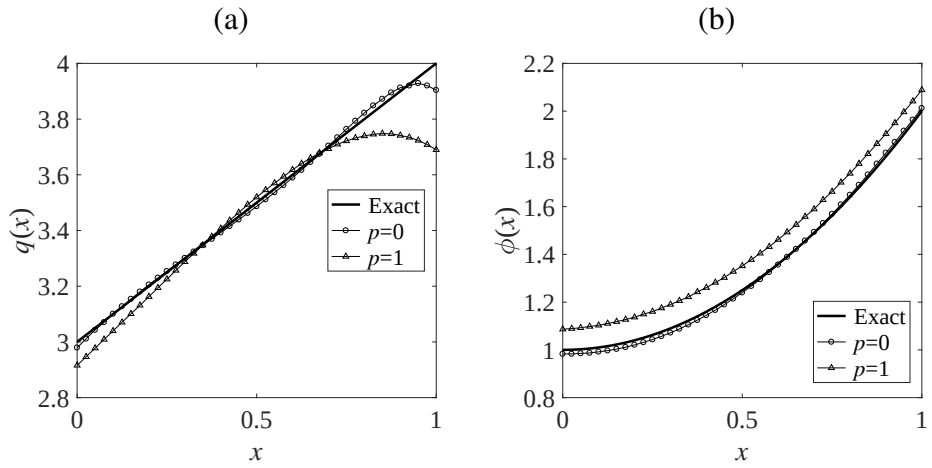

Figure 6.4: The exact and numerical results for (a) the reaction coefficient $q(x)$ and (b) the initial temperature $\phi(x)$ with $p \in \{0, 1\}$ noise, for Example 1.

p	I	M	$\bar{\epsilon}$	N	E_1	E_2
0	101	21	5.0E-07	9	1.9E-02	2.0E-02
1	101	21	3.0E-04	2	9.2E-02	6.7E-02

Table 6.1: The stopping iteration numbers N and the errors E_1 and E_2 for $p \in \{0, 1\}$ noise, for Example 1.

6.5.2 Example 2

Previous example has been concerned with the recovery of smooth functions in (6.27). In this example, we investigate a more severe situation in which the reaction coefficient in (6.28) is a discontinuous function. We take $\Omega = (0, 1)$, $t_1 = 0.5$, $T = 1$, $k \equiv 1$, $\alpha \equiv 1$, $\mu(0, t) = \mu(1, t) = e^{-t}$, and

$$f(x,t) = \pi^2 \sin(\pi x)e^{-t} + (1 + \pi + \sin(\pi x))e^{-t} \times \begin{cases} 1 - x, & x \in [0, 0.3], \\ -x + 4x^2, & x \in (0.3, 0.7), \\ 2, & x \in [0.7, 1], \end{cases}$$

$$\phi_1(x) = e^{-0.5}(1 + \pi + \sin(\pi x)), \quad \phi_2(x) = e^{-1}(1 + \pi + \sin(\pi x)).$$

Then the analytical solution of the inverse problem is

$$u(x,t) = (1+\pi+\sin(\pi x))e^{-t}, \quad \phi(x) = 1+\pi+\sin(\pi x),$$
$$q(x) = \begin{cases} 2-x, & x \in [0,0.3], \\ 1-x+4x^2, & x \in (0.3,0.7), \\ 3, & x \in [0.7,1]. \end{cases} \tag{6.28}$$

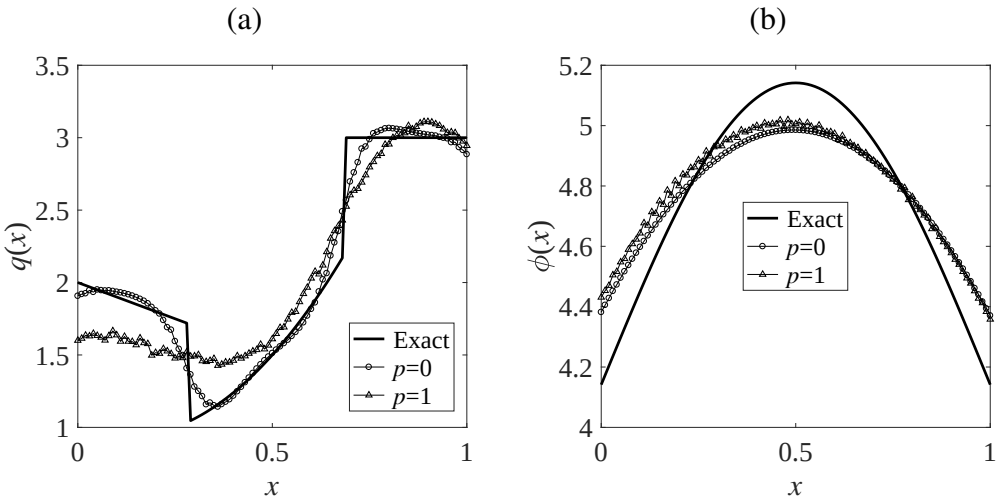

Figure 6.5: The exact and numerical results for (a) the reaction coefficient $q(x)$ and (b) the initial temperature $\phi(x)$ with $p \in \{0,1\}$ noise, for Example 2.

p	I	M	$\bar{\epsilon}$	N	E_1	E_2
0	101	101	1.0E-07	43	0.1114	0.1260
1	101	101	1.2E-03	7	0.2372	0.1309

Table 6.2: The stopping iteration numbers N and the errors E_1 and E_2 for $p \in \{0,1\}$ noise, for Example 2.

In order to obtain the components $q(x)$, $\phi(x)$ and $u(x,t)$ of the solution, the initial guesses are chosen as $q^0(x) = 1$ and $\phi^0(x) = 2$ for the two unknowns $q(x)$ and $\phi(x)$, respectively. The Crank-Nicolson FDM scheme with $I = M = 101$ is utilized to solve the PDEs involved in the CGM. The numerical results for $q(x)$ and $\phi(x)$ are illustrated in Figures 6.5(a) and 6.5(b), respectively. We also quantify the errors (6.24) and (6.25), as shown in Table 6.2. For these errors and Figure 6.5 it can be concluded that the numerical solutions are stable and reasonably accurate bearing in mind the difficult discontinuous reaction coefficient $q(x)$ in (6.28) that had to be retrieved.

6.5.3 Example 3

In the two dimensional case we take $\Omega = (0,1) \times (0,1)$. We also take $t_1 = 0.5$, $T = 1$ and

$$
\begin{aligned}
&k = \mathbf{I}_2, \quad \alpha \equiv 1, \quad f(x_1, x_2, t) = (4 + x_1 + x_2)(1 + x_1^2 + x_2^2)e^{-t} - 4e^{-t}, \\
&\mu(0, x_2, t) = (1 + x_2^2)e^{-t}, \quad \mu(1, x_2, t) = (4 + x_2^2)e^{-t}, \\
&\mu(x_1, 0, t) = (1 + x_1^2)e^{-t}, \quad \mu(x_1, 1, t) = (4 + x_1^2)e^{-t}, \\
&\phi_1(x_1, x_2) = e^{-0.5}(1 + x_1^2 + x_2^2), \quad \phi_2(x_1, x_2) = e^{-1}(1 + x_1^2 + x_2^2).
\end{aligned}
$$

The analytical solution of the inverse problem is given by

$$
\begin{aligned}
&\alpha(x_1, x_2) = 1, \quad q(x_1, x_2) = 5 + x_1 + x_2, \quad \phi(x_1, x_2) = 1 + x_1^2 + x_2^2, \\
&u(x_1, x_2, t) = (1 + x_1^2 + x_2^2)e^{-t}.
\end{aligned} \tag{6.29}
$$

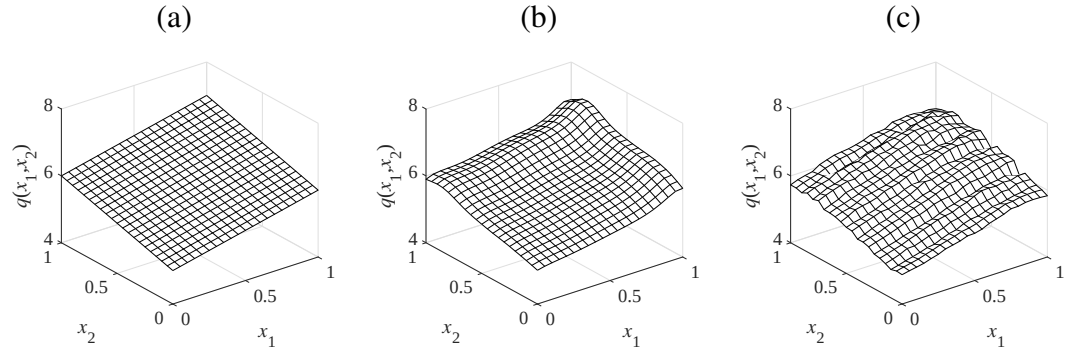

Figure 6.6: (a) The exact and numerical results for $q(x_1, x_2)$ for (b) $p = 0$ and (c) $p = 1$ noise, for Example 3.

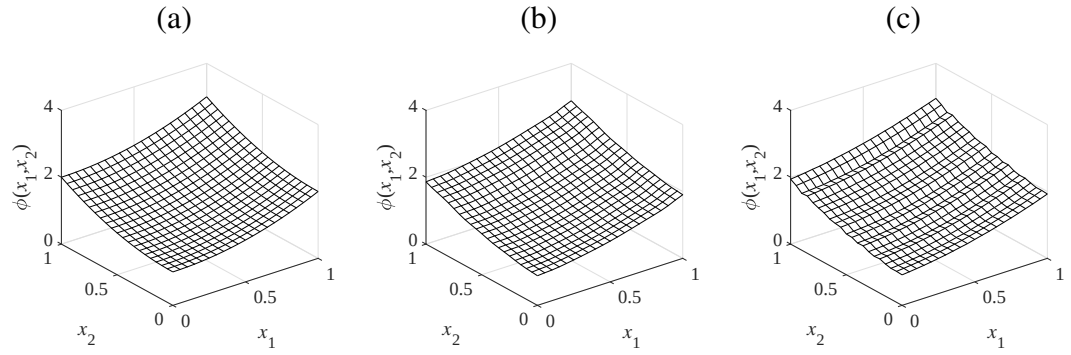

Figure 6.7: (a) The exact and numerical results for $\phi(x_1, x_2)$ for (b) $p = 0$ and (c) $p = 1$ noise, for Example 3.

For the unknown reaction coefficient $q(x_1, x_2)$ and initial temperature $\phi(x_1, x_2)$ we employ the ADI scheme with $I = J = M = 21$ to solve the PDEs involved in the CGM, with the initial guesses $q^0(x_1, x_2) = 4$ and $\phi^0(x_1, x_2) = 1.5 + x_1 + x_2$. The exact (6.29) and numerical solutions for the two unknown functions $q(x_1, x_2)$ and $\phi(x_1, x_2)$, obtained using the CGM of Section 6.4 are shown in Figures 6.5 and 6.6. The iterations are stopped after 25 for $p = 0$ and 4 for $p = 1$, giving the errors (6.24) and (6.25) in Table 6.3.

p	I	J	M	$\bar{\epsilon}$	N	E_1	E_2
0	21	21	21	1.3E-07	25	0.0884	0.0375
1	21	21	21	3.2E-04	4	0.1117	0.0454

Table 6.3: The stopping iteration numbers N and the errors E_1 and E_2 for $p \in \{0, 1\}$ noise, for Example 3.

6.6 Conclusions

In this chapter, the space-dependent reaction coefficient and the initial temperature have been reconstructed from temperature measurements at two different instants. The uniqueness of the reaction coefficient and the initial temperature in the inverse problem holds. The two unknown functions have been simultaneously reconstructed by minimizing a least-squares objective functional. The existence of a minimizer of the objective functional is proved, and the Fréchet gradients are obtained by a variational method. Then, the CGM has been applied to simultaneously determine the two unknown quantities. Three numerical experiments for one- and two-dimensional examples have been illustrated and discussed. Good accuracy and reasonable stability have been achieved.

In the next chapter, the two unknown coefficients investigated here shall be reconstructed simultaneously from time-average temperature measurements.

Chapter 7

Simultaneous reconstruction of the space-dependent reaction coefficient and initial temperature from integral temperature measurements

7.1 Introduction

In the previous chapter we have investigated the simultaneous reconstruction of the space-dependent reaction coefficient and initial temperature from temperature measurements (6.2) at two distinct instants. In this chapter, we address the same coefficient identification but additional measurements are integral observations instead of time instant temperature measurements. So, in this sense, the new inverse problem investigated in this chapter generalizes the inverse models considered in Chapter 6, which can be obtained by particular choices of the integral weights, e.g. Dirac delta functions. For the numerical reconstruction, the least-squares objective functional is minimised to obtain the quasi-solutions of the two unknown quantities. The existence of the minimizer for the objective functional is presented, and the Fréchet gradients are derived using a variational method. In addition, we show that these Fréchet gradients are Lipschitz continuous. These gradients and the adjoint problem are utilized in the CGM to reconstruct the unknown quantities simultaneously. The global convergence of the CGM with the Fletcher-Reeves formula, Fletcher & Reeves (1964), is established according to the arguments in Zoutendijk (1970) obtained from the Lipschitz continuity property of the Fréchet gradients. Since the inverse problem is unstable, our CGM is regularised by the discrepancy principle, Alifanov (1994).

This chapter is organized as follows: Section 7.2 presents the mathematical formulation of the nonlinear IHTP of reconstructing the unknown reaction coefficient and the initial temperature, together with the objective functional to be minimized. The CGM is introduced in Section 7.4, according to the Fréchet gradients obtained in Section 7.3, and the global convergence of the algorithm is obtained. Three numerical examples are discussed in Section 7.5. Finally, Section 7.6 highlights the conclusions.

7.2 Mathematical formulation

Let $\Omega \subset \mathbb{R}^{\mathrm{d}}$, $\mathrm{d} = 1, 2, 3$ be a bounded domain with sufficiently smooth boundary $\partial\Omega$, and consider the heat transfer problem given by (6.1) in the cylinder $Q_T = \Omega \times (0, T)$, and $T > 0$ is a final time of interest.

Definition 7.2.1. *A function $u(x,t) \in V_2^{1,0}(Q_T)$ is called as a weak solution to the direct initial-boundary value problem (6.1) if*

$$\begin{aligned}&\int_{Q_T} \left(-u\frac{\partial \eta}{\partial t} + (k\nabla u)\cdot\nabla\eta + qu\eta \right) dxdt + \int_{S_T} \alpha u\eta ds dt \\ &= \int_{Q_T} f\eta dx dt + \int_{S_T} \mu\eta ds dt + \int_{\Omega} \phi\eta(\cdot,0)dx, \quad \forall \eta \in H^{1,1}(Q_T) \text{ with } \eta(\cdot,T) = 0.\end{aligned} \tag{7.1}$$

The existence and uniqueness of the weak solution $u(x,t) \in V_2^{1,0}(Q_T)$ to the initial-boundary value direct problem (6.1) is presented as follows (Tröltzsch (2010), p.373):

Lemma 7.2.2. *Let $\Omega \subset \mathbb{R}^{\mathrm{d}}$ be a bounded domain with Lipschitz boundary $\partial\Omega$, and suppose that $f \in L_2(Q_T)$, $0 \le \alpha \in L_\infty(\partial\Omega)$, $\mu \in L_2(S_T)$ and $\phi \in L_2(\Omega)$. Let k satisfy (5.3) and $k_{ij} = k_{ji} \in L_\infty(\Omega)$, $i, j = \overline{1, N}$, and $q \in L_\infty(\Omega)$, $0 < q^- \le q(x) \le q^+$, a.e., $x \in \Omega$, where, q^-, q^+ are two positive constants. Then the initial-boundary value direct problem (6.1) has a unique weak solution $u \in H^{1,0}(Q_T)$ that belongs to $V_2^{1,0}(Q_T)$.*

Note that by the direct problem (6.1) for a.e., $t \in [0, T]$, we know that

$$\frac{1}{2}\frac{d}{dt}\|u(\cdot,t)\|^2_{L_2(\Omega)} + \int_\Omega (k|\nabla u|^2 + qu^2)dx + \int_{\partial\Omega} \alpha u^2 ds = \int_\Omega f u dx + \int_{\partial\Omega} \mu u ds.$$

By (5.3), $q \ge q^- > 0$, and $\alpha \ge 0$, we have

$$\begin{aligned}&\frac{1}{2}\frac{d}{dt}\|u(\cdot,t)\|^2_{L_2(\Omega)} + \min\{q^-, v_1\}\|u(\cdot,t)\|^2_{H^1(\Omega)} \\ &\le c(\|u(\cdot,t)\|^2_{L_2(\Omega)} + \|f(\cdot,t)\|^2_{L_2(\Omega)} + \|\mu(\cdot,t)\|^2_{L_2(\partial\Omega)}),\end{aligned}$$

where c is a positive constant depending on Ω. Using the Gronwall's inequality[1], we can obtain

$$\begin{aligned}\max_{t\in[0,T]}\|u(\cdot,t)\|^2_{L_2(\Omega)} &\le c(\Omega,T)\left(\|f\|^2_{L_2(Q_T)}+\|\mu\|^2_{L_2(S_T)}+\|\phi\|^2_{L_2(\Omega)}\right),\\ \|u\|^2_{H^{1,0}(Q_T)} &= \int_0^T \|u(\cdot,t)\|^2_{H^1(\Omega)}dt\\ &\le c(q^-,\upsilon_1,\Omega,T)\left(\|f\|^2_{L_2(Q_T)}+\|\mu\|^2_{L_2(S_T)}+\|\phi\|^2_{L_2(\Omega)}\right).\end{aligned}$$

Thus the weak solution $u(x,t)\in V_2^{1,0}(Q_T)$ of the initial-boundary value direct problem (6.1) satisfies the following estimate:

$$\max_{t\in[0,T]}\|u(\cdot,t)\|_{L_2(\Omega)}+\|u\|_{H^{1,0}(Q_T)}\le C_0\left(\|f\|_{L_2(Q_T)}+\|\mu\|_{L_2(S_T)}+\|\phi\|_{L_2(\Omega)}\right) \tag{7.2}$$

where $C_0(q^-,\upsilon_1,\Omega,T)$ is a positive constant.

The inverse problem is to determine the triplet $(q(x),\phi(x),u(x,t))$ satisfying (6.1) together with the time-integral temperature measurements,

$$\int_0^T \omega_1(t)u(x,t)dt=\phi_1(x),\quad x\in\Omega, \tag{7.3}$$

$$\int_0^T \omega_2(t)u(x,t)dt=\phi_2(x),\quad x\in\Omega, \tag{7.4}$$

where $\omega_1(t)$ and $\omega_2(t)\in L_\infty(0,T)$ are two given functionally independent[2] weight functions, and $\phi_1(x)$ and $\phi_2(x)$ are given data which may be subject to noise due to measurement errors. In particular, we are actually trying to recover the solution to the inverse problem (6.1), (7.3) and (7.4) from the noisy data $(\phi_1^\epsilon,\phi_2^\epsilon)$ satisfying

$$\|\phi_1^\epsilon-\phi_1\|_{L_2(\Omega)}\le\epsilon,\quad \|\phi_2^\epsilon-\phi_2\|_{L_2(\Omega)}\le\epsilon, \tag{7.5}$$

where ϵ represents the noise level.

[1] **Gronwall's inequality**. Let u be a nonnegative and continuous function on $[0,T]$, which satisfies the ordinary differential inequality

$$u'(t)\le f(t)u(t)+g(t),\quad \text{a.e. } t\in[0,T],$$

where $f(t)$ and $g(t)$ are nonnegative, integrable functions on $[0,T]$. Then

$$u(t)\le e^{\int_0^T f(\tau)d\tau}\left\{u(0)+\int_0^T g(\tau)d\tau\right\},\quad \forall t\in[0,T].$$

[2] The functions ω_1 and ω_2 are functionally independent if the only function $f:\mathbb{R}^2\mapsto\mathbb{R}$ such that $f(\omega_1,\omega_2)=0$ is $f=0$.

Note that $\phi_1(x)$ may mimic the temperature measurement at an instant time $t_1 \in (0,T]$ if $\omega_1(t) = \delta(t-t_1)$, namely,

$$u(x,t_1) = \phi_1(x), \quad x \in \Omega, \tag{7.6}$$

and $\phi_2(x)$ the temperature at another instant time $t_2 \in (0,t_1)$ if $\omega_2(t) = \delta(t-t_2)$, namely,

$$u(x,t_2) = \phi_2(x), \quad x \in \Omega, \tag{7.7}$$

where δ is the Dirac delta function. The Dirac delta function $\delta(t-t_1)$ can be approximated by the function $\delta_a = \frac{1}{a\sqrt{\pi}} e^{-(t-t_1)^2/a^2}$ with small positive parameter a, e.g., $a = 10^{-3}$, and so does $\delta(t-t_2)$, such that the approximated weighted functions belong to the space $L_\infty(0,T)$.

Other cases of potential interest may be obtained by taking the weights as cut-off functions, e.g.,

$$\omega_1(t) = \tilde{\omega}_1(t)\mathcal{X}_{[t_1,T]}(t), \quad \omega_2(t) = \tilde{\omega}_2(t)\mathcal{X}_{[0,t_1]}(t), \quad t \in [0,T], \tag{7.8}$$

where $\mathcal{X}_D$ denotes the characteristic function of the domain D and $\tilde{\omega}_1(t)$ and $\tilde{\omega}_2(t) \in L_2(0,T)$, in which case (7.3) and (7.4) yield

$$\int_{t_1}^{T} \tilde{\omega}_1(t)u(x,t)dt = \phi_1(x), \quad x \in \Omega, \tag{7.9}$$

$$\int_{0}^{t_1} \tilde{\omega}_2(t)u(x,t)dt = \phi_2(x), \quad x \in \Omega. \tag{7.10}$$

The uniqueness of the general inverse problem given by (6.1) supplemented with (7.3) and (7.4) is still to be established, but under some of the particular cases (7.6)–(7.10) the inverse problem can be split in two separate inverse problem, namely, first identifying $q(x)$ and after that $\phi(x)$. For example, when solving the inverse problem given by (6.1), (7.3) and (7.7), one can first identify $q(x)$ by solving this in the layer $\Omega \times (t_2,t_1)$ followed by retrieving the initial data $\phi(x)$ in (6.1) by solving BHCP (6.1) and (7.7) in the layer $\Omega \times (0,t_2)$. Similarly, when solving the inverse problem given by (6.1), (7.6) and (7.9), for $t_1 < T$, one can first identity $q(x)$ by solving this in the layer $\Omega \times (t_1,T)$ followed by retrieving the initial data $\phi(x)$ in (6.1) by solving the BHCP (6.1) and (7.6) in the layer $\Omega \times (0,t_1)$. We finally mention that uniqueness results and the numerical reconstructions of the reaction coefficient $q(x)$ from final time or time-average temperature measurements can be found in Chapters 5 and 6.

For the numerical reconstruction we employ a variation formulation, as described next.

7.3 Analysis

Let $u(q,\phi) := u(x,t;q,\phi)$ denote the weak solution to the initial-boundary value problem (6.1) subject to a particular pair $(q(x),\phi(x)) \in L_\infty(\Omega)\times L_2(\Omega)$. Then, given ϕ_1^ϵ and ϕ_2^ϵ in $L_2(\Omega)$ temperature measurements satisfying (7.5), the quasi-solution of the inverse problem (6.1), (7.3) and (7.4) can be obtained by minimizing the following least-squares objective functional:

$$J(q,\phi) := \frac{1}{2}\left\|\int_0^T \omega_1(t)u(q,\phi)dt - \phi_1^\epsilon\right\|^2_{L_2(\Omega)} + \frac{1}{2}\left\|\int_0^T \omega_2(t)u(q,\phi)dt - \phi_2^\epsilon\right\|^2_{L^2(\Omega)}, \tag{7.11}$$

subject to $u \in V_2^{1,0}(Q)$ satisfying the variational equality (7.1), over the admissible set $\mathcal{A}_1\times\mathcal{A}_2$, where $\mathcal{A}_1 = \{q\in L_\infty(\Omega) : 0 < q^- \le q(x) \le q^+,\ \text{a.e. } x\in\Omega\}$, $\mathcal{A}_2 = \{\phi \in L_2(\Omega) : |\phi(x)| \le \kappa,\ \text{a.e. } x\in\Omega\}$, for a positive constant κ.

Note that there exists at least one minimizer to the optimization problem (7.11), which can be proved by the approaches of Theorem 6.3.1.

In order to numerically obtain the minimizer of the objective functional $J(q,\phi)$ (7.11), the CGM can be applied together with the Fréchet gradient. Thus the adjoint problem to (6.1), (7.3) and (7.4) is introduced and given by

$$\begin{cases} \frac{\partial\lambda}{\partial t} = -\nabla\cdot(k\nabla\lambda) + q\lambda - \omega_1(t)\left(\int_0^T \omega_1(\tau)u(x,\tau)d\tau - \phi_1^\epsilon(x)\right) & \\ \qquad -\omega_2(t)\left(\int_0^T \omega_2(\tau)u(x,\tau)d\tau - \phi_2^\epsilon(x)\right), & (x,t)\in Q_T, \\ k(x)\frac{\partial\lambda}{\partial\nu} + \alpha\lambda = 0, \quad (x,t)\in S_T, \quad \lambda(x,T) = 0, & x\in\overline{\Omega}. \end{cases} \tag{7.12}$$

Its weak solution $\lambda \in V_2^{1,0}(Q)$ to the adjoint problem (7.12) is defined as satisfying

$$\begin{aligned} &\int_{Q_T}\left(\lambda\frac{\partial\eta}{\partial t} + (k\nabla\lambda)\cdot\nabla\eta + q\lambda\eta\right)dxdt + \int_{S_T}\alpha\lambda\eta dsdt \\ &= \int_\Omega\int_0^T \omega_1(t)\eta(x,t)dt\left(\int_0^T \omega_1(\tau)u(x,\tau)d\tau - \phi_1^\epsilon(x)\right)dx \\ &\quad + \int_\Omega\int_0^T \omega_2(t)\eta(x,t)dt\left(\int_0^T \omega_2(\tau)u(x,\tau)d\tau - \phi_2^\epsilon(x)\right)dx, \\ &\forall\eta\in H^{1,1}(Q) \text{ with } \eta(\cdot,0) = 0. \end{aligned} \tag{7.13}$$

Theorem 7.3.1 (Cao & Lesnic (2018b)). *The objective functional $J(q,\phi)$ is Fréchet differentiable, and $J'_q(q,\phi)$ and $J'_\phi(q,\phi)$ are given by*

$$J'_q(q,\phi) = -\int_0^T u(x,t)\lambda(x,t)dt, \tag{7.14}$$

$$J'_\phi(q,\phi) = \lambda(x,0). \tag{7.15}$$

Proof. Take $\Delta q \in L_\infty(\Omega)$ such that $q+\Delta q \in \mathcal{A}_1$, and denote by $\Delta u_q := u(q+\Delta q,\phi) - u(q,\phi)$ the increment of u with respect to q. According to the initial-boundary value problem (6.1), this increment satisfies the sensitivity problem (6.14), and using the estimate (7.2) for such parabolic problem, we have

$$\|\Delta u_q\|_{L_2(Q_T)} \le C_0\|u\Delta q\|_{L_2(Q_T)} \le C_0\|\Delta q\|_{L_\infty(\Omega)}\|u\|_{L_2(Q_T)}.$$

Denote $\Delta J_q := J(q+\Delta q,\phi) - J(q,\phi)$, then we have

$$\begin{aligned}\Delta J_q =& \frac{1}{2}\left\|\int_0^T \omega_1(t)\Delta u_q(x,t)dt\right\|^2_{L_2(\Omega)} + \frac{1}{2}\left\|\int_0^T \omega_2(t)\Delta u_q(x,t)dt\right\|^2_{L_2(\Omega)}\\ &+ \int_{Q_T}\omega_1(t)\Delta u_q(x,t)\left(\int_0^T \omega_1(\tau)u(x,\tau)d\tau - \phi_1^\epsilon(x)\right)dxdt\\ &+ \int_{Q_T}\omega_2(t)\Delta u_q(x,t)\left(\int_0^T \omega_2(\tau)u(x,\tau)d\tau - \phi_2^\epsilon(x)\right)dxdt.\end{aligned}$$

By the adjoint problem (7.12) and the sensitivity problem (6.14), we have

$$\begin{aligned}\Delta J_q =& \frac{1}{2}\left\|\int_0^T \omega_1(t)\Delta u_q(x,t)dt\right\|^2_{L_2(\Omega)} + \frac{1}{2}\left\|\int_0^T \omega_2(t)\Delta u_q(x,t)dt\right\|^2_{L_2(\Omega)}\\ &+ \int_{Q_T}\Delta u_q\left\{-\frac{\partial\lambda}{\partial t} - \nabla\cdot(k\nabla\lambda) + q\lambda\right\}dxdt,\end{aligned}$$

and

$$\begin{aligned}&\int_{Q_T}\Delta u_q\left\{-\frac{\partial\lambda}{\partial t} - \nabla\cdot(k\nabla\lambda) + q\lambda\right\}dxdt\\ =&\int_{Q_T}\lambda\left\{\frac{\partial(\Delta u_q)}{\partial t} - \nabla\cdot(k\nabla(\Delta u_q)) + q\Delta u_q\right\}dxdt\\ &+\int_{S_T}\left\{k\frac{\partial(\Delta u_q)}{\partial\nu}\lambda - k\frac{\partial\lambda}{\partial\nu}\Delta u_q\right\}dsdt - \int_\Omega \Delta u_q\lambda|_0^T dx\\ =&-\int_{Q_T}\Delta q u(q+\Delta q,\phi)\lambda dxdt = -\int_{Q_T}\Delta q\Delta u_q\lambda dxdt - \int_{Q_T}\Delta q u\lambda dxdt,\end{aligned}$$

thus

$$\begin{aligned}\Delta J_q =& \frac{1}{2}\left\|\int_0^T \omega_1(t)\Delta u_q(x,t)dt\right\|^2_{L_2(\Omega)} + \frac{1}{2}\left\|\int_0^T \omega_2(t)\Delta u_q(x,t)dt\right\|^2_{L_2(\Omega)}\\ &- \int_{Q_T}\Delta q\Delta u_q\lambda dxdt - \int_{Q_T}\Delta q u\lambda dxdt.\end{aligned}$$

We have

$$\begin{aligned}\left\|\int_0^T \omega_1(t)\Delta u_q(x,t)dt\right\|^2_{L_2(\Omega)} &\le c\|\omega_1\|^2_{L_\infty(0,T)}\|\Delta u_q\|^2_{L_2(Q_T)}\\ &\le cC_0^2\|\omega_1\|^2_{L_\infty(0,T)}\|u\|^2_{L_2(Q_T)}\|\Delta q\|^2_{L_\infty(\Omega)},\end{aligned}$$

where $c > 0$ depends on Ω, and similarly

$$\begin{aligned}\left\| \int_0^T \omega_2(t)\Delta u_q(x,t)dt \right\|^2_{L_2(\Omega)} &\le cC_0^2\|\omega_2\|^2_{L_\infty(0,T)}\|u\|^2_{L_2(Q_T)}\|\Delta q\|^2_{L_\infty(\Omega)},\\ \left| \int_{Q_T} \Delta q \Delta u_q \lambda dxdt \right| &\le \|\Delta q\|_{L_\infty(\Omega)}\|\Delta u_q\|_{L_2(Q_T)}\|\lambda\|_{L_2(Q_T)}\\ &\le C_0\|u\|_{L_2(Q_T)}\|\lambda\|_{L_2(Q_T)}\|\Delta q\|^2_{L_\infty(\Omega)}.\end{aligned}$$

Finally,

$$\Delta J_q = -\int_{Q_T} \Delta q u \lambda dxdt + o\left(\|\Delta q\|_{L_\infty(\Omega)}\right), \tag{7.16}$$

which means that the Fréchet derivative $J'_q(q,\phi)$ is given by (7.14).

Similarly, take $\Delta\phi \in L_2(\Omega)$ such that $\phi + \Delta\phi \in \mathcal{A}_2$, and denote by $\Delta u_\phi := u(q, \phi + \Delta\phi) - u(q,\phi)$ the increment of u with respect to ϕ, then this increment satisfies the sensitivity problem (6.15). Then, we can obtain that the Fréchet derivative $J'_\phi(q,\phi)$ is given by (7.15) by the same approach. The theorem is proved. □

7.4 Conjugate gradient method

The following iteration process based on the CGM scheme is applied for the reconstruction of the two unknown functions $q(x)$ and $\phi(x)$ by minimizing the objective functional $J(q,\phi)$ in (7.11):

$$q^{n+1}(x) = q^n(x) + \beta^n_q d^n_q(x), \quad \phi^{n+1}(x) = \phi^n(x) + \beta^n_\phi d^n_\phi(x), \quad n = 0,1,2,\cdots \tag{7.17}$$

with the search directions d^n_q and d^n_ϕ given by

$$d^n_q = \begin{cases} -J'^0_q, \\ -J'^n_q + \gamma^n_q d^{n-1}_q, \end{cases} \qquad d^n_\phi = \begin{cases} -J'^0_\phi, \\ -J'^n_\phi + \gamma^n_\phi d^{n-1}_\phi, \end{cases} \qquad n = 1,2,\cdots \tag{7.18}$$

where n is the subscript which denotes the number of iterations, $J'^n_q = J'_q(q^n,\phi^n)$, $J'^n_\phi = J'_\phi(q^n,\phi^n)$, q^0 and ϕ^0 are the initial guesses, β^n_q and β^n_ϕ are the step sizes for q and ϕ in passing from iteration n to the next iteration $n+1$. The Fletcher-Reeves formula in Fletcher & Reeves (1964) is utilized for the conjugate coefficients γ^n_q and γ^n_ϕ, and they are given by

$$\gamma^n_q = \frac{\|J'^n_q\|^2_{L_2(\Omega)}}{\|J'^{n-1}_q\|^2_{L_2(\Omega)}}, \quad \gamma^n_\phi = \frac{\|J'^n_\phi\|^2_{L_2(\Omega)}}{\|J'^{n-1}_\phi\|^2_{L_2(\Omega)}}, \quad n = 1,2,\cdots. \tag{7.19}$$

To determine the step sizes β_q^n and β_ϕ^n, the exact line search is utilized, i.e.,

$$J(q^n+\beta_q^n d_q^n, \phi^n+\beta_\phi^n d_\phi^n) = \min_{\beta_q,\beta_\phi\geq 0} J(q^n+\beta_q d_q^n, \phi^n+\beta_\phi d_\phi^n), \quad n=0,1,2\cdots. \tag{7.20}$$

By (7.16), (7.17) and the gradient $J_q'^{n+1}$ (7.14), we have

$$\begin{aligned}
\frac{\partial J}{\partial \beta_q^n} =& \frac{\partial J}{\partial q^{n+1}}\cdot\frac{\partial q^{n+1}}{\partial \beta_q^n} = \lim_{\beta_q^n\to 0}\frac{J(q^{n+1},\phi^{n+1})-J(q^n,\phi^{n+1})}{\beta_q^n d_q^n} d_q^n \\
=& \lim_{\beta_q^n\to 0}\frac{J(q^{n+1},\phi^{n+1})-J(q^n,\phi^{n+1})}{\beta_q^n} \\
=& \lim_{\beta_q^n\to 0}\frac{1}{\beta_q^n}\left(-\int_{Q_T} u(q^n,\phi^{n+1})\lambda(q^n,\phi^{n+1})\beta_q^n d_q^n dxdt + o(\|\beta_q^n d_q^n\|_{L_\infty(\Omega)})\right) \\
=& -\int_{Q_T} u(q^{n+1},\phi^{n+1})\lambda(q^{n+1},\phi^{n+1}) d_q^n dxdt = \int_\Omega J_q'^{n+1} d_q^n dx,
\end{aligned}$$

and similarly, we have $\frac{\partial J}{\partial \beta_\phi^n} = \int_\Omega J_\phi'^{n+1} d_\phi^n dx$. Thus, condition (7.20) implies that the step sizes β_q^n and β_ϕ^n satisfy the following conditions:

$$\langle J_q'^{n+1}, d_q^n\rangle = 0, \quad \langle J_\phi'^{n+1}, d_\phi^n\rangle = 0, \tag{7.21}$$

where $\langle\cdot,\cdot\rangle$ is the inner product in the space $L_2(\Omega)$.

7.4.1 Global convergence

For the exact data (7.3) and (7.4), the global convergence of the CGM over the admissible set $\mathcal{A}_1\times\mathcal{A}_2$ is established in the following sense:

$$\liminf_{n\to\infty}\|J_q'^n\|_{L_2(\Omega)} = 0, \quad \liminf_{n\to\infty}\|J_\phi'^n\|_{L_2(\Omega)} = 0.$$

First, we will prove that the Fréchet gradients J_q' and J_ϕ' are Lipschitz continuous over $\mathcal{A}_1\times\mathcal{A}_2$ under the following stronger assumption on the input data than in Lemma 7.2.2.

Assumption 7.4.1. *Let $\Omega\subset\mathbb{R}^{\mathrm{d}}$ ($\mathrm{d}\geq 2$) be a bounded domain of class C^{2+l} for some $l>0$. Let $p>1+\mathrm{d}/2$ and $r>\mathrm{d}+1$ and assume that $f\in L_p(Q)$ and $\mu\in L_r(S)$.*

Then we have the following lemma, see Proposition 3.3 of Raymond & Zidani (1999).

Lemma 7.4.2. *Let the Assumption 7.4.1 on Ω, f and μ hold. Let also the other assumptions of Lemma 7.2.2 on data α, k and q hold, and also let $\phi\in\mathcal{A}_2\subset L_\infty(\Omega)$. Then, the weak solution $u(x,t)\in V_2^{1,0}(Q)$ of the initial-boundary value direct problem (6.1) also belongs to $L_\infty(Q)$ and there exists a positive constant $C=C(N,p,r,q^-,\Omega,T)$ such that*

$$\|u\|_{L_\infty(Q)}\leq C(\|f\|_{L_p(Q)}+\|\mu\|_{L_r(S)}+\|\phi\|_{L_\infty(\Omega)}). \tag{7.22}$$

For the adjoint problem we also have the following lemma.

Lemma 7.4.3 (Cao & Lesnic (2018b)). *Let the assumptions of Lemma 7.4.2 hold and let ω_1 and ω_2 be given weights in $L_\infty(0,T)$. Then, there exists a unique weak solution $\lambda(x,t) \in V_2^{1,0}(Q) \cap L_\infty(Q)$ to the adjoint problem (7.12) with $\epsilon = 0$, which satisfies*

$$\|\lambda\|_{L_\infty(Q)} \leq C_1 \|u\|_{L_\infty(Q)} \tag{7.23}$$

for some positive constant C_1 depending on $N, p, r, q^-, \Omega, T, \omega_1$ and ω_2.

Proof. First, through the change of time variable $t \mapsto T - t$, the adjoint problem (7.12) can be seen of the same form as the problem (6.1) with $\mu = \phi = 0$ and the source

$$\begin{aligned} f(x,t) = \tilde{f}(x,t) :=& \omega_1(t) \left(\int_0^T \omega_1(\tau) u(x,\tau) d\tau - \phi_1(x) \right) \\ &+ \omega_2(t) \left(\int_0^T \omega_2(\tau) u(x,\tau) d\tau - \phi_2(x) \right). \end{aligned}$$

From Lemma 7.4.2 it follows that $u \in L_\infty(Q_T)$ and since ω_1 and $\omega_2 \in L_\infty(0,T)$, and using also (7.3) and (7.4), we obtain that $\tilde{f} \in L_\infty(Q_T)$. Moreover, from (7.3) and (7.4), and using the inequality (7.22) of Lemma 7.4.2 for the function λ satisfying the adjoint problem (7.12) with $\epsilon = 0$, we obtain

$$\begin{aligned} \|\lambda\|_{L_\infty(Q_T)} \leq& C \|\tilde{f}\|_{L_p(Q_T)} \leq C \|\tilde{f}\|_{L_\infty(Q_T)} \\ \leq& 2C(\|\omega_1\|^2_{L_\infty(0,T)} + \|\omega_2\|^2_{L_\infty(0,T)}) \|u\|_{L_\infty(Q_T)}, \end{aligned}$$

which implies that (7.23) holds. □

Theorem 7.4.4 (Cao & Lesnic (2018b)). *Under the assumptions of Lemma 7.4.3, the gradients J'_q in (7.14) and J'_ϕ in (7.15) are Lipschitz continuous, namely, there exist two positive constants M_q and M_ϕ such that*

$$\|J'_q(q^1,\phi^1) - J'_q(q^2,\phi^2)\|_{L_2(\Omega)} \leq M_q(\|q^1 - q^2\|_{L_2(\Omega)} + \|\phi^1 - \phi^2\|_{L_2(\Omega)}), \tag{7.24}$$

$$\|J'_\phi(q^1,\phi^1) - J'_\phi(q^2,\phi^2)\|_{L_2(\Omega)} \leq M_\phi(\|q^1 - q^2\|_{L_2(\Omega)} + \|\phi^1 - \phi^2\|_{L_2(\Omega)}), \tag{7.25}$$

for any $q^1, q^2 \in \mathcal{A}_1$, $\phi^1, \phi^2 \in \mathcal{A}_2$.

Proof. By Lemma 7.4.2 and using the estimate (7.22), it is easy to see that

$$\|u(q,\phi)\|_{L_\infty(Q_T)} \leq C(\|f\|_{L_p(Q_T)} + \|\mu\|_{L_r(S_T)} + \kappa) =: K_1 \tag{7.26}$$

for any $q \in \mathcal{A}_1$ and $\phi \in \mathcal{A}_2$, and K_1 is a positive constant depending on N, p, r, q^-, κ, Ω, T, f and μ (independent of q and ϕ). Similarly, using Lemma 7.4.3, (7.23) and (7.26), we have

$$\|\lambda(q,\phi)\|_{L_\infty(Q_T)} \leq C_1 K_1 =: K_2, \tag{7.27}$$

where K_2 is a positive constant depending on N, p, r, q^-, κ, Ω, T, ω_1, ω_2, f and μ (independent of q and ϕ).

Denote $u_q := u(q^1, \phi^1) - u(q^2, \phi^1)$ and by the direct problem (6.1), we have

$$\begin{cases} \frac{\partial u_q}{\partial t} = \nabla \cdot (k \nabla u_q) - q^1 u_q - (q^1 - q^2) u(q^2, \phi^1), & (x,t) \in Q_T, \\ k \frac{\partial u_q}{\partial \nu} + \alpha u_q = 0, \quad (x,t) \in S_T, \quad u_q(x,0) = 0, & x \in \Omega. \end{cases}$$

Since $q^1, q^2 \in \mathcal{A}_1 \subset L_\infty(\Omega)$, then $q^1 - q^2 \in L_\infty(\Omega) \subset L_2(\Omega)$, and by using the estimate (7.2), we have

$$\|u_q\|_{L_2(Q_T)} \leq C_0 \|(q^1 - q^2) u(q^2, \phi^1)\|_{L_2(Q_T)} \leq C_0 K_1 \|q^1 - q^2\|_{L_2(\Omega)}.$$

Similarly, denoting $u_\phi := u(q^2, \phi^1) - u(q^2, \phi^2)$, we have

$$\begin{cases} \frac{\partial u_\phi}{\partial t} = \nabla \cdot (k \nabla u_\phi) - q^2 u_\phi, & (x,t) \in Q_T, \\ k \frac{\partial u_\phi}{\partial \nu} + \alpha u_q = 0, \quad (x,t) \in S_T, \quad u_\phi(x,0) = \phi^1 - \phi^2, & x \in \Omega, \end{cases}$$

and $\|u_\phi\|_{L_2(Q_T)} \leq C_0 \|\phi^1 - \phi^2\|_{L_2(\Omega)}$.

Define $\lambda_q := \lambda(q^1, \phi^1) - \lambda(q^2, \phi^1)$ and by the adjoint problem (7.12), we have

$$\begin{cases} \frac{\partial \lambda_q}{\partial t} = -\nabla \cdot (k \nabla \lambda_q) + q^1 \lambda_q + (q^1 - q^2) \lambda(q^2, \phi^1) \\ \qquad -\omega_1(t) \int_0^T \omega_1(\tau) u_q(x,\tau) d\tau - \omega_2(t) \int_0^T \omega_2(\tau) u_q(x,\tau) d\tau, & (x,t) \in Q_T, \\ k \frac{\partial \lambda_q}{\partial \nu} + \alpha \lambda_q = 0, \quad (x,t) \in S_T, \quad \lambda_q(x,T) = 0, & x \in \Omega, \end{cases}$$

and by Lemma 7.4.2, we have

$$\begin{aligned} &\|\lambda_q\|_{L_2(Q_T)} \\ \leq & C_0 \left\| (q^1 - q^2) \lambda(q^2, \phi^1) + \omega_1 \int_0^T \omega_1(\tau) u_q(\cdot, \tau) d\tau + \omega_2 \int_0^T \omega_2(\tau) u_q(\cdot, \tau) d\tau \right\|_{L_2(Q_T)} \\ \leq & C_0 K_2 \|q^1 - q^2\|_{L_2(\Omega)} + C_0 \left(\|\omega_1\|^2_{L_\infty(0,T)} + \|\omega_2\|^2_{L_\infty(0,T)} \right) \|u_q\|_{L_2(Q_T)} \\ \leq & K_3 \|q^1 - q^2\|_{L_2(\Omega)}, \end{aligned}$$

where $K_3 := C_0 K_2 + C_0^2 K_1 \left(\|\omega_1\|^2_{L_\infty(0,T)} + \|\omega_2\|^2_{L_\infty(0,T)} \right)$. Similarly, denoting $\lambda_\phi := \lambda(q^2, \phi^1) - \lambda(q^2, \phi^2)$, we have

$$\begin{cases} \frac{\partial \lambda_\phi}{\partial t} = -\nabla \cdot (k \nabla \lambda_\phi) + q^2 \lambda_\phi \\ \qquad -\omega_1(t) \int_0^T \omega_1(\tau) u_\phi(x,\tau) d\tau - \omega_2(t) \int_0^T \omega_2(\tau) u_\phi(x,\tau) d\tau, & (x,t) \in Q_T, \\ k \frac{\partial \lambda_\phi}{\partial \nu} + \alpha \lambda_\phi = 0, \quad (x,t) \in S_T, \quad \lambda_\phi(x,T) = 0, & x \in \Omega, \end{cases}$$

and

$$\begin{aligned}\|\lambda_\phi\|_{L_2(Q_T)} \leq & C_0 \left\| \omega_1 \int_0^T \omega_1(\tau) u_\phi(\cdot,\tau) d\tau + \omega_2 \int_0^T \omega_2(\tau) u_\phi(\cdot,\tau) d\tau \right\|_{L_2(Q_T)} \\ \leq & C_0 \left(\|\omega_1\|^2_{L_\infty(0,T)} + \|\omega_2\|^2_{L_\infty(0,T)} \right) \|u_\phi\|_{L_2(Q_T)} \leq K_4 \|\phi^1 - \phi^2\|_{L_2(\Omega)},\end{aligned}$$

where $K_4 := C_0^2 \left(\|\omega_1\|^2_{L_\infty(0,T)} + \|\omega_2\|^2_{L_\infty(0,T)} \right)$. Denote $\Delta J'_q := J'_q(q^1,\phi^1) - J'_q(q^2,\phi^2)$, then we have $\|\Delta J'_q\|_{L_2(\Omega)} = \left\| \int_0^T [u(q^1,\phi^1)\lambda(q^1,\phi^1) - u(q^2,\phi^2)\lambda(q^2,\phi^2)] dt \right\|_{L_2(\Omega)}$, and $u(q^1,\phi^1)\lambda(q^1,\phi^1) - u(q^2,\phi^2)\lambda(q^2,\phi^2) = (u_q + u_\phi)\lambda(q^1,\phi^1) + (\lambda_q + \lambda_\phi)u(q^2,\phi^2)$, thus

$$\begin{aligned}\|\Delta J'_q\|_{L_2(\Omega)} \leq & \left\| \int_0^T (u_q + u_\phi)\lambda(q^1,\phi^1) dt \right\|_{L_2(\Omega)} + \left\| \int_0^T (\lambda_q + \lambda_\phi) u(q^2,\phi^2) dt \right\|_{L_2(\Omega)} \\ \leq & c(\|u_q\|_{L_2(Q_T)} + \|u_\phi\|_{L_2(Q_T)}) \|\lambda(q^1,\phi^1)\|_{L_\infty(Q_T)} \\ & + c(\|\lambda_q\|_{L_2(Q_T)} + \|\lambda_\phi\|_{L_2(\Omega)}) \|u(q^2,\phi^2)\|_{L_\infty(Q_T)} \\ \leq & c(C_0 K_1 K_2 + K_1 K_3) \|q^1 - q^2\|_{L_2(\Omega)} + c(C_0 K_2 + K_1 K_4) \|\phi^1 - \phi^2\|_{L_2(\Omega)} \\ \leq & M_q (\|q^1 - q^2\|_{L_2(\Omega)} + \|\phi^1 - \phi^2\|_{L_2(\Omega)}),\end{aligned}$$

where c is a positive constant depending on Ω and T, and $M_q := c \times \max\{C_0 K_1 K_2 + K_1 K_3, C_0 K_2 + K_1 K_4\} > 0$, which is independent of q^1, q^2, ϕ^1 and ϕ^2.

Denote $\Delta J'_\phi = J'_\phi(q^1,\phi^1) - J'_\phi(q^2,\phi^2)$, then by (7.2) we have

$$\begin{aligned}& \|\Delta J'_\phi\|_{L_2(\Omega)} = \|\Delta\lambda(x,0)(q^1,\phi^1) - \lambda(x,0)(q^2,\phi^2)\|_{L_2(\Omega)} \\ \leq & \|\lambda_q(x,0)\|_{L_2(\Omega)} + \|\lambda_\phi(x,0)\|_{L_2(\Omega)} \\ \leq & C_0 \left\| (q^1 - q^2)\lambda(q^2,\phi^1) + \omega_1 \int_0^T \omega_1(\tau) u_q(\cdot,\tau) d\tau + \omega_2 \int_0^T \omega_2(\tau) u_q(\cdot,\tau) d\tau \right\|_{L_2(Q_T)} \\ & + C_0 \left\| \omega_1 \int_0^T \omega_1(\tau) u_\phi(\cdot,\tau) d\tau + \omega_2 \int_0^T \omega_2(\tau) u_\phi(\cdot,\tau) d\tau \right\|_{L_2(Q_T)} \\ \leq & K_3 \|q^1 - q^2\|_{L_2(\Omega)} + K_4 \|\phi_1 - \phi_2\|_{L_2(\Omega)} \leq M_\phi (\|q^1 - q^2\|_{L_2(\Omega)} + \|\phi^1 - \phi^2\|_{L_2(\Omega)}),\end{aligned}$$

where $M_\phi := \max\{K_3, K_4\} > 0$ independent of q^1, q^2, ϕ^1 and ϕ^2. The theorem is proved. □

Lemma 7.4.5. *Under the assumptions of Theorem 7.4.4, for the step sizes β_q^n and β_ϕ^n satisfying (7.20), we have*

$$\sum_{n\geq 0} \frac{\|J'^n_q\|^4_{L_2(\Omega)}}{\|d^n_q\|^2_{L_2(\Omega)}} < \infty, \quad \sum_{n\geq 0} \frac{\|J'^n_\phi\|^4_{L_2(\Omega)}}{\|d^n_\phi\|^2_{L_2(\Omega)}} < \infty. \tag{7.28}$$

Proof. We use the arguments of Dai & Yuan (1996); Wolfe (1969, 1971); Zoutendijk (1970). By (7.20), we have

$$J(q^{n+1},\phi^{n+1}) = J(q^n + \beta_q^n d_q^n, \phi^n + \beta_\phi^n d_\phi^n) \leq J(q^n + \beta_1 d_q^n, \phi^n + \beta_2 d_\phi^n), \quad \forall \beta_1, \beta_2 \geq 0.$$

Taking $\beta_2 = 0$ and using the mean value theorem[1], we obtain

$$\begin{aligned}
&J(q^n, \phi^n) - J(q^{n+1}, \phi^{n+1}) \\
\geq &J(q^n, \phi^n) - J(q^n + \beta_1 d_q^n, \phi^n) = -\beta_1 \int_0^1 \langle J_q'(q^n + t\beta_1 d_q^n, \phi^n), d_q^n \rangle dt \\
= &-\beta_1 \langle J_q'^n, d_q^n \rangle - \beta_1 \int_0^1 \langle J_q'(q^n + t\beta_1 d_q^n, \phi^n) - J_q'^n, d_q^n \rangle dt. \qquad (7.29)
\end{aligned}$$

Taking $n = 0$ and using (7.18), we have $\langle J_q'^0, d_q^0 \rangle = -\|J_q'^0\|^2_{L_2(\Omega)}$. For $n \geq 1$, using (7.18) and (7.21), we have $\langle J_q'^n, d_q^n \rangle = \langle J_q'^n, -J_q^n + \gamma_q^n d_q^{n-1} \rangle = -\|J_q'^n\|^2_{L_2(\Omega)} + \gamma_q^n \langle J_q'^n, d_q^{n-1} \rangle = -\|J_q'^n\|^2_{L_2(\Omega)}$, which means $\langle J_q'^n, d_q^n \rangle = -\|J_q'^n\|^2_{L_2(\Omega)}, \forall n \geq 0$.

For $\int_0^1 \langle J_q'(q^n + t\beta_1 d_q^n, \phi^n) - J_q'^n, d_q^n \rangle dt$ in (7.29), the Lipschitz continuity of the gradient J_q' from Theorem 7.4.4 implies that

$$\begin{aligned}
&\int_0^1 \langle J_q'(q^n + t\beta_1 d_q^n, \phi^n) - J_q'^n, d_q^n \rangle dt \\
\leq &\|d_q^n\|_{L_2(\Omega)} \int_0^1 \|J_q'(q^n + t\beta_1 d_q^n, \phi^n) - J_q'(q^n, \phi^n)\|_{L_2(\Omega)} dt \\
\leq &M_q \|d_q^n\|_{L_2(\Omega)} \int_0^1 \|t\beta_1 d_q^n\|_{L_2(\Omega)} dt = \frac{1}{2}\beta_1 M_q \|d_q^n\|^2_{L_2(\Omega)}.
\end{aligned}$$

Thus, we obtain $J(q^n, \phi^n) - J(q^{n+1}, \phi^{n+1}) \geq \beta_1 \|J_q'^n\|^2_{L_2(\Omega)} - \frac{1}{2}\beta_1^2 M_q \|d_q^n\|^2_{L_2(\Omega)}, \forall \beta_1 \geq 0$. Taking $\beta_1 = \frac{\|J_q'^n\|^2_{L_2(\Omega)}}{M_q \|d_q^n\|^2_{L_2(\Omega)}} \geq 0$, then we have $J(q^n, \phi^n) - J(q^{n+1}, \phi^{n+1}) \geq \frac{\|J_q'^n\|^4_{L_2(\Omega)}}{2M_q \|d_q^n\|^2_{L_2(\Omega)}}$. By the definition of the objective functional (7.11), it is easy to see that the sequence $\{J(q^n, \phi^n)\}$ is bounded. Then, we have

$$\sum_{n \geq 0} \frac{\|J_q'^n\|^4_{L_2(\Omega)}}{\|d_q^n\|^2_{L_2(\Omega)}} \leq 2M_q \{[J(q^0, \phi^0) - J(q^1, \phi^1)] + [J(q^1, \phi^1) - J(q^2, \phi^2)] + \cdots] \} < \infty,$$

which means the first inequality in (7.28) holds. And by the same approaches, we can obtain the second inequality in (7.28), which concludes the proof. □

Theorem 7.4.6. *Under the assumptions of Theorem 7.4.4, the CGM either terminates at a stationary point or converges in the following senses:*

$$\liminf_{n \to \infty} \|J_q'^n\|_{L_2(\Omega)} = 0, \quad \liminf_{n \to \infty} \|J_\phi'^n\|_{L_2(\Omega)} = 0. \qquad (7.30)$$

[1] Let f be a continuously differentiable real-valued function defined on an open interval $I \subset \mathbb{R}$, and let x as well as $x + h$ be points of I. Then,

$$f(x + h) - f(x) = \left(\int_0^1 f'(x + th) dt \right) \cdot h.$$

Proof. From (7.18), we have $\|d_q^0\|_{L_2(\Omega)}^2 = \|J_q'^0\|_{L_2(\Omega)}^2$, and

$$\|d_q^n\|_{L_2(\Omega)}^2 = \|J_q'^n\|_{L_2(\Omega)}^2 + (\gamma_q^n)^2\|d_q^{n-1}\|_{L_2(\Omega)}^2 - 2\gamma_q^n\langle J_q'^n, d_q^{n-1}\rangle, \quad \forall n \geq 1.$$

Then (7.19) and (7.21) imply that $\|d_q^n\|_{L_2(\Omega)}^2 = \|J_q'^n\|_{L_2(\Omega)}^2 + \frac{\|J_q'^n\|_{L_2(\Omega)}^4}{\|J_q'^{n-1}\|_{L_2(\Omega)}^4}\|d_q^{n-1}\|_{L_2(\Omega)}^2$. Dividing both sides by $\|J_q'^n\|_{L_2(\Omega)}^4$ and using $\frac{\|d_q^0\|_{L_2(\Omega)}^2}{\|J_q'^0\|_{L_2(\Omega)}^4} = \frac{1}{\|J_q'^0\|_{L_2(\Omega)}^2}$, we obtain

$$\frac{\|d_q^n\|_{L_2(\Omega)}^2}{\|J_q'^n\|_{L_2(\Omega)}^4} = \frac{1}{\|J_q'^n\|_{L_2(\Omega)}^2} + \frac{\|d_q^{n-1}\|_{L_2(\Omega)}^2}{\|J_q'^{n-1}\|_{L_2(\Omega)}^4} = \sum_{i=0}^{n}\frac{1}{\|J_q'^i\|_{L_2(\Omega)}^2}.$$

Assuming that $\liminf_{n\to\infty}\|J_q'^n\|_{L_2(\Omega)} \neq 0$, then there exists a constant $c > 0$ such that

$$\|J_q'^n\|_{L_2(\Omega)} \geq c, \quad n \geq 0,$$

which leads to

$$\frac{\|d_q^n\|_{L_2(\Omega)}^2}{\|J_q'^n\|_{L_2(\Omega)}^4} \leq \frac{n+1}{c}, \quad \sum_{n\geq 0}\frac{\|J_q'^n\|_{L_2(\Omega)}^4}{\|d_q^n\|_{L_2(\Omega)}^2} \geq c\sum_{n\geq 0}\frac{1}{n+1} = \infty.$$

This is in contradiction with the first inequality in (7.28). Thus, the first result in (7.30) holds, and the second result in (7.30) can be obtained by the same method. The proof is complete. □

7.4.2 CGM

Based on the above discussions, all the coefficients of the iteration process (7.17) and (7.18) are expressed in explicit form except for the search step sizes β_q^n and β_ϕ^n which satisfy (7.21). These can be found by minimizing

$$\begin{aligned} J(q^{n+1}, \phi^{n+1}) =& \frac{1}{2}\int_\Omega\left(\int_0^T \omega_1 u(q^n + \beta_q^n d_q^n, \phi^n + \beta_\phi^n d_\phi^n)dt - \phi_1^\epsilon\right)^2 dx \\ &+ \frac{1}{2}\int_\Omega\left(\int_0^T \omega_2 u(q^n + \beta_q^n d_q^n, \phi^n + \beta_\phi^n d_\phi^n)dt - \phi_2^\epsilon\right)^2 dx. \end{aligned}$$

Since the above expression shows that the step sizes β_q^n and β_ϕ^n are in implicit form, the Taylor series expression can be applied to approximate $J(q^{n+1}, \phi^{n+1})$ such that the step sizes β_q^n and β_ϕ^n become explicit in the new formulation. Therefore, setting $\Delta q^n = d_q^n$ and $\Delta\phi^n = d_\phi^n$, the temperature $u(x, t; q^n + \beta_q^n d_q^n, \phi^n + \beta_\phi^n d_\phi^n)$ is linearised by a Taylor series expression in the form

$$\begin{aligned} &u(x, t; q^n + \beta_q^n d_q^n, \phi^n + \beta_\phi^n d_\phi^n) \\ \approx& u(x, t; q^n, \phi^n) + \beta_q^n d_q^n\frac{\partial u(x, t; q^n, \phi^n)}{\partial q^n} + \beta_\phi^n d_\phi^n\frac{\partial u(x, t; q^n, \phi^n)}{\partial \phi^n} \\ \approx& u(x, t; q^n, \phi^n) + \beta_q^n\Delta u_q(x, t; q^n, \phi^n) + \beta_\phi^n\Delta u_\phi(x, t; q^n, \phi^n). \end{aligned}$$

Here the functions $\Delta u_q(x,t;q^n,\phi^n)$ and $\Delta u_\phi(x,t;q^n,\phi^n)$ can be obtained by solving the sensitivity problems (6.14), and (6.15). Then, we rewrite

$$u_1^n = \int_0^T \omega_1 u(q^n,\phi^n)dt, \quad u_2^n = \int_0^T \omega_2 u(q^n,\phi^n)dt,$$
$$\Delta u_{q,1}^n = \int_0^T \omega_1 \Delta u_q(q^n,\phi^n)dt, \quad \Delta u_{q,2}^n = \int_0^T \omega_2 \Delta u_q(q^n,\phi^n)dt,$$
$$\Delta u_{\phi,1}^n = \int_0^T \omega_1 \Delta u_\phi(q^n,\phi^n)dt, \quad \Delta u_{\phi,2}^n = \int_0^T \omega_2 \Delta u_\phi(q^n,\phi^n)dt,$$

and then

$$J(q^{n+1},\phi^{n+1}) = \frac{1}{2}\int_\Omega \Big\{ \left(u_1^n + \beta_q^n \Delta u_{q,1}^n + \beta_\phi^n \Delta u_{\phi,1}^n - \phi_1^\epsilon\right)^2 + \left(u_2^n + \beta_q^n \Delta u_{q,2}^n + \beta_\phi^n \Delta u_{\phi,2}^n - \phi_2^\epsilon\right)^2 \Big\} dx.$$

The partial derivatives of the objective functional $J(q^{n+1},\phi^{n+1})$ with respect to β_q^n and β_ϕ^n are given by

$$\frac{\partial J(q^{n+1},\phi^{n+1})}{\partial \beta_q^n} = C_1\beta_q^n + C_2\beta_\phi^n + C_3, \quad \frac{\partial J(q^{n+1},\phi^{n+1})}{\partial \beta_\phi^n} = C_2\beta_q^n + C_4\beta_\phi^n + C_5,$$

where

$$C_1 = \int_\Omega \left[(\Delta u_{q,1}^n)^2 + (\Delta u_{q,2}^n)^2\right] dx, \quad C_2 = \int_\Omega \left(\Delta u_{q,1}^n \Delta u_{\phi,1}^n + \Delta u_{q,2}^n \Delta u_{\phi,2}^n\right) dx,$$
$$C_3 = \int_\Omega \left[(u_1^n - \phi_1^\epsilon)\Delta u_{q,1}^n + (u_2^n - \phi_2^\epsilon)\Delta u_{q,2}^n\right] dx, \quad C_4 = \int_\Omega \left[(\Delta u_{\phi,1}^n)^2 + (\Delta u_{\phi,2}^n)^2\right] dx,$$
$$C_5 = \int_\Omega \left[(u_1^n - \phi_1^\epsilon)\Delta u_{\phi,1}^n + u_2^n - \phi_2^\epsilon)\Delta u_{\phi,2}^n\right] dx.$$

According to the conditions (7.21), we set $\frac{\partial J(q^{n+1},\phi^{n+1})}{\partial \beta_q^n} = \frac{\partial J(q^{n+1},\phi^{n+1})}{\partial \beta_\phi^n} = 0$, and then obtain the search step sizes β_q^n and β_ϕ^n as follows:

$$\beta_q^n = \frac{C_3C_4 - C_2C_5}{C_2^2 - C_1C_4}, \quad \beta_\phi^n = \frac{C_1C_5 - C_2C_3}{C_2^2 - C_1C_4}, \quad n = 0,1,2,\cdots. \tag{7.31}$$

The iteration process given by (7.17) does not provide the CGM with the stabilisation necessary for the minimizing of the objective functional (7.11) to be classified as well-posed because of the errors inherent in the time-average temperature measurements (7.3) and (7.4). However, the method may become well-posed if the discrepancy principle is applied to stop the iteration procedure. According to the discrepancy principle, the iterative procedure is stopped when the following criterion is satisfied:

$$J(q^n,\phi^n) \le \overline{\epsilon}, \tag{7.32}$$

where $\bar{\epsilon}$ is some small positive value, e.g., $\bar{\epsilon} = 10^{-5}$, for the exact temperature measurements, and

$$\bar{\epsilon} = \frac{1}{2}\left(\|\phi_1^\epsilon - \phi_1\|^2_{L_2(\Omega)} + \|\phi_2^\epsilon - \phi_2\|^2_{L_2(\Omega)}\right) \leq \epsilon^2,$$

when the measured temperatures contain noise. Then, the CGM for the numerical reconstruction of the reaction coefficient $q(x)$ and initial temperature $\phi(x)$ is shown as follows:

S1. Set $n = 0$ and choose initial guesses q^0 and ϕ^0 for the unknowns q and ϕ, respectively.

S2. Solve the initial-boundary value direct problem (6.1) numerically by applying the FDM to compute $u(x, t; q^n, \phi^n)$, and the objective functional $J(q^n, \phi^n)$ by (7.11).

S3. If the stopping condition (7.32) is satisfied, then go to S7. Else go to S4.

S4. Solve the adjoint problem (7.12) to get the function $\lambda(x, t; q^n, \phi^n)$, and the gradients $J'_q(q^n, \phi^n)$ in (7.14) and $J'_\phi(q^n, \phi^n)$ in (7.15). Compute the conjugate coefficients γ_q^n and γ_ϕ^n in (7.19), and the search directions (7.18).

S5. Solve the sensitivity problems given by (6.14) for $\Delta u_q(x, t; q^n, \phi^n)$, and (6.15) for $\Delta u_\phi(x, t; q^n, \phi^n)$ by taking $\Delta q^n = d_q^n$ and $\Delta\phi^n = d_\phi^n$, and compute the step sizes β_q^n and β_ϕ^n by (7.31).

S6. Compute q^{n+1} and ϕ^{n+1} by (7.17). Set $n = n + 1$ and return to S2.

S7. End.

7.5 Numerical results and discussions

In this section, the reaction coefficient $q(x)$ and the initial temperature $\phi(x)$ are reconstructed numerically and simultaneously by the nonlinear CGM proposed in Section 7.4. The FDM, based on the C-N scheme for the one-dimensional $(\mathrm{d} = 1)$ case and the ADI scheme for the two-dimensional $(\mathrm{d} = 2)$ case, are applied to solve the direct, sensitivity and adjoint problems involved. The accuracy errors, as functions of the iteration number n, are defined by (6.24) and (6.25).

The integral temperature observations ϕ_1^ϵ and ϕ_2^ϵ are corrupted by Gaussian additive noise as

$$\phi_1^\epsilon = \phi_1 + \sigma \times \mathrm{random}(1), \quad \phi_2^\epsilon = \phi_2 + \sigma \times \mathrm{random}(1), \tag{7.33}$$

where $\sigma = \frac{p}{100} \max_{x\in\overline{\Omega}} \{|\phi_1|, |\phi_2|\}$ is the standard deviation, $p\%$ represents the percentage of noise, and the term random(1) generates random values from the normal distribution with zero mean and standard deviation equal to unity.

In the following sections, three numerical examples are considered in one- and two-dimensions.

7.5.1 Example 1

In the the one-dimensional $(\mathrm{d} = 1)$ case, we take $\Omega = (0,1)$, $T = 1$, $\omega_1(t) = 1$, $\omega_2(t) = 2t$ and

$$
\begin{aligned}
&k \equiv 1, \quad \alpha \equiv 1, \quad \mu(0,t) = \mu(1,t) = e^{-t},\\
&f(x,t) = \left(x^2(1+\pi+\sin\pi x) + \pi^2 \sin\pi x\right) e^{-t},\\
&\phi_1(x) = (1-e^{-1})(1+\pi+\sin\pi x), \quad \phi_2(x) = (2-4e^{-1})(1+\pi+\sin\pi x).
\end{aligned}
$$

With this input data, an analytical solution for the combined inverse coefficient or backward bio-heat conduction problem (6.1), (7.3) and (7.4) is given by

$$q(x) = 1 + x^2, \quad \phi(x) = 1 + \pi + \sin\pi x, \quad u(x,t) = (1+\pi+\sin\pi x)e^{-t}. \tag{7.34}$$

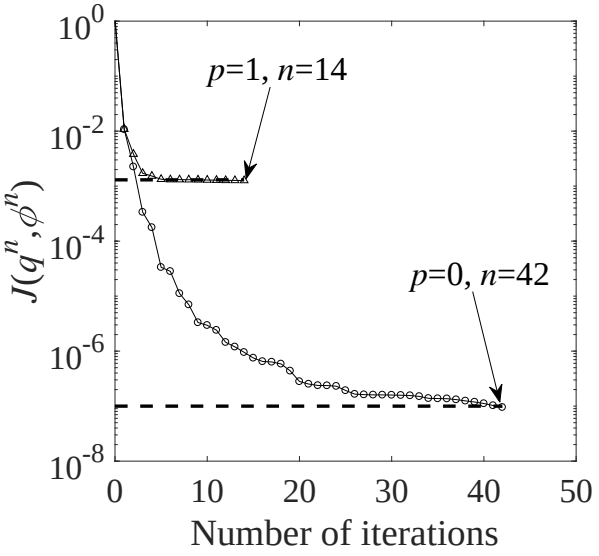

Figure 7.1: The objective functional (7.11) with $p \in \{0,1\}$ noise, for Example 1.

The Crank-Nicolson FDM is used to solve the problems (direct, sensitivity and adjoint problems) in the CGM with $I = M = 101$. The initial guesses are chosen arbitrary, say

$q^0(x) = 1.5$ and $\phi^0(x) = 1$. Figures 7.1 and 7.2 show the objective functional $J(q^n, \phi^n)$ given by (7.11) and the accuracy errors $E_1(q^n)$ given by (6.24) and $E_2(\phi^n)$ given by (6.25), for the reconstruction of the two unknown functions, simultaneously, in case of no noise, i.e., $p = 0$, and with $p = 1$ noise. Figure 7.1 illustrates the rapid monotonic decreasing convergence of the objective functional, as a function of iteration number n. The stopping number of the iterative process is 42 for exact data, i.e., for $p = 0$, whilst the iteration process is stopped at iteration number 14 according to the discrepancy principle (7.32) for $p = 1$ noise. On comparing Figures 7.1(a) and 7.2 it can be seen that there is some consistency and agreement between the stopping iteration numbers given by the discrepancy principle (7.32) and the optimal iteration numbers given by the minimum of the errors (6.24) and (6.25).

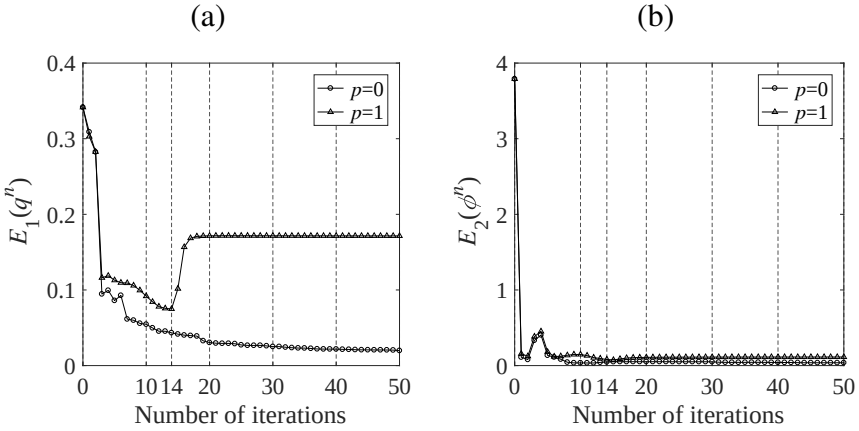

Figure 7.2: The accuracy errors (a) (6.24) and (b) (6.25), with $p \in \{0, 1\}$ noise, for Example 1.

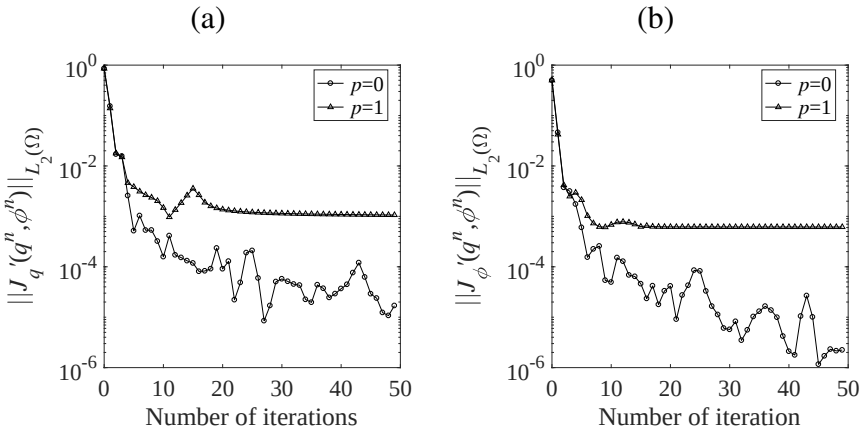

Figure 7.3: The norm of gradients (a) $\|J_q'(q^n, \phi^n)\|_{L_2(\Omega)}$ and (b) $\|J_\phi'(q^n, \phi^n)\|_{L_2(\Omega)}$, with $p \in \{0, 1\}$ noise, for Example 1.

Figure 7.3 shows the convergence of the norms of gradients $\|J'_q(q^n, \phi^n)\|_{L_2(\Omega)}$ and $\|J'_\phi(q^n, \phi^n)\|_{L_2(\Omega)}$ to small positive values with the increasing of the iteration number for $p = 0$. For $p\% = 1\%$ noise, the two norms are decreasing after the stopping iteration number 14, whilst the errors in Figures 7.2(a) and 7.3(b) are increasing after this discrepancy principle threshold. Such phenomenon means that while the CGM is convergent, the numerical solution is unstable, since the inverse problem is ill-posed. This is why the discrepancy principle (7.32) is applied to regularise the CGM to attain the stable solutions.

The numerical solutions of the reaction coefficient $q(x)$ and the initial temperature $\phi(x)$ are presented in Figures 7.4(a) and 7.4(b) for $p \in \{0, 1\}$ noise. As previously inferred from Figure 7.1, the plotted results are after 42 iterations in the case of no noise, while for noisy data the results are plotted after 14 iterations. From Figure 7.4 it can be seen that the accurate and stable results are obtained for both reaction coefficient $q(x)$ and the initial temperature $\phi(x)$.

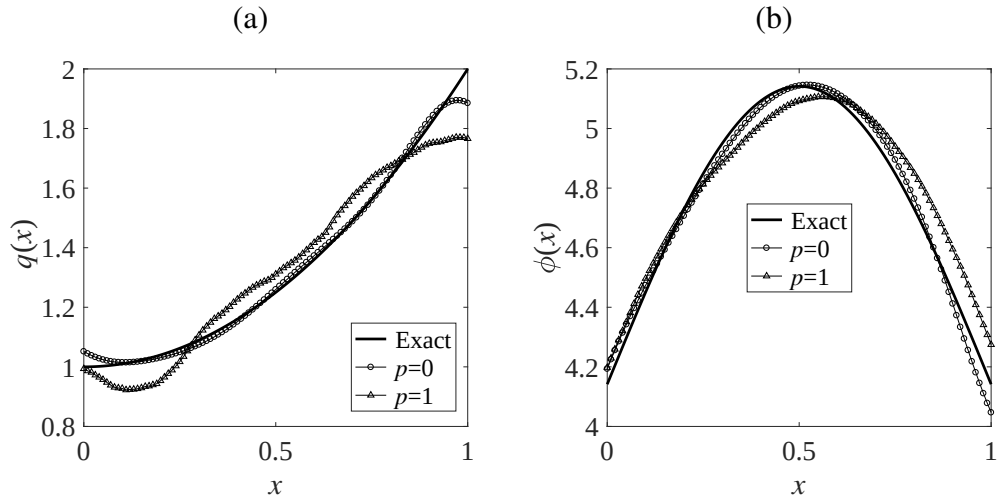

Figure 7.4: The exact and numerical results for (a) the reaction coefficient $q(x)$ and (b) the initial temperature $\phi(x)$, with $p \in \{0, 1\}$ noise, for Example 1.

p	I	M	$\bar{\epsilon}$	N	E_1	E_2
0	101	101	1.0E-07	42	2.4E-02	3.7E-02
1	101	101	1.3E-03	14	4.3E-02	4.6E-02

Table 7.1: The stopping iteration numbers N and the errors E_1 and E_2 for $p \in \{0, 1\}$ noise, for Example 1.

7.5.2 Example 2

We take $\Omega = (0,1)$, $T = 1$, $\omega_1(t) = 1$, $\omega_2(t) = 4t$ and

$$
\begin{aligned}
&k \equiv 1, \quad \alpha \equiv 1, \quad \mu(0,t) = \mu(1,t) = e^{-t},\\
&f(x,t) = 2e^{-t} + (2 + x - x^2)e^{-t} \times \begin{cases} 1 - x, & x \in [0, 0.3],\\ -x + 4x^2, & x \in (0.3, 0.7),\\ 2, & x \in [0.7, 1], \end{cases}\\
&\phi_1(x) = (1 - e^{-1})(2 + x - x^2), \quad \phi_2(x) = (4 - 6e^{-1})(2 + x - x^2),
\end{aligned}
$$

with this data the analytical solution of the inverse problem (6.1), (7.3) and (7.3) is given by

$$
\begin{aligned}
q(x) &= \begin{cases} 2 - x, & x \in [0, 0.3],\\ 1 - x + 4x^2, & x \in (0.3, 0.7),\\ 3, & x \in [0.7, 1], \end{cases}\\
\phi(x) &= 2 + x - x^2, \quad u(x,t) = (2 + x - x^2)e^{-t}.
\end{aligned} \tag{7.35}
$$

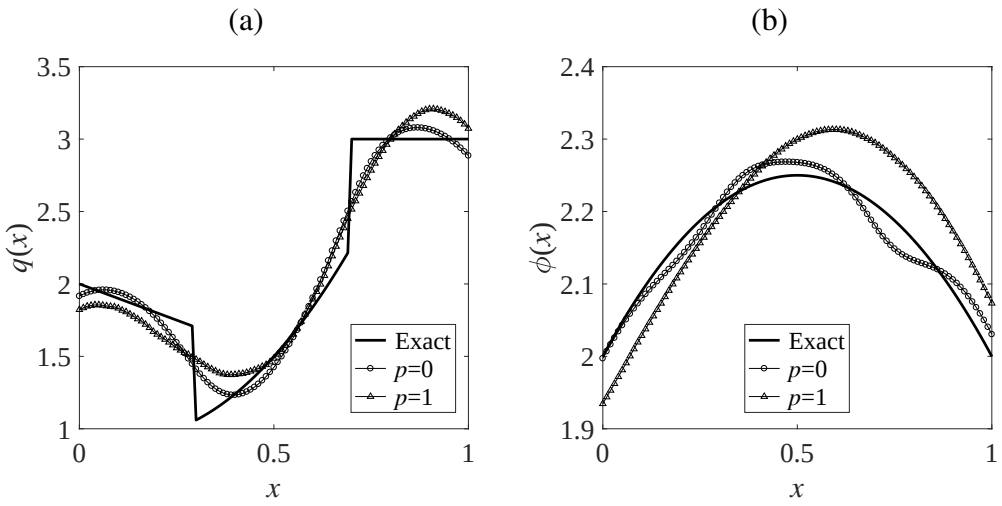

Figure 7.5: The exact and numerical results for (a) the reaction coefficient $q(x)$ and (b) the initial temperature $\phi(x)$, with $p \in \{0, 1\}$ noise, for Example 2.

In comparison with the previous Example 1, this example is more severe since the reaction coefficient to be retrieved is a discontinuous function. We take the initial guesses $q^0(x) = 1$ and $\phi^0(x) = 1$ and employ the Crank-Nicolson FDM with the mesh sizes $I = M = 101$.

The corresponding numerical solutions for the reaction coefficient $q(x)$ and initial temperature $\phi(x)$ at these stopping iteration numbers are shown in Figures 7.5(a) and

p	I	M	$\overline{\epsilon}$	N	E_1	E_2
0	101	101	1.5E-07	45	0.1319	2.0E-02
1	101	101	4.4E-04	5	0.1721	6.4E-02

Table 7.2: The stopping iteration numbers N and the errors E_1 and E_2 for $p \in \{0, 1\}$ noise, for Example 2.

7.5(b), respectively. From these figures it can be seen that the numerical solutions are stable and reasonably accurate bearing in mind the severe discontinuous reaction coefficient that had to be retrieved simultaneously with the initial temperature.

7.5.3 Example 3

We now consider a two-dimensional example and take $\Omega = (0, 1) \times (0, 1)$, $T = 1$, $\omega_1(t) = 1$, $\omega_2(t) = 3t$ and

$$
\begin{aligned}
&k = \mathbf{I}_2, \quad \alpha \equiv 1, \quad \mu(0, x_2, t) = \mu(1, x_2, t) = \mu(x_1, 0, t) = \mu(x_2, 1, t) = e^{-t},\\
&f(x_1, x_2, t) = (2\pi^2 + x_1^2 + x_2^2)(\sin^2(\pi x_1)\sin^2(\pi x_2) + 1)e^{-t}\\
&\qquad\qquad - 2\pi^2(\cos(2\pi x_1)\sin^2(\pi x_2) + \sin^2(\pi x_1)\cos(2\pi x_2))e^{-t},\\
&\phi_1(x_1, x_2) = (1 - e^{-1})(\sin^2(\pi x_1)\sin^2(\pi x_2) + 1),\\
&\phi_2(x_1, x_2) = (3 - 5e^{-1})(\sin^2(\pi x_1)\sin^2(\pi x_2) + 1).
\end{aligned}
$$

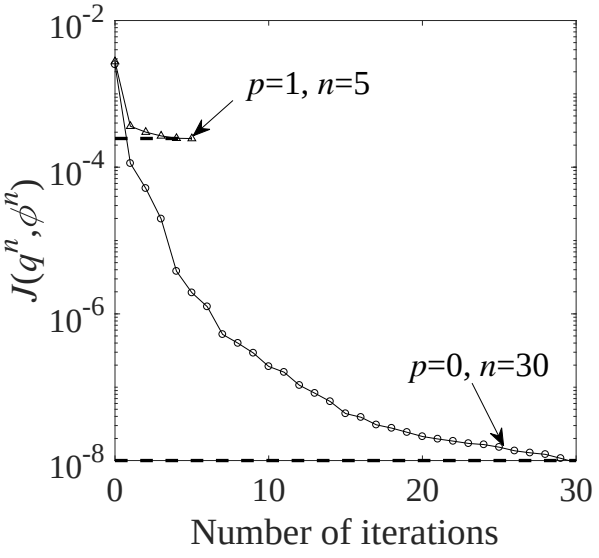

Figure 7.6: The objective functional (7.11) with $p \in \{0, 1\}$ noise, for Example 3.

With this data, the analytical solution of the inverse problem (6.1), (7.3) and (7.4) is given by

$$q(x_1, x_2) = 1 + 2\pi^2 + x_1^2 + x_2^2, \quad \phi(x_1, x_2) = \sin^2(\pi x_1)\sin^2(\pi x_2) + 1,$$
$$u(x_1, x_2, t) = (\sin^2(\pi x_1)\sin^2(\pi x_2) + 1)e^{-t}. \tag{7.36}$$

The ADI scheme with mesh sizes $I = J = M = 101$ is used to obtain the numerical solutions for the direct, sensitivity and adjoint problems in the algorithm for the two-dimensional $(\mathrm{d} = 2)$ case. The initial guesses are chosen as $q^0(x_1, x_2) = 20$ and $\phi^0(x_1, x_2) = 1$. Figures 7.6–7.10 for Example 3 represent analogous quantities to Figures 7.1–7.4 of Example 1 and similar conclusions can be observed.

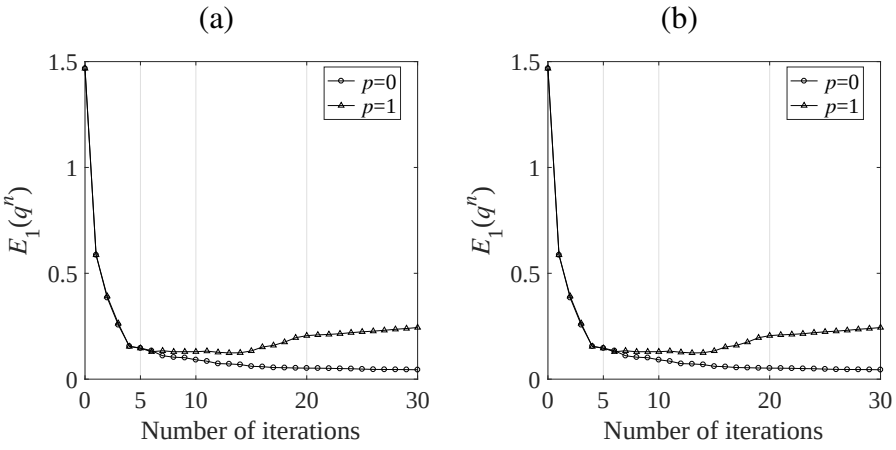

Figure 7.7: The accuracy errors (a) (6.24) and (b) (6.25), with $p \in \{0, 1\}$ noise, for Example 3.

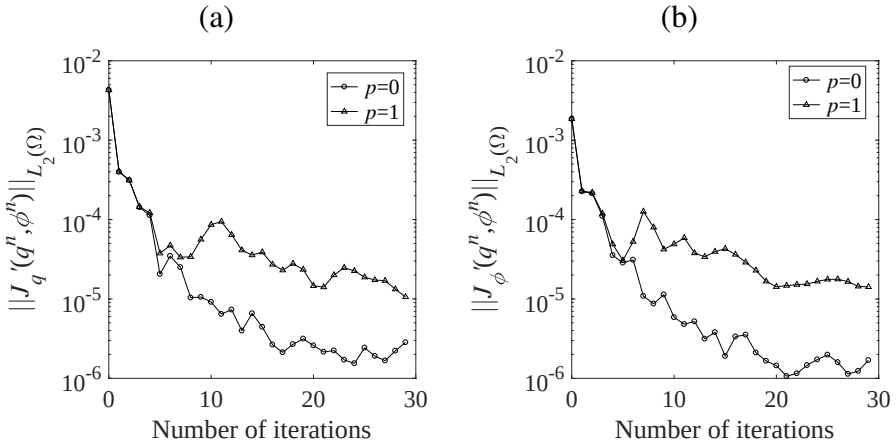

Figure 7.8: The norm of gradients (a) $\|J'_q(q^n, \phi^n)\|_{L_2(\Omega)}$ and (b) $\|J'_\phi(q^n, \phi^n)\|_{L_2(\Omega)}$, with $p \in \{0, 1\}$ noise, for Example 3.

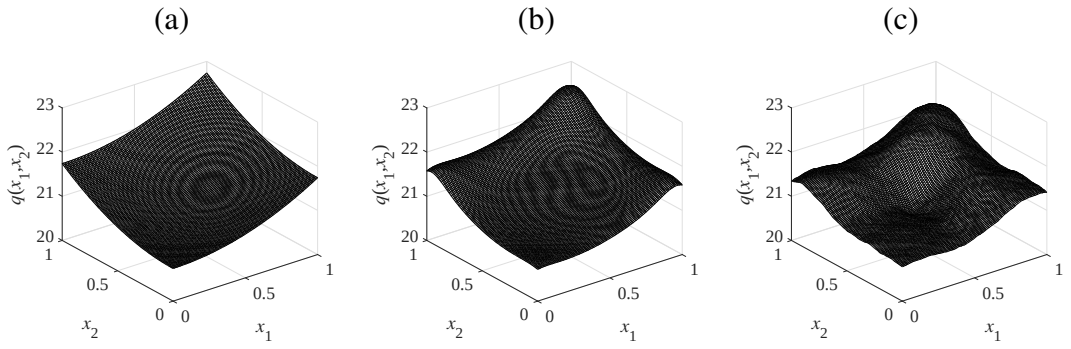

Figure 7.9: (a) The exact reaction coefficient, and numerical results with (b) $p = 0$ and (c) $p = 1$, for Example 3.

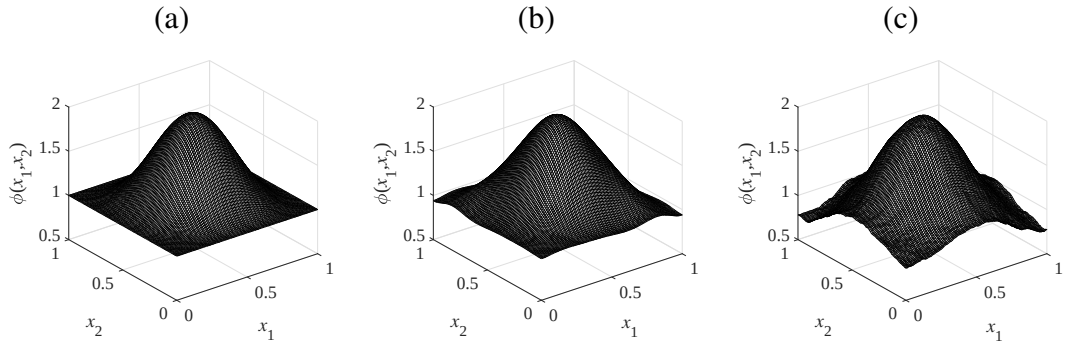

Figure 7.10: (a) The exact initial temperature, and numerical results with (b) $p = 0$ and (c) $p = 1$, for Example 3.

p	I	J	M	$\bar{\epsilon}$	N	E_1	E_2
0	101	101	101	1.0E-08	30	0.0444	0.0297
1	101	101	101	2.5E-04	5	0.1462	0.1000

Table 7.3: The stopping iteration numbers N and the errors E_1 and E_2 for $p \in \{0, 1\}$ noise, for Example 3.

7.6 Conclusions

In this chapter, the simultaneous retrieval of the space-dependent reaction coefficient and initial temperature from time-integral weighted temperature observations has been investigated. The two unknown functions have been identified simultaneously by minimizing the least-squares objective functional using the CGM based on the newly derived adjoint

problem (7.12), the sensitivity problems (6.14) and (6.15) presented in Chapter 6, and the gradient equations (7.14) and (7.15). Stability has been achieved by stopping the iterations according to the discrepancy criterion (7.32). Three numerical examples in both one- and two-dimensions have been presented, and discuss showing the accuracy and stability of the numerical reconstruction.

Chapter 8

Simultaneous reconstruction of the space-dependent reaction coefficient, initial temperature and source term

8.1 Introduction

The simultaneous identification of several non-constant physical properties along with initial and/or boundary conditions is very challenging, especially when it cannot be decoupled, as it combines both nonlinear as well as ill-posedness features. One such new inverse problem, that is investigated in this chapter, is to identify the space-dependent reaction coefficient, the initial temperature and the source term from measured temperatures at two instants and at the final time, simultaneously.

The nonlinear identification of the space-dependent reaction coefficient from final or time-average temperature observations has been investigated in Chapters 5. The reaction coefficient and the initial temperature have been simultaneously identified from temperature measurements at two different time instants in Chapters 6. Also, the linear identification of the space-dependent source term from temperature measurements at the final time was also widely studied, e.g., Isakov (1990, 2006); Prilepko *et al.* (2000).

In this chapter, the simultaneous reconstruction of the spatially-distributed reaction coefficient, the initial temperature, the heat source, and the temperature throughout the solution domain from temperature measurements at three different instants, is investigated for the first time. The least-squares objective functional, whose minimizer is proven to exist, is minimized to obtain a quasi-solution to the inverse problem. A variational method is applied to derive the Fréchet gradient with respect to the three unknown coefficients based on the adjoint and sensitivity problems. The CGM which is based on

the gradient, the adjoint and sensitivity problems, are utilized to simultaneously reconstruct the three unknown functions. Furthermore, since the inverse problem is ill-posed, the CGM is regularized by the discrepancy principle, Alifanov (1994), to obtain stable numerical results.

This chapter is organized as follows: Section 8.2 presents the inverse problem to reconstruct the unknown space-dependent reaction coefficient, initial temperature and source term. The least-squares objective functional to be minimized is described having several properties in Section 8.3. The CGM is established in Section 8.4 based on the gradients of the objective functional, and the adjoint and sensitivity problems, and the global convergence for the CGM algorithm is obtained. Two numerical examples for the one-dimensional inverse problem are discussed in Section 8.5. Finally, Section 8.6 highlights the conclusions of this work.

8.2 Mathematical formulation

Let $\Omega \subset \mathbb{R}^{\mathrm{d}}$, $\mathrm{d} = 1, 2, 3$ be a bounded domain with sufficiently smooth boundary $\partial\Omega$. We consider the heat transfer problem given by (6.1) in the cylinder $Q_T = \Omega \times (0, T)$, and $T > 0$ is a final time. Moreover, the heat source $f(x,t)$ in (6.1) has the form $f(x,t) = F(x)h(x,t) + g(x,t)$. Then, the mathematical model becomes

$$\begin{cases} \frac{\partial u}{\partial t}(x,t) = \nabla \cdot (k(x)\nabla u(x,t)) - q(x)u(x,t) & \\ \qquad\qquad +F(x)h(x,t) + g(x,t), & (x,t) \in Q_T, \\ k(x)\frac{\partial u}{\partial \nu} + \alpha(x)u(x,t) = \mu(x,t), & (x,t) \in S_T, \\ u(x,0) = \phi(x), & x \in \overline{\Omega}, \end{cases} \tag{8.1}$$

where $F(x)$, $h(x,t)$ and $g(x,t)$ are the components of the heat source $f(x,t)$. The direct problem is to determine the temperature $u(x,t)$ in (8.1) when the thermal conductivity $k(x)$, reaction coefficient $q(x)$, the source components $F(x)$, $h(x,t)$ and $g(x,t)$, the heat flux $\mu(x,t)$ and the initial temperature $\phi(x)$ are specified. The weak solution $u(x,t) \in H^{1,0}(Q_T)$ of the direct problem (8.1) is defined as follows.

Definition 8.2.1. *A function $u \in H^{1,0}(Q_T)$ is called as a weak solution to the initial-boundary value direct problem (8.1) if*

$$\begin{aligned} &\int_{Q_T} \left(-u\frac{\partial \eta}{\partial t} + k\nabla u \cdot \nabla \eta + qu\eta \right) dxdt + \int_{S_T} \alpha u\eta dsdt \\ &= \int_{Q_T} Fh\eta dxdt + \int_{Q_T} g\eta dxdt + \int_{S_T} \mu\eta dsdt + \int_{\Omega} \phi\eta(\cdot,0)dx, \end{aligned} \tag{8.2}$$

for $\forall \eta \in H^{1,1}(Q_T)$ with $\eta(\cdot, T) = 0$.

Then, the existence and uniqueness of the weak solution to the initial-boundary value direct problem (8.1) is stated in the following theorem (Tröltzsch (2010), p.373).

Theorem 8.2.2. *Let $\Omega \subset \mathbb{R}^{\mathrm{d}}$ be a bounded domain with Lipschitz boundary $\partial\Omega$, and suppose that the matrix $k = (k_{ij})_{i,j=\overline{1,d}}$ is symmetric and positive definite, i.e., $k_{ij} = k_{ji} \in L_\infty(\Omega)$ and satisfy (5.3), $q \in L_\infty(\Omega)$, $F \in L_2(\Omega)$, $h \in L_\infty(Q_T)$, $g \in L_2(Q_T)$, $\alpha \in L_\infty(\partial\Omega)$, $\mu \in L_2(S_T)$ and $\phi \in L_2(\Omega)$. Then the initial-boundary value direct problem (8.1) has a unique weak solution $u \in H^{1,0}(Q)$. In addition, the solution satisfies the estimate*

$$\begin{aligned}&\max_{t\in[0,T]} \|u(\cdot,t)\|_{L_2(\Omega)} + \|u\|_{H^{1,0}(Q_T)} \\ \leq& c\left(\|F\|_{L_2(\Omega)}\|h\|_{L_\infty(Q_T)} + \|g\|_{L_2(Q_T)} + \|\mu\|_{L_2(S_T)} + \|\phi\|_{L_2(\Omega)}\right)\end{aligned} \tag{8.3}$$

for some positive constant c which is independent of F, h, g, μ and ϕ.

The inverse problem is to reconstruct $(q(x), \phi(x), F(x), u(x,t)) \in L_\infty(\Omega) \times L_2(\Omega) \times L_2(\Omega) \times H^{1,0}(Q_T)$ satisfying (8.1) together with the temperature measurements at two time instants t_1, t_2, $0 < t_1 < t_2 < T$ and at the final time T, i.e.

$$u(x,t_1) = \phi_1(x), \quad x \in \Omega, \tag{8.4}$$

$$u(x,t_2) = \phi_2(x), \quad x \in \Omega, \tag{8.5}$$

$$u(x,T) = \phi_T(x), \quad x \in \Omega, \tag{8.6}$$

where $\phi_1(x)$, $\phi_2(x)$ and $\phi_T(x)$ are given data in $L_2(\Omega)$ which may be subject to noise due to measurement errors, as

$$\|\phi_1^\epsilon - \phi_1\|_{L_2(\Omega)} \leq \epsilon, \quad \|\phi_2^\epsilon - \phi_2\|_{L_2(\Omega)} \leq \epsilon, \quad \|\phi_T^\epsilon - \phi_T\|_{L_2(\Omega)} \leq \epsilon, \tag{8.7}$$

where $\epsilon \geq 0$ represents the noise level.

8.3 Analysis

Define the sets $\mathcal{A}_1 = \{q \in L_\infty(\Omega) : 0 \leq q(x) \leq \kappa_1, \text{ a.e. } x \in \Omega\}$, $\mathcal{A}_2 = \{\phi \in L_2(\Omega) : |\phi(x)| \leq \kappa_2, \text{ a.e. } x \in \Omega\}$ and $\mathcal{A}_3 = \{F \in L_2(\Omega) : |F(x)| \leq \kappa_3, \text{ a.e. } x \in \Omega\}$, where κ_1, κ_2 and κ_3 are given positive constants.

Let $u(q,\phi,F) := u(x,t;q,\phi,F) \in H^{1,0}(Q_T)$ denote the solution to the initial-boundary value direct problem (8.1) for a particular triplet $(q(x), \phi(x), F(x)) \in \mathcal{A}_1 \times$

$\mathcal{A}_2 \times \mathcal{A}_3$. The quasi-solution of the inverse problem (8.1), (8.4)–(8.6) can be attained by minimizing the following least-squares objective functional

$$J(q,\phi,F) = \frac{1}{2}\left\{\|u_1 - \phi_1^\epsilon\|^2_{L_2(\Omega)} + \|u_2 - \phi_2^\epsilon\|^2_{L_2(\Omega)} + \|u_T - \phi_T^\epsilon\|^2_{L_2(\Omega)}\right\}, \tag{8.8}$$

where $u_1(x) = u(x,t_1;q,\phi,F)$, $u_2(x) = u(x,t_2;q,\phi,F)$ and $u_T(x) = u(x,T;q,\phi,F)$.

The existence of a minimizer to the optimization problem (8.8) over the admissible set $\mathcal{A}_1 \times \mathcal{A}_2 \times \mathcal{A}_3$ is established in the following theorem.

Theorem 8.3.1. *There exists at least one minimizer to the optimization problem* (8.8).

Proof. We follow the same ideas as in the proof of Theorem 6.3.1 of Chapter 6. Based on the estimate (8.3), it is obvious that $\min J(q,\phi,F)$ is finite over the admissible set $\mathcal{A}_1 \times \mathcal{A}_2 \times \mathcal{A}_3$. Thus, there exists a minimizing sequence $\{q^n,\phi^n,F^n\}$ from $\mathcal{A}_1 \times \mathcal{A}_2 \times \mathcal{A}_3$ such that

$$\lim_{n\to\infty} J(q^n,\phi^n,F^n) = \inf_{q\in\mathcal{A}_1,\phi\in\mathcal{A}_2,F\in\mathcal{A}_3} J(q,\phi,F).$$

The boundedness of $\{q^n,\phi^n,F^n\}$ in $L_\infty(\Omega)\times L_2(\Omega)\times L_2(\Omega)$ implies that there exists a subsequence, still denoted by $\{q^n,\phi^n,F^n\}$, such that q^n, ϕ^n and F^n converge weakly to q^* in $L_\infty(\Omega)$, ϕ^* in $L_2(\Omega)$, and F^* in $L_2(\Omega)$. Clearly $q^* \in \mathcal{A}_1$, $\phi^* \in \mathcal{A}_2$ and $F^* \in \mathcal{A}_3$, since the sets $\mathcal{A}_1$, $\mathcal{A}_2$ and $\mathcal{A}_3$ are closed and convex. The *a-priori* estimate (8.3) implies that the sequence $\{u^n := u(q^n,\phi^n,F^n)\}$ is bounded in $H^{1,0}(Q_T)$. Thus, we may extract a subsequence, still denoted by $\{u^n\}$, and some $u^* \in H^{1,0}(Q_T)$ such that $u^n \to u^*$, weakly in $H^{1,0}(Q_T)$.

By Definition 8.2.1, for any $\eta \in H^{1,1}(Q)$ with $\eta(\cdot,T) = 0$, we have

$$\begin{aligned}&\int_{Q_T}\left(-u^n\frac{\partial\eta}{\partial t} + k\nabla u^n\cdot\nabla\eta + q^n u^n\eta\right)dxdt + \int_{S_T}\alpha u^n\eta dsdt\\ &= \int_{Q_T} F^n h\eta dxdt + \int_{Q_T} g\eta dxdt + \int_{S_T}\mu\eta dsdt + \int_\Omega \phi^n\eta(\cdot,0)dx.\end{aligned} \tag{8.9}$$

Since $H^{1,0}(S_T)$ is compactly embedded in $L_2(S_T)$, $u^n|_{S_T}$ converges to $u^*|_{S_T}$ in $L_2(S_T)$. The weak convergence of u^n to u^* in $H^{1,0}(Q_T)$ and the convergence of $u^n|_{S_T}$ to $u^*|_{S_T}$ in $L_2(S_T)$ imply that

$$\begin{aligned}\lim_{n\to\infty}\int_{Q_T} -u^n\frac{\partial\eta}{\partial t}dxdt &= \int_{Q_T} -u^*\frac{\partial\eta}{\partial t}dxdt,\\ \lim_{n\to\infty}\int_{Q_T} k\nabla u^n\cdot\nabla\eta dxdt &= \int_{Q_T} k\nabla u^*\cdot\nabla\eta dxdt,\\ \lim_{n\to\infty}\int_{S_T}\alpha u^n\eta dsdt &= \int_{S_T}\alpha u^*\eta dsdt,\end{aligned}$$

and the weak convergence of ϕ^n to ϕ^* and F^n to F^* in $L_2(\Omega)$ implies that

$$\lim_{n\to\infty}\int_{Q_T} F^n h\eta dxdt = \int_{Q_T} F^* h\eta dxdt, \quad \lim_{n\to\infty}\int_{\Omega}\phi^n\eta(\cdot,0)dx = \int_{\Omega}\phi^*\eta(\cdot,0)dx.$$

The third term in the left hand side of (8.9) can be rewritten as

$$\int_{Q_T} q^n u^n \eta dxdt = \int_{Q_T} q^* u^n \eta dxdt + \int_{Q_T}(q^n - q^*)u^n\eta dxdt.$$

Since u^n weakly converges to u^* in $H^{1,0}(Q_T)$, we have

$$\lim_{n\to\infty}\int_{Q_T} q^* u^n \eta dxdt = \int_{Q_T} q^* u^* \eta dxdt,$$

and due to q^n weakly converges to q^* in $L_\infty(\Omega)$, using the estimate (8.3) for u^n and the Lebesgue dominant convergence theorem we obtain that the term $\int_{Q_T}(q^n - q^*)u^n\eta dxdt$ converges to zero, and hence

$$\lim_{n\to\infty}\int_{Q_T} q^n u^n \eta dxdt = \int_{Q_T} q^* u^* \eta dxdt,$$

and (8.9) yields

$$\begin{aligned}&\int_{Q_T}\left(-u^*\frac{\partial\eta}{\partial t} + (k\nabla u^*)\cdot\nabla\eta + q^*u^*\eta\right)dxdt + \int_{S_T}\alpha u^*\eta dsdt\\ &= \int_{Q_T} F^* h\eta dxdt + \int_{Q_T} g\eta dxdt + \int_{S_T}\mu\eta dsdt + \int_{\Omega}\phi^*\eta(\cdot,0)dx,\end{aligned}$$

which means that $u^* = u(q^*, \phi^*, F^*)$, due to the uniqueness of solution to the initial-boundary value direct problem (8.1) in Theorem 8.2.2, with $q = q^*$, $F = F^*$ and $\phi = \phi^*$ in (8.1). The lower semi-continuity of norms implies

$$\begin{aligned}J(q^*,\phi^*,F^*) =& \frac{1}{2}\left\{\|u_1^* - \phi_1^\epsilon\|^2_{L_2(\Omega)} + \|u_2^* - \phi_2^\epsilon\|^2_{L_2(\Omega)} + \|u_T^* - \phi_T^\epsilon\|^2_{L_2(\Omega)}\right\}\\ \le& \frac{1}{2}\lim_{n\to\infty}\left\{\|u_1^n - \phi_1^\epsilon\|^2_{L_2(\Omega)} + \|u_2^n - \phi_2^\epsilon\|^2_{L_2(\Omega)} + \|u_T^n - \phi_T^\epsilon\|^2_{L_2(\Omega)}\right\}\\ =& \lim_{n\to\infty} J(q^n,\phi^n,F^n) = \min_{q\in\mathcal{A}_1,\phi\in\mathcal{A}_2,F\in\mathcal{A}_3} J(q^n,\phi^n,F^n),\end{aligned}$$

which indicates that the triplet $\{q^*, \phi^*, F^*\}$ is a minimizer of the optimization problem (8.8) over $\mathcal{A}_1 \times \mathcal{A}_2 \times \mathcal{A}_3$. □

Lemma 8.3.2. *The mapping $(q, \phi, F) \mapsto u(q, \phi, F)$ is Lipschitz continuous, i.e.,*

$$\|u(q+\Delta q,\phi,F) - u(q,\phi,F)\|_{H^{1,0}(Q_T)} \le c\|\Delta q\|_{L_\infty(\Omega)}, \tag{8.10}$$

$$\|u(q,\phi+\Delta\phi,F) - u(q,\phi,F)\|_{H^{1,0}(Q_T)} \le c\|\Delta\phi\|_{L_2(\Omega)}, \tag{8.11}$$

$$\|u(q,\phi,F+\Delta F) - u(q,\phi,F)\|_{H^{1,0}(Q_T)} \le c\|\Delta F\|_{L_2(\Omega)}, \tag{8.12}$$

for any $q, q+\Delta q \in \mathcal{A}_1$, $\phi, \phi+\Delta\phi \in \mathcal{A}_2$ and $F, F+\Delta F \in \mathcal{A}_3$.

Proof. Denote by $\Delta u_q = u(q+\Delta q, \phi, F) - u(q, \phi, F)$, $\Delta u_\phi = u(q, \phi+\Delta\phi, F) - u(q, \phi, F)$ and $\Delta u_F = u(q, \phi, F+\Delta F) - u(q, \phi, F)$ the increments of the temperature u with respect to q, ϕ and F. Then, based on the initial-boundary value problem (8.1) they satisfy the following problems:

$$\begin{cases} \frac{\partial(\Delta u_q)}{\partial t} = \nabla\cdot(k\nabla(\Delta u_q)) - q\Delta u_q - \Delta q u(q+\Delta q, \phi, F), & (x,t)\in Q_T, \\ k\frac{\partial(\Delta u_q)}{\partial \nu} + \alpha \Delta u_q = 0, \quad (x,t)\in S_T, \quad \Delta u_q(x,0) = 0, & x\in\overline{\Omega}, \end{cases} \tag{8.13}$$

$$\begin{cases} \frac{\partial(\Delta u_\phi)}{\partial t} = \nabla\cdot(k\nabla(\Delta u_\phi)) - q\Delta u_\phi, & (x,t)\in Q_T, \\ k\frac{\partial(\Delta u_\phi)}{\partial \nu} + \alpha \Delta u_\phi = 0, \quad (x,t)\in S_T, \quad \Delta u_\phi(x,0) = \Delta\phi, & x\in\overline{\Omega}, \end{cases} \tag{8.14}$$

and

$$\begin{cases} \frac{\partial(\Delta u_F)}{\partial t} = \nabla\cdot(k\nabla(\Delta u_F)) - q\Delta u_F + \Delta F h, & (x,t)\in Q_T, \\ k\frac{\partial(\Delta u_F)}{\partial \nu} + \alpha \Delta u_F = 0, \quad (x,t)\in S_T, \quad \Delta u_F(x,0) = 0, & x\in\overline{\Omega}, \end{cases} \tag{8.15}$$

Using the estimate (8.3) to the above problem problems, we obtain

$$\begin{aligned} &\|\Delta u_q\|_{H^{1,0}(Q_T)} \le c\|\Delta q u\|_{L_2(Q_T)} \le c\|\Delta q\|_{L_\infty(\Omega)}\|u\|_{L_2(Q_T)}, \\ &\|\Delta u_\phi\|_{H^{1,0}(Q_T)} \le c\|\Delta\phi\|_{L_2(\Omega)}, \\ &\|\Delta u_F\|_{H^{1,0}(Q_T)} \le c\|\Delta F h\|_{L_2(Q_T)} \le c\|\Delta F\|_{L_2(\Omega)}\|h\|_{L_\infty(Q_T)}, \end{aligned}$$

which conclude the proof of the lemma. □

Lemma 8.3.3. *The mapping $(q, \phi, f) \mapsto u(q, \phi, f)$ is Fréchet differentiable.*

Proof. Consider the problem

$$\begin{cases} \frac{\partial v}{\partial t} = \nabla\cdot(k\nabla v) - qv - \Delta q u(q,\phi,F), & (x,t)\in Q_T, \\ k\frac{\partial v}{\partial \nu} + \alpha v = 0, \quad (x,t)\in S_T, \quad v(x,0) = 0, & x\in\overline{\Omega}, \end{cases} \tag{8.16}$$

where $\Delta q \in L_\infty(\Omega)$ such that $q+\Delta q \in \mathcal{A}_1$. Then, there exists a unique solution $v(x,t) \in H^{1,0}(Q_T)$ for the initial-boundary value problem (8.16), and the mapping $\Delta q \mapsto v$ from $L_\infty(\Omega)$ to $H^{1,0}(Q_T)$ defines a bounded linear operator $\mathcal{U}_q$ by the estimate (8.3).

Denote $w = u(q+\Delta q, \phi, F) - u(q, \phi, F) - \mathcal{U}_q\Delta q = \Delta u_q - v$, where Δu_q satisfies the problem (8.13). Then, w satisfies the problem

$$\begin{cases} \frac{\partial w}{\partial t} = \nabla\cdot(k\nabla w) - qw - \Delta q \Delta u_q, & (x,t)\in Q_T, \\ k\frac{\partial w}{\partial \nu} + \alpha w = 0, \quad (x,t)\in S_T, \quad w(x,0) = 0, & x\in\overline{\Omega}. \end{cases}$$

By applying (8.3), we obtain

$$\|w\|_{H^{1,0}(Q_T)} \leq c\|\Delta q \Delta u_q\|_{L_2(Q_T)} \leq c\|\Delta q\|_{L_\infty(\Omega)}\|\Delta u_q\|_{H^{1,0}(Q_T)},$$

then via (8.10) in Lemma 8.3.2, we obtain

$$\|u(q+\Delta q,\phi,F) - u(q,\phi,F) - \mathcal{U}_q\Delta q\|_{H^{1,0}(Q_T)} = \|w\|_{H^{1,0}(Q_T)} \leq c\|\Delta q\|^2_{L_\infty(\Omega)},$$

which implies that

$$\lim_{\|\Delta q\|_{L_\infty(\Omega)}\to 0} \frac{\|u(q+\Delta q,\phi,F) - u(q,\phi,F) - \mathcal{U}_q\Delta q\|_{H^{1,0}(Q_T)}}{\|\Delta q\|_{L_\infty(\Omega)}} = 0.$$

For the initial-boundary value problem (8.14), it is obvious that there exists a unique solution $\Delta u_\phi \in H^{1,0}(Q_T)$, and then the mapping $\Delta\phi \mapsto \Delta u_\phi$ from $L_2(\Omega)$ to $H^{1,0}(Q_T)$ defines a bounded linear operator $\mathcal{U}_\phi$ and $\mathcal{U}_\phi\Delta\phi = \Delta u_\phi$.

Similarly, the problem (8.15) and Theorem 8.2.2 imply that there exists a unique solution $\Delta u_F \in H^{1,0}(Q_T)$, and the mapping $\Delta F \mapsto \Delta u_F$ from $L_2(\Omega)$ to $H^{1,0}(Q_T)$ defines a bounded linear operator $\mathcal{U}_F$ such that $\mathcal{U}_F\Delta F = \Delta u_F$. Therefore, the lemma is proved. □

The CGM based on the gradient of $J(q,\phi,F)$ is applied to obtain the minimizer of the objective functional numerically. In order to obtain the gradient, we introduce the following adjoint problem:

$$\begin{cases} \frac{\partial\lambda}{\partial t} = -\nabla\cdot(k\nabla\lambda) + q\lambda - (u_1-\phi_1^\epsilon)\delta(t-t_1) \\ \qquad -(u_2-\phi_2^\epsilon)\delta(t-t_2) - 2(u_T-\phi_T^\epsilon)\delta(t-T), & (x,t)\in Q_T, \\ k\frac{\partial\lambda}{\partial\nu} + \alpha\lambda = 0, \quad (x,t)\in S_T, \quad \lambda(x,T) = 0, & x\in\overline{\Omega}, \end{cases} \tag{8.17}$$

where $\delta(\cdot)$ is the Dirac delta function. According to Definition 8.2.1, the weak solution $\lambda \in H^{1,0}(Q_T)$ of the adjoint problem (8.17), satisfies the variational equality

$$\int_{Q_T}\left(\lambda\frac{\partial\eta}{\partial t} + k\nabla\lambda\cdot\nabla\eta + q\lambda\eta\right)dxdt + \int_{S_T}\alpha\lambda\eta dsdt = \int_\Omega\{(u_1-\phi_1^\epsilon)\eta(x,t_1) + (u_2-\phi_2^\epsilon)\eta(x,t_2) + (u_T-\phi_T^\epsilon)\eta(x,T)\}\,dx, \quad \forall\eta\in H^{1,1}(Q_T) \text{ with } \eta(\cdot,0)=0.$$

Theorem 8.3.4. *The objective functional $J(q,\phi,F)$ is Fréchet differentiable, and the partial derivatives $J'_q(q,\phi,F)$, $J'_\phi(q,\phi,F)$ and $J'_F(q,\phi,F)$ are given by*

$$J'_q(q,\phi,F) = -\int_0^T u(x,t)\lambda(x,t)dt, \tag{8.18}$$

$$J'_\phi(q,\phi,F) = \lambda(x,0), \tag{8.19}$$

$$J'_F(q,\phi,F) = \int_0^T \lambda(x,t)h(x,t)dt. \tag{8.20}$$

Proof. Taking $\Delta q \in L_\infty(\Omega)$ such that $q + \Delta q \in \mathcal{A}_1$, and denoting by $\Delta J_q = J(q + \Delta q, \phi, F) - J(q, \phi, F)$, the increment of the objective functional $J(q, \phi, F)$ in the q direction, then equation (8.8) yields

$$\begin{aligned}\Delta J_q = &\int_\Omega \{\Delta u_{q,1}(u_1 - \phi_1^\epsilon) + \Delta u_{q,2}(u_2 - \phi_2^\epsilon) + \Delta u_{q,T}(u_T - \phi_T^\epsilon)\}\, dx \\ &+ \frac{1}{2}\left\{\|\Delta u_{q,1}\|^2_{L_2(\Omega)} + \|\Delta u_{q,2}\|^2_{L_2(\Omega)} + \|\Delta u_{q,T}\|^2_{L_2(\Omega)}\right\},\end{aligned}$$

where $\Delta u_{q,i} := \Delta u_q(x, t_i; q, \phi, F)$, $i = 1, 2$, and $\Delta u_{q,T} := \Delta u_q(x, T; q, \phi, F)$. Using the property of the Dirac delta function, the first term of the right hand side in the above formula can be written as

$$\begin{aligned}&\int_\Omega \{\Delta u_{q,1}(u_1 - \phi_1^\epsilon) + \Delta u_{q,2}(u_2 - \phi_2^\epsilon) + \Delta u_{q,T}(u_T - \phi_T^\epsilon)\}\, dx \\ =&\int_{Q_T} \Delta u_q \left\{(u_1 - \phi_1^\epsilon)\delta(t - t_1) + (u_2 - \phi_2^\epsilon)\delta(t - t_2) + 2(u_T - \phi_T^\epsilon)\delta(t - T)\right\} dxdt,\end{aligned}$$

and by the adjoint problem (8.17), we have

$$\begin{aligned}\Delta J_q = &\int_{Q_T} \Delta u_q \left\{-\frac{\partial \lambda}{\partial t} - \nabla \cdot (k\nabla\lambda) + q\lambda\right\} dx \\ &+ \frac{1}{2}\left\{\|\Delta u_{q,1}\|^2_{L_2(\Omega)} + \|\Delta u_{q,2}\|^2_{L_2(\Omega)} + \|\Delta u_{q,T}\|^2_{L_2(\Omega)}\right\}.\end{aligned}$$

Also, by (8.13) for Δu_q and integration by parts, we get

$$\begin{aligned}&\int_{Q_T} \Delta u_q \left\{-\frac{\partial \lambda}{\partial t} - \nabla \cdot (k\nabla\lambda) + q\lambda\right\} dxdt \\ =&\int_{Q_T} \lambda \left\{\frac{\partial(\Delta u_q)}{\partial t} - \nabla \cdot (k\nabla(\Delta u_q)) + q\Delta u_q\right\} dxdt \\ &+ \int_{S_T} \left\{k\frac{\partial(\Delta u_q)}{\partial \nu}\lambda - k\frac{\partial \lambda}{\partial \nu}\Delta u_q\right\} dsdt - \int_\Omega \Delta u_q \lambda|_0^T dx \\ =&-\int_{Q_T} \Delta q u(q + \Delta q, \phi, F)\lambda dxdt \\ =&-\int_{Q_T} \Delta q \Delta u_q \lambda dxdt - \int_{Q_T} \Delta q u \lambda dxdt.\end{aligned}$$

Thus, the above two equations and the property of the Dirac delta function imply

$$\begin{aligned}\Delta J_q = &-\int_{Q_T} \Delta q \Delta u_q \lambda dxdt - \int_{Q_T} \Delta q u \lambda dxdt \\ &+ \frac{1}{2}\left\{\|\Delta u_{q,1}\|^2_{L_2(\Omega)} + \|\Delta u_{q,2}\|^2_{L_2(\Omega)} + \|\Delta u_{q,T}\|^2_{L_2(\Omega)}\right\}.\end{aligned}$$

By the same approach for the problems (8.14) for Δu_ϕ and (8.15) for Δu_F, we can obtain

$$\Delta J_\phi = \int_\Omega \Delta\phi\lambda(x,0)dx + \frac{1}{2}\left\{\|\Delta u_{\phi,1}\|^2_{L_2(\Omega)} + \|\Delta u_{\phi,2}\|^2_{L_2(\Omega)} + \|\Delta u_{\phi,T}\|^2_{L_2(\Omega)}\right\},$$
$$\Delta J_F = \int_Q \Delta F h\lambda dxdt + \frac{1}{2}\left\{\|\Delta u_{F,1}\|^2_{L_2(\Omega)} + \|\Delta u_{F,2}\|^2_{L_2(\Omega)} + \|\Delta u_{F,T}\|^2_{L_2(\Omega)}\right\}.$$

From (8.3), we can obtain that

$$\max\{\|\Delta u_{q,1}\|^2_{L_2(\Omega)}, \|\Delta u_{q,2}\|^2_{L_2(\Omega)}, \|\Delta u_{q,T}\|^2_{L_2(\Omega)}\} \le c\|\Delta q\|^2_{L_\infty(\Omega)},$$
$$\max\{\|\Delta u_{\phi,1}\|^2_{L_2(\Omega)}, \|\Delta u_{\phi,2}\|^2_{L_2(\Omega)}, \|\Delta u_{\phi,T}\|^2_{L_2(\Omega)}\} \le c\|\Delta\phi\|^2_{L_2(\Omega)},$$
$$\max\{\|\Delta u_{F,1}\|^2_{L_2(\Omega)}, \|\Delta u_{F,2}\|^2_{L_2(\Omega)}, \|\Delta u_{F,T}\|^2_{L_2(\Omega)}\} \le c\|\Delta F\|^2_{L_2(\Omega)},$$

and via Lemma 8.3.2, we get

$$\left|\int_{Q_T} \Delta q\Delta u_q\lambda dxdt\right| \le \|\Delta q\|_{L_\infty(\Omega)}\|\lambda\|_{L_2(Q_T)}\|\Delta u_q\|_{L_2(Q_T)} \le c\|\Delta q\|^2_{L_\infty(\Omega)},$$

thus

$$\Delta J_q = -\int_{Q_T} \Delta q u\lambda dxdt + o(\|\Delta q\|_{L_\infty(\Omega)}),$$
$$\Delta J_\phi = \int_\Omega \Delta\phi\lambda(x,0)dx + o(\|\Delta\phi\|_{L_2(\Omega)}),$$
$$\Delta J_F = \int_{Q_T} \Delta F h\lambda dxdt + o(\|\Delta F\|_{L_2(\Omega)}),$$

which means that the formulae (8.18)–(8.20) for the Fréchet derivatives hold. The theorem is proved. □

8.4 Conjugate gradient method

In this section, the CGM will be developed and applied to obtain the numerical solutions for the reaction coefficient $q(x)$, the initial temperature $\phi(x)$ and the source term $F(x)$ to the inverse problem (8.1), (8.4)–(8.6). The following iterative process is used for the estimation of the triplet of functions (q,ϕ,F) by minimizing the objective functional (8.8):

$$q^{n+1} = q^n + \beta_q^n d_q^n, \quad \phi^{n+1} = \phi^n + \beta_\phi^n d_\phi^n, \quad F^{n+1} = F^n + \beta_F^n d_F^n, \quad n = 0,1,2,\cdots \tag{8.21}$$

with the search directions d_q^n, d_ϕ^n and d_F^n given by

$$d_q^n = \begin{cases} -J_q'^0, \\ -J_q'^n + \gamma_q^n d_q^{n-1}, \end{cases} \quad d_\phi^n = \begin{cases} -J_\phi'^0, \\ -J_\phi'^n + \gamma_\phi^n d_\phi^{n-1}, \end{cases} \quad d_F^n = \begin{cases} -J_F'^0, \\ -J_F'^n + \gamma_F^n d_F^{n-1}, \end{cases} \tag{8.22}$$

where the subscript n indicates the number of iterations, q^0, ϕ^0 and F^0 are the initial guesses for the three unknown functions, $J_q'^n = J_q'(q^n, \phi^n, F^n)$, $J_\phi'^n = J_\phi'(q^n, \phi^n, F^n)$, $J_F'^n = J_F'(q^n, \phi^n, F^n)$, β_q^n, β_ϕ^n and β_F^n are the step sizes with respect to q, ϕ and F in passing from iteration n to the next iteration $n+1$. The Fletcher-Reeves formula, Fletcher & Reeves (1964), is applied for the conjugate gradient coefficients γ_q^n, γ_ϕ^n and γ_F^n given by

$$\gamma_q^n = \frac{\|J_q'^n\|^2_{L_2(\Omega)}}{\|J_q'^{n-1}\|^2_{L_2(\Omega)}}, \quad \gamma_\phi^n = \frac{\|J_\phi'^n\|^2_{L_2(\Omega)}}{\|J_\phi'^{n-1}\|^2_{L_2(\Omega)}}, \quad \gamma_F^n = \frac{\|J_F'^n\|^2_{L_2(\Omega)}}{\|J_F'^{n-1}\|^2_{L_2(\Omega)}}, \quad n = 1, 2, \cdots \tag{8.23}$$

Denote $u_i^n := u(x, t_i; q^n, \phi^n, F^n)$, $i = 1, 2$, and $u_T^n := u(x, T; q^n, \phi^n, F^n)$, then the step sizes β_q^n, β_ϕ^n and β_F^n can be found by minimizing

$$J(q^{n+1}, \phi^{n+1}, F^{n+1}) = \frac{1}{2}\int_\Omega \left\{(u_1^{n+1} - \phi_1^\epsilon)^2 + (u_2^{n+1} - \phi_2^\epsilon)^2 + (u_T^{n+1} - \phi_T^\epsilon)^2\right\} dx.$$

Setting $\Delta q^n = d_q^n$, $\Delta\phi^n = d_\phi^n$ and $\Delta F^n = d_F^n$, the functions u_1^{n+1}, u_2^{n+1} and u_T^{n+1} are linearised by the Taylor series expansion in the following form:

$$\begin{aligned}
&u(x, \bar{t}; q^n + \beta_q^n d_q^n, \phi^n + \beta_\phi^n d_\phi^n, F^n + \beta_F^n d_F^n) \\
\approx &u(x, \bar{t}; q^n, \phi^n, F^n) + \beta_q^n d_q^n \frac{\partial u(x, \bar{t}; q^n, \phi^n, F^n)}{\partial q^n} \\
&+ \beta_\phi^n d_\phi^n \frac{\partial u(x, \bar{t}; q^n, \phi^n, F^n)}{\partial \phi^n} + \beta_F^n d_F^n \frac{\partial u(x, \bar{t}; q^n, \phi^n, F^n)}{\partial F^n} \\
\approx &u(x, \bar{t}; q^n, \phi^n, F^n) + \beta_q^n \Delta u_q(x, \bar{t}; q^n, \phi^n, F^n) \\
&+ \beta_\phi^n \Delta u_\phi(x, \bar{t}; q^n, \phi^n, F^n) + \beta_F^n \Delta u_F(x, \bar{t}; q^n, \phi^n, F^n)
\end{aligned}$$

where $\bar{t}$ represents t_1, t_2 and T.

Denote $\Delta u_{q,1}^n = \Delta u_q(x, t_1; q^n, \phi^n, F^n)$, $\Delta u_{q,2}^n = \Delta u_q(x, t_2; q^n, \phi^n, F^n)$ and $\Delta u_{q,T}^n = \Delta u_q(x, T; q^n, \phi^n, F^n)$, and $\Delta u_{\phi,1}^n$, $\Delta u_{\phi,2}^n$, $\Delta u_{\phi,T}^n$, $\Delta u_{F,1}^n$, $\Delta u_{F,2}^n$ and $\Delta u_{F,T}^n$ can be defined in the same way. We have

$$\begin{aligned}
J(q^{n+1}, \phi^{n+1}, F^{n+1}) = &\frac{1}{2}\int_\Omega \left(u_1^n + \beta_q^n \Delta u_{q,1}^n + \beta_\phi^n \Delta u_{\phi,1}^n + \beta_F^n \Delta u_{F,1}^n - \phi_1^\epsilon\right)^2 dx \\
&+ \frac{1}{2}\int_\Omega \left(u_2^n + \beta_q^n \Delta u_{q,2}^n + \beta_\phi^n \Delta u_{\phi,2}^n + \beta_F^n \Delta u_{F,2}^n - \phi_2^\epsilon\right)^2 dx \\
&+ \frac{1}{2}\int_\Omega \left(u_T^n + \beta_q^n \Delta u_{q,T}^n + \beta_\phi^n \Delta u_{\phi,T}^n + \beta_F^n \Delta u_{F,T}^n - \phi_T^\epsilon\right)^2 dx.
\end{aligned}$$

The partial derivatives of the objective functional $J(q^{n+1}, \phi^{n+1}, F^{n+1})$ with respect to β_q^n, β_ϕ^n and β_F^n are given by

$$\frac{\partial J}{\partial \beta_q^n} = A_{11}\beta_q^n + A_{12}\beta_\phi^n + A_{13}\beta_F^n - B_1, \quad \frac{\partial J}{\partial \beta_\phi^n} = A_{21}\beta_q^n + A_{22}\beta_\phi^n + A_{23}\beta_F^n - B_2,$$
$$\frac{\partial J}{\partial \beta_F^n} = A_{31}\beta_q^n + A_{32}\beta_\phi^n + A_{33}\beta_F^n - B_3,$$

where $A_{12} = A_{21}$, $A_{13} = A_{31}$, $A_{23} = A_{32}$,

$$A_{11} = \sum_{i=1,2,T} \|\Delta u_{q,i}^n\|_{L_2(\Omega)}^2, \quad A_{22} = \sum_{i=1,2,T} \|\Delta u_{\phi,i}^n\|_{L_2(\Omega)}^2,$$
$$A_{12} = \sum_{i=1,2,T} \langle \Delta u_{q,i}^n, \Delta u_{\phi,i}^n \rangle, \quad A_{13} = \sum_{i=1,2,T} \langle \Delta u_{q,i}^n, \Delta u_{F,i}^n \rangle,$$
$$A_{23} = \sum_{i=1,2,T} \langle \Delta u_{\phi,i}^n, \Delta u_{F,i}^n \rangle, \quad A_{33} = \sum_{i=1,2,T} \|\Delta u_{F,i}^n\|_{L_2(\Omega)}^2,$$

and

$$B_1 = -\sum_{i=1,2,T} \langle u_i^n - \phi_i^\epsilon, \Delta u_{q,i}^n \rangle, \quad B_2 = -\sum_{i=1,2,T} \langle u_i^n - \phi_i^\epsilon, \Delta u_{\phi,i}^n \rangle,$$
$$B_3 = -\sum_{i=1,2,T} \langle u_i^n - \phi_i^\epsilon, \Delta u_{F,i}^n \rangle.$$

Setting $\frac{\partial J}{\partial \beta_q^n} = \frac{\partial J}{\partial \beta_\phi^n} = \frac{\partial J}{\partial \beta_F^n} = 0$, the search step sizes β_q^n, β_ϕ^n and β_F^n can be obtained by solving the following linear system:

$$\mathbf{A}\mathbf{x} = \mathbf{b}, \tag{8.24}$$

where $\mathbf{A} = \{A_{ij}\}$, $i, j = \overline{1,3}$ is a symmetric matrix, $\mathbf{x} = \{\beta_q^n, \beta_\phi^n, \beta_F^n\}^{\mathrm{T}}$ and $\mathbf{b} = \{B_1, B_2, B_3\}^{\mathrm{T}}$.

The iteration process given by (8.21) does not provide the CGM with the stabilization necessary for the minimizing of the objective functional (8.8) to be classified as well-posed because of the errors inherent in the measured temperatures (8.4)–(8.6). However, the CGM may become well-posed if the discrepancy principle, Alifanov (1994), applied to stop the iteration procedure at the smallest threshold n for which

$$J(q^n, \phi^n, F^n) \le \bar{\epsilon}, \tag{8.25}$$

where $\bar{\epsilon}$ is a small positive value, e.g., $\bar{\epsilon} = 10^{-5}$ for exact temperature measurements, and

$$\bar{\epsilon} = \frac{1}{2}\left(\|\phi_1^\epsilon - \phi_1\|_{L_2(\Omega)}^2 + \|\phi_2^\epsilon - \phi_2\|_{L_2(\Omega)}^2 + \|\phi_T^\epsilon - \phi_T\|_{L_2(\Omega)}^2\right),$$

if the measured temperatures contain noise. Based on (8.7), we indicate that $\bar{\epsilon} \le 3\epsilon^2/2$.

In summary, the CGM for the numerical estimation of the space-dependent reaction coefficient $q(x)$, initial temperature $\phi(x)$ and source term $F(x)$ is presented as follows:

S1. Set $n = 0$ and choose initial guesses q^0, ϕ^0 and F^0 for the three unknown coefficients $q(x)$, $\phi(x)$ and $F(x)$, respectively.

S2. Solve the initial-boundary value direct problem (8.1) numerically by using the FDM to compute $u(x, t; q^n, \phi^n, F^n)$, and $J(q^n, \phi^n, F^n)$ by (8.8).

S3. If the stopping criterion (8.25) is satisfied, then go to S7. Else go to S4.

S4. Solve the adjoint problem (8.17) to obtain $\lambda(x, t; q^n, \phi^n, F^n)$, and the Fréchet gradients $J_q'^n$ in (8.18), $J_\phi'^n$ in (8.19) and $J_F'^n$ in (8.20). Compute the conjugate coefficients γ_q^n, γ_ϕ^n and γ_F^n in (8.23), and the search directions d_q^n, d_ϕ^n and d_F^n in (8.22).

S5. Solve the sensitivity problems (8.13) for $\Delta u_q(x, t; q^n, \phi^n, F^n)$, (8.14) for $\Delta u_\phi(x, t; q^n, \phi^n, F^n)$, and (8.15) for $\Delta u_F(x, t; q^n, \phi^n, F^n)$ by taking $\Delta q^n = d_q^n$, $\Delta\phi^n = d_\phi^n$ and $\Delta f^n = d_F^n$, and compute the search step sizes β_q^n, β_ϕ^n and β_F^n by (8.24).

S6. Update q^{n+1}, ϕ^{n+1} and F^{n+1} by (8.21). Set $n = n + 1$ and return to S2.

S7. End.

8.5 Numerical results and discussions

In this section, the space-dependent reaction coefficient $q(x)$, the initial temperature $\phi(x)$ and the source term $F(x)$ are simultaneously reconstructed by the CGM proposed in Section 8.4. The FDM based on the Crank-Nicolson scheme is applied to solve the direct, sensitivity and adjoint problem involved. Note that in the adjoint problem (8.17), we approximate the Dirac delta function $\delta(\cdot)$ by $\delta_a(t - \tilde{t}) = \frac{1}{a\sqrt{\pi}} e^{-(t-\tilde{t})^2/a^2}$, where a is a small positive constant taken as, e.g., $a = 10^{-3}$ and $\tilde{t}$ represents t_1, t_2 and T. The accuracy errors, as functions of the iteration numbers n, for $q(x)$, $\phi(x)$ and $F(x)$ are defined as

$$E_1(q^n) = \|q^n - q\|_{L_2(\Omega)}, \tag{8.26}$$

$$E_2(\phi^n) = \|\phi^n - \phi\|_{L_2(\Omega)}, \tag{8.27}$$

$$E_3(F^n) = \|F^n - F\|_{L_2(\Omega)}, \tag{8.28}$$

where q^n, ϕ^n and F^n are the numerical solutions obtained by the CGM at the iteration number n, and q, ϕ and F are the analytical expression for the reaction coefficient, initial temperature and source term, if available.

The measured noisy temperatures ϕ_1^ϵ, ϕ_2^ϵ and ϕ_T^ϵ are simulated by adding the Gaussian noisy term to the exact temperature

$$\phi_i^\epsilon = \phi_i + \sigma \times \text{random}(1), \quad i = 1, 2, T,$$

where $\sigma = \frac{p}{100} \max_{x \in \overline{\Omega}} \{|\phi_1(x)|, |\phi_2(x)|, |\phi_T(x)|\}$ is the standard deviation, $p\%$ represents the percentage of noise, and $\text{random}(1)$ generates random values from a normal distribution with zero mean and unit standard deviation.

We consider a couple of one-dimensional ($\text{d} = 1$) test examples in a finite slab $\Omega = (0, 1)$ over the time period $T = 1$. For the numerical discretisation we employ the FDM with a mesh of 100 equidistant nodes equally spread over each of the space and time intervals.

8.5.1 Example 1

In this example, we take $t_1 = 0.5$, $t_2 = 0.7$ and

$$\begin{aligned}
&k \equiv 1, \quad \alpha \equiv 1, \quad g(x,t) = x(1+x)^2 e^{-t} - (1+x)(1+x^3)t^3, \\
&h(x,t) = (1+x)t^3, \quad \mu(0,t) = e^{-t}, \quad \mu(1,t) = 4e^{-t}, \\
&\phi_1(x) = e^{-0.5}(1+x^2), \quad \phi_2(x) = e^{-0.7}(1+x^2), \quad \phi_T(x) = e^{-1}(1+x^2).
\end{aligned}$$

Based on this input data, the analytical solution to the inverse problem (8.1), (8.4)–(8.6) is given by

$$q(x) = 3 + x, \quad F(x) = 1 + x^3, \quad \phi(x) = 1 + x^2, \quad u(x,t) = (1+x^2)e^{-t}. \tag{8.29}$$

The initial guesses are chosen as $q^0(x) = 2$, $\phi^0(x) = 2 + x$ and $F^0(x) = 1$. Figure 8.1(a) shows the objective functional $J(q^n, \phi^n, F^n)$ given by (8.8) for the simultaneous reconstruction of the three unknown coefficients with $p \in \{0, 1\}$ noise. From this figure it can be seen that the objective functional (8.8), as a function of iteration numbers n, is rapidly monotonic decreasing convergent. The stopping iteration number is 17 for the exact data, i.e., $p = 0$, whilst the algorithm is stopped at the iteration number 4 for $p = 1$ noise, obtained according to the discrepancy principle (8.25). The accuracy errors $E_1(q^n)$ given by (8.26), $E_2(\phi^n)$ given by (8.27) and $E_3(F^n)$ given by (8.28) are shown in Figures 8.1(b)–8.1(d), respectively. From these figures, it can be seen that for $p = 0$, the accuracy errors keep decreasing as the iterations proceed, but for $p = 1$ noise the errors start quickly increasing after just a few iterations. Therefore, stopping the CGM iterations after 4 iterations, (cf. Figure 8.1(a)), is expected to yield stable and reasonably accurate numerical solutions, as illustrated in Figure 8.2.

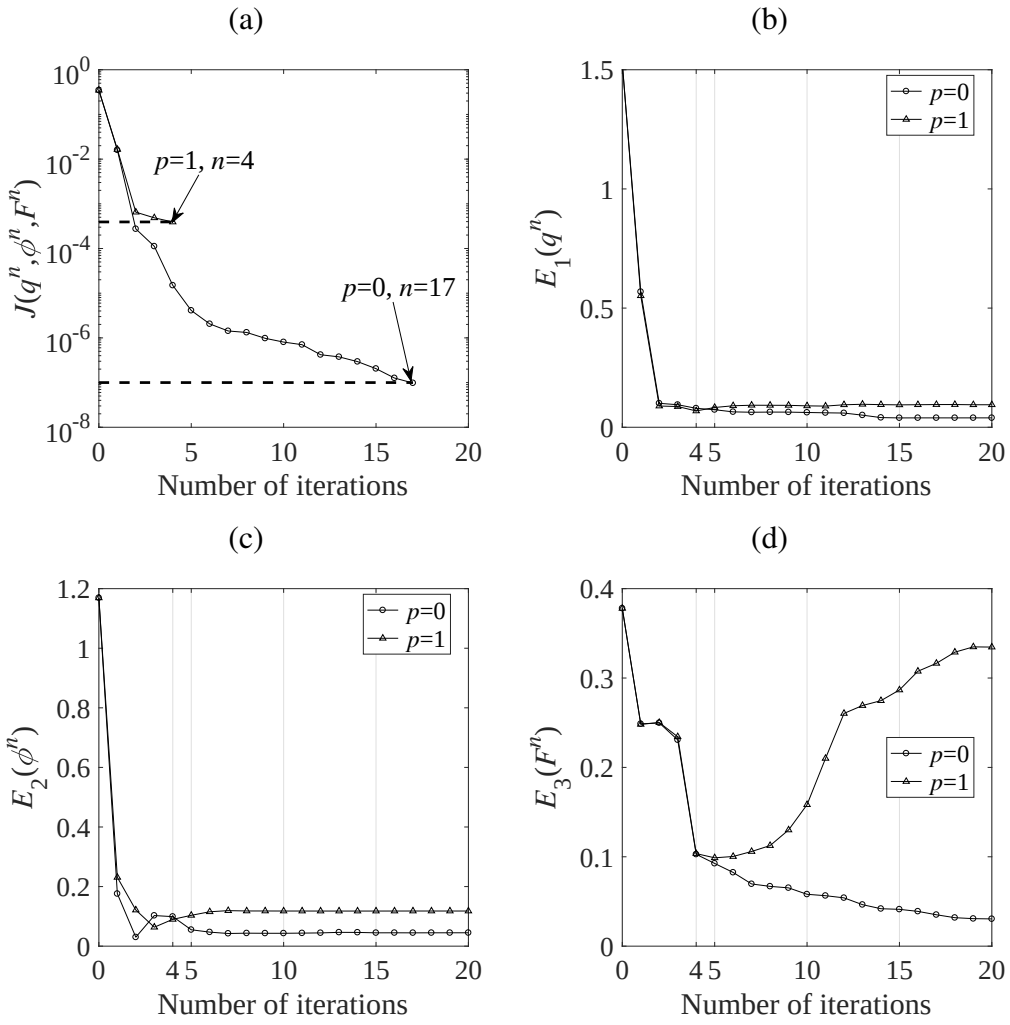

Figure 8.1: (a) The objective functional (8.8) and the accuracy errors (b) (8.26) (c) (8.27) and (d) (8.28), with $p \in \{0, 1\}$ noise, for Example 1.

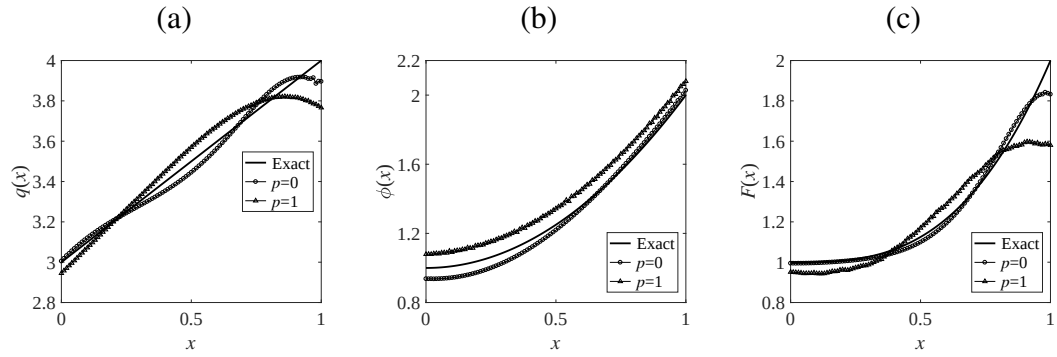

Figure 8.2: The exact and numerical solutions for (a) the reaction coefficient $q(x)$, (b) the initial temperature $\phi(x)$ and (c) the source term $F(x)$, with $p \in \{0, 1\}$ noise, for Example 1.

p	I	M	$\overline{\epsilon}$	N	E_1	E_2	E_3
0	101	101	1.0E-07	17	2.7E-02	2.0E-02	3.0E-03
1	101	101	3.9E-04	4	6.4E-02	5.4E-02	0.1077

Table 8.1: The stopping iteration numbers N and the errors E_1, E_2 and E_3 for $p \in \{0, 1\}$ noise, for Example 1.

8.5.2 Example 2

We take $t_1 = 0.3$, $t_2 = 0.7$, and

$$
\begin{aligned}
&k \equiv 1, \quad \alpha \equiv 1, \quad h(x,t) = (2+x^3)e^t, \quad \mu(0,t) = \mu(1,t) = e^{-t},\\
&g(x,t) = \pi^2 \sin(\pi x)e^{-t} - (3-2x^2)(2+x^3)e^t\\
&\qquad + (1+\pi+\sin(\pi x))e^{-t} \begin{cases} 1-x, & x \in [0, 0.3],\\ -x+4x^2, & x \in (0.3, 0.7),\\ 2 & x \in [0.7, 1], \end{cases}\\
&\phi_1(x) = e^{-0.3}(1+\pi+\sin(\pi x)), \quad \phi_2(x) = e^{-0.7}(1+\pi+\sin(\pi x)),\\
&\phi_T(x) = e^{-1}(1+\pi+\sin(\pi x)).
\end{aligned}
$$

Based on this input data, the analytical solution to the inverse problem (8.1), (8.4)–(8.6) is given by

$$
\begin{aligned}
&q(x) = \begin{cases} 2-x, & x \in [0, 0.3],\\ 1-x+4x^2, & x \in (0.3, 0.7),\\ 3, & x \in [0.7, 1], \end{cases} \qquad F(x) = 3 - 2x^2,\\
&\phi(x) = 1+\pi+\sin(\pi x), \quad u(x,t) = (1+\pi+\sin(\pi x))e^{-t}.
\end{aligned} \tag{8.30}
$$

In comparison with the Example 1, this example is more severe since the reaction coefficient $q(x)$ in (8.30) to be retrieved is a discontinuous function. The initial guesses are taken as $q^0(x) = 1$, $\phi^0(x) = 1$ and $F^0(x) = 1$. Figure 8.3(a) shows the convergence of the objective functional $J(q^n, \phi^n, F^n)$ given by (8.8) with the iterative CGM stopped at the iteration numbers $\{50, 18\}$ for $p \in \{0, 1\}$ noise, respectively. The corresponding numerical solutions to the reaction coefficient $q(x)$, the initial temperature $\phi(x)$ and the source term $F(x)$ at these stopping iteration numbers are illustrated in Figures 8.3(b)–8.3(d), respectively. From these figures, it can be seen that the retrieved results are reasonably accurate and stable bearing in mind the severe discontinuous reaction coefficient that had to be recovered along with the initial temperature and the source term, simultaneously.

p	I	M	$\overline{\epsilon}$	N	E_1	E_2	E_3
0	101	101	1.0E-06	50	0.1343	6.2E-02	2.5E-03
1	101	101	2.7E-03	18	0.3402	0.1640	0.1420

Table 8.2: The stopping iteration numbers N and the errors E_1, E_2 and E_3 for $p \in \{0, 1\}$ noise, for Example 2.

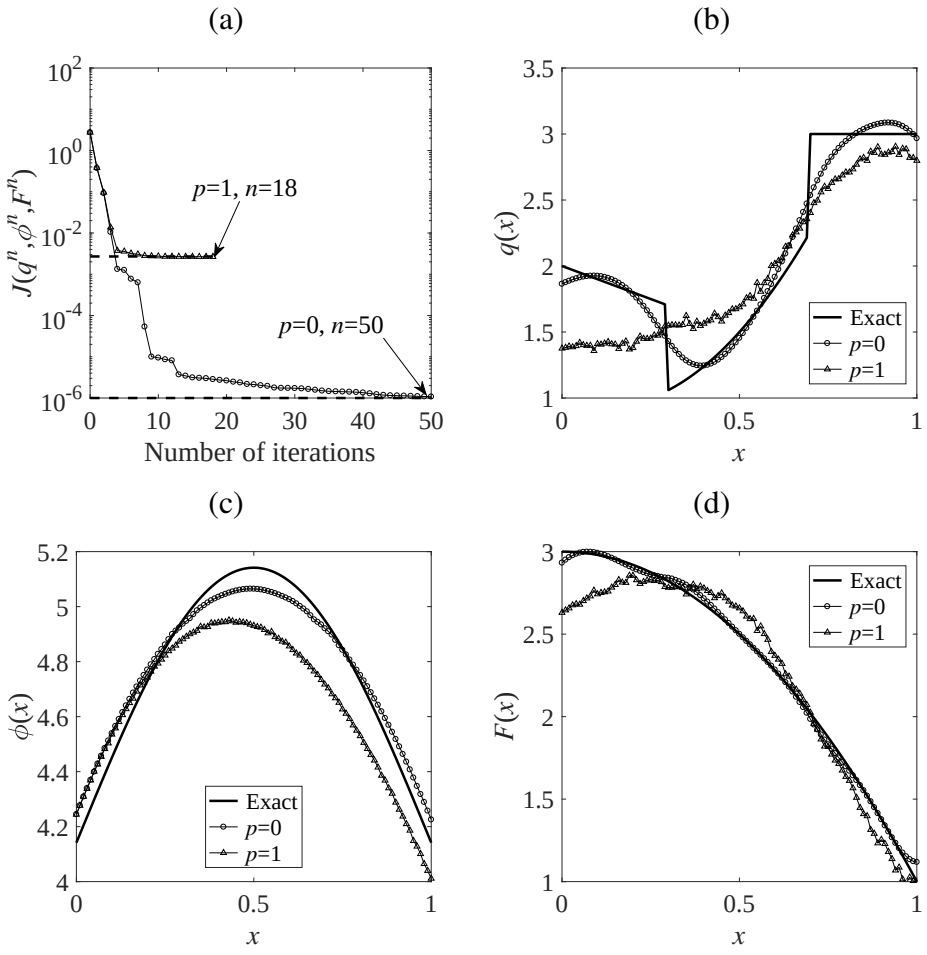

Figure 8.3: (a) The objective functional (8.8) and the exact and numerical solutions for (b) the reaction coefficient $q(x)$, (c) the initial temperature $\phi(x)$ and (d) the source term $F(x)$, with $p \in \{0, 1\}$ noise, for Example 2.

8.6 Conclusions

The simultaneous retrieval of the space-dependent reaction coefficient, the initial temperature and the source term from the measured temperatures at two time instants t_1, t_2 and at the final time T has been investigated. The three unknown coefficients have been

reconstructed by minimizing the least-squares objective functional. Based on a variational method, the Fréchet derivatives with respect to the three unknowns are obtained together with the adjoint and sensitivity problems. The CGM has then been applied to numerically retrieve the three unknown coefficients. Two numerical examples for one-dimensional inverse problems have been illustrated for continuous and discontinuous reaction coefficient. The numerical solutions regularized by the discrepancy principle have been obtained accurate and stable for all the three space-dependent unknown quantities that have been simultaneously retrieved.

Chapter 9

General conclusions and future work

9.1 Conclusions

The objective of this thesis was to reconstruct unknown space-dependent coefficients and/or the initial temperature in the IHTPs. Such inverse problems have practical physical applications in heat and bio-heat conduction, melting or cooling processes, etc.

Since one or more space-dependent coefficients and/or the initial temperature in the inverse problems is/are unknown, extra information is required to retrieve these unknown quantities. Such information is usually provided as measured over-specified observation which contains random noise. This random noise causes huge oscillations and unbounded behaviour in the numerical solutions to the inverse problem under investigation, when this problem is ill-posed. Consequently, the traditional numerical methods are not appropriate unless combined with some sort of regularization.

In this thesis, the inverse problems have been transformed to nonlinear optimization problems of the least squares objective functionals. Then, the quasi-solutions to the inverse problems can be approximated by the minimizers of these objective functionals. The CGM regularized by the discrepancy principle was utilized to stabilize the solution with respect to errors in the temperature measurements.

The existence of the minimizer for the optimization problem was proved by applying basic arguments of functional analysis. The Fréchet gradient of the objective functional is derived using the variational method, the adjoint problem and the sensitivity problem.

The CGM is established to obtain the numerical solutions to the unknown coefficients. The choice of the conjugate gradient parameter is taken into consideration, and the Fletcher-Reeves formula is applied throughout the thesis. The temperature can be transformed into a linear function of the step size using the Taylor series expansion. Then, the objective functional can be approximated by the above temperature, and the

step size is obtained by vanishing the partial derivatives of the objective function subject to the step size. In summary, the steps of the CGM includes: (S1) set $n = 0$ and choose initial guesses for the unknown coefficients; (S2) solve the direct problem and calculate the objective functional; (S3) if the stopping criterion based on the discrepancy principle is satisfied, then go to S7, else go to S4; (S4) solve the adjoint problem, Fréchet gradient, conjugate coefficients and directions of descent; (S5) solve the sensitivity problem and compute the search step sizes; (S6) update the unknown coefficients, set $n = n + 1$ and go to S2; (S7) end.

For all the inverse problems considered in this thesis, their accurate and stable numerical results have been thoroughly investigated for various noise levels in the temperature measurements. The direct, adjoint and sensitivity problems have been solved by using the FDM, i.e. the C-N scheme for one dimensional problems and the ADI scheme for two dimensional problems. The temperature measurement has been statistically simulated by adding to the exact temperature random noise generated from a normal distribution by MATLAB.

In Chapter 1, a general introduction to the direct parabolic problems and the IHTPs has been provided. The ill-posedness of the IHTP has been presented, especially the instability of the solution to linear or nonlinear inverse problems. Then, the Tikhonov regularization can be used to regularize ill-posed problems for a suitable choice of regularization parameter. Iteration regularization methods, such as the Landweber's method and the CGM can be used to obtain stable solutions to the inverse problems when the iteration process is stopped according to the discrepancy principle.

In Chapter 2, the IHTP which requires to reconstruct the unknown space-dependent thermal conductivity in an isotropic medium has been investigated. The interior measured temperature is used as additional information. The quasi-solution of the inverse problem is approximated by the minimizer of the objective functional, which is the gap between the computed and the measured temperature. The existence of the minimizer to the optimization problem is proved based on basic functional analysis arguments. The Fréchet gradient is derived using the variational method based on the sensitivity and adjoint problems. Then, the CGM is established based on such gradient. The Sobolev gradient can also be applied in the CGM to obtain smoother results, especially for the conventional gradient with zero boundary values. The stable results can be reconstructed by the CGM regularized by the discrepancy principle, in such case the iterations are stopped at the level at which the objective functional becomes just below the noise threshold with which the data is contaminated. Three numerical numerical examples have been presented for one- or two-dimensional problems obtaining accurate and stable numerical solutions.

In Chapter 3, the space-dependent thermal conductivity orthotropic tensor has been numerically reconstructed from internal temperature observations using the CGM. The Sobolev gradient has been utilized in the CGM to determine smoother and significantly more accurate and stable numerical results.

In Chapter 4, the inverse problem of identifying the space-dependent thermal conductivity and reaction coefficient from internal temperature measurements has been considered using the CGM. The Fréchet gradient with respect to the coefficients has been utilized to establish the CGM, and then regularized by discrepancy principle to obtain stable numerical solutions. The numerical results of the three continuous and discontinuous examples showed that CGM is an accurate and stable regularization method for reconstructing spatially-varying coefficients.

In Chapter 5, the unknown space-dependent reaction coefficient has been reconstructed from the final or time-average temperature measurements using the CGM regularized by the discrepancy principle. Three examples for both inverse problems have been tested obtaining stable and accurate numerical results. Moreover, the numerical solution for the inverse problem based on the time-average measured temperature has been obtained slightly more accurate than the numerical solution for the inverse problem based on the final data.

Chapter 6 has been concerned with the simultaneous reconstruction of the space-dependent reaction coefficient and the initial temperature from temperature measurements at two different instants. The uniqueness of the inverse problem holds under some assumptions. The regularized CGM has been applied to obtain the numerical solutions for the two unknown quantities. Three numerical examples for one- and two-dimensional examples have been illustrated and discussed, and accurate and stable results have been achieved.

In Chapter 7, the same unknown coefficients as in Chapter 6 have been retrieved, but from time-integral weighted temperature observations. The CGM has been established based on the Fréchet gradient and the adjoint and sensitivity problems. The global convergence of the CGM has been established for exact data from the Lipschitz continuity of the gradient. Three numerical examples in both one- and two-dimensional inverse problems have been presented, and the numerical solutions showed the accuracy and stability of the numerical reconstruction.

Finally, in Chapter 8, the space-dependent reaction coefficient, the initial temperature and the source component have been simultaneously reconstructed from temperature measurements at two time instants and at the final time. The CGM has been again utilized

to retrieve the numerical solutions of the three unknown quantities. The numerical solutions of two examples for one-dimensional inverse problems illustrate that all the three space-dependent unknown coefficients can be retrieved in an accurate and stable manner.

Overall, the numerical results obtained by using the methods established in this thesis, i.e. the FDM combined with CGM regularized by the discrepancy principle, illustrate that accurate and stable solutions can be obtained for recovering one or more unknown space-dependent coefficients in nonlinear and ill-posed IHTPs. Moreover, the CGM semi-converges fast, i.e. the iteration process are stopped rapidly. In general, up to 5% noisy data, which is a realistic amount noise in practical measurement, can be inverted to produce reasonably accurate and stable numerical results.

In the simultaneous reconstruction of three unknowns investigated in Chapter 8, the three search step sizes cannot be obtained in the two-dimensional case, since the matrix $\mathbf{A}$ in (8.24) becomes singular. Thus, the method proposed in this thesis may not be useful for reconstructing three or more coefficients in IHTPs, simultaneously.

In addition, since the FDM is applied to solve the PDEs, which may limit the applications of the CGM proposed in this thesis, the FEM could be a better method to solve the PDEs in irregular domains. Besides, the weak solutions, which are used in the definition of the least-squares objective functional in Chapters 2–8, can also be applied in the establishment of the FEM.

Much work remains to be done in the future and some possible avenues are proposed in the next section.

9.2 Future work

The numerical solutions produced in this thesis confirm the fact that the CGM can be applied for efficiently reconstructing the unknown coefficients of IHTPs and the initial temperature of the BHCPs. Some possible future work may consist of:

- Extend the unknown space-dependent coefficients in Chapters 2-4 to time- and space-dependent or temperature-dependent coefficients.
- Investigate the global convergence of the inverse problems in Chapters 2-4 based on the approach applied in Chapter 7.
- Reconstruct the space-dependent reaction coefficient, the Robin boundary coefficient and the initial temperature from the measured temperatures at two distinct time instants, simultaneously.

- Investigate the uniqueness of the reaction coefficient and the initial temperature in the IHTP from time-average measured temperatures in Chapter 7.
- Investigate the uniqueness of the reaction coefficient, the source component and the initial temperature of the IHTP from temperature observations at two distinct time instants and at the final time in Chapter 8.
- Extend the one-dimensional numerical implementation of Chapter 8 to higher dimensional inverse problems.
- The numerical solutions to the discontinuous coefficient examples are not sufficiently accurate throughout the work, especially near the areas of the discontinuity points. One may employ the TV regularization to improve the accuracy in recovering these discontinuous coefficients.
- Use the FEM combined with CGM to reconstruct unknown coefficients in IHTPs for irregular solution domains.

References

ALIFANOV, O.M. (1994). *Inverse Heat Transfer Problems*. Springer, Berlin. 1, 2, 4, 31, 33, 84, 103, 105, 121, 145, 154

ALIFANOV, O.M. & TRYANIN, A.P. (1985). Determination of the coefficient of internal heat exchange and the effective thermal conductivity of a porous solid on the basis of a nonstationary experiment. *Journal of Engineering Physics and Thermophysics*, **48**, 356–365. 21

BANERJEE, P.K. & BUTTERFIELD, R. (1981). *Boundary Element Methods in Engineering Science*, vol. 17. McGraw-Hill, London. 3

BECK, J.V. & AL-ARAJI, S. (1974). Investigation of a new simple transient method of thermal property measurement. *Journal of Heat Transfer*, **96**, 59–64. 18

BECK, J.V., BLACKWELL, B. & CLAIR JR, C.S. (1985). *Inverse Heat Conduction Problems*. Wiley&Interscience, New York. 2

CANNON, J.R. & DOUGLAS, J. (1967). The Cauchy problem for the heat equation. *SIAM Journal on Numerical Analysis*, **4**, 317–336. 103

CANNON, J.R. & DUCHATEAU, P. (1974). Determination of the conductivity of an isotropic medium. *Journal of Mathematical Analysis and Applications*, **48**, 699–707. 18

CANNON, J.R. & JONES, B.F. (1963). Determination of the diffusivity of an anisotropic medium. *International Journal of Engineering Science*, **1**, 457–460. 18

CANNON, J.R. & LIN, Y. (1990). An inverse problem of finding a parameter in a semi-linear heat equation. *Journal of Mathematical Analysis and Applications*, **145**, 470–484. 19

CANNON, J.R. & YIN, H.M. (1990). Numerical solutions of some parabolic inverse problems. *Numerical Methods for Partial Differential Equations*, **6**, 177–191. 19

CANNON, J.R., DOUGLAS, J. & JONES, B.F. (1963). Determination of the diffusivity of an isotropic medium. *International Journal of Engineering Science*, **1**, 453–455. 18

CANNON, J.R., DUCHATEAU, P. & STEUBE, K. (1990). Unknown ingredient inverse problems and trace-type functional differential equations. In *Inverse Problems in Partial Differential Equations*, (D. Colton, R. Ewing, and W. Rundell, eds.), SIAM, Philadelphia, 187–202. 106

CANNON, J.R., LIN, Y. & WANG, S. (1992). Determination of source parameter in parabolic equations. *Meccanica*, **27**, 85–94. 19

CAO, K. & LESNIC, D. (2018a). Reconstruction of the perfusion coefficient from temperature measurements using the conjugate gradient method. *International Journal of Computer Mathematics*, **95**, 797–814. 5, 19

CAO, K. & LESNIC, D. (2018b). Simultaneous reconstruction of the perfusion coefficient and initial temperature from time-average integral temperature measurements. *Accepted by Applied Mathematical Modelling*. 125, 129

CAO, K., LESNIC, D. & LIU, J.J. (2018). Simultaneous reconstruction of space-dependent heat transfer coefficients and initial temperature. *Submitted to Journal of Computational and Applied Mathematics*. 105, 107

CHEN, Q. & LIU, J.J. (2006). Solving an inverse parabolic problem by optimization from final measurement data. *Journal of Computational and Applied Mathematics*, **193**, 183–203. 19, 84

CHEN, Z. & ZOU, J. (1999). An augmented Lagrangian method for identifying discontinuous parameters in elliptic systems. *SIAM Journal on Control and Optimization*, **37**, 892–910. 25

CHOULLI, M. & YAMAMOTO, M. (2008). Uniqueness and stability in determining the heat radiative coefficient, the initial temperature and a boundary coefficient in a parabolic equation. *Nonlinear Analysis: Theory, Methods & Applications*, **69**, 3983–3998. 104

COLAÇO, M.J. & ORLANDE, H.R.B. (1999). Comparison of different versions of the conjugate gradient method of function estimation. *Numerical Heat Transfer: Part A: Applications*, **36**, 229–249. 14, 19

COLAÇO, M.J., ORLANDE, H.R.B. & DULIKRAVICH, G.S. (2006). Inverse and optimization problems in heat transfer. *Journal of the Brazilian Society of Mechanical Sciences and Engineering*, **28**, 1–24. 14, 18, 21, 69

COLTON, D. (1979). The approximation of solutions to the backwards heat equation in a nonhomogeneous medium. *Journal of Mathematical Analysis and Applications*, **72**, 418–429. 104

DAI, Y.H. & YUAN, Y. (1996). Convergence properties of the Fletcher-Reeves method. *IMA Journal of Numerical Analysis*, **16**, 155–164. 17, 131

DAI, Y.H. & YUAN, Y. (1999). A nonlinear conjugate gradient method with a strong global convergence property. *SIAM Journal on Optimization*, **10**, 177–182. 15, 17

DEHGHAN, M. (2005). Efficient techniques for the second-order parabolic equation subject to nonlocal specifications. *Applied Numerical Mathematics*, **52**, 39–62. 19

DEMIRCI, E., ACAR, M., POURDEYHIMI, B. & SILBERSCHMIDT, V.V. (2012). Computation of mechanical anisotropy in thermally bonded bicomponent fibre nonwovens. *Computational Materials Science*, **52**, 157–163. 51

DENG, Z.C., YU, J.N. & YANG, L. (2008). Optimization method for an evolutional type inverse heat conduction problem. *Journal of Physics A: Mathematical and Theoretical*, **41**, 035201. 19

DENG, Z.C., YANG, L. & YU, J.N. (2009). Identifying the radiative coefficient of heat conduction equations from discrete measurement data. *Applied Mathematics Letters*, **22**, 495–500. 84

DENG, Z.C., YANG, L., YU, J.N. & LUO, G.W. (2010). Identifying the radiative coefficient of an evolutional type heat conduction equation by optimization method. *Journal of Mathematical Analysis and Applications*, **362**, 210–223. 19

EICKE, B., LOUIS, A.K. & PLATO, R. (1990). The instability of some gradient methods for ill-posed problems. *Numerische Mathematik*, **58**, 129–134. 13

ENGL, H.W., KUNISCH, K. & NEUBAUER, A. (1989). Convergence rates for Tikhonov regularisation of non-linear ill-posed problems. *Inverse Problems*, **5**, 523–540. 33

ENGL, H.W., HANKE, M. & NEUBAUER, A. (1996). *Regularization of Inverse Problems*, vol. 375. Springer Science & Business Media. 7, 8, 9, 10, 11, 15, 25, 33

FLETCHER, R. (2013). *Practical Methods of Optimization*. John Wiley & Sons, New York. 15

FLETCHER, R. & REEVES, C.M. (1964). Function minimization by conjugate gradients. *The Computer Journal*, **7**, 149–154. 15, 32, 59, 74, 90, 121, 127, 153

FRIEDMAN, A. (2008). *Partial Differential Equations of Parabolic Type*. Courier Dover Publications, New York. 3

FU, C.L., XIONG, X.T. & QIAN, Z. (2007). Fourier regularization for a backward heat equation. *Journal of Mathematical Analysis and Applications*, **331**, 472–480. 104

GEL'FAND, I.M. & LEVITAN, B.M. (1951). On the determination of a differential equation from its spectral function. *Izvestiya Rossiiskoi Akademii Nauk. Seriya Matematicheskaya*, **15**, 309–360. 19

GOLUB, G.H. & VAN LOAN, C.F. (2012). *Matrix Computations*, vol. 3. Johns Hopkins University Press, Baltimore. 7

HADAMARD, J. (1923). *Lectures on Cauchy's Problem in Linear Partial Differential Equations*. Dover Publications, New York. 3

HAGER, W.W. & ZHANG, H. (2006). A survey of nonlinear conjugate gradient methods. *Pacific Journal of Optimization*, **2**, 35–58. 16

HAN, H., INGHAM, D.B. & YUAN, Y. (1995). The boundary element method for the solution of the backward heat conduction equation. *Journal of Computational Physics*, **116**, 292–299. 103

HANKE, M. (1995). *Conjugate Gradient Type Methods for Ill-Posed Problems*, vol. 327. CRC Press, New York. 15, 33

HANKE, M., NEUBAUER, A. & SCHERZER, O. (1995). A convergence analysis of the landweber iteration for nonlinear ill-posed problems. *Numerische Mathematik*, **72**, 21–37. 11

HANSEN, P.C. & OLEARY, D.P. (1993). The use of the L-curve in the regularization of discrete ill-posed problems. *SIAM Journal on Scientific Computing*, **14**, 1487–1503. 33

HÀO, D.N., VAN DUC, N. & LESNIC, D. (2009). Regularization of parabolic equations backward in time by a non-local boundary value problem method. *IMA Journal of Applied Mathematics*, **75**, 291–315. 104

HÀO, D.N., THANH, P.X. & LESNIC, D. (2013). Determination of the heat transfer coefficients in transient heat conduction. *Inverse Problems*, **29**, 095020. 108

HÀO, D.N., HUONG, B.V., OANH, N.T.N. & THANH, P.X. (2017). Determination of a term in the right-hand side of parabolic equations. *Journal of Computational and Applied Mathematics*, **309**, 28–43. 5

HARRIS, S.D., MUSTATA, R., ELLIOTT, L., INGHAM, D.B. & LESNIC, D. (2008). Numerical identification of the hydraulic conductivity of composite anisotropic materials. *Computer Modeling in Engineering and Sciences*, **25**, 69–79. 19, 51

HESTENES, M.R. & STIEFEL, E. (1952). Methods of conjugate gradients for solving linear systems. *Journal of Research of the National Bereau of Standards*, **49**, 409–436. 12, 15

HIBBINS, S.G. (1982). Characterization of heat transfer in the secondary cooling system of a continuous slab caster. *Iron and Steel Society of AIME*, **2**, 139–152. 21

HUANG, C.H. & CHIN, S.C. (2000). A two-dimensional inverse problem in imaging the thermal conductivity of a non-homogeneous medium. *International Journal of Heat and Mass Transfer*, **43**, 4061–4071. 5, 19

HUANG, C.H. & ÖZIŞIK, M.N. (1990). A direct integration approach for simultaneously estimating spatially varying thermal conductivity and heat capacity. *International Journal of Heat and Fluid Flow*, **11**, 262–268. 18, 21

HUANG, C.H. & ÖZIŞIK, M.N. (1991). Direct integration approach for simultaneously estimating temperature dependent thermal conductivity and heat capacity. *Numerical Heat Transfer, Part A Applications*, **20**, 95–110. 19, 21

ISAKOV, V. (1990). *Inverse Source Problems*. 34, American Mathematical Society, Providence. 5, 144

ISAKOV, V. (1991). Inverse parabolic problems with the final overdetermination. *Communications on Pure and Applied Mathematics*, **44**, 185–209. 19, 83

ISAKOV, V. (2006). *Inverse Problems for Partial Differential Equation*. Springer-Verlag, Berlin. 22, 144

JARNY, Y., OZISIK, M.N. & BARDON, J.P. (1991). A general optimization method using adjoint equation for solving multidimensional inverse heat conduction. *International Journal of Heat and Mass Transfer*, **34**, 2911–2919. 33

JIN, B. & ZOU, J. (2009). Numerical estimation of the Robin coefficient in a stationary diffusion equation. *IMA Journal of Numerical Analysis*, **30**, 677–701. 31

JOHANSSON, B.T. & LESNIC, D. (2008). A procedure for determining a spacewise dependent heat source and the initial temperature. *Applicable Analysis*, **87**, 265–276. 114

KALTENBACHER, B., NEUBAUER, A. & SCHERZER, O. (2008). *Iterative Regularization Methods for Nonlinear Ill-Posed Problems*, vol. 6. Walter de Gruyter, Berlin. 11, 12, 13

KAMYNIN, V.L. & KOSTIN, A.B. (2010). Two inverse problems of finding a coefficient in a parabolic equation. *Differential Equations*, **46**, 375–386. 19, 84, 86

KEUNG, Y.L. & ZOU, J. (1998). Numerical identifications of parameters in parabolic systems. *Inverse Problems*, **14**, 83–100. 26, 70, 108

KOHN, R. & VOGELIUS, M. (1984). Determining conductivity by boundary measurements. *Communications on Pure and Applied Mathematics*, **37**, 289–298. 18

KOHN, R.V. & VOGELIUS, M. (1985). Determining conductivity by boundary measurements II. interior results. *Communications on Pure and Applied Mathematics*, **38**, 643–667. 18

KOZHANOV, A.I. (2004). A nonlinear loaded parabolic equation and a related inverse problem. *Mathematical Notes*, **76**, 784–795. 19, 84, 86

KRAVARIS, C. & SEINFELD, J.H. (1986). Identifiability of spatially-varying conductivity from point observation as an inverse Sturm–Liouville problem. *SIAM Journal on Control and Optimization*, **24**, 522–542. 18

KURPISZ, K. & NOWAK, A. (1995). *Inverse Thermal Problems*. Computational Mechanics Publications, Southampton. 103

LADYZHENSKAIA, O.A., SOLONNIKOV, V.A. & URAL'TSEVA, N.N. (1968). *Linear and Quasi-Linear Equations of Parabolic Type*, vol. 23. American Mathematical Society, Providence. 3, 22, 86, 106

LANDWEBER, L. (1951). An iteration formula for Fredholm integral equations of the first kind. *American Journal of Mathematics*, **73**, 615–624. 11

LAX, P.D. (2002). *Functional Analysis*. John Wiley & Sons, Inc., New York. 26

LESNIC, D., ELLIOTT, L. & INGHAM, D.B. (1998). An iterative boundary element method for solving the backward heat conduction problem using an elliptic approximation. *Inverse Problems in Engineering*, **6**, 255–279. 103, 114

LESNIC, D., MUSTATA, R., CLENNELL, M.B., ELLIOTT, L., HARRIS, S.D. & INGHAM, D.B. (2007). Genetic algorithm to identify the hydraulic properties of heterogeneous rocks from laboratory flow-pump experiments. *Journal of Porous Media*, **10**, 71–91. 51

LIU, Y. & STOREY, C. (1991). Efficient generalized conjugate gradient algorithms, part 1: theory. *Journal of Optimization Theory and Applications*, **69**, 129–137. 15

MARIN, L. & LESNIC, D. (2002). Boundary element solution for the Cauchy problem in linear elasticity using singular value decomposition. *Computer Methods in Applied Mechanics and Engineering*, **191**, 3257–3270. 10

MEJIAS, M.M., ORLANDE, H.R.B. & OZISIK, M.N. (1999). Design of optimum experiments for the estimation of the thermal conductivity components of orthotropic solids. *Hybrid Methods in Engineering*, **1**, 37–53. 51

MIRANKER, W.L. (1961). A well posed problem for the backward heat equation. *Proceedings of the American Mathematical Society*, **12**, 243–247. 103

MOROZOV, V.A. (1966). On the solution of functional equations by the method of regularization. *Soviet Mathematical Doklady*, **7**, 414–417. 12

MUNIZ, W.B., DE CAMPOS VELHO, H.F. & RAMOS, F.M. (1999). A comparison of some inverse methods for estimating the initial condition of the heat equation. *Journal of Computational and Applied Mathematics*, **103**, 145–163. 104

NATTERER, F. (2001). *The Mathematics of Computerized Tomography*. Wiley, Chichester. 12

NEUBAUER, A. & SCHERZER, O. (1995). A convergence rate result for a steepest descent method and a minimal error method for the solution of nonlinear ill-posed problems. *Zeitschrift für Analysis und ihre Anwendungen*, **14**, 369–377. 13

NEUBERGER, J. (2009). *Sobolev Gradients and Differential Equations*. Springer Science & Business Media, Berlin. 31

ORLANDE, H.R.B., COLAÇO, M.J. & MALTA, A.A. (1997). Estimation of the heat transfer coefficient in the spray cooling of continuously cast slabs. *ASME-Publications-HTD*, **340**, 109–116. 21

ÖZIŞIK, M.N. & ORLANDE, H.R.B. (2000). *Inverse Heat Transfer: Fundamentals and Applications*. CRC Press, New York. 1, 4, 17, 19, 84, 103, 105

PATTERSON, W.M. (1974). *Iterative Methods for the Solution of a Linear Operator Equation in Hilbert Space: A Survey*. Springer-Verlag, Berlin. 12

PEACEMAN, D.W. & RACHFORD, H.H., JR (1955). The numerical solution of parabolic and elliptic differential equations. *Journal of the Society for Industrial and Applied Mathematics*, **3**, 28–41. 37

PENNES, H.H. (1948). Analysis of tissue and arterial blood temperatures in the resting human forearm. *Journal of Applied Physiology*, **1**, 93–122. 83, 85

PHILLIPS, D.L. (1962). A technique for the numerical solution of certain integral equations of the first kind. *Journal of the Association for Computing Machinery*, **9**, 84–97. 9

PIERCE, A. (1979). Unique identification of eigenvalues and coefficients in a parabolic problem. *SIAM Journal on Control and Optimization*, **17**, 494–499. 19

POLAK, E. & RIBIERE, G. (1969). Note sur la convergence de méthodes de directions conjuguées. *Revue française d'informatique et de recherche opérationnelle. Série rouge*, **3**, 35–43. 15

POWELL, M.J.D. (1977). Restart procedures for the conjugate gradient method. *Mathematical Programming*, **12**, 241–254. 14

PRILEPKO, A.I. & KOSTIN, A.B. (1993). On certain inverse problems for parabolic equations with final and integral observation. *Russian Academy of Science, Siberian Mathematics*, **75**, 473–490. 19, 84, 86, 87, 106

PRILEPKO, A.I. & SOLOVEV, V.V. (1987). Solvability of the inverse boundary-value problem of finding a coefficient of a lower-order derivative in a parabolic equation. *Differential Equations*, **23**, 101–107. 19, 83, 86

PRILEPKO, A.I., ORLOVSKY, D.G. & VASIN, I.A. (2000). *Methods for Solving Inverse Problems in Mathematical Physics*. CRC Press, New York. 144

RAYMOND, J.P. & ZIDANI, H. (1999). Hamiltonian Pontryagin's principles for control problems governed by semilinear parabolic equations. *Applied Mathematics and Optimization*, **39**, 143–177. 128

REDDY, J.N. (1993). *An Introduction to the Finite Element Method*, vol. 2. McGraw-Hill, New York. 3

RICHTER, G.R. (1981a). An inverse problem for the steady state diffusion equation. *SIAM Journal on Applied Mathematics*, **41**, 210–221. 25

RICHTER, G.R. (1981b). Numerical identification of a spatially varying diffusion coefficient. *Mathematics of Computation*, **36**, 375–386. 25

RICHTMYER, R.D. & MORTON, K.W. (1967). *Difference Methods for Initial-Value Problems*. John Wiley & Sons, Inc., New York. 35, 37

ROBINSON, P.S., SCOTT, E.P. & DILLER, T.E. (1998). Validation of methodologies for the estimation of blood perfusion using a minimally invasive probe. *ASME-Publication-HTD*, **362**, 109–116. 83

RUNDELL, W. (1987). The determination of a parabolic equation from initial and final data. *Proceedings of the American Mathematical Society*, **99**, 637–642. 19, 83, 84

SAWAF, B. & ÖZISIK, M.N. (1995). Determining the constant thermal conductivities of orthotropic materials by inverse analysis. *International Communications in Heat and Mass Transfer*, **22**, 201–211. 19, 51

SCHERZER, O. (1996). A convergence analysis of a method of steepest descent and a two–step algorothm for nonlinear ill–posed problems. *Numerical Functional Analysis and Optimization*, **17**, 197–214. 15, 33

SCHOPFER, F. (2016). Linear convergence of descent methods for the unconstrained minimization of restricted strongly convex functions. *SIAM Journal on Optimization*, **26**, 1883–1911. 16

SCOTT, E.P., ROBINSON, P.S. & DILLER, T.E. (1997). Estimation of blood perfusion using a minimally invasive blood perfusion probe. *ASME-Publications-HTD*, **355**, 205–212. 83

SCOTT, E.P., ROBINSON, P.S. & DILLER, T.E. (1998). Development of methodologies for the estimation of blood perfusion using a minimally invasive thermal probe. *Measurement Science and Technology*, **9**, 888–897. 83

SMITH, G.D. (1985). *Numerical Solution of Partial Differential Equations: Finite Difference Methods*. Oxford University Press, Oxford. 3, 35

STEWART, I., MASSINGHAM, J.D. & HAGERS, J. (1996). Heat transfer coefficient effects on spray cooling. *Iron and Steel Engineer*, **63**, 17–23. 21

SUZUKI, T. (1983). Uniqueness and nonuniqueness in an inverse problem for the parabolic equation. *Journal of Differential Equations*, **47**, 296–316. 19

TADI, M., KLIBANOV, M.V. & CAI, W. (2002). An inversion method for parabolic equations based on quasireversibility. *Computers & Mathematics with Applications*, **43**, 927–941. 86

TERVOLA, P. (1989). A method to determine the thermal conductivity from measured temperature profiles. *International Journal of Heat and Mass Transfer*, **32**, 1425–1430. 19

THOMAS, M., BOYARD, N., LEFÈVRE, N., JARNY, Y. & DELAUNAY, D. (2010). An experimental device for the simultaneous estimation of the thermal conductivity 3-D tensor and the specific heat of orthotropic composite materials. *International Journal of Heat and Mass Transfer*, **53**, 5487–5498. 19, 51

TIKHONOV, A.N. (1963a). Regularization of incorrectly posed problems. *Soviet Mathematics Doklady*, **4**, 1624–1627. 9

TIKHONOV, A.N. (1963b). Solution of incorrectly formulated problems and the regularization method. *Soviet Mathematics Doklady*, **4**, 1035–1038. 9

TRÖLTZSCH, F. (2010). *Optimal Control of Partial Differential Equations*, vol. 112. Graduate Studies in Mathematics, American Mathematical Sciety, Providence. 22, 24, 53, 108, 122, 146

TROMBE, A., SULEIMAN, A. & LE MAOULT, Y. (2003). Use of an inverse method to determine natural convection heat transfer coefficients in unsteady state. *Journal of Heat Transfer*, **125**, 1017–1026. 105

TRUCU, D., INGHAM, D.B. & LESNIC, D. (2008). Inverse time-dependent perfusion coefficient identification. *Journal of Physics: Conference Series*, **124**, 012050. 19, 86

TRUCU, D., INGHAM, D.B. & LESNIC, D. (2010a). Inverse temperature-dependent perfusion coefficient reconstruction. *International Journal of Non-Linear Mechanics*, **45**, 542–549. 19

TRUCU, D., INGHAM, D.B. & LESNIC, D. (2010b). Space-dependent perfusion coefficient identification in the transient bio-heat equation. *Journal of Engineering Mathematics*, **67**, 307–315. 10, 19, 84, 93, 95, 96

TRUCU, D., INGHAM, D.B. & LESNIC, D. (2011). Reconstruction of the space- and time-dependent blood perfusion coefficient in bio-heat transfer. *Heat Transfer Engineering*, **32**, 800–810. 19

TUAN, N.H., VAN AU, V., KHOA, V.A. & LESNIC, D. (2017). Identification of the population density of a species model with nonlocal diffusion and nonlinear reaction. *Inverse Problems*, **33**, 055019. 104

VERSTEEG, H.K. & MALALASEKERA, W. (2007). *An Introduction to Computational Fluid Dynamics: The Finite Volume Method*. Pearson Education, England. 3

WAHBA, G. (1990). *Spline Models for Observational Data*, vol. 59. SIAM, Philadelphia. 33

WOLFE, P. (1969). Convergence conditions for ascent methods. *SIAM Review*, **11**, 226–235. 17, 131

WOLFE, P. (1971). Convergence conditions for ascent methods. II: Some corrections. *SIAM Review*, **13**, 185–188. 131

YAMAMOTO, M. & ZOU, J. (2001). Simultaneous reconstruction of the initial temperature and heat radiative coefficient. *Inverse Problems*, **17**, 1181–1202. 70, 104, 108

YANG, L., YU, J.N. & DENG, Z.C. (2008). An inverse problem of identifying the coefficient of parabolic equation. *Applied Mathematical Modelling*, **32**, 1984–1995. 84

YUE, K., ZHANG, X. & ZUO, Y.Y. (2008). Noninvasive method for simultaneously measuring the thermophysical properties and blood perfusion in cylindrically shaped living tissues. *Cell Biochemistry and Biophysics*, **50**, 41–51. 83

ZEIDLER, E. (1995). *Applied Functional Anlysis: Main Principles and Their Applications*. Springer, New York. 26

ZOUTENDIJK, G. (1970). Nonlinear programming, computational methods. *Integer and Nonlinear Programming*, **143**, 37–86. 17, 121, 131